Neuropilin 2 role in the regulation of disseminated tumour cells dormancy and metastasis in breast and head and neck cancer

Leire Recalde-Percaz

UNIVERSITAT DE BARCELONA

PhD Thesis
Doctoral programme in Biomedicine

Neuropilin 2 role in the regulation of disseminated tumour cells dormancy and metastasis in breast and head and neck cancer

Leire Recalde-Percaz

A thesis to obtain the degree of

Doctor in Philosophy by the University of Barcelona

This PhD thesis has been performed under the direction of Dra. Paloma Bragado Domingo and Dr. Pere Gascon Vilaplana, in the laboratory of Molecular and Traslational Oncology (IDIBAPS-Fundació Clinic) and New Strategies against Cancer (Faculty of Biology, University of Barcelona).

Paloma Bragado Domingo
Director

Pere Gascón Vilaplana
Director

Neus Carbó Carbó
Tutor

Maria Neus Carbo Carbo - DNI 79285171P (TCAT)
Signat digitalment per Maria Neus Carbo Carbo - DNI 79285171P (TCAT)
Data: 2021.04.26 16:53:04 +02'00'

Leire Recalde-Percaz
Candidate

Faculty of Medicine
2021

The work presented in this doctoral dissertation has been developed with the financial support from the Ministry of Education, Culture and Sports of the Spanish Government by the *Ayuda del Programa de Formación de Profesorado Universitario* (**FPU2016**) pre-doctoral fellowship and the financial support from the University and Research Grants Management Agency (AGAUR) of the Government of Catalonia by the *Ajuts per a la Contractació de Personal Investigador Novell* (**FI-2017**) pre-doctoral fellowship. Moreover, the research project has been funded by ***Fundació Cellex*** (Barcelona, Spain), *Asociación Española Contra el Cancer* (**AECC**) (Spain), **Carlos III Health Institute** from the Ministry of Economy and Competitiveness of the Spanish Government (PI15/00661), *Fundació per a la Recerca en Oncologia i Immunologia* (**FROI**) (Barcelona, Spain), ***Fundación BBVA**: Beca Leonardo a Investigadores y Creadores Culturales* (2018) (Spain) and the **national research programme** of the Ministry of Science and Innovation of the Spanish Government (PID2019-104991RB-I00).

The international internship in Dr. Aguirre-Ghiso's laboratory in the Icahn School of Medicine at Mount Sinai (New York, USA) was funded by the **Boehringer Ingelheim Fonds** travel grant and the **European Association for Cancer Research** travel fellowship. Furthermore, assistance to congresses and workshops was financed by the Scholar-in-Training award for the **AACR**, Meeting Bursary Award for the **Metastasis Research Society** and *Fundació Cellex*.

Index

Abbreviations I
Abstract III
Resum V
Introduction 1
1.1. Breast cancer 3
1.1.1. Breast anatomy and development 3
1.1.2. Epidemiology and prognosis 4
1.1.3. BrCa origin and evolution 5
1.1.4. BrCa classification 7
1.1.4.1. Histopathological classification 8
1.1.4.1.1. Non-invasive BrCa 8
1.1.4.1.2. Invasive BrCa 8
1.1.4.1.3. Metastatic BrCa 9
1.1.4.2. Tumour stage and histological grade classification 9
1.1.4.3. Classification by biomarkers 10
1.1.4.4. Molecular classification 11
1.1.5. BrCa diagnosis 12
1.1.6. BrCa therapeutic approaches 13
1.1.6.1. Early BrCa treatment 13
1.1.6.2. Advanced BrCa treatment 14
1.2. Head and neck cancer 15
1.2.1. Upper aerodigestive track anatomy 15
1.2.2. Epidemiology and prognosis 16
1.2.2.1. HNSCC aetiology 16
1.2.3. HNSCC classification 18
1.2.3.1. TNM staging 18
1.2.3.2. Genetic classification 18
1.2.4. HNSCC molecular pathogenesis 20
1.2.4.1. Pathogenesis of HPV-negative HNSCCs 20
1.2.4.2. Pathogenesis of HPV-positive HNSCCs 21
1.2.5. HNSCC diagnosis 21
1.2.6. HNSCC treatment 22
1.2.6.1. Early-stage HNSCC treatment 22

1.2.6.2. Advanced HNSCC treatment 22
1.2.6.3. HPV-positive HNSCC treatment 23
1.3. Tumour microenvironment 23
1.3.1. Extracellular matrix 24
1.3.2. Fibroblasts 24
1.3.3. Endothelial cells 25
1.3.4. Immune inflammatory cells 26
1.3.4.1. Lymphocytes 26
1.3.4.2. Macrophages 26
1.3.4.3. Dendritic cells 27
1.3.4.4. Neutrophils 27
1.3.4.5. Natural killer cells 27
1.3.5. Nerve cells 28
1.4. Metastasis 29
1.4.1. Metastasis models: early *vs* late metastasis 29
1.4.2. Metastatic cascade, step by step 30
1.4.2.1. Local invasion and intravasation 31
1.4.2.2. Circulation 32
1.4.2.3. Extravasation and colonization 32
1.4.2.4. Metastasis growth or expansion 33
1.4.3. Dormancy 34
1.4.3.1. Dormancy, an evolutionary conserved process 35
1.4.3.2. Mechanisms for dormancy regulation 36
1.4.3.2.1. Microenvironmental regulation of cellular dormancy 37
1.4.3.2.2. Cell intrinsic regulation of dormancy: signalling mechanisms 39
1.4.4. Metastasis treatment 41
1.4.4.1. Dormancy diagnosis and treatment 41
1.5. Neuropilins, semaphorins and plexins 42
1.5.1. Structure and classification 43
1.5.2. NRPs, SEMA3s and PLXNs physiological functions 45
1.5.2.1. Axonal guidance 45
1.5.2.2. Vasculogenesis 46
1.5.3. NRPs, SEMA3s and PLXNs in cancer 46
1.5.3.1. NRPs, SEMA3s and PLXNs in metastasis 49
1.6. Background of the group 50

1.6.1. Role of neural mediators in breast cancer 50
1.6.2. Microenvironmental regulation of tumour dormancy 50
Hypothesis & Aims 51
Materials & Methods 55
3.1. Cell cultures 57
3.1.1. BrCa cell lines culture 57
3.1.1.1. Lung metastatic MDA-MB-453 cell lines generation 58
3.1.2. HNSCC cell lines culture 58
3.1.3. Other cell lines culture 59
3.1.3.1. Human bone marrow mesenchymal stromal cells 59
3.1.3.2. Macrophages 60
3.1.3.3. Fibroblasts 60
3.1.3.4. HEK293 cell line 60
3.1.4. Generation of conditioned media 60
3.1.5. 3D cultures 61
3.1.6. Cell treatments: drugs and inhibitors 61
3.2. Gene expression modulation 62
3.2.1. Small interfering RNA transfection 62
3.2.2. CRISPR-Cas9 system 62
3.2.2.1. CRISPR design 63
3.2.2.2. Generation of NRP2 cloning vector 63
3.2.2.2.1. Vector digestion and purification 63
3.2.2.2.2. sgRNAs annealing and ligation with lentiviral plasmids 64
3.2.2.2.3. Transformation and plasmid amplification 64
3.2.2.2.4. NRP2 CRISPR lentivirus production 64
3.2.2.3. Generation of Cas9-positive cell lines 65
3.2.2.3.1. Generation of Cas9 lentiviral particles 65
3.2.2.3.2. Cell infection and selection 65
3.2.2.4. Generation of NRP2 silenced cell lines 65
3.3. Gene expression studies 66
3.3.1. Isolation and quantification of RNA 66
3.3.2. Reverse transcription 66
3.3.3. Quantitative polymerase chain reaction 66
3.4. Protein analyses 67
3.4.1. Cell lysis 67

3.4.2. Western blotting 67
3.4.3. TGFβ1 depletion by immunoprecipitation assay 69
3.4.4. Human TGFβ1 immunoassay 69
3.5. Cell proliferation and viability assays 69
3.5.1. Cell proliferation assays: MTT assay 69
3.5.2. Colony formation assay 70
3.5.3. Annexin V assay 70
3.5.4. Cell cycle analysis: PI assay 71
3.6. Cell adhesion, migration and invasion assays 71
3.6.1. Cell adhesion assay 71
3.6.2. Wound-healing assay 71
3.6.3. Transwell invasion assay 71
3.6.4. DQ Collagen invasion assay 72
3.7. Immunofluorescence staining 72
3.7.1. Immunofluorescence in 2D cultures 72
3.7.2. Immunofluorescence in 3D cultures 73
3.7.3. Immunofluorescence in tissue samples 74
3.8. *In vivo* experiments 74
3.8.1. Chicken embryo chorioallantoic membrane assay 74
3.8.2. *In vivo* 1: xenograft mouse model, orthotopic inoculation 75
3.8.3. *In vivo* 2: tail vein injection 76
3.9. Studies with patients 77
3.10. Statistical analysis 77
Results 79
4.1. NRPs, SEMA3s and PLXNs expression characterization in BrCa and HNSCC cell lines 81
4.1.1. Characterization of NRPs expression in BrCa and HNSCC cell lines 81
4.1.2. Characterization of PLXNs expression in BrCa and HNSCC cell lines 84
4.1.3. Characterization SEMA3s expression in BrCa and HNSCC cell lines 86
4.2. Role of SEMA3F as a dormancy-inducer in BrCa and HNSCC models 88
4.2.1. SEMA3F treatment increases p27 quiescence marker expression *in vitro* 90
4.2.2. SEMA3F has no effect on cell proliferation, clonogenicity and cell cycle regulation *in vitro* 90
4.2.3. SEMA3F does not regulate cell migration and invasion *in vitro* 92
4.2.4. SEMA3F induces dormancy genes expression on primary tumours and reduces tumour cell dissemination to secondary organs *in vivo* 94

4.3. Role of PLXNA2 and PLXNA3 in BrCa 97
4.3.1. Regulation of PLXNA2 and PLXNA3 expression by signals present in the tumour microenvironment *in vitro* 99
4.3.2. PLXNA2 regulates breast tumour growth by inhibiting cell migration, invasion and stemness 101
4.3.2.1. PLXNA2 inhibition does not regulate quiescence markers expression 101
4.3.2.2. PLXNA2 inhibition enhances cell migration and invasion in BrCa cells 102
4.3.2.3. PLXNA2 negatively regulates BrCa stemness and tumour-initiation capacity 104
3.2.4. PLXNA2 regulates tumour growth *in vivo*, likely inducing cell quiescence 105
4.3.3. PLXNA3 might restrain tumour growth in ER-positive breast tumours 106
4.3.3.1. PLXNA3 down-regulation enhances luminal A breast tumours growth *in vivo* 106
4.3.3.2. Oestrogens regulate PLXNA3 expression in ER-positive BrCa cells 108
4.4. NRP2 induces tumour growth and DTCs proliferation promoting lung metastases development 109
4.4.1. NRP2 expression negatively correlates with metastatic risk and BrCa and HNSCC patients' survival 109
4.4.2. NRP2 regulates cell proliferation while reducing p27 expression, triggering tumour growth *in vivo* 110
4.4.2.1. NRP2 deletion inhibits cell proliferation and cell cycle progression 110
4.4.2.2. NRP2 inhibition up-regulates p27 levels in BrCa and HNSCC cell lines 112
4.4.2.3 NRP2 inhibition decreases the *in vitro* tumour-initiation capacity of BrCa and HNSCC cells 113
4.4.2.4. NRP2 expression modulation might induce cell apoptosis by the intrinsic signalling pathway 114
4.4.2.5 NRP2 deletion reduces cell adhesion, inhibits migration and blocks invasion of BrCa and HNSCC cells 115
4.4.2.6. NRP2 expression modulation increases p27 expression and induces cleaved caspase 3 in the chicken embryo CAM *in vivo* model 116
4.4.2.7. NRP2 deletion completely blocks T-HEp3 tumour growth in xenograft models 120
4.4.3. NRP2 induces proliferation in lung DTCs and promotes lung metastases development *in vivo* 121
4.4.3.1. NRP2 blocking reduces lung DTCs derived cell lines proliferation *in vivo* 121
4.4.3.2. Lung DTCs up-regulate NRP2 expression to form micrometastases 122
4.3.3. NRP2 promotes lung DTCs proliferation resulting in a higher number and bigger lung metastases 125
4.4.4. Microenvironmental signals regulate NRP2 expression *in vitro* 130
4.4.4.1. Canonical TGFβ1 signalling pathway up-regulates NRP2 expression 133
4.4.5. Lung fibroblasts and macrophages-secreted TGFβ1 increases NRP2 expression 135

4.4.5.1. Lung-derived TGFβ1 up-regulates NRP2 expression by the canonical signalling pathway 135
4.4.5.2. Macrophages and fibroblasts-released TGFβ1 might be responsible of NRP2 up-regulation in lung DTCs 137
4.4.5.3. Lung fibrosis is associated with NRP2 up-regulation 138
Discussion 141
5.1. SEMA3F is a dormancy-inducer protein in BrCa and HNSCC prompting dormancy in lung DTCs 144
5.2. PLXNA2 inhibits tumorigenic cell properties in ER-negative BrCa cells 146
5.3. PLXNA3 expression is regulated by oestrogens and it might be inducing dormancy in ER-positive breast tumours 148
5.4. NRP2 enhances tumour growth and promotes lung DTCs proliferation triggering lung metastases development 150
5.4.1. NRP2 induces proliferation and inhibits quiescence in cancer cells, promoting tumour growth 150
5.4.2. NRP2 regulates cell survival 152
5.4.3. NRP2 induces tumour initiation 153
5.4.4. NRP2 promotes cell adhesion, migration and invasion 153
5.4.5. NRP2 triggers lung DTCs proliferation inducing lung metastases development *in vivo* 154
5.4.6. NRP2 expression is up-regulated in lung DTCs by lung fibroblasts and macrophages-derived TGFβ1 155
5.5. Concluding remarks 160
Conclusions 161
Bibliography 165

Abbreviations

#

αNRP2 Neuropilin 2 blocking antibody
2D Two dimensions
3D Three dimensions

A

ATCC American Type Culture Collection
ATF Activating transcription factor
atRA all-trans retinoic acid

B

BM Bone marrow
BMP Bone morphogenetic protein
BrCa Breast cancer
BSA Bovine serum albumin

C

CAM Chorioallantoic membrane
CC3 Cleaved caspase-3
CCL2 Chemokine C-C motif ligand 2
CDK Cyclin-dependent kinase
ch Chronic
CIN Chromosomal instability
CM Conditioned media
CRISPR Clustered regularly interspaced short palindromic repeats
CSC Cancer stem cell
CSF Colony stimulating factor
CTC Circulating tumour cell
CT Computed tomography

D

DC Dendritic cell
DCIS Ductal carcinoma *in situ*
DMEM Dulbecco's Modified Eagle Medium
DMFS Distant metastasis-free survival
DTC Disseminated tumour cell

E

E2 Oestradiol
EBV Epstein-Barr Virus
EC Extracellular
ECM Extracellular matrix
EGF Epidermal growth factor
EMT Epithelial to mesenchymal transition
ER Oestrogen receptor
ERK Extracellular regulated kinase

F

FAK Focal adhesion kinase
FBS Foetal bovine serum
FGF Fibroblast growth factor

G

GAP GTPase-activating protein
GAS6 Growth arrest-specific 6
GFP Green fluorescent protein

GNB Galunisertib
Gtx Glutamax

H

HDS High dormancy-score
HER2 Human epidermal growth factor receptor 2
HNSCC Head and neck squamous cell carcinoma
HGF Hepatocyte growth factor
HPV Human Papilloma Virus
HSC Hematopoietic stem cell

I

IC Intracellular
IDC Invasive ductal carcinoma
IF Immunofluorescence
IFN Interferon
IHC Immunohistochemistry
IL Interleukin
ILC Invasive lobular carcinoma
IPT Immunoglobulin-plexin-transcription

L

LB Luria-Bertani
LCIS Lobular carcinoma *in situ*
LDS Low dormancy-score
LG Lentiguide

M

MAPK Mitogen-activated protein kinase
MET Mesenchymal-to-epithelial transition
Mfi Mean fluorescence intensity
MIC Metastasis-initiating cell
MMP Matrix Metalloproteinases
MRD Minimal residual disease
MRI Magnetic resonance imaging
mTOR Mammalian target of rapamycin

N

NDRG1 N-myc downstream-regulated gene 1
NF-κB Nuclear factor kappa B
NGS Normal goat serum
NK Natural killer
NK1 Neurokinin 1
NRS Normal rabbit rerum
NRP Neuropilin

ns non-significant
NS Nervous system

O

ON Over-night
OS Overall survival

P

P/S Penicillin-Streptomycin
PAM50 Prediction Analysis of Microarray of 50 genes
PBS Phosphate-Buffered Saline
PD-L1 Programmed death Ligand 1
PDGF Platelet-derived growth factor
PERK Protein kinase R-like endoplasmic reticulum kinase
PFA Paraformaldehyde
PI3K Phosphatidylinositol-3-kinase
PLXN Plexin
PMN Pre-metastatic niche
PR Progesterone receptor
PSI Plexin-semaphorin-integrin
PT Primary tumour

Q

qPCR Quantitative polymerase chain reaction

R

RANKL Receptor activator of nuclear factor-κB ligand
Rb Retinoblastoma
RBD Rho GTPase-binding domain
RPMI Roswell Park Memorial Institute 1640
RT Room temperature
RTK Receptor tyrosine kinase
RQ Relative quantification

S

S.E.M. Standard error of the mean
SC Stem cell
SEMA Semaphorin
sgRNA specific single-guide RNA

siA2 small interfering RNA for PLXNA2
siA3 small interfering RNA for PLXNA3
siNRP2 small interfering RNA for NRP2
siRNA small interfering RNA
SP Substance P

T

TAF Tumour-associated fibroblast
TAM Tumour-associated macrophage
TCGA The Cancer Genome Atlas
TGF Transforming growth factor
TME Tumour microenvironment
TNBC Triple-negative breast cancer
TNF Tumour necrosis factor
TSP Thrombospondin

U

uPAR Urokinase plasminogen activator receptor
UPR Unfolded protein response

V

VCAM Vascular cell adhesion protein
VEGF Vascular endothelial growth factor

W

WHO World Health Organization

Abstract

Metastases are considered the last stage of tumour progression and the main cause of death associated to solid tumours. There are no effective treatments for metastasis which remain non-curable with more than 90% of patients dying from metastatic disease. They derive from disseminated tumour cells (DTCs) that can remain occult in a dormant state while adapting to the new microenvironment. By mechanisms that are still unclear, dormant DTCs can re-activate and become proliferative giving rise to metastatic outgrowth. Therefore, understanding the mechanisms by which metastases are formed is essential to face one of the most important problems in clinical oncology. Metastasis development depends on DTCs survival in circulation as well as on their ability to colonize new microenvironments. Therefore, we propose that the tumour microenvironment regulates the fate and survival of DTCs in secondary organs, hence regulating metastases.

This project has been developed in order to decipher the role of the nervous system in breast cancer (BrCa) and head and neck cancer (HNSCC) progression and metastasis. Particularly, we have investigated whether the neurogene neuropilin 2 (NRP2) has a crucial role in regulating DTCs biology and in remodelling the metastatic niche generating a favourable microenvironment for the survival and proliferation of the DTCs, all stimulating metastasis. As classical partners of NRPs, we have also studied the effect of class 3 semaphorins (SEMA3s) and their receptors, plexins (PLXNs), on tumour cells biology.

On one hand, we have shown that SEMA3F has an anti-tumour effect *in vivo* increasing quiescence markers expression and inducing a switch in primary tumours behaviour to a more dormant phenotype. We have also shown that it diminishes cell dissemination to secondary organs, which makes SEMA3F a potential good prognosis factor in BrCa and HNSCC. On the other hand, our results suggest that PLXNA2 inhibits tumour growth as well as prevents cell migration and invasion while it might modulate cell stemness. Moreover, we have also found that PLXNA3 might restrain tumour growth in oestrogen receptor (ER)-positive breast tumours and that the oestrogen signalling up-regulates PLXNA3 expression, associating PLXNA3 with longer dormancy periods of ER-positive breast tumours.

Finally, we have mainly focused on deciphering the role of NRP2 in regulating DTCs biology and lung metastases. Here, we have shown that NRP2 positively regulates BrCa and HNSCC cells proliferation, adhesion, migration, invasion and survival *in vitro* and *in vivo*. NRP2 deletion clearly inhibits tumour growth *in vivo* as well as decreases the number and size of lung metastases. Moreover, NRP2 is essential for lung DTCs proliferative phenotype, hence promoting lung metastases growth *in vivo*. Highlighting the role of the microenvironment, we have shown that the lung microenvironment up-regulates NRP2 expression partly by macrophages and fibroblasts-derived TGFβ1. Altogether, this thesis contributes to a better understanding of DTCs biology describing TGFβ1-NRP2 axis as a dormancy inhibitor pathway, promoting DTCs re-awakening and lung metastases development. The negative correlation of NRP2 expression with metastasis free survival in BrCa and HNSCC patients' and our results emphasizing the metastatic role of NRP2, suggest that NRP2 could be a bad prognosis biomarker and a good target to design new drugs against metastasis.

Resum

Les metàstasis, principal causa de mortalitat associada a tumors sòlids que provoquen la mort de més del 90% dels pacients, no disposen d'un tractament efectiu. Les metàstasis deriven de cèl·lules tumorals disseminades (CTDs) que escapen del tumor primari i, després d'un període d'adaptació al nou microambient, proliferen donant lloc a la metàstasi. Durant aquest període d'adaptació, les CTDs entren en un estat de latència que es caracteritza per una parada del cicle cel·lular, fet que les fa invisibles davant de les teràpies actuals. Mitjançant mecanismes parcialment desconeguts, les CTDs es reactiven i proliferen generant la metàstasi. Per tant, és imprescindible millorar el coneixement sobre la biologia de les CTDs per fer front a un dels principals problemes de l'oncologia clínica actual. Per tal que es generi una metàstasi, es requereix la supervivència de les CTDs tant en circulació com al nou microambient que colonitzaran. Tenint tot això en compte, proposem que el microambient tumoral influencia el fenotip i la supervivència de les CTDs, regulant així la formació de metàstasis.

Aquesta tesi ha tingut com a objectiu l'estudi de la influència de factors neuronals en el desenvolupament del tumor i la metàstasi als càncers de mama i de cap i coll. Concretament, hem estudiat el paper de la Neuropilina 2 (NRP2) en la regulació de la biologia i supervivència de les CTDs, així com en la modulació del microambient tumoral, afavorint la formació de metàstasis. Així mateix, hem analitzat l'efecte i la contribució de les semaforines de classe 3 (SEMA3s) i els seus receptors, les plexines (PLXNs), als càncers de mama i de cap i coll.

D'una banda, hem posat de manifest la funció anti-tumoral de la SEMA3F en augmentar l'expressió de marcadors de latència, a més de reduir la disseminació tumoral i d'induir fenotips menys proliferatius a les CTDs *in vivo*. D'altra banda, els nostres resultats suggereixen que la PLXNA2 semblaria inhibir el creixement de tumors de mama receptor d'estrogen (ER)-negatius, disminuint la migració i invasió cel·lular. Altrament, l'expressió de la PLXNA3 està regulada per la via dels estròGens, associant la seva expressió als períodes de latència més perllongats en tumors de mama ER-positius. Finalment, el nostre estudi s'ha centrat a determinar la funció de la NRP2 a les CTDs i al desenvolupament de metàstasis al pulmó. En concret, hem demostrat la relació de l'expressió de NRP2 amb una major proliferació, adhesió, migració, invasió i supervivència cel·lular *in vitro* i *in vivo*. En concordança, hem mostrat que la inhibició de NRP2 redueix tant el creixement del tumor primari com la formació de metàstasis als pulmons *in vivo*. Finalment, destacant el paper del microambient tumoral als pulmons, hem vist que el TGFβ1 secretat pels macròfags i fibroblasts pulmonars augmenta l'expressió de NRP2 a les cèl·lules tumorals.

En definitiva, aquesta tesi contribueix a un major coneixement de les CTDs descrivint l'eix TGFβ1-NRP2 com a inhibidor de la latència cel·lular i promotor de les metàstasis pulmonars. Tenint en compte la correlació de l'expressió de NRP2 en pacients de càncer de mama i de cap i coll amb una major incidència de metàstasis, definim la NRP2 com a marcador de mala prognosi contra la qual generar possibles noves eines terapèutiques per a millorar els tractaments de la malaltia metastàtica.

Introduction

1.1. Breast cancer

1.1.1. Breast anatomy and development

The breast, also referred as mammary gland, is a bilateral organ present in mammals including humans. Each mammary gland contains different types of tissues that give rise to a highly modified and specialized sweat gland. The mammary gland is formed by a glandular system composed of 15-20 lobes each of them subdivided in smaller lobes called lobules, which produce milk in adult females, and ducts which collect the milk and conduct it to the nipple. Lobes and ducts are surrounded by fibrotic and connective tissue while everything is surrounded by adipose tissue that, together with the fibrotic and connective tissue, forms the mammary gland stroma (**fig. 1**). Although the mammary glands do not contain muscles, muscles around the mammary gland hold the structure to the chest wall[1]. Both females and males have identical mammary gland architecture, but male's mammary gland lack the lactiferous function of this organ.

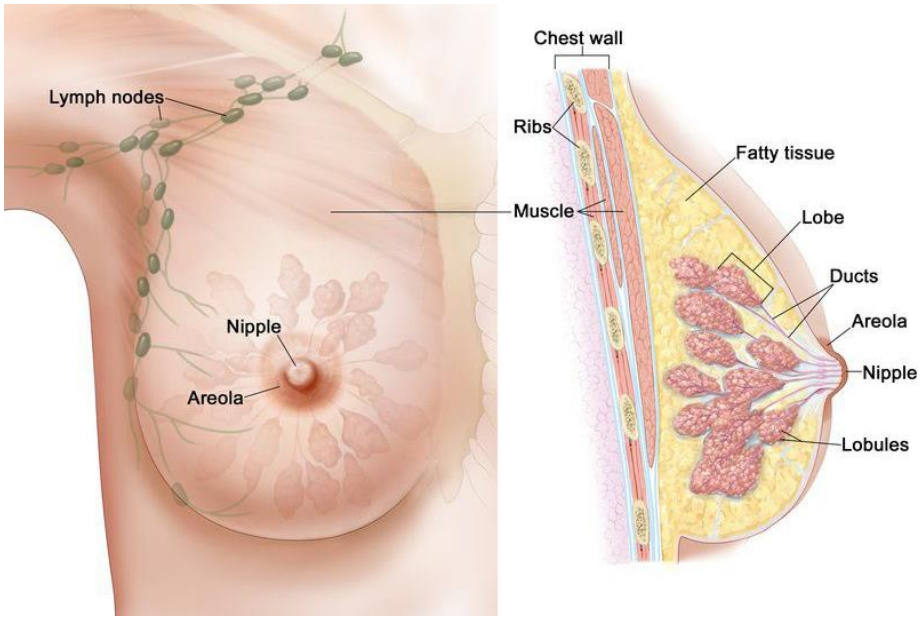

Figure 1. Anatomy of the female breast. Mammary glands are composed of several groups of lobules called lobes, connected with the nipple by ducts. Surrounding fatty and connective tissue complete breast stroma. Several lymph nodes are located within the tissue and nearby. Adapted from National Breast Cancer Foundation (NBCF).

Mammary glands are developed from very early stages in embryos and they suffer a complex process to achieve their total development through prenatal and postnatal stages. The ectoderm is responsible for the formation of lobes and ducts whereas the stroma develops from the mesenchyme[2]. Although the normal mammary gland remains quiescent during the first decade, the pubertal period is a greater impulse and the mammary gland reaches its mature structure with the biggest tissue modulation. Parenchymal changes involve duct branching and functional but no secretory lobe formation. Stromal changes consist on fibrous and fatty tissue enlargement, which occur prior to parenchymal changes[2,3]. Mammary gland changes during puberty are influenced by sex hormones, in particular oestrogen and progesterone[4,5]. The last developmental stage comes during pregnancy where the secretion of progesterone and peptidic hormones such as prolactin promotes the proliferation of ducts and the development of the secretory acini to allow lactation for new-born

feeding. During the weaning phase, there is an involution process of the mammary gland where it returns to the initial phenotype through tissue remodelling[3]. Apart from sex and peptidic hormones, diverse systemic endocrine signals and genes involved in developmental processes such as homeobox genes regulate branching morphogenesis. Dysregulation in the expression or function of any of these components might cause poor cell differentiation or uncontrolled cell proliferation increasing cancer risk[3,6].

1.1.2. Epidemiology and prognosis

Cancer is the first leading cause of death worldwide and its incidence and mortality are rapidly growing due to the population ageing[7]. According to the most recent data based on GLOBOCAN 2020, an estimated 19.3 million people would be diagnosed of cancer (incidence) and 9.9 million people would die from cancer (mortality) in 2020 [8]. Breast cancer (BrCa) is the most commonly diagnosed cancer among females (2.3 million new cases) and the main leading cause of cancer death (685.000 new cases), followed by colorectal and lung cancer (**fig. 2**). There is no association between geographical or socio-economic development with BrCa incidence rate. However, incidence increases in both developed or in transition countries as well as in different ethnical populations[8].

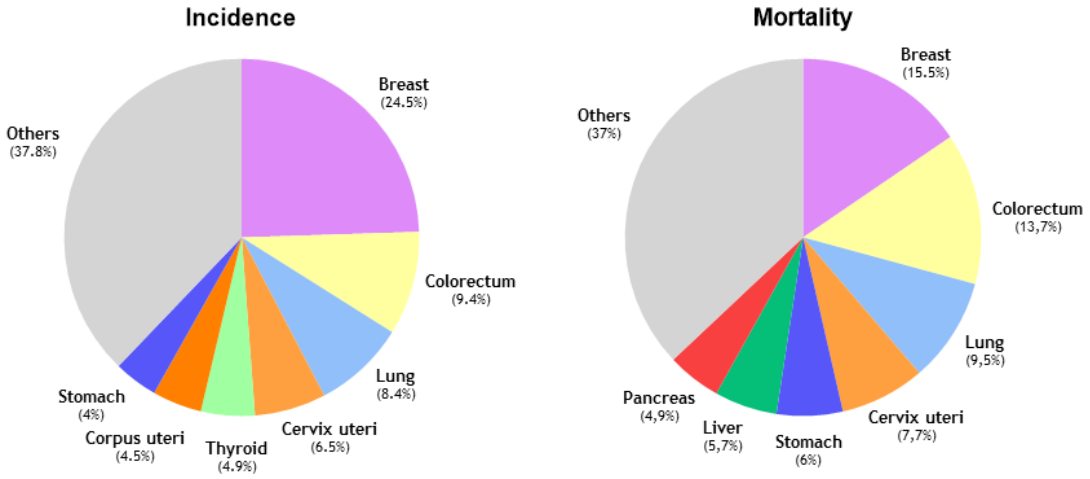

Figure 2. Distribution of cancer incidence and mortality in females worldwide in 2020. Adapted from Globocan (2020)[8].

Concerning cancer incidence and mortality in Europe, BrCa is the most commonly diagnosed cancer among European females with 25.8% incidence, significantly beyond the second and third cancer types (colorectal and lung, respectively). In terms of mortality, BrCa is the first leading cause (16.3%) followed by lung (14.3%) and colorectal (13%) cancer[9]. The International Agency for Research on Cancer and the European Cancer Information System reports in 2020 agreed on the number of more than 34.000 diagnoses of BrCa patients in Spain, representing the 28.7% of new diagnosed female cancer cases. BrCa is the second leading cause of cancer death in Spain (14.6%), behind colorectal cancer (15.1%)[8,9].

Early detection, correct diagnosis and better treatments have greatly improved global cancer average survival[10]. However, around 20-30% of diagnosed cancers could be prevented as well as its survival improved by avoiding risk factors (tobacco, infectious agents, alcohol, unhealthy diet and physical inactivity) and implementing existing prevention and treatment strategies worldwide[8,11]. Nevertheless, the five-year survival rate of BrCa is higher than other cancer types, with more than an

80% in most of the countries[12]. Spain has a rate of 84.7% of five-year survival, being higher than the European average (83.2%)[9]. Cancer survival is closely related with the stage of the disease at the time of diagnosis. Thus, the five-year survival rate of metastatic BrCa dramatically decreases close to 30% when it is diagnosed as a distant disease[7], reflecting a lack in effective metastatic cancer clinical management.

1.1.3. BrCa origin and evolution

Despite all the advances of the last decades, the morbidity and mortality associated with BrCa still makes crucial the development of more effective treatments. Nevertheless, the complexity and heterogeneity of BrCa makes the improvement of existing therapies and the experimentation of new approaches to counteract the disease an arduous task.

Tumour heterogeneity is one of the hallmarks of cancer described by Hanahan and Weinberg in 2011 [13]. On one hand, breast tumours can be different among different individuals (inter-tumour heterogeneity) either at clinical, histopathological and/or molecular level[14,15]. Due to a large gene expression profiling breast tumours can be classified in several independent groups (described in *Introduction, section 1.1.4*), each of them with their own gene expression pattern and associated clinical outcomes[14–16]. On the other hand, breast tumours are composed of different cell populations within the same tumour (intra-tumour heterogeneity). These cells can differ either at the genetic and epigenetic level or in their phenotype and functional characteristics[15–17], making more complex the study of tumour biology and cancer initiation and progression.

Actually, at the cellular level, there are two different theories to explain the establishment and maintenance of tumour heterogeneity as well as cancer initiation: the cancer stem cell hypothesis and the clonal evolution model (**fig. 3**). Both theories agree on the acquisition of mutations in a single cell as the origin of a tumour even though they differ in the cell of origin where the mutations are originated[16–18]. However, these two models might not be mutually exclusive but complementary. Moreover, the tumour microenvironment must be also considered as contributor to tumour heterogeneity (described in *Introduction, section 1.3*). The **cancer stem cell hypothesis** postulates that only a small portion of cells present in the mammary tissue are aberrantly mutated, becoming tumour initiating cells. These particular subsets of cells, known as BrCa stem cells, are considered the cell diversity and cell hierarchy modulators in a tumour (**fig. 3A**)[16–18]. By definition, cancer stem cells (CSCs) are a small group of cells present in tumours with self-renewal capacity and differentiation potential which confers them the ability to generate an heterogeneous lineage of cancer cells[19]. In addition, they are thought to be not only responsible for tumorigenesis due to its pluripotency and plasticity but also for recurrence and metastasis[20]. Mutations during the division of these cells will give rise to wide phenotypes of cells that all together will lead to the formation of a heterogeneous tumour. Nevertheless, a CSC does not always have to be the cell of origin or tumour initiating cell. According to the **clonal evolution model,** the accumulation of mutations (genomic instability) occurs in already differentiated epithelial cells and only those acquiring new potentially advantageous mutations will survive (clonal selection) (**fig. 3B**)[16–18,20]. This model does not rely on a hierarchical model but on a stochastic model with a natural or Darwinian selection of the “best prepared” cell able to survive the selection pressure. Any tumour cell will acquire different mutations when dividing that will accumulate over time. Some of these random mutations can be damaging, useless or positive conferring cells a biological advance. The genetic mutations promoting cell proliferation and tumour progression are known as driver-mutations. These are usually accompanied by passenger-mutations that confer no

selective advantages under selective pressure[17]. The combination of cell subpopulations with several common and unique genetic aberrations is the one determining tumour heterogeneity. Therefore, in line with this model, any of the cells present in the tumour will have self-renewal capacity, metastasis initiating capacity and therapeutic resistance[16,17]. Since the CSC hypothesis and the clonal evolution model may complement each other, BrCa heterogeneity may be determined by the differentiation state of tumour initiating cells, by the dynamic phenotype of the cells present in the mammary gland and by the genetic aberrations acquired[15].

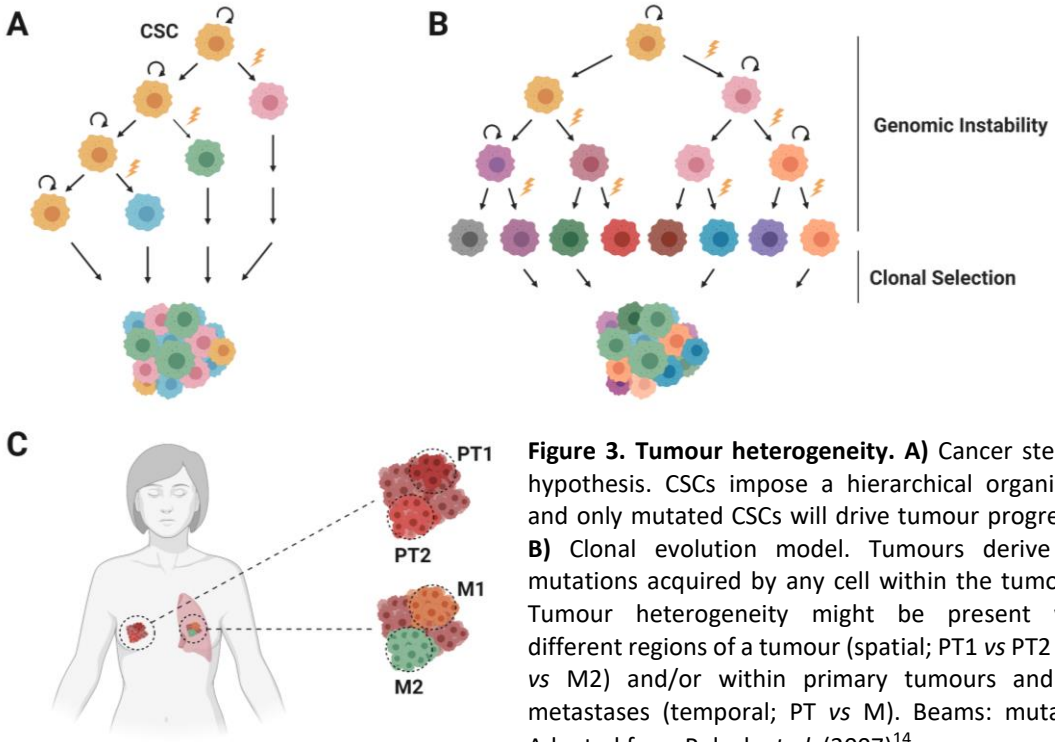

Figure 3. Tumour heterogeneity. A) Cancer stem cell hypothesis. CSCs impose a hierarchical organization and only mutated CSCs will drive tumour progression. **B)** Clonal evolution model. Tumours derive from mutations acquired by any cell within the tumour. **C)** Tumour heterogeneity might be present within different regions of a tumour (spatial; PT1 *vs* PT2 or M1 *vs* M2) and/or within primary tumours and their metastases (temporal; PT *vs* M). Beams: mutations. Adapted from Polyak *et al.* (2007)[14].

Although most of the tumour cells are thought to have a clonal origin, diversity within tumour cells phenotypes can be found between primary tumours (PT) and their metastases (M). Studies of tumour heterogeneity at the genomic level have described the existence of populations of cancer cells across different regions within a tumour (spatial heterogeneity) as well as in a tumour at different time points, including PT and its relapses (temporal heterogeneity) (**fig. 3C**)[21,22]. Tumours evolve in a branching model rather than in a linear model generating different subclonal populations. Therefore, the aberration spectra of cancer cells generate wide genomic landscapes, which may vary within the same patient. Typically, more abundant than monogenomic tumours, polygenomic tumours refer to tumours with multiple genetically different subpopulations. This results in spatial or histological heterogeneity where morphologically distinct areas with different genetic aberrations are present within a single tumour[17]. Moreover, clonal diversity can be detected as cancer progresses through time with synchronous or metachronous metastases. In synchronous metastases, metastases share most of the somatic genetic aberrations with the PT whereas metachronous metastases markedly differ from the initial tumour[22]. The tumour microenvironment and/or treatments exert pressure over metastases and might have an influence on driving that variability. With all, heterogeneity and its dynamism need to be considered to avoid as much as possible the tumour-sampling bias. Most of the therapeutic decisions are based on a single biopsy of the PT, which might be effective if the genetic alterations are common in all tumour subclones. However, the changing dynamics of tumour subclones over space

and time may result in diverse molecular profiles unresponsive or resistant to actual therapies[21]. Multiple biopsies of a tumour as well as of the metastases would be more appropriate to better fight the neoplasia, even though such invasive methods are far from being implemented in the clinic.

1.1.4. BrCa classification

BrCa is a heterogeneous disease in terms of molecular alterations, cellular composition and clinical outcome. As mentioned in *Introduction, section 1.1.3*, BrCa heterogeneity is not only defined by spatial and temporal intra-tumour heterogeneity but also by inter-tumour heterogeneity[15]. The discovery of the existence of different BrCa subtypes in patients unveiled the necessity of developing specific therapies for each, reaching almost individualized treatments. In the following section, currently used classification systems based on intrinsic breast tumours will be discussed.

Several hypotheses have been proposed to explain the inter-tumour heterogeneity in BrCa, including subtype-specific cell of origin and subtype-specific transforming event. The mammary gland is a dynamic tissue and, according to the CSC hypothesis, hierarchically organised[17,18]. The lineage-restricted basal and luminal progenitors derive from undifferentiated and pluripotent oestrogen receptor (ER)-negative mammary stem cells (SC) (**fig. 4A**)[14,23]. Therefore, in accordance with the **subtype-specific cell of origin** model, different subtypes of BrCa would derive from the same cell of origin which will divide, differentiate and evolve to one subtype or the other, carrying with it specific genetic and epigenetic alterations (**fig. 4A**)[14,23,24]. Conversely, the **subtype-specific transforming event** model claims that the malignant transformation of a differentiated subpopulation of mammary epithelial cells is the origin of basal and luminal subtypes of BrCa[23]. Based on the molecular similarities between normal and cancer cells, basal-like tumours would come from the transformation of basal-like mammary epithelial cells whereas luminal tumours would originate from the transformation of luminal epithelial cells (**fig. 4B**). However, gene expression analyses have demonstrated that not all BrCa subtypes have the same molecular pattern[25,26] and that some basal-like tumours might also come from luminal progenitors[27]. Consequently, there might be multiple ways to develop each tumour subtype and as with intra-tumour heterogeneity, inter-tumour heterogeneity may be explained by a combination of both models.

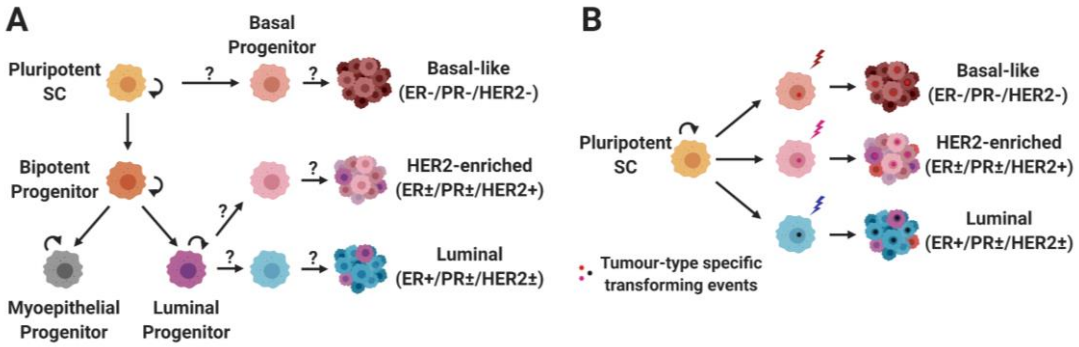

Figure 4. Hypothetical models explaining breast cancer subtypes origin. According to the cell of origin model (**A**), each tumour subtype derives from a different cell type while the subtype-specific transforming event model (**B**) designates cells acquired specific mutations as tumour subtypes determination. Adapted from Polyak *et al.* (2007)[14].

In the last decades, there have been significant advances in our understanding and classification of BrCa, some of which have been incorporated into the worldwide clinical oncologist recommendations

with important implications in diagnosis and treatment. In the next sections, the most relevant clinical criteria for BrCa classification will be discussed.

1.1.4.1. Histopathological classification

The histological classification has been the basis of the World Health Organization (WHO) for breast tumours classification for a long time[28]. It considers tumour morphology and structural organization as mainstays for tumour stratification[15]. Depending on the transformed cell, the type of BrCa will be classified into two broad groups: carcinomas, when the affected cells come from the epithelial components of the breast and sarcomas, when the stromal component of the breast is altered. Although different types of cells exist within the mammary tissue, most BrCa arise from the epithelial compartment and thus are carcinomas[29,30]. There are several tumour subtypes among breast carcinomas based on their invasiveness, which will have different treatment and prognosis implications.

1.1.4.1.1. Non-invasive BrCa

Non-invasive or *in situ* BrCa comes from the proliferation of malignant ductal or lobular epithelial cells[29,31]. Due to the total integrity of the basement membrane, there is no stromal invasion and thus the tumours are considered localized. The main characteristic that defines the non-invasive BrCa is the presence of the myoepithelial cell layer surrounding the neoplastic proliferation[28,31]. However, a reduction in myoepithelial cell number or in its integrity may be observed in some non-invasive carcinomas[30]. In the second edition of BrCa classification, the WHO introduced two new subtypes of *in situ* BrCa based on the transformed luminal epithelial cells. With this, ductal carcinoma *in situ* (DCIS) and lobular carcinoma *in situ* (LCIS) were segregated[28]. Of all the *in situ* reported BrCa an 80% are DCIS[32]. **LCIS** is an aberrant proliferation of malignant lobular epithelial cells commonly diagnosed in pre-menopausal women [31]. It is associated with an increase in the risk of developing invasive diseases[31] and although it is not mandatory, LCIS becomes invasive in 25-35% of cases[30]. **DCIS** comes from the proliferation of malignant ductal epithelial cells and is one of the most common types of BrCa[29]. DCIS is an heterogeneous group of pre-malignant diseases, mainly asymptomatic and usually diagnosed after mammography which increased the number of detected DCIS from 1% in 1980s to an actual incidence of 20-25% [32,33], since its widespread use as a screening technique. DCIS has a very good clinical outcome with more than 95% 10-years survival[32]. Many of the DCIS-related deaths are associated to an undetected invasive disease or to a recurrent invasive lesion[30]. Many of the DCIS will become invasive and thus DCIS is considered a precursor lesion of an invasive carcinoma. However, according to the finding of Farabegoli *et al.*, (2002) DCIS is a possible but not an obligate precursor of invasive BrCa[34].

1.1.4.1.2. Invasive BrCa

The term invasive makes reference to those breast tumours whose cells have invade the surrounding stroma spreading outside the lobules and ducts[29]. Once again, based on the mutated epithelial cell type, invasive cancers will be subdivided in invasive ductal or lobular carcinoma, both with different prognosis and treatment options. **Invasive lobular carcinoma** (ILC) refers to the aberrant proliferation and spreading of lobular epithelial cells. It affects 10-15% of women with invasive lesions[15,29,31], which are in their 60s. However, ILC incidence is associated with hormone exposure and thus it may vary depending on the cohort studied due to female exposure to hormones as well as to hormone replacement treatments[35]. On the other hand, **invasive ductal carcinoma** (IDC) is originated when ductal epithelial cells proliferate and invade local stroma[29,31]. It is the most common invasive

carcinoma with approximately 80% of women in their 50s being diagnosed[29]. However, IDC is a very heterogeneous group of invasive diseases including the more common tubular carcinoma or mucinous carcinoma as well as the less common clear cell carcinoma or sebaceous carcinoma[28,29], all with very distinctive histological and morphological phenotypes as well as with different clinical outcomes.

1.1.4.1.3. Metastatic BrCa

Diagnosis of metastatic BrCa is based on the spreading of breast tumour cells to other organs[29]. Metastatic BrCa is the most advanced stage of the tumour and it is also known as stage IV invasive BrCa. This histological type of BrCa classification is closely linked to the clinical staging, described in the next section (*Introduction, section 1.1.4.2*). As described in *Introduction, section 1.4.3*, the metastatic disease can appear long time after PT diagnosis and treatment. Metastasis causes the death of half a million people worldwide every year, having a median survival of 2-3 years in developed countries[36], depending on the subtype. Indeed, at present, metastatic BrCa cannot be cured.

Regarding to most recent studies, only 5-10% of newly diagnosed BrCa patients will be initially diagnosed with metastatic BrCa. However, it is known that approximately 35% of women diagnosed with invasive BrCa will develop metastasis[37].

1.1.4.2. Tumour stage and histological grade classification

Stage classification at diagnosis is essential for proper treatment selection and prognosis determination. The clinical stage of the tumour is assessed based on physical examination, biopsies and imaging, which inform about the extent of the disease before any treatment. On the other hand, the pathological stage of the tumour is determined after patients undergo treatment[38]. Both stages will define the TNM categories corresponding to the TNM-staging system having a meaningful impact on survival, treatment and prognosis.

The **TNM-staging system** was first used in 1943 by Pierre Denoix trying to unify the multiple staging classifications at the time and is mainly used in epithelial and solid tumours[39]. He based his categorizations in primary tumour size (T category), in the presence and dimensions of regional lymph node metastases (N category) and in the presence of distant metastases (M category)[40,41]. These categories can be differentiated into clinically (c) or pathologically (p) detected categories. Then, the size of a primary tumour (T) can be divided in tumours of 20mm or smaller (T1), tumours between 20-50mm (T2) and tumours bigger than 50mm (T3). There is an additional T subgroup referring to those tumours of any size but with direct extension to the chest wall and/or the skin (T4). The lymph node category (N) is divided in further subcategories by colonized lymph node site. It includes metastasis in movable ipsilateral lymph nodes (N1), metastasis in ipsilateral level (N2) and metastasis in ipsilateral infraclavicular, supraclavicular or ipsilateral internal lymph nodes (N3). Finally, in the distant metastasis category (M) three groups can be distinguished depending on the absence (M0) or presence (M1) of distant metastasis. When the distant metastasis cannot be determined the tumour is grouped in the MX category[42]. After clinical staging, when biomarkers analyses cannot be implemented, the T-N-M categories can be complemented with the stage I-II-III-IV categories which inform about the localization or spreading of the tumour. Stage I tumours are those confined to the organ of origin whereas stage IV tumours are widespread tumours, with distant metastatic diseases[29,39].

It is known that tumour stage does not always reflect the biology of the tumour and thus its complementation with the grade classification system is required for proper treatment and prognosis prediction. **Histological tumour grade** is a classification method based on the degree of differentiation

of cancer cells within a tumour. It is a cost-effective and semi-quantitative evaluation of morphological features that gives robust prognostic information[43]. The most used grading system is the modified Nottingham Grading System. It has been incorporated in algorithms and guidelines for determining the use of adjuvant chemotherapy[43]. According to the 8th edition of the American and international Committees on cancer manuals[42], tumour histological grade (G) analyses three morphological features of the breast. It studies the degree of tubule or gland formation, the nuclear pleomorphism and the mitotic count giving a score from 1 (favourable) to 3 (unfavourable) for each feature. The total value of the three categories together will determine the total score that will classify the tumour in GX (grade cannot be assessed), G1 (score of 3-5; low histologic grade), G2 (score of 6-7; intermediate histologic grade) or G3 (score of 8-9; high histologic grade). However, the Nottingham Grading System is only used for invasive BrCa while for DCIS nuclear grade is used, where GX (grade cannot be assessed), G1 (low nuclear grade), G2 (intermediate nuclear grade) and G3 (high nuclear grade) are differentiated. Altogether, the histological grade can predict tumour behaviour and correlates with the clinical outcome[43,44]. Low grade tumours have better clinical outcome and have non to few metastatic events whereas tumours classified as grade 3 have a poorer prognosis and higher risk of developing metastasis. Histological grading of a tumour is well settled for early-stage BrCa, considered as local tumours or tumours only spread to the axillary lymph nodes, providing crucial information about therapy options and prognosis, both improving clinical outcomes. In more advanced and invasive breast tumours, histologic grade does not contribute to predict prognosis and survival. Nevertheless, Schwartz and colleagues (2014) demonstrated that histologic grade is still informative in highly-invasive breast tumours despite tumour size and nodal invasion status[45].

1.1.4.3. Classification by biomarkers

Testing of classical tumour biomarkers by immunohistochemistry (IHC) techniques is recognized by international guidelines and it is routinely performed in patients in pre-surgical biopsies[46]. Nevertheless, the number of clinically used biomarkers is extremely low despite the technological progression and the increasing number of emerging biomarkers. Variations in technical factors such as sample preparation or inter-laboratory agreement for antibody type, inaccurate experimental design and inappropriate statistical data analysis contribute to discordance and lack of validated biomarkers[47].

Clinical classical subtyping of BrCa analyses the expression of hormone receptors (ER, PR -progesterone receptor-), human epidermal growth factor receptor 2 (HER2) and the proliferation protein Ki67. The expression of other factors such as cytokeratins may also be important for clinical classification[48]. ER is expressed in 70-75% of BrCa and is related with good prognosis. In addition, it is predictive of hormone therapy response with 30-40% of patients responding positively[46]. The staining intensity and the percentage of ER-positive cells might vary between and within samples but a consensus of more than 1% of positive nuclei was established as the cut-off to define an ER-positive tumour[46–48]. PR expression is also analysed through IHC staining and as for ER, PR-positive tumours are those with more than 1% of positive nuclei. PR is expressed in approximately 60-70% of breast tumours and being regulated by ER, the correlation between ER and PR expression is good. However, around 10% of samples will be ER+/PR- being more aggressive than the ER+/PR+ tumours while less than 5% will be ER-/PR+, having a similar prognosis to ER+/PR+ tumours[46]. HER2 is a transmembrane tyrosine-kinase receptor (RTK) and regarding guidelines recommendations, a HER2-positive sample requires more than 10% of cells with strong and circumferential staining. HER2-negative tumours will be either those with less than 10% of cells with incomplete membrane staining or those with more than 10% of cells with weak membrane staining[49]. HER2-enriched subtypes are characterized by the amplification

of the *HER2/neu* oncogene and thus gene amplification assays like fluorescence *in situ* hybridization (FISH) might be used for proper analysis. Although gene amplification occurs prior to protein over-expression, HER2 over-expression occurs in 95% of the cases being the IHC the most clinically used technique for HER2 status evaluation[48]. HER2 is a prognostic biomarker correlated with tumour aggressiveness but also a predictive marker related to targeted molecular therapies. Therefore, is important to identify patients with HER2-positive tumours since they will positively respond to anti-HER2 treatments such as pertuzumab, trastuzumab, trastuzumab emtansine or lapatinib[46–48,50].

The differential expression of biomarkers between tumours provides complementary information about tumour heterogeneity and complements the basis for BrCa classification. Unfortunately, intra-tumour heterogeneity also plays a determinant role in the classification by biomarkers expression since they can be represented non-homogeneously within a tumour. Some studies have tabulated how powerful intra-tumour heterogeneity is since 35-56% of the samples analysed were misclassified due to spatial heterogeneity, which was observed in 2% of the cases for ER, 7% for PR and 8% for HER2 [51].

1.1.4.4. Molecular classification

Due to high screening techniques developed during the last years, gene expression profiling has leaded the way of the arduous task of BrCa molecular classification. With that aim, in the 2000s, by microarray-based gene expression analysis and unbiased hierarchical clustering five molecular subtypes (also referred as intrinsic subtypes) were defined based on the variation in gene expression patterns[25,26]: luminal A, luminal B, HER2-enriched, basal-like and normal breast-like. Later, a new molecular subtype was identified, referred to as claudin-low (**fig. 5**)[52,53]. These molecular subtypes of BrCa have different prediction of survival[25,26,53,54] as well as differ in treatment response[53,54]. Diagnosis by intrinsic subtypes helps in prognosis and prediction of clinical responses but a complete diagnosis based on molecular alterations, cellular composition and clinical outcome might be required for trying to be as close to the reality as possible.

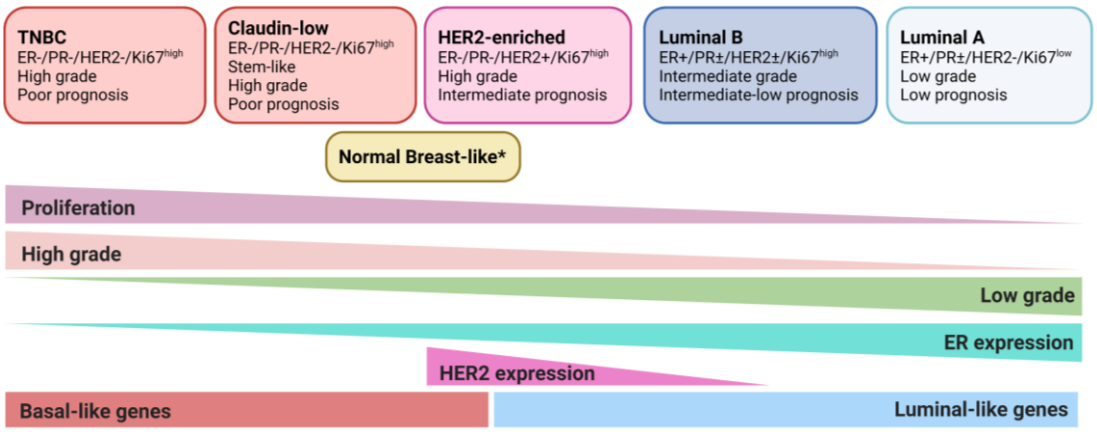

Figure 5. Intrinsic breast cancer subtypes. Triple-negative breast cancer (TNBC), claudin-low, HER2-enriched, luminal B and luminal A subtypes are classified based on their genetic expression pattern and on the histology/immunohistochemistry expression of ER, PR, HER2 and the proliferation marker Ki67. Each subtype has different characteristics and clinical outcome. * means not well established. Adapted from Harbeck *et al.* (2019)[57].

The luminal cluster has relative high expression of many genes expressed by the mammary luminal cells and are defined as ER-positive cells[25,26]. Deeper analysis demonstrated that within the luminal

cluster there were two different subtypes. Based on Ki67 level, ER expressing tumours can be differentiated in luminal A (<14%, Ki67^{low}) or luminal B (>20%, Ki67^{high})[55,56]. **Luminal A** is an ER-positive and/or PR-positive subtype with tumours negative for HER2. Luminal A is the most common BrCa with 30-40% of incidence and it is considered a low-grade tumour, being the intrinsic subtype with better survival. **Luminal B**, accounting up to 20% of diagnosed breast tumours, is an ER-positive and/or PR-positive subtype that can include HER2-positive or HER2-negative tumours on it. Hence, luminal B tumours grow faster than luminal A tumours having worse prognosis[48,57]. **HER2-enriched** subtype is determined by the amplification of *ErbB2* or *HER2/neu* oncogene and a specific subset of genes associated with it but not with the expression of luminal or basal-cluster genes[25]. It is less frequent than luminal tumours accounting for 12% to 20% and is defined by ER and PR-negative and Ki67-high. They are aggressive tumours leading to an intermediate prognosis. However, HER2-targeted therapies such as trastuzumab and lapatinib have improved patients outcome[47,48]. Conversely, the basal-like hierarchical group has relative high expression of genes expressed in mammary basal cells[25,26]. The basal-like cluster comprises intrinsic subtypes characterized by low to absent hormone receptors (ER and PR) and no luminal gene expression[26]. Among basal-like subtype, **triple negative BrCa** (TNBC) is the most frequent subtype and it has low to absent expression of hormone receptors (ER-/PR-) and HER2 gene cluster (HER2-). It is less frequent than luminal tumours representing 15-20% of breast tumours. TNBC tumours are Ki67-high and are classified as high grade being the most aggressive BrCa with the worst prognosis[48,57]. However, the basal-like cluster is a morphologically, genetically and clinically heterogeneous category so it includes additional subtypes. **Claudin-low** tumours are ER-/PR-/HER2- as TNBC tumours but they are enriched in epithelial-to-mesenchymal transition features, immune system responses and stem cell-associated biological processes. Clinically, they are considered highly metaplastic and high grade, both making claudin-low poor prognosis tumours[53]. **Normal breast-like** subtype is typified by the high expression of basal-like cluster and many genes expressed in adipose and non-epithelial cells as well as by the low expression of luminal-cluster cells[25,26]. Pathological studies show less than 50% of tumour cellularity in this subtype[52] which makes its survival higher than the TNBC survival[26,57] and its prognosis intermediate[54]. Small numbers of tumours are classified as normal breast-like due to its similarity to normal mammary tissue[54]. The lack of consensus makes the normal breast-like subtype not to be considered in all the molecular intrinsic classifications. In this context, molecular intrinsic subtypes are broadly defined as described below: TNBC as ER-/PR-/HER2- and Ki67^{high}, HER2-enriched as ER-/PR-/HER2+ and Ki67^{high}, luminal B as ER+/PR±/HER2± and Ki67^{high} and luminal A as ER+/PR±/HER2- and Ki67^{low} (**fig. 5**).

The definition of the molecular intrinsic subtypes based on the differential gene expression patterns among tumours provides the opportunity to use them in the clinical practice. Due to the high cost of the microarray analyses, there is a standardized method of classification termed PAM50 (Prediction Analysis of Microarray of 50 genes). The expression of 50 genes is studied through classic techniques such as the quantitative reverse transcriptase polymerase chain reaction being able to effectively contribute to distinguishing the different molecular subtypes. This analysis complements prognostic and predictive values obtained from the clinical variables (pathologic stage, tumour grade and clinical markers expression)[54].

1.1.5. BrCa diagnosis

The incidence of BrCa in developed countries increases every year while the mortality decreases in numbers, mainly due to more effective treatments and more accurate and earlier diagnosis.

Screening analyses aim for malignant diseases detection early in their progression, before symptoms appear, by checking patients' body. Complete BrCa diagnosis is based on a triple test comprising clinical examination, imaging and a needle biopsy[57]. First suspicious come from a breast self-examination or clinical breast exam, which were first implemented in 1960s when image screening was not yet available[58]. They do not reduce mortality but help in early detection of BrCa. The best implemented screening strategy in developed countries is the **mammography,** which reduces BrCa mortality a 28% [58–60]. Being a cost-effective and reproducible prevention method, mammography is performed in symptomatic or high-risk women population younger than 40 or in women older than 40 for mortality and morbidity reduction. While reliable, it has several limitations identifying tumours without a clear mass (ex.: ILC), without calcifications or in dense breasts[59]. Therefore, the sensitivity of mammography is estimated to be between 70-90%, being lower in younger women with highly dense breasts[58,59]. Another recent method for screening is the **digital breast tomosynthesis**, also known as three dimensions (3D) mammography since it provides a 3D image of the breast. Digital breast tomosynthesis improves image and results interpretation and in combination with 2D mammography, the sensitivity increases 33-53% and the false-positives are reduced in 30-40% [61].

Within high-risk women population, the use of more sensitive and accurate screening methods is recommended. **Ultrasonography,** whose intermediate-high sensitivity (81.7%) and specificity (88%) as well as its high resolution make it a good choice for high-risk women and mammographic suspicious patients[59]. In addition, it is recommended for women younger than 30 and lactating or pregnant women[57,59]. For some women, **magnetic resonance imaging** (MRI) is also recommended giving a 3D breast image and contributing with a higher sensitivity (90%). Nevertheless, its specificity is low-intermediate (72%) having weaknesses in discriminating between malignant and benign lesions. Both sensitivity and specificity increase when combining with other screening methods[59,62]. Although MRI has been demonstrated to be the highest sensitive screening method, its use is restricted to patients in high-risk due to its high cost[62]. Even though mammography is the gold standard screening method, its limitations require for new and improved detection methods. In this sense, **microwave breast imaging** offers a rapid and cost-effective breast imaging based on the differences in dielectric properties of tissues[59]. Although further studies are required for its validation, this non-ionizing, non-invasive and painless method seems to be a true alternative for mammographic analyses in the future.

1.1.6. BrCa therapeutic approaches

While total breast surgery was the only treatment for BrCa patients in the beginning, improvements in surgical methods and new and targeted therapies development have lessened mortality lower than estimated based on BrCa incidence and increase patient's treatment options[7].

BrCa has two main molecular targets, ER and HER2, which have been successfully therapeutically used improving patients' prognosis and survival. Therefore, luminal and HER2-enriched subtypes can benefit from hormone therapy and HER2-targeted therapy, respectively, while TNBC is only treated by chemotherapy[63].

1.1.6.1. Early BrCa treatment

Early BrCa are defined as cancers that have not developed metastasis so treatments are used to eradicate the PT and loco-regional lymph nodes lesions as well as to prevent metastatic recurrence. For that, **surgery** is first applied in order to remove the tumour and excise the affected regional lymph nodes, regardless of the molecular subtype. Moreover, patients can be given systemic therapy before

(neoadjuvant) or after (adjuvant) surgery for tumour burden reduction or for therapeutic approaches, respectively. Different strategies are used as neoadjuvant or adjuvant therapies in early BrCa. As local approach, **radiation therapy** is widely used and it can be delivered to the whole or to a portion of the breast, to the chest wall or locally to the regional lymph nodes. Radiation improves the disease-free and overall survival (OS) of the patients reducing the loco-regional recurrences in approximately 75%. However, fewer benefits have been demonstrated in terms of distant metastasis[57,63]. By contrast, systemic therapies chemotherapy, hormone therapy and molecular target therapies can be used significantly reducing BrCa associated mortality. **Chemotherapy** uses cytotoxic drugs to inhibit cancer cells proliferation and growth, with many different drugs available depending on the tumour type. The main types of chemotherapy used are anthracyclines (doxorubicin), taxanes (paclitaxel, docetaxel), oxazaphosphorines (cyclophosphamide) and platinum-based drugs (cisplatin, carboplatin). They can be given alone but mostly in combinations such as docetaxel-cyclophosphamide, doxorubicin-cyclophosphamide or doxorubicin-cyclophosphamide-paclitaxel[63,64]. However, many healthy and rapidly dividing normal cells will be also affected by chemotherapy having many toxic side effects. Chemotherapy is the only effective systemic therapy for TNBC but it can also be used in other subtypes. BrCa subtypes showed different pathologic complete response to chemotherapy being the basal-like and HER2-enriched subtypes the most sensitive with 45% complete response. Conversely, luminal tumours had a complete response of 6% whereas in normal breast-like tumours no pathological complete response was observed[65]. In HER2-positive tumours, chemotherapy is combined with **HER2-targeted therapies** where antibodies targeting HER2 (trastuzumab, pertuzumab) or small-molecule tyrosine kinase inhibitors (lapatinib, neratinib) are used[63]. As neoadjuvant therapy, combinative treatment of two HER2-blocking antibodies (trastuzumab and pertuzumab) with chemotherapy is considered as standard[66]. For adjuvant therapy, chemotherapy is combined with one year of anti-HER2 treatment better than with 2 years[67]. All patients with ER-positive and/or PR-positive tumours should be treated with hormone-therapy regardless of the HER2 status. **Hormone therapy** aims to block ER activity either targeting the receptor or inhibiting aromatase activity which is involved in oestrogen synthesis. Tamoxifen is a selective ER modulator that inhibits oestrogen binding to ER[63]. Tamoxifen is used for the first 5 years as systemic standard treatment both in pre- and post-menopausal women reducing the mortality by 34% [68] and recurrence by 50% [69]. Aromatase inhibitors (anastrozole, letrozole, exemestane) decrease oestrogen circulating levels inhibiting the conversion of androgens to oestrogen[63]. They can be used in some post-menopausal women for replacing or combining tamoxifen improving the disease-free survival due to reduced distant metastasis[68]. Hormone therapy can be extended for 10 or 15 years in luminal subtypes in order to reduce recurrent disease but the benefit is small compared with the toxic side effect that it produces.

1.1.6.2. Advanced BrCa treatment

Advanced BrCa includes inoperable locally advanced tumours without dissemination to distant organs and metastatic tumours that have colonized secondary organs, such as bones, lungs and the liver. They are treatable but incurable tumours where therapies are used for relieving the symptoms and prolonging the quality-adjusted life expectancy[57,63]. Treatment strategies will differ depending in whether the metastatic disease is a *de novo* stage IV BrCa or a recurrent disease, which is more aggressive and resistant to therapies.

In general, surgery of the PT is not recommended in advanced BrCa even though palliative surgery may be done if it improves patient's quality of life. Radiation therapy as local treatment is neither recommended unless otherwise agreed for alleviating symptoms of distant metastases[57]. However,

some studies have demonstrated that local radiation might induce a systemic immune response attacking surrounding cancer cells and reducing tumour recurrence[70]. Regarding systemic treatments, different programs are approved depending on the subtype. Therefore, the assessment of the receptor status should be performed preferably in the first metastatic site, to detect whether PTs and metastases are different and thus determine the most effective treatment. For metastatic luminal tumours with ER+/HER2- molecular pattern, different approaches of hormonal therapy are used until tumours develop endocrine resistance where cyclin-dependent kinase (CDK) 4/6 inhibitors or mammalian target of rapamycin (mTOR) inhibitors (everolimus) are prescribed[57,63]. If resistance to CDK4/6 and mTOR inhibitors is developed, chemotherapy can also be used[63]. In HER2-positive tumours, regardless of ER status, the initial combination of chemotherapy and anti-HER2 agents is used even after resistance but using other approved drug combinations. More effective treatments are required for basal-like subtypes since chemotherapy is the only option. In a recent study where data from 13 studies were analysed, Li and colleagues (2019) observed that currently approved cytotoxic drugs for metastatic TNBCs were ineffective and associated with unfavourable toxicity profiles[71], highlighting the need for specific treatments for metastatic TNBC. The only treatment accepted for metastatic TNBCs is the use of atezolizumab, an immune checkpoint inhibitor against programmed death ligand-1 (PD-L1), in combination with chemotherapy that was proved to enhance anti-tumour immune response prolonging patients' progression-free survival[72].

1.2. Head and neck cancer

1.2.1. Upper aerodigestive track anatomy

Head and neck cancer comprises a very heterogeneous group of cancers that arise from the epithelial cells of the mucosal lining of the upper aerodigestive tract. The epithelial mucosal barrier, composed of the surface squamous epithelial cells and the deeper lamina propia, protects the mobile structures from the external environment it covers[73]. The vast majority of the head and neck cancers originate from the squamous epithelial cells[74], and hence are referred as head and neck squamous cell carcinomas (HNSCCs).

The upper aerodigestive tract is organized into several major sites which in turn are subdivided into various anatomic subsites (**fig. 6**). The **oral cavity** includes the buccal mucosa, lips, anterior tongue, floor of the mouth and hard palate, gingiva and retromolar trigone (small area behind the wisdom teeth in the lower jaw). The **pharynx** is composed by the nasopharynx, oropharynx and hypopharynx while the **larynx** comprises the supraglottic, glottis and subglottic larynx. The **nasal cavity** and **paranasal sinuses** include the maxillary, ethmoid, sphenoid, and frontal sinuses. The vocal folds, salivary glands, thyroid, bones and the skin and soft tissues from this anatomical region are also part of the upper aerodigestive tract. From all these anatomical sites, HNSCCs arise mainly in the tongue (13%) and mouth (11%) from the oral cavity, the pharynx (12%) and the larynx (28%)[74,75].

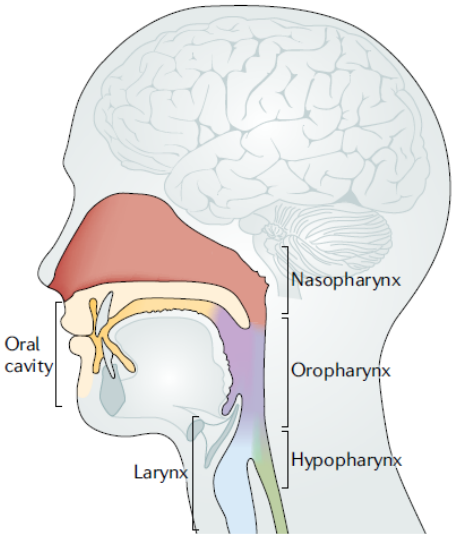

Cancer subtype	World Incidence	World Mortality
Oral cavity	354.864 (2.0)	177.384 (1.9)
Larynx	177.422 (1.0)	94.771 (1.0)
Nasopharynx	129.079 (0.7)	72.987 (0.8)
Oropharynx	92.887 (0.5)	51.005 (0.5)
Hypopharynx	80.608 (0.4)	34.984 (0.4)

Figure 6. Head and neck cancer incidence rates and mortality for worldwide patients. New cases and deaths for HNSCCs, with the percentage of each subtype combining all cancers in parentheses. Adapted from Cramer *et al.* (2019)[115].

1.2.2. Epidemiology and prognosis

According to the most recent epidemiologic data, HNSCC was the sixth most frequent cancer worldwide with approximately 1.5 million new cases diagnosed (8.3%) and 950.000 deaths (10%)[8,11,76], combining all cancers, sexes and ages. Site by site, oral cavity cancers are the most prevalent with more than 350.000 new cases followed by larynx cancers with approximately 180.000 new cases and pharynx cancers with around 300.000 new cases (counting naso-, oro- and hypopharynx together) (**fig. 6**). Regarding mortality, oral cavity accounts for more than 170.000 deaths while larynx and pharynx cancers are responsible for around 95.000 and 160.000 [76], respectively. In Europe, more than 120.000 individuals were diagnosed with head and neck cancer in 2020 whereas around 70.000 of the deaths were related to HNSCC[9]. Data from the EUROCARE-5 population-based study, where more than 250.000 head and neck cancer cases were analysed, determined that the relative survival was cancer-subtype dependent being the poorest for hypopharynx (25%) and the highest for larynx (59%) cancer. Moreover, geographical or socio-economic development seemed to be associated with survival rate since Eastern countries had 28% 5-year relative survival rate whereas developed countries had an average of 50%[77]. The Spanish 5-year relative survival was calculated to be 38.12%, slightly below the European average (39.88%)[9].

In general, males are affected more than females regardless of the tumour type with a ratio ranging from 2:1 to 4:1, either in incidence or mortality. Worldwide, Asian countries have the highest incidence and mortality rates considering all head and neck cancer types together or individually[12,76].

1.2.2.1. HNSCC aetiology

HNSCC is a multi-factorial tumour which results from a combination of genetic predisposition and environmental factors. Lifestyle habits including smoking, alcohol consumption and diet are determinants in head and neck cancers development, with 8 out of 10 cases being potentially avoidable[78]. From all the aetiological factors, tobacco and alcohol as well as virus infections are the primary risk factors associated with head and neck cancers. Prolonged exposures to tobacco and alcohol can potentially result in dysplasia or premalignant lesions in the epithelial mucosa which in the

end could develop malignant HNSCCs[79]. Therefore, the incidence of HNSCCs may be in part related to environmental and social influences more than to geographical variation.

Tobacco industry had its global expansion in the late 16th century, before which few oral cancers were reported[80]. **Tobacco** is implicated in multiple cancer types including lung and oesophagus cancers while it is the most important risk factor in HNSCCs, being directly related with oral cavity cancers. Around 20-30% of oral cancers are directly associated to any kind of tobacco[78], either cigarettes, pipe smoking or chewing tobacco. However, the association between tobacco and other HNSCCs such as nasopharynx is less clear. By using data from the International Head and Neck Cancer Epidemiology (INHANCE) Consortium, Wyss *et al.* (2013) [81] observed that smokers had around a 6-fold increase in the risk of developing HNSCC compared with non-smokers. Moreover, several studies have demonstrated that there is a time and dose-response relationship with tobacco and its associated risk of developing cancer. Studies made by the International Agency for Research on Cancer working group revealed that HNSCCs risk increased with the duration and amount of smoking, having duration a greater impact on risk[81,82]. Environmental tobacco smoke exposure is also a contributing factor. A study within 59 tobacco non-user HNSCCs patients showed that smoke exposure at home and in the workplace significantly increased the risk when compared to a control population without cancer[83].

Tobacco and alcohol are responsible for 75% of all HNSCCs cases and even though in the majority of the cases is difficult to separate the effects of smoking and alcohol alone, both independently increase the risk of cancer in the upper aerodigestive tract. **Alcohol** is a well stablished primary risk factor for HNSCCs and it is responsible for 19% of oral cavity cancers worldwide[78]. Chronic alcohol consumption increases the risk for cancer 2-3 times[84]. In addition, there is a synergistic effect between tobacco and alcohol consumption since alcohol increases the solubility of tobacco's carcinogens as well as it dehydrates cell membranes increasing their absorption by the oral mucosa[85,86].

HNSCCs were typically diagnosed in older patients due to its association with tobacco and alcohol. However, at present, it is slowly decreasing simultaneously to increasing global tobacco quitting. Nevertheless, in the last decades, the incidence is increasing among younger people in virus-associated head and neck cancers mainly because of viral infections in sexual exposures[87]. In head and neck cancers, several viruses have been implicated in carcinogenesis including human papilloma virus (HPV) and Epstein-Barr virus (EBV). **HPV** is now stablished as an independent risk factor for HNSCCs, above all for oropharynx cancer, and is closely associated with sexual behaviour. Changes in sexual practices have increased the HPV-positive oropharynx cancer incidence in young men, sexually active and non-smokers whereas the increase is not that evident for women. HPV contributes to 25-30% of oropharynx cancers and 3% of oral cancers, where HPV-16 is the most predominant subtype causing more than 90% of the HPV-positive oral cancers and more than 95% of oropharynx cancers[88]. Therefore, oral HPV infection has become a principal risk factor for HPV-positive oropharynx cancer, with more than 90% being sexually acquired[87]. Determining the HNSCCs proportion attributable to HPV infection is of considerable interest in order to potentially prevent it by HPV vaccination. Besides, HPV-positive tumours have better overall prognosis (82%) than HPV-negative tumours (57%)[89] and thus defining the HPV status is also important for HNSCC prognosis and treatment implications. HPV-16 has two viral oncogenic proteins (E6 and E7) that target *TP53* and retinoblastoma (*Rb*) tumour-suppressor genes, disrupting the cell cycle and promoting aberrant cell proliferation[90].

Herpes viruses have several immune evasion strategies and some of them are known to be oncogenic. Of them, **EBV** is the most oncogenic subtype with more than 90% of the world population infected with EBV, even though most of them asymptomatically[91]. EBV infection is associated with nasopharyngeal cancer and although considering the whole world population it is a rare disease, it is one of the most common HNSCCs in southern Asia[76] where the presence of EBV is higher[91].

1.2.3. HNSCC classification

The fact that more than 95% of head and neck cancers develop from the squamous epithelial cells of the mucosa implies that it might be a homogeneous disease. Far from this assumption, HNSCC is a very heterogeneous group of malignant diseases, each having different prognosis and treatment options. Given this circumstance, it is imperative to properly classify the tumour at diagnosis to be able to address the disease in an effective mode.

1.2.3.1. TNM staging

Due to its simplicity, TNM staging is the most accepted and used classification system for HNSCCs in the clinical practice. HNSCCs heterogeneity requires an individualized tumour staging specific to each site.

As in BrCa, HNSCCs are classified in different tumour stages based on three anatomic characteristics: primary tumour size and extent (T category), absence or presence and extent of regional lymph node spread (N category) and absence or presence of distant metastases (M category). In the last TNM staging system that came into effect in 2018 [92], the HNSCCs staging was classified as shown in **table 1**.

Stage	T category	N category	M category
I	T1-T2	N0-N1	
II	T1-T2	N2	
	T3		
III	T4		
		N3	
IV			M1

Table 1. HNSCCs staging following the last cancer staging manual published (2018). Tumours are classified based on tumour features (T category), lymph node spread (N category) and distant metastases (M category).

1.2.3.2. Genetic classification

Gene expression analyses are widely used for solid tumours classification, as we have previously described for BrCa. During the last years, gene expression arrays have been performed to molecularly classify HNSCCs in different subgroups. However, genetic HNSCCs classification has not been clinically implemented yet due to huge variations within subtypes. Only HPV status has been established as a genetic marker for HNSCCs subtype aggrupation although genetic profiling might be effective in the near future.

Analysing the gene expression patterns of 60 HNSCCs, Chung *et al.* (2004)[93] identified 4 distinct subtypes as well as patterns of gene expression that could predict lymph node metastases. The first group was the group with the worst clinical outcome and it had very high expression of a gene set related to basal-like cancers[25] such as collagens and laminins. Group 1 was also characterized by the expression of transforming growth factor alpha (TGFα) and epidermal growth factor receptor (EGFR)-pathway associated genes. Group 2 was poorly differentiated lacking epithelial gene signature (low E-Cadherin, high Vimentin) and expressing many genes produced by fibroblast and mesenchymal cells.

Group 3 comprised the normal epithelial samples and normal-like malignant samples with high cytokeratin 15 expression. Lastly, Group 4 showed an increase in gene expression induced by exposure to cigarette smoke, but it could be derived either from a specific response to smoke of those tumours or from a contaminant of smoking patients aggrupation in that group. Further genetic studies showed that HNSCCs can be diploid, although most have chromosomal instability (CIN) having simple to more complex chromosome number changes[94]. Moreover, additional subtypes of HNSCCs can be found regarding HPV infection, since HPV-positive and HPV-negative tumours have different genetic profiles. Through gene clustering, copy number profiling and HPV status, five subtypes of HNSCCs were identified (**fig. 7**)[95,96]. Three different HPV-negative subtypes could be classified depending on the number of DNA copy change events (none-low, high, very high) correlating with prognosis[97]. The two HPV-positive subtypes differed in the expression of genes implicated in keratinocyte differentiation and oxidation-reduction processes (HPV-KRT) or genes implicated in immune response and mesenchymal differentiation (HPV-IMU) (**fig. 7**)[96].

Except for HPV status, many of the studied molecular and clinical risk factors have limited clinical utility. To address this issue, The Cancer Genome Atlas (TCGA) analysed more than 270 head and neck tumour samples to determine somatic mutations specific for different subtypes[98]. In HPV-positive tumours, they observed deletion of tumour necrosis factor (TNF) receptor-associated factor 3 (*TRAF3*) which is implicated in anti-viral responses[99] as well as *E2F1* and *PIK3CA* amplification which will promote cell proliferation. Because HPV induces cellular transformation and prevent apoptosis inhibiting p53 and Rb protein[90], *TP53* and *Rb* gene mutations were rarely detected. In the vast majority of HPV-negative tumours, amplification of RTKs (*EGFR*, *HER2*) and genes implicated in cell death/nuclear factor-kappa B (NF-κB) pathways was observed while they showed deletions in tumour suppressor genes (*TP53*, *Rb*). A small subset of HPV-negative subtype was found with few copy number alterations and wild-type *TP53* which had better prognosis. On the basis of HPV status and high or low chromosome instability DNA profiles, a viable genetic classification model for HNSCCs is proposed in **figure 7**.

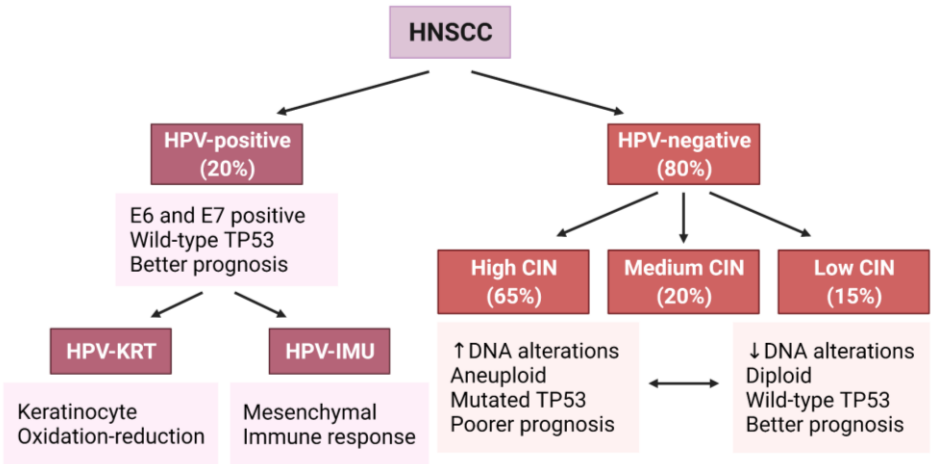

Figure 7. Overview of the genetic classification of head and neck cancers. HNSCCs can be divided in HPV-positive (left) and HPV-negative (right) subtypes. The later can be subdivided regarding cells' chromosome instability (CIN) as high, medium and low. Each of the categories has different characteristics and clinical outcome. Adapted from Leemans *et al.* (2011)[105].

1.2.4. HNSCC molecular pathogenesis

Most of the tumour progression models for HNSCCs are based on oral cavity cancer since it is the commonest diagnosed cancer. The fact that the vast majority are diagnosed at advanced stages makes difficult to assess the correct progression model from precursor lesions to invasive tumours. Nevertheless, two pathogenesis models have been proposed for HNSCCs depending on their HPV status.

1.2.4.1. Pathogenesis of HPV-negative HNSCCs

Most HNSCCs derive from transformed cells that accumulate genetic and epigenetic changes. However, some patients present macroscopically recognized precursor lesions as white or red areas of the mucosa, known as leukoplakia and erythroplakia respectively. Leukoplakia is the most common premalignant lesion, with an estimated prevalence between 1.5% and 2.5% [100]. Defined by the WHO as a "white plaque of questionable risk", leukoplasia is an off-white epithelial lesion that has features of hyperplasia that can progress and transform to invasive cancer[101]. However, not all leukoplakias end up in an invasive carcinoma mainly depending on the type, location and risk factors associated to the population of study[102]. Besides, malignant lesions can develop outside the leukoplakia or after treating and removing it[101], which means that other malignant process may be participating in HNSCCs tumorigenesis.

To develop HNSCC, the hyperplastic lesion progresses to squamous dysplasia in various stages (mild, moderate and severe) depending on the degree of the affected epithelial cells. The evolution from dysplasia to malignant and invasive tumour is mainly unknown although several studies have identified some potential tumour initiation genes. Early in disease progression, tumour suppressor *TP53* and *CDKN2A* (encoding p16, involved in Rb pathway) genes as well as *FAT1* and *NOTCH1* and the oncogene *PIK3CA* related to cell cycle, cell-cell adhesion and cell proliferation were found to be mutated[103,104]. An increased frequency of copy number alteration was also observed in high grade dysplasia than in lower grade dysplasia, correlating with higher immortalization rate and tumorigenesis[103]. From the gene expression array performed for genetic classification[98], those genes frequently mutated were also defined as tumour initiation gene candidates. Besides *TP53* and *CDKN2A*, *EGFR* and *MET* are commonly amplified and activated as well as genes from the TGFβ, Ras-MAPK (mitogen-activated protein kinase) and phosphatidylinositol 3-kinase (PI3K/PTEN/AKT) signalling pathways supporting, their role as driver genes in HNSCC[104,105]. Crucial genes involved in the regulation of disease malignancy and HNSCC development are shown in **figure 8**.

As we will describe later, the tumour microenvironment is a crucial component in the tumorigenic process of every cancer including head and neck cancers. In 1953, Slaughter *et al.*[106] first proposed the concept of field cancerization to explain the development of multiple independent PTs and locally recurrent oral cancers. His classical idea is nowadays well stablished and refers to the predisposition of the epithelium surrounding a HNSCC for developing premalignant or malignant lesions. This epithelium is macroscopically normal but might be histologically and/or genetically aberrant, with similar mutations to the PT. Found in the surgical margins after tumour excision, they can be source of the local recurrences and second PTs[105].

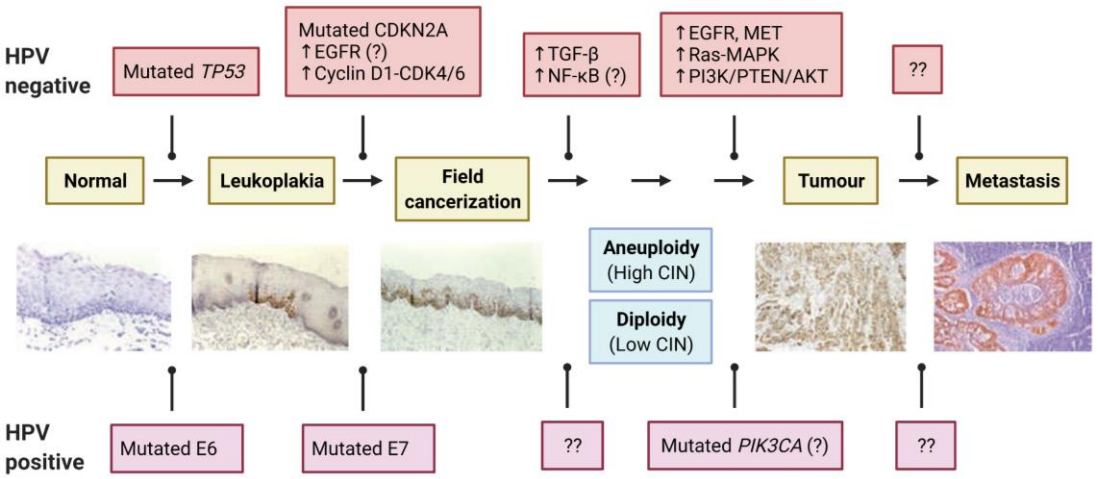

Figure 8. Model of molecular carcinogenesis for head and neck cancers. Cells acquire one (or more) genetic alterations, including mutations in *TP53* and form a precursor lesion (leukoplakia) with genetically altered daughter cells. By uncontrollable proliferation, this lesion develops into an expanding field which eventually will evolve into an invasive cancer and metastasis. Genetic mutations and signalling pathways are indicated in red (for HPV-negative; upper diagrams) or pink (for HPV-positive; lower diagrams) boxes whereas chromosome alterations are indicated in blue boxes. Adapted from Leemans *et al.* (2011)[105].

1.2.4.2. Pathogenesis of HPV-positive HNSCCs

There is now consensus that HPV-positive HNSCCs should be considered as a specific subclass of HNSCCs. However, the natural progression of HPV-induced tumours remains still unknown. Between 25-40% of the oropharynx cancers (particularly tonsillar cancers) are associated with HPV infections, mainly due to HPV-16 subtype infection[87,107]. From studies based on cervical carcinogenesis in which HPV infection has also a determinant role, a hypothetical tumorigenic model for HPV-positive HNSCCs has been defined (**fig. 8**; lower diagram). Apparently, the squamous epithelial cells from the head and neck are highly sensitive to HPV infections, which will increase the viral yield. These productive infections are more common in the epithelial cells from the oral cavity, pharynx and larynx although they seem to have a low propensity to change into a transforming infection[107]. Increasing the viral yield, a deregulation of E6 and E7 oncoproteins expression in proliferative cells will occur, which will make oropharynx and tonsillar epithelial cells become more susceptible of suffering malignant transformation[90,104]. Therefore, even though tonsil epithelial cells might be less sensitive to HPV productive infections than oral or larynx epithelial cells, they are presumed to be more susceptible to transforming infections. Most of the mutations found in HPV-negative tumours were not found in HPV-positive HNSCCs, except from the tumour suppressor *TP53* and *CDKN2A* genes and the *PIK3CA* oncogene[98,103]. Further studies are needed to determine whether tonsillar epithelial cells constitute a different cellular entity that might have high transformation susceptibility.

1.2.5. HNSCC diagnosis

Head and neck cancers have a very poor prognosis mainly because they are usually diagnosed late. Despite the recommendations for early detection, the lack of symptoms in early stages hampers early detection and management of HNSCCs. Symptoms vary regarding the anatomic site of the tumour but the commonest are swelling or leukoplakia/erytroplakia for oral cavity cancers, sore throat and dysphagia for oropharynx cancers and dysphagia and otalgia for larynx cancers. Those cancers with nonspecific symptoms are usually late diagnosed, such as nasopharynx and hypopharynx cancers, and thus have worse prognosis[108].

As for all cancers, stage and anatomical localization at diagnosis is the main prognostic factor. Hence, the initial assessment is based on a **physical examination** by palpation, mirror examination or flexible fibre optic endoscope. A **biopsy** should be performed for any suspicious lesion through a fine needle aspiration, for a sensitive and specific initial tissue diagnosis with more than 90% of accuracy[109]. To better characterize the tumour, **imaging analyses** are also recommended for all newly-diagnose patients to determine lymph node spread or distant metastases. Consequently, for detecting primary tumour sites computed tomography (CT) and MRI are mostly used while whole body CT or positron emission tomography (PET)/CT imaging systems are used for detecting regional nodal metastases as well as distant metastases and secondary tumours[110,111].

1.2.6. HNSCC treatment

HNSCC heterogeneity makes vital a multi-disciplinary treatment approach since the undertaken therapies will depend on the anatomical site and stage of the disease at diagnosis. Genetic profiling supports the decision-making process due to the significant difference in prognosis of HPV-positive and HPV-negative tumours. Organ preservation, morbidity amelioration and good quality of life maintenance are determinants when choosing the treatments to be implemented.

1.2.6.1. Early-stage HNSCC treatment

Around 30-40% of patients will be diagnosed with tumours in stage I or II whose 3-year survival rate will be in 70-90% after treatment[112]. Single modality treatment with surgery or radiotherapy is recommended for early-stage HNSCCs, both with similar survival rates. Minimally invasive surgeries are recommended in early-stage cancers to reduce morbidity where robots or lasers are used. In addition, although negative for lymph node spread (N0 category), elective neck dissection may also be performed where regional nodes from common dissemination pathways are removed. However, this approach is not well supported by data given that there was only a little improvement (12.5%) in 3 years OS after neck dissection[113]. Regarding radiotherapy, novel intensity-modulated and image-guided radiotherapies are used decreasing patient's morbidity[114]. Intensity-modulated radiotherapy allows directing high doses of radiotherapy to the tumour but not to the adjacent tissue. Several studies have demonstrated better OS and better quality of life in patients following intensity-modulated radiotherapy, having become the routine treatment for early-stage HNSCCs[112,115].

1.2.6.2. Advanced HNSCC treatment

Advanced HNSCCs refer to stage III and IV tumours which are characterized by large tumours with local invasions and/or distant metastasis or patients with recurrent diseases. Advanced tumours will be diagnosed at first in more than 60% of patients having higher risk for local relapse and metastasis, involving very poor prognosis (<50%)[114]. The main objective for advance diseases is either cure (if surgery or radiation are feasible) or palliation (if tumour is unresectable). When resectable, PTs might be surgically removed following an elective neck dissection (for N0) or a comprehensive neck dissection (for N3) where all lymph nodes are removed. Nevertheless, the standard treatment for newly diagnosed advanced diseases is concurrent chemotherapy (high-dose cisplatin as the preferred) and radiotherapy[112,115]. For resectable recurrent diseases surgery is recommended whereas in unresectable relapses chemoradiotherapy will be administered if any prior radiotherapy has been used. For metastatic diseases, palliative adjuvant therapies are recommended which may include site-specific radiotherapy and drugs such as analgesics for controlling disease dissemination effects[112,114].

In addition to surgery, chemotherapy and radiotherapy have been widely used as standard treatments for HNSCCs. However, since the 2000s, target therapies and immunotherapy have become outstanding complements for HNSCCs treatment. In 2006, the monoclonal antibody targeting EGFR, cetuximab, was first approved for its use in combination with radiotherapy. EGFR is highly mutated and activated in advanced HNSCCs[98,104,105] and thus its blockade showed a significant improvement in locoregional control and survival[116]. In 2011, cetuximab was also approved for treating recurrent or and/or metastatic HNSCCs as well as platinum-resistant recurrent or metastatic HNSCCs in combination with systemic chemotherapy[112,117]. Although mild improvements in survival rates were reported, recurrent and/or metastatic diseases become resistant after few months of treatment. In 2016, two different immunotherapeutic agents were approved for HNSCC treatment paving the way to synergistic combinative therapies. Pembrolizumab is a monoclonal antibody against PD-1 approved as a single agent for recurrent and/or metastatic HNSCC patients. It showed an overall response of 18% as well as a median duration response higher than for cetuximab[118]. Nivolumab is a monoclonal antibody against PD-1 approved for using as a single agent in recurrent and/or metastatic HNSCC patients. In comparison with standard therapy, nivolumab showed an improvement of 2 months in OS and a 20% increase in 1-year survival rate[119]. Despite the low response rate of both antibodies (<20%), the light improvements in OS increases life expectancy of a HNSCCs subtype from 5 to 9 months without following any treatment[114,115,117].

1.2.6.3. HPV-positive HNSCC treatment

Given the better prognosis of HPV-positive HNSCCs and the morbidities associated with standard therapies, determining the HPV status is often a key to decide which patients could follow a de-intensification in therapy. The aim of treatment de-intensification is to control the disease but with less toxicities[115]. Many strategies are used in the clinical practice for the treatment of HPV-positive patients depending on the HNSCC subtype, resulting in similar clinical improvements than the standard treatments.

1.3. Tumour microenvironment

Each tissue has a physical structure and an established functional anatomy sustained by many cellular, organic and inorganic elements. Cancer cells are exogenous units that may overcome different stresses enforced by the environment. Such pressures will select tumour cells with the capability of growing despite the hardships by acquiring an aggressive phenotype. Since healthy tissues ban tumour growth whereas the tumour microenvironment sustains tumour cells proliferation, it is reasonable to deduce that the microenvironment itself contains intrinsic mechanisms to regulate tumour growth and metastasis.

The tumour microenvironment (TME) is the set of cellular and extracellular components around cancer cells, which is in turn an essential supportive element for tumour growth[13]. The stroma of solid tumours is composed of tumour-infiltrating cells of two different origins. Stromal cells of haematopoietic origin comprise monocytes, neutrophils, dendritic cells and lymphocytes whereas stromal cells of non-haematopoietic origin refers to bone marrow-derived endothelial and mesenchymal progenitors as well as tissue resident fibroblasts and macrophages[120]. In addition to the cellular component, the extracellular matrix is also part of this TME. Furthermore, blood vessels, lymphatic vessels and nerves also form part of the TME and influence the fate of tumour cells[121].

1.3.1. Extracellular matrix

The extracellular matrix (ECM) is a non-cellular complex and dynamic network between cells that modulates cell function, spatial arrangement and tissue organization. It is generated during embryonic development and being specific for each tissue, plays an essential role in development and disease[122].

This proteinaceous network is composed of more than 300 proteins. **Collagens** are the main structural proteins of the ECM and can be classified as fibrillary (collagens I-III, V and XI) and non-fibrillary, both providing tensile arrangement. **Proteoglycans** are located interspersed with collagens, filling the interstitial space between cells and conferring hydration. **Glycoproteins** such as laminins, elastin, fibronectins and thrombospondins are involved in the assembling of the ECM structure, ECM-cells interactions and growth factors storage[123]. Structurally, two types of ECM are found. The interstitial matrix comprises collagen I and fibronectins and provides tissue support when locating around the cells. The basement membrane, mainly composed of collagen IV and laminins, is a layer-like compact structure that separates epithelial or endothelial cells from the surrounding stroma. The basement membrane expresses receptors, such as integrins and hemidesmosomes, which bind to ECM proteins providing physical scaffold and regulating cellular functions[123].

The ECM influences the migration and invasion of cancer cells. Its composition regulates cells migration: fibronectin enriched environments allow cell migration whereas fibronectin-laminin low environments decrease cell movement[124]. ECM organization, with aligned fibres, also modulates cell migration favouring movement[125]. With all, tumour and stromal cells might modulate ECM to favour their movement. As tumour cells proliferate, there is a composition change where collagens I, II and IV and fibronectin are increased promoting malignant behaviour[126]. The major ECM components involved in tissue remodelling are proteinase substrates which are degraded by matrix metalloproteinases (MMPs) secreted by tumour and stromal cells[127]. Their activity is low in normal conditions but increased during cancer disease negatively correlating with prognosis[127,128]. For example, MMP9 promotes cancer development and progression in most cancers[129–132] as well as MMP2 [133,134]. Moreover, MMPs not only modulate ECM organization to allow cell migration but also release ECM-anchored growth factors such as TGFβ1 [130,131] and vascular endothelial growth factor (VEGF)[133] promoting cell migration, invasion and tumour growth as well as they have also been reported to contribute to chemoresistance[135,136]. Therefore, targeting MMPs could be a promising therapeutic approach.

1.3.2. Fibroblasts

Fibroblasts arise from the mesoderm during the embryonic development as do adipocytes, pericytes, chondrocytes and osteoblasts. In healthy tissues, fibroblasts are the main source of connective tissue in ECM also acting as regulators of angiogenesis, immune response and tissue repair[137]. These functions will backfire when tumour cells modulate healthy fibroblasts appropriating their functions for tumour progression. Not only tumour cells but also other cells within the TME will activate fibroblasts to become **tumour associated fibroblasts** (TAFs). Several signals have been described to promote TAFs activation, including TGFβ and inflammatory signals (interleukin -IL-1, IL-6), ECM modelling and several growth factors such as EGF, platelet-derived growth factor (PDGF) and fibroblast growth factor (FGF)[137,138].

TAFs participate in tumour progression and metastasis by remodelling the ECM and synthesizing growth factors, cytokines and chemokines. Tumours are generally stiffer than the normal tissue with

surrounding ECM alterations mainly induced by TAFs, which control integrin-mediated adhesions[139]. TAFs regulate both tumour cells and TME by increasing cell proliferation, invasion and survival as well as activating angiogenesis and immunosuppressive response[137,138], by modulation of chemokine signalling[140,141] and growth factor signalling[142,143]. TAFs have been classically implicated in mediating therapy resistance by secreting cytokines and remodelling tumour cells[144]. For instance, in BrCa, TAFs promoted HER2 targeted therapy resistance via FGFR2 and Src signalling[145]. These and other mechanisms foster the selection of cancer cell subpopulations resistant to therapies with improved tumour-initiating capacity. Moreover, fibroblasts are important mediators of secondary tumour growth by secretion of pro-inflammatory cytokines, induction of proliferation and EMT programs, promoting BrCa lung dissemination[146] or colorectal lung or liver metastases[147].

1.3.3. Endothelial cells

Blood vessels supply cells and tissues with oxygen and nutrients. Located in the inner surface, **endothelial cells** are the main components of vessels forming a lumen with a pericytes layer in the outer surface. During development and several diseases the formation of new blood vessels from pre-existing ones (angiogenesis) is activated, leading to aberrant blood vessels formation[148]. Angiogenesis requires the activation of endothelial cells by pro-angiogenic signals present in the microenvironment[148]. VEGF is the main angiogenesis promoting cue that binds to VEGF receptor (VEGFR) expressed in endothelial cells. Multiple VEGFs and VEGFRs have been described being the VEGF-A/VEGFR2 signalling pathway the best characterized[149]. When a VEGF gradient is recognized by endothelial cells, some of them acquire a filopodious phenotype spreading towards the gradient as a tip cell. Along behind it, the so-called stalk cells, although less motile, support the sprouting forming the lumen of the new vessel[148].

Hypoxia, tumour and/or stromal cells-derived VEGF-A induces angiogenesis favouring cell intravasation and dissemination. Early-stage tumours are poorly infiltrated but as tumours progress, there is an angiogenic switch that activates the development of the vascular network. Nevertheless, vessels pattern will depend on tumour type and stage, stromal composition and the pro-angiogenic/anti-angiogenic factors balance[120]. New formed blood vessels have an anomalous morphology with hundreds of branching arms, discontinuous endothelial cell barrier and altered basement membrane and pericyte cover[120]. **Pericytes** are a heterogeneous cell population with mesenchymal origin that cover capillaries, inhibiting endothelial cells proliferation but increasing their survival and cell-cell interaction. Due to the lack of pericytes, tumour-associated blood vessels are dysfunctional, hyperplastic, with defective cell junctions and vascular leakiness[150]. All these traits favour tumour cell intravasation and escape.

In addition to angiogenesis, tumour cells trigger the formation of new lymphatic vessels, a process known as lymphangiogenesis. Lymph vessels are composed of a lymphatic endothelial cell layer coated by smooth muscle cells. They transfer fluids and cells from the interstitial space to the blood. Besides protein-rich fluids, macromolecules and immune cells, cancer cells can also be transported by the lymph, which will first arrive to sentinel lymph nodes and distal lymph nodes prior to flowing into the blood stream[151]. Lymph vessels formation is activated by VEGF-C/VEGF-D binding to VEGFR2/VEGFR3[151,152]. Intra-tumour lymphangiogenesis has been commonly described in melanoma[153] and HNSCCs[154,155] and it is significantly associated with reduced patients' survival and tumour metastasis[156]. Being relatively leaker than blood vessels, lymph vessels are considered essential for tumour dissemination.

1.3.4. Immune inflammatory cells

Cancer immunoediting is a dynamic process which integrates the capacity of the immune system to either protect the host from cancer or promote cancer growth[157]. Three phases compose cancer immunoediting: elimination of malignant cells by innate and adaptive immunity following by an equilibrium phase due to immune-mediated tumour dormancy and a last phase of escape where tumour cells grow out of control and the tumour emerges as a clinically detectable disease[157]. Immunity-related components of the TME include tumour-promoting inflammation, active innate immunity and effective adaptive immunity, all mediated by a plethora of immune cells.

1.3.4.1. Lymphocytes

Following the *Th1/Th2 paradigm*, Th1 cells will have a pro-inflammatory and anti-tumour phenotype whereas Th2 cells will be immunosuppressive[158]. Thus, tumour-infiltrating lymphocytes positively correlate with tumour inhibition and good prognosis in patients[159,160]. **CD8+ T lymphocytes** are responsible for cancer cells death by the perforin/granzyme exocytosis pathway or by induction of FasL-mediated apoptosis[160]. However, for tumour cells killing, T cells have to be primed by interactions with dendritic cells (DCs), natural killer (NK) cells and CD4+ T cells[159,160]. Beyond the cytotoxic direct effect, CD8+ T cells also release the pro-inflammatory cytokines interferon-γ (IFN-γ) and TNF-α to indirectly cause cytotoxic cell death[161,162]. Besides the positive crosstalk with some immune cells, CD8+ T cells also negatively interact with other immune cell as well as with cancer cells and TAFs, which will inhibit the anti-tumour functions of CD8+ T cells[160]. As tumours progress, effector T cells will slowly become regulatory T cells evolving towards an immunosuppressive TME[163].

In addition to CD8+ T cells, other T cells are also present in immune TMEs. Helper **CD4+ T lymphocytes** release several cytokines for CD8+ T cells priming through specific DCs to optimize the CD8+ T cells response[164]. Conversely, **regulatory T cells** (Tregs) are an immunosuppressive subset of CD4+ T cells which suppress the innate and adoptive immune responses and release TGFβ, altogether suppressing CD8+ T cells[165]. As for T cells, **B lymphocytes** can also be tumour-infiltrating cells which can be divided in different subtypes with opposite functions. They can not only inhibit tumour development by cytokines and antibodies secretion and antigen presentation but also promote tumour progression by differentiation into regulatory B cells (Bregs). These will have an immunosuppressive effect directly interacting with tumour cells or inhibiting the function of NKs and CD8+ T cells through TGFβ, IL-10 and IL-35 secretion[166].

1.3.4.2. Macrophages

Macrophages represent the vast majority of the infiltrated cells in the stroma. Tissue resident macrophages derive from the yolk sac during embryo development whereas the majority of macrophages in adult tissues come from circulatory bone marrow monocytes[167–169]. Initially, **tumour-associated macrophages** (TAMs) were thought to derive from monocytes although it is actually well established that they arise both from yolk sac and circulating monocytes. However, their origin can partly affect their tumorigenic role since yolk sac macrophages are more likely to be immunosuppressive than monocyte-derived TAMs[170].

Two subtypes of macrophages are distinguished[168]. Classically activated macrophages (M1) have pro-inflammatory and anti-tumour functions while alternatively activated macrophages (M2), also referred as TAMs, repress the immune system being pro-tumorigenic. In an initial tumour stage, macrophages are polarized towards M1 phenotype by IFN-γ[167,171]. Macrophages will support the

inflammatory conditions by secreting IFN-γ, TNF-α and IL-6 promoting tumour cell death[160,169,171]. However, when tumours progress, the immune TME will be modified and M1 macrophages will be educated to become M2 macrophages mainly through IL-4 and IL-13[172–174], colony-stimulating factor 1 (CSF-1) and granulocyte-macrophage CSF (GM-CSF)[167,175]. M2 macrophages will regulate different pro-tumoral functions depending on their location within the tumour and the panel of secreted factors[168,176]. In PTs, TAMs activate the angiogenic switch by VEGF-A secretion[168,177] while promoting invasion through EGFR ligands expression and MMP9 up-regulation[178]. TAMs will also maintain an immunosuppressive TME by inhibiting T cells expansion and promoting regulatory T cells activation by IL-10 and TGFβ expression[168,169]. Further, M2 macrophages participate in metastasis where they support disseminated tumour cells survival by vascular cell adhesion protein 1 (VCAM-1)-dependent binding to the tumour cells[179]. Tissue-resident M2 macrophages are involved in melanoma[180] or breast[181] metastasis, inducing an inflammatory pre-metastatic niche and thus promoting tumour cell lung dissemination.

1.3.4.3. Dendritic cells

DCs are a heterogeneous population of immune cells that infiltrate tumours and have anti-tumour response. They connect both innate and adaptive immune system when presenting tumour-derived antigens to effector T cells[176]. There are multiple DCs subsets with specific immune functions and their role during cancer will depend on their stage of maturation and differentiation. While DCs are mainly involve in T cells priming and maintenance of local immunity in early tumour stages, some immunosuppressive DCs populations will increase as tumour progresses[182].

1.3.4.4. Neutrophils

Neutrophils are short-lived phagocytes which protect the host against infections although their role in cancer remains controversial. In the context of cancer, 3 types of neutrophils have been described: normal density and mature and immature low-density neutrophils. Normal density neutrophils are usually associated with anti-tumour cytotoxic neutrophils while low density neutrophils have immunosuppressive functions becoming pro-tumoral[183]. The neutrophil to lymphocyte ratio correlates with prognosis in several cancer types where a higher number of neutrophils is associated with poorer prognosis[184]. Low density neutrophils are the most abundant white blood cells in circulation promoting circulating tumour cells survival[185]. Moreover, once neutrophils are homed to the TME, they release neutrophil extracellular traps (NET) for angiogenesis activation, through VEGFs secretion, and ECM remodelling via MMPs production[184,186], among others. Although most of the data supports a pro-tumorigenic role, neutrophils might also inhibit tumour progression eliminating cancer cells during early stages and metastasis and stimulating anti-tumour effector T cells response[184,186].

1.3.4.5. Natural killer cells

NK cells are part of the innate lymphoid cells that, when circulating in the blood, eliminate cells expressing surface markers associated with oncogenic transformation[187]. As in effector CD8+ T cells, they eliminate tumour cells by perforin/granzyme-mediated cytotoxicity and death receptor-mediated apoptosis[187]. However, their cytotoxicity is highly effective in destroying circulating tumour cells whereas is less efficient at killing cells in TMEs[176]. The differentiation stage will also determine the function and effectiveness of NK cells since immature NKs will be pro-inflammatory whereas differentiated NKs will facilitate tumour progression[160].

NK T cells are the link between the innate and adaptive immune systems. These CD1d-restricted cells specifically recognize lipid antigens and, after being stimulated, they release high amount of cytokines and chemokines (like NKs) as well as respond to antigenic stimulation (like T cells)[188]. However, depending on the T cell of origin NK T cells can either inhibit tumour progression or be immunosuppressive favouring tumour evolution[176,188].

1.3.5. Nerve cells

Although the presence of nerves in the TME has received little attention, the actual implication of the nervous system (NS) in cancer progression has begun to be elucidated in the past few years. Nerves are present in the TME and as with other stromal cells, tumour cells are in contact with them through tumour-nerve connections. This way, both nerve and tumour cells reciprocally regulate each other controlling tumour cell biology, tumour progression and nerves outgrowth[189,190]. Similarly to angiogenesis, the growth of new axons from pre-existing nerves into the tumour tissue can be detected in many solid tumours, in a process called neoneurogenesis[191]. Recently, a unique crosstalk between the central NS and tumours has been described where progenitors from the central NS reached tumour sites and directly induced the formation of new neurons[192]. Nerves infiltration is correlated with poor prognosis and might be the cause of cancer-associated pain[193–195]. The neuroendocrine system, and in particular the autonomic NS, regulates tumour cell functions and thus tumour progression[196]. Sympathetic and parasympathetic nerves have been demonstrated to act complementary in prostate cancer, the former regulating early tumours while the latter induced cell dissemination and metastasis[195]. Three types of molecules take part in tumour-nerve connections. Tumour cells release neurotrophic factors (such as neural growth factor –NGF- and brain-derived neurotrophic factor –BDNF-) and axon guidance molecules (netrins, ephrins and semaphorins) which promote axon growth towards tumour sites[189,190]. Neurotransmitters act as cellular communicators and can be synthetized and released not only by neurons but also by non-neural cells such as cancer cells[189]. Tumour cells express neurotransmitter receptors and consequently neurotransmitters can modulate the so-called neuro-neoplastic synapses[197]. Nevertheless, such interaction has not been clearly characterized morphologically but only described functionally[198]. These neural cues can also act as an autocrine or paracrine stimulation of cancer or surrounding stromal cells when binding and activating the corresponding receptors[190,198,199]. As potential oncological targets, it is already accepted that nervous system targeting therapies can be used for cancer treatment[200].

Tumour cells can also use the newly developed nerves as an exit route for cell dissemination and metastasis. Neurotrophic factors, growth factors and axon guidance molecules are thought to regulate nerve invasion[201]. Tumour cells will migrate towards the nerve following the cues gradient and due to nerves low-resistance, cells will be able to either migrate along or invade it[202]. Through the perineural invasion, tumour cells can invade surrounding nerves when degrading the perineurium cover of the nerves fascicles[203,204]. The presence of tumour cells in the perineurium space of local nerves is associated with poor prognosis and shorter relapse-free periods[203,205,206]. Although clinically accepted, the mechanism by which tumour cells invade nerves is fully unknown. Although removal of nerves is sufficient for decreasing tumour growth and dissemination[194,195], denervation cannot be clinically used. Acting directly on the tumour and its environment using neurotransmitter modulators might be a solution[200], even though the possible significant side effects should be considered.

1.4. Metastasis

By definition, metastasis is the dissemination of tumour cells to a nearby or distant secondary organ where a macroscopic secondary tumour will grow. Therefore, it is considered the last stage of the tumour progression on the way of becoming an autonomous entity within the host[207]. Metastasis is the main cause of death associated to solid tumours where more than 90% of patients will die from metastatic diseases[208]. Although the 5-year relative survival rate for all cancers combined is 67%, it strongly depends on the stage at which the tumour is diagnosed. Whatever the tumour type, survival rates decrease dramatically when they are first diagnosed as stage IV or metastatic diseases, even in tumours with good prognosis[7]. For example, BrCa has a 99% five-year relative survival rate when localized which falls to 25% when the tumour has spread, as do oral cavity and pharynx cancers whose 5-year relative survival rate drops from 84% to 39% [7].

1.4.1. Metastasis models: early *vs* late metastasis

Metastases derive from disseminated tumour cells (DTCs) that escape from the PT and invade secondary organs, where they will be able to proliferate giving rise to a secondary tumour bulk. Metastases usually appear after PT diagnosis and treatment and thus, classically it was assumed that tumour cells that had disseminated before tumour resection or/ treatment were responsible for the metastatic growth. This classical hypothesis constituted the **linear progression model** that is based on the clonal evolution model and suggests that highly malignant tumour cells are responsible of dissemination and metastasis formation. It sustains that metastases emerge from the clonal evolution of a genetically modified PT cell whose random mutations confer it metastatic ability. This cell will be selected in a Darwinian mode from other cancer cells due to the expression of genes that provide the cell with the ability to disseminate and colonize distant organs[209,210]. The new tissue environment that DTCs will have to colonize as well as the treatment the patient will receive, will exert selective pressure that only the best adapted tumour cells will overcome. Cancer cells at the primary site will pass through multiple successive rounds of mutations and selection until they are able to proliferate autonomously. These independent cancer cells will eventually disseminate and generate metastasis at secondary sites. Therefore, metastases will arise from the most advanced clones within the PT, whose molecular characteristics will be determined by and similar to the PT[211]. This theory has been supported by genomic analyses that have revealed that most of the PT cells mutations were also present in metastatic cells[212,213]. Overriding genes mutated both in PT and metastatic cells are *TP53*, *CDKN2A*, *PIK3CA* and *RB1*[214,215].

However, molecular profiling analyses have also revealed that metastatic cells not only have mutations acquired by ancestral cells but also mutations acquired during metastatic dissemination, unique for every metastatic cell. Compared with normal tissues, metastatic tumours show an increase in migration, proliferation, stress response, and metabolism-related genes[216–219]. Most of these genetic studies were performed comparing advanced PTs with advanced metastatic lesions. In the last 20 years several new evidence have arisen showing that dissemination can also occur early in the disease. In fact, DTCs can be detected in patients that have only pre-malignant lesions. Furthermore, genetic studies that compared PTs, DTCs and metastases, found that DTCs are genetically divergent from PTs, suggesting that they have evolved in parallel[220]. These evidence, have led to a new metastasis model, the **parallel progression model**. In this model, dissemination is initiated long before the PT is diagnosed. The parallel progression model relies on several waves of early disseminated cells whose genetic alterations acquired in parallel in a different organ during tumour progression provide them

with enough tumorigenic features for surviving and growing independently in this distant organ. Meanwhile, the PT will continue growing and thus its cells mutating. This view is consistent with the differences in gene expression patterns found between PT and metastatic cells[216–219] as well as between PT cells and DTCs[221,222]. Genetically distinct metastatic cells at different distant sites and at different times[223,224] reinforce the idea of multiple waves of dissemination or continuous spread of DTCs from the PT.

In addition to clonal evolution and the parallel model, hierarchical organization and CSCs have also been a topic of discussion in metastasis development. Self-renewal capacity and differentiation potential properties define CSCs as tumour initiating cells[19]. Thus, both features may also confer the ability to disseminate and develop metastasis giving rise to the term metastasis-initiating cells (MICs). MICs are thought to be responsible for metastatic growth and although roughly characterized, are believed to have high plasticity and stemness. This plasticity may help in adapting their behaviour to new environments while invading, expressing different genotypes and phenotypes regarding the metastatic step[225]. The stronger evidence supporting that DTCs have metastasis-initiating capacity and are able to grow into metastases, has come from transplantation studies where it was found that the cancer was transmitted from donors that were considered being free of disease for more than 16 years to immunosuppressed transplant patients[226]. The occult non-proliferative DTCs where then activated by the transplantation process and subsequently formed tumours in the recipient organ[227]. These studies strongly suggest that DTCs can remain clinically asymptomatic for prolonged periods of time and still maintain their metastasis-initiating capacity. However, whether are the early, the late or both DTCs responsible of metastasis initiation and thus the MICs is still under debate in the scientific community and an open and exciting field of study in metastasis research.

Therefore, traditionally, metastasis was considered the last stage of cancer development, and it was exclusively explained lineally whereas new data from the last decades has revealed that both early and late dissemination events occur, suggesting that metastasis development is probably a combination of both linear and parallel progression models. Early DTCs will be genetically divergent from the PTs whereas late DTCs will be genetically closer[228]. Which one, early *vs* late DTCs are ultimately responsible for metastasis growth is still under study.

1.4.2. Metastatic cascade, step by step

Metastasis is a stochastic multi-step process caused by the dissemination of malignant cells from the PT and growth at distant sites. It comprises cell migration, local invasion, intravasation entering the circulation, arrest at secondary sites for extravasation, colonization, adaptation to the new environment or dormancy and, finally, growth to form a metastatic mass (**fig. 9**). Hence, metastasis is a very inefficient process that requires the circulation and survival of DTCs, the permissiveness of capillary walls to extravasation and a viable and supportive target organ which will facilitate the survival of foreign DTCs in a non-receptive target organ[229,230].

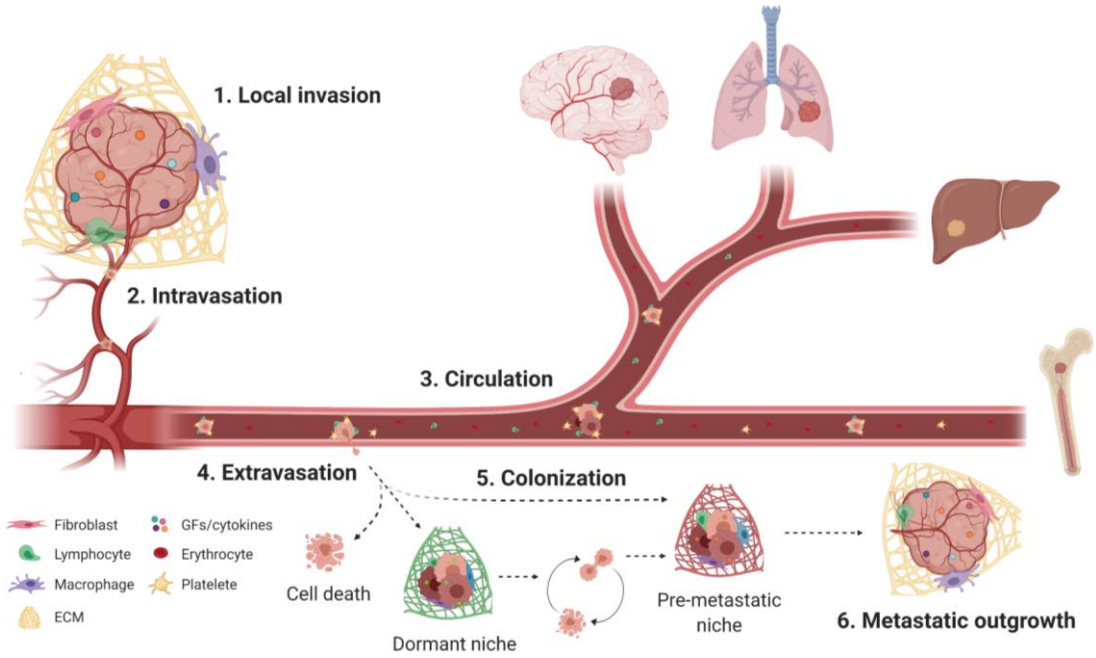

Figure 9. Metastatic cascade. Metastasis is an inefficient process deriving from DTCs from the primary tumour. Tumour cells locally invade the surrounding stroma (1) followed by their intravasation into the tumour vasculature (2). Circulating as single cells or clusters (3), circulating tumour cells would be arrested by endothelial cells. After extravasation (4), colonizing DTCs (5) will have to adapt to survive in the new environment. In dormant niches, DTCs enter a dormant state as single cells or micro-metastases. In pre-metastatic niches, DTCs have support to initiate overt metastatic outgrowth (6). Adapted from Vanharanta & Massagué (2013)[230].

1.4.2.1. Local invasion and intravasation

After malignant transformation, a cell may divide to form a small and growing colony of cells. The colony is initially confined to the epithelium, separated from the stroma by the epithelial basement membrane. At some point, some of these cells will acquire motile and invasive traits penetrating the basement membrane and invading the local stroma. Tumour cells and stromal cells interaction favours invasion. Tumour-derived factors will pass through the basement membrane to activate resident stromal cells and to recruit circulating mesenchymal cells. TAFs and TAMs support the invasion by secreting angiogenic factors and proteolytic enzymes stimulating the formation of new blood and lymph vessels (angiogenesis and lymphangiogenesis, respectively) and ECM remodelling. Tissue remodelling favours phenotypic changes of tumour cells triggering tumour cells penetration into new and immature vessels, giving rise to intravasation[207,231]. Tumour cells go through the abnormal and leaky tumour vasculature without completely disrupting endothelial tight junctions. In addition to the weak endothelial connections, tumour derived VEGF increases vascular permeability favouring tumour entrance to vessels lumen[232].

For a tumour cell to migrate and invade, cell plasticity is required and thus they reorganize their cytoskeleton in response to chemoattractant stimuli[233]. Cell plasticity enables changes from more epithelial to more mesenchymal phenotype in a process called epithelial-to-mesenchymal transition (EMT). After EMT, tumour cells lose polarization, reduce cell-cell and cell-ECM adhesions being more mobile and acquiring stem-like features[233,234]. Once tumour cells reach secondary organs, they will need to recover the epithelial phenotype through the so called mesenchymal-to-epithelial transition (MET) process to be able to proliferate and form the secondary tumour bulk[233]. EMT-MET are

reversible and dynamic traits and thus a wide variety of phenotypes will be present in a tumour, not all cells being completely epithelial or mesenchymal[235]. Although tumour cells can migrate as single cells, the commonest type of motility is the collective migration where cells will migrate as a group[236]. Therefore, within an invading tumour, inner cells will be mostly epithelial whereas cells at the invasive front will display EMT features expressing integrins and proteolytic enzymes for ECM remodelling[237,238].

EMT is associated with motility and might be essential in early metastatic steps. However, it is not essential to complete the metastatic cascade and cells not performing EMT may cooperate with surrounding cells to migrate. Then, those cells that have not undergone EMT might be responsible for the secondary tumour formation. Similarly, invasion is required for metastasis even though is not sufficient. Despite being invasive, some cancers such as glioblastoma almost never metastasize[239]. Adhesion has also been described as a critical aspect in metastasis since even tumour cells decrease cell-cell and cell-ECM adhesions, they must also attach to ECM through integrins even weakly to move forward[238].

1.4.2.2. Circulation

Once tumour cells enter the circulation they are termed circulating tumour cells (CTCs) and interactions with components of their environment will determine their survival and extravasation capacities. Although metastatic low performance, metastasis inefficiency may not seem to steam from circulation since $4 \cdot 10^6$ CTCs are estimated to be released per gram of PT[240]. Cells in circulation can disseminate throughout the whole body either actively through intrinsic motile mechanisms or passively using the fluid flow[241].

Metastatic cells can disseminate directly via blood vessels or through lymph vessels near the PT site. Carcinomas develop mainly lymphatic metastasis whereas sarcomas perform hematogenous metastasis. Anyhow, bloodstream will be the main systemic spread way since lymph vessels drain into blood[152]. CTCs can either circulate as single cells or as small cell clusters, both accompanied by stromal cells from the microenvironment of origin[185,241]. While transported by blood circulatory system, CTCs will go unnoticed by immune cells due to a platelet coating shield and interaction with neutrophils. Platelets will also facilitate CTCs arrest at the endothelium promoting cells extravasation[242]. Despite neutrophils can have an anti-metastatic role, they also facilitate CTCs extravasation by secreting MMPs that increase vascular permeability[243].

1.4.2.3. Extravasation and colonization

Cancer cells exit blood circulation in small capillaries where their diameter is similar to tumour cells diameter and thus, they are easily physically arrested. Extravasation for exiting a vessel and entering into an organ parenchyma is thought to occur in two ways: by mechanical disruption of capillary vessels or by transendothelial migration. In some organs, such as liver and bone marrow, vessels are not completely continuous and CTCs can go through the gaps between endothelial cells. In those organs, microvessels are made of highly permeable sinusoids and being permissive, CTCs display a high rate of colonization[244]. Conversely, in most organs, vessels comprise a continuous endothelial barrier formed by strong tight junctions and thus CTCs require interactions with endothelial cells. Here, platelets and leukocytes in the cover sustain sialyl-Lewis glycans expression binding to L- or P-selectins expressed by endothelial cells favouring CTCs arrest[245,246]. Due to the low affinity binding, tumour cells might roll on the endothelial surface until stronger bindings are formed for immobilization as do leukocytes in inflammation[245]. Immobilization in some areas but not in others is regulated by unique lectins and

chemokines expression by activated endothelial cells which may regulate metastatic organotropism. Once arrested, CTCs enter distant parenchyma by transendothelial migration inducing endothelial cells retraction and tumour cells squeezing between them[245,246]. Alternatively, CTCs can remain stationed alone and after cell proliferation, CTC clusters will be able to mechanically disrupt the endothelial barrier entering the secondary organ parenchyma[247].

Colonization, adaptation and growth are the final steps of the metastatic cascade. Once a tumour cell extravasates and colonizes a secondary organ it becomes a DTC. The main bottleneck of metastasis is the colonization of distant organs. Colonization is highly inefficient and only a minority of the millions of cells spread from the tumour will lead to a metastasis[248,249]. Experimental studies estimated that only 0.01% of tumour cells would colonize secondary organs[250,251]. Cancer cells follow a metastatic organotropism where they metastasise to specific distant sites. Organotropism was defined by Paget's *seed and soil* hypothesis in 1889 [252] where interactions between metastatic cells and the organ environment were first postulated for describing an organ-specific pattern of metastasis. He proposed that a DTC with metastatic capacities (seed) has a special affinity for a specific organ (soil) and thus metastasis will only develope when the seed and soil are compatible. Therefore, although cells are released broadly into circulation, every cancer type colonize a particular set of specific organ(s) (**table 2**)[253]. Notwithstanding, the metastatic compatibility of certain tissues defined by the *seed and soil* hypothesis is only relative and many cancer cells still die at distant sites.

Primary tumour	Metastatic site	Primary tumour	Metastatic site
Breast	Bone, lung, brain, adrenal, lymph nodes, ovary	**Melanoma**	Lymph nodes, lung, liver, bone, brain
Head and neck	Lymph nodes, lungs, bone	**Prostate**	Bone, lymph nodes
Lung	Bone, brain, lymph nodes, pleura, diaphragm, liver…	**Ovary**	Diaphragm, peritoneum, lymph nodes
Colon	Liver, lymph nodes, lung, bladder, stomach	**Uterus**	Lung, lymph nodes, liver, ovary

Table 2. Metastatic organotropism.

1.4.2.4. Metastasis growth or expansion

Once the cells have colonized the secondary organ, they will need to adapt, and depending on the microenvironment and on the conditions, they will start metastatic cell proliferation or become dormant. In most patients there is a delay between CTCs colonization and DTCs growth into metastasis. In fact, metastasis can appear months or years after PT growth, as in breast and prostate cancers, where metastatic diseases can develop 10-15 years after diagnosis[254,255]. This delay in metastatic growth is explained by tumour dormancy where tumour cells at metastatic sites remain quiescent for extended periods of time until something changes and they re-activate and proliferate forming secondary tumours[256]. Tumour dormancy and quiescence mechanisms will be treated and expanded in *Introduction, section 1.4.3*.

For DTCs to grow into metastasis, the same elements as for PT formation are required. DTCs need a supportive environment with sufficient oxygenation, nutrients and new vessels network[257]. There is a theory that proposes that cells within PTs communicate with other parts of the body to establish the so-called **pre-metastatic niche** (PMN). Apart from cell-intrinsic changes in a metastatic cell, complex molecular and cellular changes occur in the target-organ preconditioning it for metastatic seeding and outgrowth. These alterations comprise vascular permeability increase, local stroma modulation,

alteration of local resident cells and the recruitment of non-resident cells to promote metastatic cells attraction and survival[257]. The PMN formation is a multi-step process where the initial arrival of tumour-secreted factors and tumour-derived extracellular vesicles starts modulating the stroma favouring the recruitment of bone-marrow derived and suppressive immune cells. Altogether, they generate a mature PMN before metastatic cells arrive to colonize the niche. Finally, additional tumour cells will be hosted promoting their growth and expansion[258]. Conversely, some factors instead of forming the PMN will be determinant for **sleepy/dormant niches** formation, which will promote tumour cell dormancy instead of metastatic growth resulting in the delay in metastasis development shown in some patients[257]. Factors required for each niche formation are only functional in the context of specific tissues defined by tumours organotropism. Therefore, cells seeding in non-conditioned environments (restrictive-microenvironments) will lack the support and will fail in colonization whereas cells seeding in pre-conditioned environments (permissive-microenvironments) will promote cell survival and proliferation producing metastasis[257,258]. Nevertheless, several questions remain unresolved regarding pre-metastatic or sleepy niches such as their existence prior to colonization or their origin after PT removal.

These niches might be dynamic and as the metastasis evolves, they might also modulate their composition and their effect over the metastasis. Many of the factors involved in PMN formation are also required for metastatic expansion of tumour cells while sleepy niches regulating factors will inhibit metastasis. Thus, lymph nodes metastases in BrCa require VEGFR1 expressing bone-marrow derived myeloid cells recruitment before metastatic cells arrival[259] whereas for bone metastases development IL-6 [260] and MMPs [261] need to be released. They will promote receptor activator of NF-κB ligand (RANKL) secretion by osteoblasts for osteoclasts differentiation and activation, priming osteolytic metastases characteristic of BrCa[260,262]. Lungs are commonly colonized in several cancers and tumour-associated factors such as VEGF-A, TGFβ and chemokine C-C motif ligand 2 (CCL2) are described as lung metastases inducers[263]. Thrombospondin 1 (TSP-1) accumulation in the microvasculature in response to bone morphogenetic proteins (BMP4 [264], BMP7 [265]) and TGFβ2 [266] is essential for DTCs dormancy induction in lung and bone-marrow. After DTCs activation, proliferation and metastatic expansion, tumour cells from metastasis can in turn metastasize and form new tumours in other organs. Re-entering circulation, metastatic cells can disseminate to new organs as well as to their PT increasing tumour heterogeneity[267].

In view of all the above, as for PTs, the hallmarks of metastasis have been recently described[207]. Four essential characteristics define metastatic cells for the metastatic cascade and formation of secondary tumour: motility and invasion, modulation of the microenvironment, cell plasticity and colonization. Although most of the mechanisms used by metastatic cells are common to PT cells and so to normal cells, defining the principles of metastases aims to simplify the process to control and hopefully one day cure the metastatic disease.

1.4.3. Dormancy

When CTCs cross the endothelial barrier and invade the stroma of the target organs, from then on, they are termed DTCs, and they are the main source of metastasis. However, DTCs are not immediately proliferative having to adapt to the new microenvironment before initiating metastatic growth. Therefore, these DTCs undergo a period of dormancy/latency defined by non-dividing cells arrested in G0/G1 (quiescence) resistant to targeted and cytotoxic treatments[268]. Not only the cell cycle remains paused but also biochemical, biophysical and metabolic activities are reprogrammed during dormancy

to survive inhospitable environments[269]. As a result, some DTCs or micro-metastases can remain asymptomatic during months or years after PT diagnosis and treatment in a period known as minimal residual disease (MRD). MRDs comprise tumour cells that survive treatment and cannot be detected, which can persist in a dormant state without causing any clinical symptom. Conversely to cell senescence, dormancy is a reversible phenotype. Therefore, through mechanisms that are being investigated, dormant cells can re-activate, proliferate and grow as a secondary tumour (**fig. 10**)[268,270].

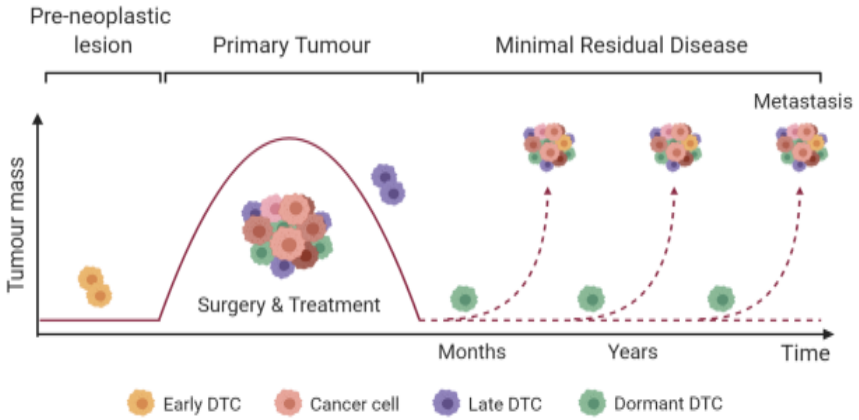

Figure 10. Tumour dormancy. Metastasis may evolve from early DTCs coming from pre-neoplastic lesions and/or from late DTCs coming directly from the PT. After surgery and treatment of the PT that result in tumour regression, DTCs can remain in a dormant state and become undetectable minimal residual disease for months or years (dashed line). By mechanisms still not well established, these dormant DTCs re-activate, proliferate and grow as metastatic tumour masses. Adapted from Sosa *et al.* (2014)[280].

DTCs are the main source of metastases but dormancy, re-activation and proliferation mechanisms are still not well understood. Despite metastatic cascade being somehow similar in all tumour types, metastasis tempo is clearly tumour-type dependent and the complete evolution of a metastasis will be mostly affected by the dormancy period. Very aggressive tumours such as lung cancer relapse early after PT resection and have high mortality rate[271] while in less aggressive tumours, such as prostate cancer, metastases are asynchronously manifested, with very long dormancy periods[255]. Conversely, BrCa can be classified either as medium or long dormancy depending on the stage and molecular subtype. ER-negative subtypes are more aggressive and recur early within the first 2 years whereas less relapses are found 5 years after diagnosis. Hence, they can be classified as high-medium dormancy cancer types. ER-positive subtypes have lower risk of recurrence during the first 5 years although the rate increases slow but constantly thereafter, with more than half of the ER-positive metastasis occurring more than 5 years after diagnosis[254]. Concerning HNSCCs, aggressiveness is closely related to the stage at the time of diagnosis, since they are commonly diagnosed at late stages and thus around 20% to 70% of patients will relapse 2 to 5 years after diagnosis. Besides, they are usually unresectable and resistant to treatments[272].

1.4.3.1. Dormancy, an evolutionary conserved process

DTCs regulate their signalling pathways depending on factors present in the microenvironment to ensure their survival. Therefore, DTCs dormancy is considered an evolutionary conserved mechanism of adaptation to a new foreign microenvironment. Nevertheless, dormancy is not exclusive of cancer cells and can also be observed in hematopoietic stem cells (HSCs)[273] and other organisms[268]. Several plants, insects and animal species will only have progeny with external favourable conditions or

conversely, they will enter quiescence. Then, after the conditions change and become propitious, they will retrieve proliferation resulting in embryonic development[268]. Many of the genes involved in this evolutionary conserved adaptation process were found to be up-regulated in dormant DTCs, including cell cycle and metabolic pathways-related genes[274].

During development, HSCs migrate from the liver to the bone marrow where, after fully matured, they will be located in the endosteal lining of the inner bone. HSCs will be maintained in a non-proliferative phenotype regulated by the endosteal microenvironment[275]. HSCs can reversibly acquire dormant, homeostatic and injury-activated states. During homeostasis, HSCs are kept dormant, preserving long-term self-renewal. However, in response to hematopoietic stress or injury, HSCs are activated and proliferate giving rise to new blood cells[273]. G-CSF and IFN-α induce the proliferation of dormant HSCs[273], which could be also activators of dormant DTCs proliferation. Therefore, pluripotency signalling pathways in HSCs may be closely related with dormancy signalling pathways in DTCs.

1.4.3.2. Mechanisms for dormancy regulation

Metastatic dormancy has been clinically relevant during many years, in part because of the high metastasis-associated deaths in solid tumours. Two types of dormancy can be distinguished: tumour mass dormancy and cellular dormancy[268,270]. In **tumour mass dormancy**, a tumour mass remains constant due to a balance between proliferative and apoptotic cells, mainly regulated by vascular and immune systems.

Tumour cells do proliferate but there is a lack in tumour bulk expansion maintained by blood supply limitation (angiogenic dormancy) and/or active immune response (immune dormancy). For tumour growth, the formation of new vessels is required for oxygen and nutrients supply and can be regulated activating the angiogenic switch by the expression of FGF and VEGF[276]. Angiogenesis can be also regulated by high expression of angiogenesis suppressors such as TSP-1 [276]. Therefore, the balance between pro-angiogenic and anti-angiogenic factors and thus the equilibrium between proliferation and death of DTCs regarding tumour vascularization is called **angiogenic dormancy**. Despite competent vasculature system, tumour mass dormancy can be given by the immune system as well. **Immune dormancy** maintains a tumour mass constant balancing the anti-tumour and pro-tumour functions of the immune system[277]. Importantly, the immune system could also be involved in tumour mass dormancy by regulating angiogenic dormancy through the release of anti-angiogenic chemokines (CXCL9 and CXCL10) and aberrant expression of α5β3-integrin by CD4+ T cells, which results in decreased formation of tumour vessels[278]. Tumour cell death is mainly regulated by the immune-surveillance of cytotoxic effector T cells, in cooperation with NK cells whereas tumour proliferation is promoted by the immune-evasion of regulatory T cells and myeloid-derived suppressor cells[277,279]. Myeloid-derived suppressor cells consist of immature macrophages, neutrophils and dendritic cells that are reported both as pro-metastatic and anti-metastatic cells.

In contrast, **cellular dormancy** derives from extrinsic and/or intrinsic changes in single tumour cells mediated by different signalling pathways. Here, cell cycle is arrested and cells enter quiescence without generating offspring. Both models of metastatic dormancy are not exclusive and in fact, cellular dormancy can be found in tumour mass dormancy where some cells will proliferate but others will be slow-proliferating cells[268,270]. As both dormancy mechanisms are complementary and there is a

dormancy switch for quiescent DTCs to proliferate into micro-metastases, the focus of this study will be the cellular dormancy.

1.4.3.2.1. Microenvironmental regulation of cellular dormancy

Metastatic cell dissemination is not sufficient for metastasis development. It will also be regulated by the microenvironment at distant organs, determining the likelihood of DTCs colonization. The microenvironment and epigenetic mechanisms exert growth control over DTCs[280]. As in PMN, dormant niches will regulate dormancy of DTCs as well as their engraftment, survival and chemoresistance[281,282]. Depending on the balance of growth factors and cytokines, a microenvironment could be considered restrictive or permissive allowing cells to enter or escape dormancy (**table 3**).

Restrictive-microenvironment (pro-dormancy signals)	**Permissive-microenvironment** (pro-proliferation signals)
– Organized ECM [253,283]	– Inflammation [294]
– Hypoxia [284–286]	– Periostin [295,296]
– Effector T and NK cells infiltration [278,287,288]	– TGFβ1 [266,296–298]
– TSP-1 [289]	– Tenascin C [299]
– Gas6 [290]	– Fibrosis [300]
– TGFβ2 [266,291,292]	– BMP4 [264]
– BMP7 [265]	– RANKL [301]
– atRA [293]	– IL-6, IL-8, TNFα [297]
	– Noradrenaline [302]

Table 3. Tumour cells dormancy and proliferation regulating signals present in restrictive or permissive microenvironments.

The availability of these molecules will be dynamic and heterogeneous within the tissue, regulating the tempo and the localization of a metastasis. The distribution is mainly regulated by the ECM. During metastasis, MMPs, integrins and metastasis-associated stromal cells (TAMs, TAFs) modulate ECM promoting cancer cells dissemination[128,207,231,253]. When degraded by MMPs, ECM-embedded growth factors and cytokines secreted by stromal components will be released[127]. Physical properties of the ECM have been implicated as well, in that organized fibronectin surfaces support BrCa quiescence through α5β3 and α5β1-integrins binding[283].

As a permissive-microenvironment, lungs are usually colonized by several types of cancers[253]. Periostin is an abundant ECM molecule in lungs involved in the metastatic colonization, promoting the survival of DTCs by Wnt signalling[295]. While tenascin C is synthetized by fibroblasts or BrCa cells in lungs and it helps in PMN formation and metastasis initiation[299], induction of lung fibrosis induces dormant BrCa cells to form proliferative metastatic lesions through β1 integrin signalling[300]. Furthermore, BMP4 expression inhibits BrCa DTCs proliferation in lungs[264].

Bone is usually colonized by cancer cells as an intermediate site to their target organs where bone-marrow stromal cells will be educated for PMN formation[268,303]. Tumour cells express molecules and factors produced by bone cells, mimicking osteoblasts and osteoclasts to adapt and survive in the bone microenvironment[303]. Once in the bone, DTCs locate in osteoblast-rich regions where growth arrest-specific 6 (GAS6) protein synthetized by osteoblasts induces DTCs dormancy when binding to GAS6 receptor AXL[290]. Bone microenvironment is also rich in TGFβ2, BMP7 and all-trans retinoic acid (atRA) which induce breast, prostate and head and neck cancers dormancy[265,266,291–293]. Nevertheless, bone is not always a restrictive microenvironment and re-activation and proliferation of DTCs can give rise to

bone and overt metastases. While osteoblasts might induce cells dormancy, osteoclasts might mediate escape from dormancy[301,304]. VCAM-1 expressing DTCs recruit osteoclast progenitors through α4β1-integrin providing an osteoclastic niche triggering micro-metastases activation to form overt bone metastases[304]. In addition, osteoclasts are activated by osteoblasts-derived RANKL, inducing myeloma cells proliferation in the bone[301]. Tumour-derived factors such as IL-6, IL-8 and TNFα also promote osteoclast activation and bone degradation which in turn will induce tumour cells proliferation in a positive feedback loop called the vicious cycle[297]. Ca^{2+}, TGFβs and several growth factors released from bone ECM remodelling will enhance tumour cells proliferation[297,298,305,306], where several compounds blocking TGFβs have been successfully used in preclinical trials for bone metastasis treatment[298]. Moreover, blood vessels, immune cells and nerves are also important components of the microenvironment and hence can also influence DTCs fate. The first barrier DTCs cross in their colonization process is the vascular basement membrane and thus it is reasonable to find them closely settled. Hence, it is assured the role of the microenvironment surrounding the microvasculature (termed perivascular niche) in DTCs phenotype[281]. Dormant BrCa DTCs were shown to reside close to the stable vasculature system which is rich in TSP-1 in secondary organs. However, in neoangiogenic vessels TGFβ1 and periostin induced DTCs proliferation[296]. In lung endothelial cells, TSP-1 expression is regulated by BMP4 [307], whose inhibition by tumour-derived Coco was shown to induce proliferation of dormant BrCa cells in lungs[264]. Furthermore, TSP-1 has recently been implicated in glioblastoma cells dormancy, reducing their angiogenic potential[289]. In addition, it has recently been shown that the perivascular niche is a protective site for DTCs and inhibition of integrin-mediated interactions between DTCs and the perivascular niche sensitizes DTCs to chemotherapy, preventing metastasis[308]. In this regard, therapeutic strategies to target tumour vasculature, such as VEGF targeting treatments, are the current approaches to oppose dormant cells.

Hypoxia is associated with poor-prognosis in solid tumours and although most tumour cells die in low concentration of oxygen, some cells will adapt and survive in a dormant state[284]. Few studies have been published trying to determine how oxygen influences the fate of DTCs in target organs. A recent study by Fluegen *et al.* (2017)[285] reported that BrCa and HNSCC cells were dormant under hypoxic conditions. In addition, hypoxia also activated dormancy programs in HPV-positive HNSCC and when repressing E6 and E7 oncogenes, cells enter quiescence in a p53-independent manner[286]. With all, hypoxic microenvironments seem to activate dormancy programs in DTCs, being likely to survive better after extravasation.

Regarding the regulatory role of the immune system in dormancy, neutrophils-derived inflammation in the lung induced awakening of dormant DTCs, through the activation of the EMT transcription factor Zeb1 [294]. Several studies have demonstrated the role of tissue resident macrophages or infiltrating monocytes as pro-metastatic immune cells, although no clear evidence have yet related them with DTCs dormancy. VCAM-1 expressing BrCa cells activated Akt signalling and had better survival in lungs when binding metastasis-associated macrophages through α4-integrins[179]. In addition to immune-surveillance, CD4+ and CD8+ effector T cells may regulate cell dormancy since dormant BrCa DTCs persist together with CD4+ and CD8+ T cells in the bone marrow. Here, more NK and effector T lymphocytes were found in the bone marrow of patients containing dormant DTCs[287]. Depletion of these cells induced dormancy exit and increased cell proliferation[278,288], both promoting metastasis.

Nervous system as a TME component and a key element in tumour progression regulator began to be studied in the last decades. Hence, whether it may also be an important factor that regulates DTCs fate in secondary organs remains elusive. In a recent study, it was demonstrated that the neural cue noradrenaline reactivated dormant prostate cancer cells in the bone marrow directly though β2-adrenergic receptor activation in tumour cells or indirectly by reducing osteoblast-secreted GAS6 [302]. Therefore, the observed reduction in metastases by blocking β-adrenergic receptors[309,310] may be, in part, due to longer dormancy periods.

Dormancy inducing signals can be very stable since relapses can appear 10-15 years after PT diagnosis. However, most of the dormancy escape studies describe which signals regulate dormancy exit but do not define how these exit cues are activated.

1.4.3.2.2. Cell intrinsic regulation of dormancy: signalling mechanisms

Growth factors, cytokines, angiogenic and immune signals present in secondary organs microenvironment determine DTCs phenotype by regulating intrinsic signalling pathways[280]. In general, reduction in mitogenic signalling by down-regulating specific kinases activity induces dormancy. However, certain kinases are up-regulated triggering cell cycle arrest. Therefore, the balance between MAPK-signalling pathways will determine the proliferative or quiescent cells phenotype (**fig. 11**). The very first studies demonstrating the role of the mitogenic extracellular regulated kinase (ERK) and the apoptotic/growth suppressive stress-activated protein kinase 2 (p38) ratio were performed in HNSCC, where a high ERK/p38 ratio was found in proliferative cells bound to fibronectin through urokinase plasminogen activator receptor (uPAR) activated α5β1-integrin[311–313]. ERK activation can be regulated by p38 and Cdc42 –downstream of integrin signalling- which in turn can be involved in p38 deactivation[313]. In addition, uPAR down-regulation inhibited focal adhesion kinase (FAK) and Src kinases blocking ERK and Ras activity, promoting cellular dormancy *in vivo*[314].

p38α MAPK was later found to regulate a transcription factor network that control dormant cells quiescence and survival (**fig. 11**)[315]. In HNSCC, activation of p38α by TGFβ2 resulted in the induction of the cell cycle inhibitor p27 and Dec2 (dormancy markers), down-regulation of CDK4 and subsequent dormancy entrance in the bone marrow microenvironment[266]. Similarly, bone stromal cells derived BMP7 activated p38 signalling in prostate DTCs and induced the cell cycle inhibitor p21 and the metastasis suppressor gene NDRG1 (N-myc downstream-regulated gene 1), all inhibiting tumour recurrence[265]. The mitogen-activated protein kinase family MKK induces dormancy of micro-metastatic colonies, where MKK4-induced dormancy was regulated by p38 activation[316] and induced p21 expression[317] in ovarian cancer. However, dormancy mechanisms might be different in early and late DTCs since HER2-positive early lung DTCs enter dormancy in a p38-independent manner[318].

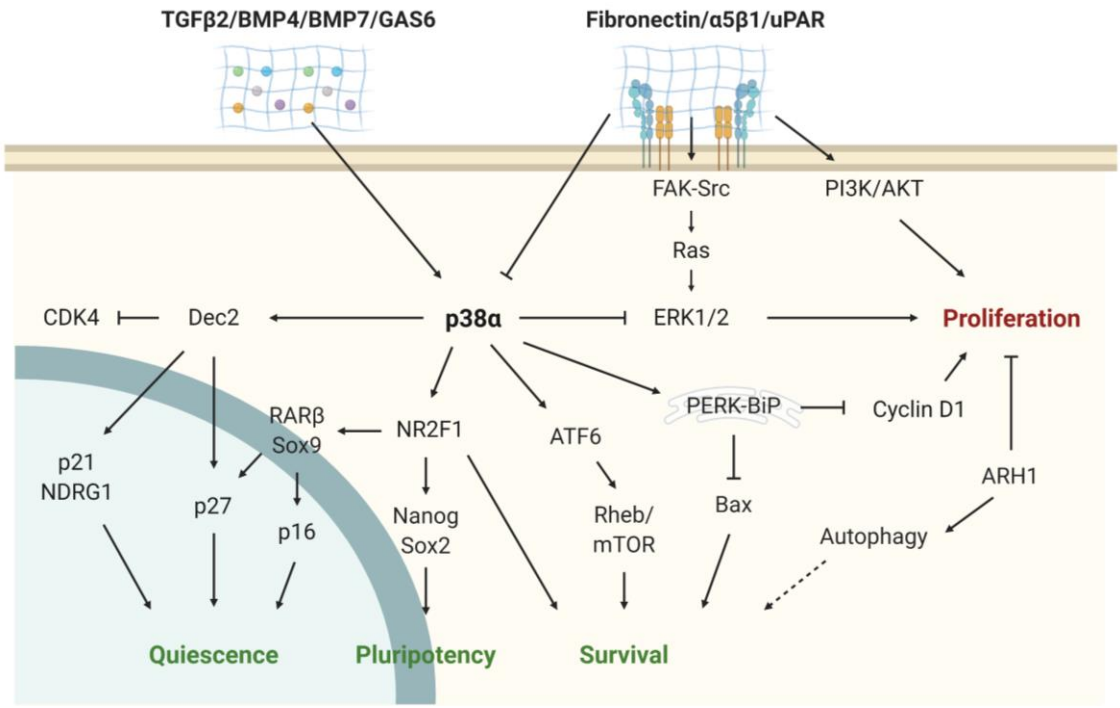

Figure 11. Cellular dormancy signalling pathways. Extrinsic (TGFβ2, BMPs, GAS6) or intrinsic mechanisms can activate p38α, which remains the central component of the dormancy intracellular pathways. p38α activation induces quiescence by Dec2 and cyclin-dependent kinase inhibitors (p16, p21, p27) activation. Moreover, p38α is a key component regulating pluripotency and DTCs survival. Conversely, it might indirectly inhibit cell proliferation by CDK4 and ERK1/2 expression regulation. On the other hand, proliferative DTCs induce uPAR and β1-integrin signalling by ECM molecules activating growth-promoting pathways such as PI3K/AKT, FAK-Src and Ras-ERK.

Activation of p38α is also linked to endoplasmic unfolded protein response (UPR) in dormant DTCs. It regulates the expression of endoplasmic reticulum chaperone BiP/Grp78 and protein kinase R-like endoplasmic reticulum kinase (PERK) promoting drug resistance while inhibiting drug-induced apoptosis of dormant HEp3 cells[319]. The latter was also shown to decrease Ki67, phosphorylated-histone 3 (p-H3) and cyclin D1 levels in pancreatic cancer cells keeping them dormant[320]. Besides, the endoplasmic reticulum stress-related transcription factor activating transcription factor 6 (ATF6), also regulated by p38α, induced dormant HNSCC cells survival through mTOR-Rheb pathway activation[321]. mTOR activation was independent of PI3K/AKT signalling, which is usually found down-regulated in slow-proliferative or dormant-like cells[321–323]. Thus, activation of UPR pathways promotes cell cycle arrest and survival, both regulating a dormancy-like state allowing them to resist stress-induced death. Autophagy has been also demonstrated to regulate dormant DTCs survival. ARHI expression induced cell death *in vitro* while activated tumour dormancy *in vivo*. Autophagy inhibition blocked tumour regrowth suggesting that autophagy, besides cell dormancy, may also regulate dormant DTCs survival[324].

Dormant cells can be related with stem cells concerning their pluripotent ability to switch between proliferation and dormancy, through epigenetic reprogramming mechanisms[280]. The NR2F1 orphan nuclear receptor, which is also activated downstream of p38, was demonstrated to increase *SOX9*, *SOX2* and *NANOG* genes expression in HNSCCs regulating both quiescence and pluripotency programs[293]. Interestingly, molecular profiling studies have revealed an enrichment in drug resistance, stemness and immune system related genes in slow-cycling cancer cells[325]. For instance, TET2

epigenetic enzyme was required for survival and chemoresistance of colorectal slow-cycling cancer cells[325]. Several studies have also related active pluripotency programs in embryonic stem cells entering quiescence[326] and lung and breast latent cells[288].

The loss of metastasis suppressor genes expression or function by DTCs is also associated with dormancy exit and metastasis development. Metastasis-suppressor genes comprise a group of genes participating each in different signalling pathways. They are defined by their ability to inhibit overt metastases without affecting tumorigenicity[327]. KISS1 was shown to induce dormancy in solitary melanoma cells in target organs[328] whereas KAI1 induced dormancy in solitary prostate cancer cells by regulating cell adhesion to endothelial cells[329,330]. Nm23 expression correlates with good prognosis in several cancer types and its mechanisms of action may be multi-functional suppressing several steps in the metastatic cascade[331]. Although metastasis suppressor genes are not directly linked to dormancy, a study by Takács-Vellai (2014)[332] suggested that Nm23 may exert its anti-metastatic effect by blocking Ras/ERK signalling and thus it could mediate dormancy entrance in DTCs.

1.4.4. Metastasis treatment

Metastases are correlated with poor prognosis mainly because they are resistant to the therapies used and designed for PTs [333]. Although PT cells share genetic mutations with metastatic cells, the latter also have unique alterations which facilitate colonization that might be in part responsible for resistance. Epigenetic mutations modulated by tumour microenvironment are also part of the resistance mechanisms in metastatic cells[231]. In addition, metastatic cells express high levels of multidrug resistance channels as well as they activate desmoplastic reactions increasing fibrous density of the colonized tissue both reducing drug internalization[333].

There are not clinically available metastasis targeting treatments and thus the same treatments as for PTs are employed. In fact, surgery is only used in single metastasis or in small and clinically detectable reduced number of metastases since widespread metastases are not surgically removed. Studies are being developed in order to prevent metastasis formation focusing on PMNs, CTCs and dormant DTCs targeting[231,333].

1.4.4.1. Dormancy diagnosis and treatment

Dormant cells may be the source of tumour recurrence and thus understanding dormancy is essential to face metastasis, one of the most significant challenges of clinicians. Minimal residual disease is often observed in cancer patients where DTCs are frequently found and the detection of DTCs in the bone marrow is associated with worse clinical outcome[334–337]. However, not all patients with clinically detectable DTCs will develop relapse. Therefore, it would be essential to predict which dormant DTCs will eventually grow and which will stay dormant in order to not over-treat patients. Interestingly, p38-associated dormancy genes helped defining a dormancy signature enriched in ER-positive BrCa cell lines over ER-negative cells and that correlated with longer metastasis-free periods in ER-positive patients[338]. Moreover, p38α and p38-regulated NR2F1 have been shown to be up-regulated in prostate cancer[293,339] or BrCa patients' bone marrow DTCs[340] and their expression correlated with prognosis[339,340], suggesting altogether these genes could be interesting biomarkers of dormancy. Treatment-imposed stress has been also related with dormancy[256]. In ER-positive BrCa, although initial hormone-therapy reduces tumour growth and increases relapse-free survival, Ogba *et al.* (2014) [341] demonstrated that ER and PR-positive dormant cells become proliferative and metastatic

after hormone-therapy. In addition, the metastatic lesions showed cell heterogeneity with ER/PR-positive and ER/PR-negative cells within the tumour, the latter being therapy resistant[341].

Currently, two tactics are widely studied to target dormant DTCs: maintain DTCs dormant indefinitely or eradicate dormant DTCs[281,342–344]. Treatments to keep dormant DTCs asleep aim to inhibit tumour re-growth while reducing the use of chemotherapies and their side effects. Bisphosphonate and anti-RANK treatments such as denosumab inhibit osteoclasts activity in bone metastases and their use reduces metastatic recurrence and improve patient survival[345], evidencing the role of osteoclasts in bone DTCs dormancy exit. Moreover, combination of the Food and Drugs Administration (FDA)-approved 5-azadeoxycytidine and atRA up-regulate NR2F1 inducing pluripotency and quiescence in HNSCCs[293], showing its therapeutic potential to sustained dormancy. The first clinical trial combining 5-azadeoxycytidine and atRA to target dormant DTC is undergoing at the moment at Mount Sinai in prostate cancer castration resistant patients (#NTC03572387). Therefore, inhibition of metastasis-inducing components such as uPAR or ERK, in combination with induction of dormancy initiating factors such as p38α and NR2F1, would be the best strategy to prevent awakening from dormancy. Nevertheless, as in cancer patients, we could not assume that treatment-induced dormancy will not eventually become subverted, DTCs could become resistant, re-activate and proliferate developing metastasis. Conversely, eradicating DTCs while they are dormant in secondary organs would avoid the sudden awakening of the cells. While dormant DTCs have enhanced survival mechanisms, blocking survival signals might push cells to suicide. Chloroquine treatment inhibited ovarian cancer growth *in vivo* by impeding autophagy-promoted cell survival[324]. Moreover, the combination of the proteasome inhibitor bortezomib and the specific inhibitor of eIF2α phosphatase (PERK downstream) salubrinal reduced the number of quiescent myeloma cells surviving to bortezomib treatment alone. Survival cells had activated UPR signalling which was down-regulated after drug combination which in turn enhanced bortezomib-induced apoptosis of dormant cells[346].

Alternatively, promoting dormant cells awakening by external stimuli or through dormancy niche cells mobilization could sensitize DTCs to anti-proliferative therapies. As DTCs are moved to endosteal niche in bone marrow through CXCL12-CXCR4 binding, the use of an oncolytic virus expressing a CXCR4 antagonist inhibited the attachment of cells to bone marrow niches and inhibited BrCa metastasis *in vivo*[347]. It remains unclear whether DTCs mobilization sensitize them to chemotherapy without affecting HSCs or whether DTCs exit from the dormancy niches would result in their awakening. However, using cytotoxic therapies to kill newly awakened chemosensitive and proliferative cells before they undergo multiple divisions could address the problem. At the moment, several clinical trials are being developed targeting the persistent DTCs with the goal of eradicating dormant cells[342,343]. In a phase II clinical trial with BrCa patients that have been treated with adjuvant chemotherapy, if DTCs are detected in the bone marrow, they are treated with docetaxel to reduce the burden of dormant and persistent DTCs (NCT00248703). Detectable DTCs and metastasis-free survival are analysed and docetaxel treated patients show lower number of DTCs as well as higher disease-free survival[348].

1.5. Neuropilins, semaphorins and plexins

Neuropilins (NRPs) are proteins that act as co-receptors for both class 3 semaphorins (SEMA3s) and VEGFs, regulating axonal guidance and angiogenesis, respectively. However, since they were discovered, NRPs have been increasingly implicated in physiological and disease-related processes such as tumour progression, immune diseases and viral infections[349,350].

1.5.1. Structure and classification

Neuropilin 1 and 2 (NRP1, NRP2) form a small family of type I transmembrane glycoproteins, present in all vertebrates. Although functionally diverse, their genomic and structural similarities suggest that they were originated from a gene duplication event[351]. With 17 exons, the *NRP1* gene is located in the short arm of chromosome 10 (10p12) encoding a 923 amino acids protein of approximately 120kDa of molecular weight. The *NRP2* gene is located in the long arm of the chromosome 2 and its 17 exons codify for a 926 amino acids protein of 112kDa[352,353].

Both NRPs have an overall amino acid homology of 44% with a conserved domain structure (**fig. 12**). The extracellular N-terminal region is essential for ligand binding and is structured in five different domains. Farthest from the membrane, NRPs have two calcium-binding C1r/C1s/Uegf/Bmp1 (CUB) domains (also referred as a1/a2 domains), two coagulation factor V/VIII-like domains (also referred as b1/b2 domains) and a Meprin/A5-antigen/ptp-Mu (MAM) domain (also referred as c domain). Following the extracellular region, NRPs have a single transmembrane helical region linked to a very short intracellular domain (44 amino acids in NRP1 and 42 or 46 in NRP2). The latter has a PDZ domain-binding motif in the C-terminal with which NRPs bind PDZ-containing intracellular proteins (**fig. 12**)[350,351,353,354].

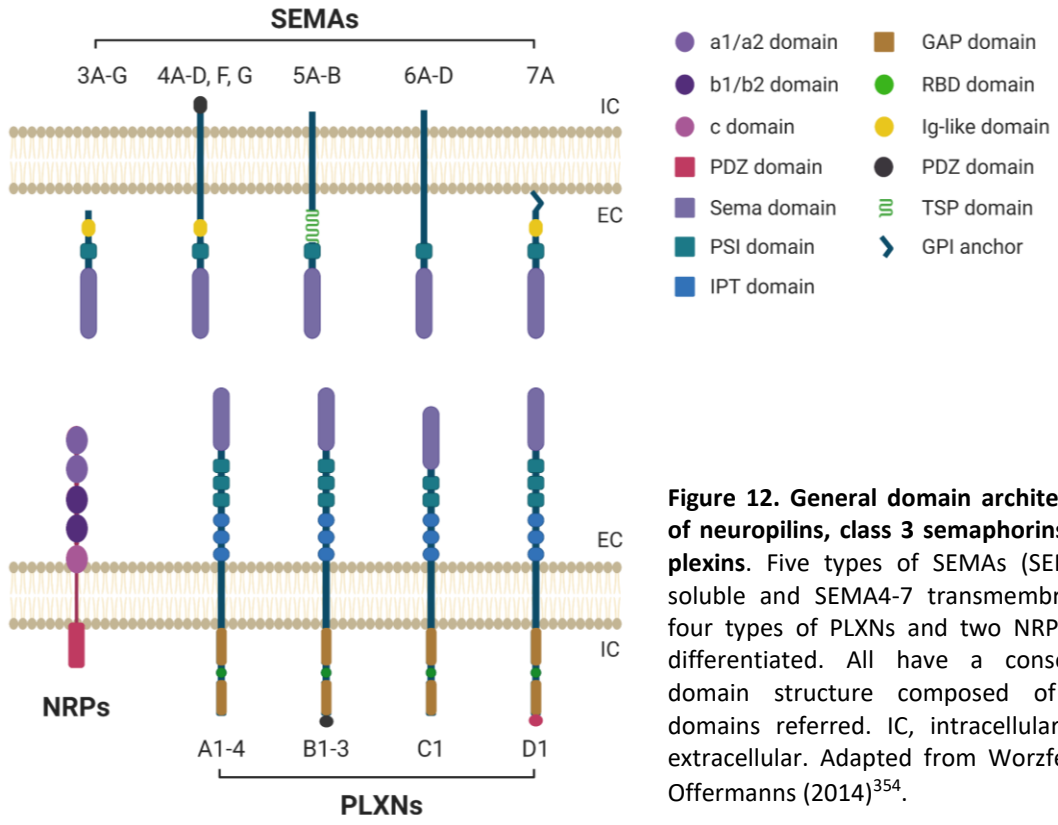

Figure 12. General domain architecture of neuropilins, class 3 semaphorins and plexins. Five types of SEMAs (SEMA3s soluble and SEMA4-7 transmembrane), four types of PLXNs and two NRPs are differentiated. All have a conserved domain structure composed of the domains referred. IC, intracellular; EC, extracellular. Adapted from Worzfeld & Offermanns (2014)[354].

NRPs bind to SEMA3s through a bivalent mechanism where a1 domain specifically binds to the sema domain while the b1 domain confers affinity when binding the basic C-terminal region of a particular SEMA3. The b1 domain forms a basic binding pocket specific for ligands with a C-terminal arginine such as those of SEMA3s. Besides SEMA3s, VEGFs also bind the b1 domain of NRPs and thus both may compete for NRP binding[349–351]. The relative concentration of both ligands and the NRP-expressing cell type might control NRPs function[350]. The c domain mediates protein-protein interactions essential for

NRPs oligomerization or dimerization[351]. Despite homodimers are more often described, NRPs heterodimers can be also formed for signalling activation[355].

Due to the alternative splicing, several NRP1 isoforms, two membrane-associated NRP2 isoforms and a soluble NRP2 isoform have been described in humans[351]. Membrane-bound NRP2s, NRP2a and NRP2b, differ in the transmembrane and cytoplasmic regions, where NRP2b lacks the PDZ domain[352]. Therefore, although maintaining the ligand-binding abilities, both isoforms might vary in their functions. This is underpinned by the different tissue expression pattern [352]. Conversely, the soluble isoform is constituted by two a1/a2 domains, a complete b1 domain and a truncated b2 domain[352] which can act as an endogenous inhibitory protein when binding NRPs ligands[356]. NRP1 and NRP2 can be post-translationally modulated by asparagine N-linked glycosylation[357,358] but only NRP1 is modulated by addition of glycosaminoglycans to the N-terminal, forming a high molecular mass NRP1 (>250kDa)[359,360]. These variants modulate NRPs function either in physiological[359] or pathological[358,360] conditions.

Semaphorins (SEMAs) constitute a large family of secreted and membrane-associated proteins, initially described as axonal guidance molecules in the nervous system but currently involved in many biological processes[361]. SEMAs are structurally and functionally conserved proteins present in many different vertebrate and non-vertebrate species but absent in non-animals. There are eight classes of SEMAs and vertebrates have members in classes 3-7 (**fig. 12**). Genes codifying for SEMAs are distributed along the genome and their sequence is highly heterogeneous and alternatively spliced[362]. However, the SEMA family is defined by a highly conserved cysteine extracellular domain called sema domain, which characterizes SEMAs function (**fig. 12**)[363]. This single copy domain mediates the homophilic dimerization required for SEMAs signalling and receptor binding[364]. Next to the sema domain, in almost all SEMAs there is a cysteine-rich domain known as plexin-semaphorin-integrin (PSI) domain. Other domains are also described but vary among the different SEMA family members (**fig. 12**). Within SEMAs in vertebrates, only the SEMA3s are produced as secreted proteins while class 4-6 SEMAs are transmembrane proteins and SEMA7 is a membrane-anchored protein[362,365]. SEMA3s are thought to be secreted as inactive pro-SEMA3s that require a proteolytic cleavage of the C-terminal pro-peptide by furin-like proteases for their activation[366].

Plexins (PLXNs) are the main receptors for SEMAs. They are transmembrane glycoproteins widely expressed in the neural system but also outside of it. Initially described as receptor complexes in the guidance of neuronal axons with SEMAs, currently PLXNs are also implicated in the development of the nervous and cardiovascular system, immune system and tumour progression[367]. There are four classes of PLXNs in vertebrates with a total of nine subtypes: PLXNA1-A4, PLNXB1-B3, PLXNC and PLXND1 (**fig. 12**). In their extracellular domain, PLXNs have a sema domain which will bind SEMAs, two or three PSI domains and several immunoglobulin-plexin-transcription (IPT) glycine-proline-rich domains. Inside in the cytosol, PLXNs contain two conserved and unique GTPase-activating protein (GAP) domains separated by an insertion region (**fig. 12**)[368]. SEMAs binding through the extracellular sema and PSI domains induces a conformational change in PLXNs, folding together the two GAP domains. The conformational change activates PLXNs GAP domains regulating the activity of small GTPases like Ras[368–370]. Plexins GAP activity seems to be more directed to Rap proteins, a sub-family of Ras proteins[371]. Rho family small GTPases including Rdn,Rac1 and RhoD will bind to the insertion domain between the two GAP domains, known as Rho GTPase-binding domain (RBD), contributing to PLXNs signalling[368,369,372].

Most SEMAs bind to one or several PLXNs, which exist as monomeric or homodimeric inactive receptors in the membrane. With a dimeric SEMAs binding, a 2:2 SEMA-PLXN protein complex is formed[364,373]. However, these complexes usually include PLXNs-associated RTKs or intracellular tyrosine kinases for PLXNs phosphorylation and activation[368]. In addition, SEMA3s signalling pathway activation requires the presence of NRPs as co-receptors whereas other SEMAs seem to be co-receptor binding-independent[364,373]. Excluding SEMA3E that can regulate several functions directly through PLXND1 without NRPs binding[374,375], the formation of a 2:2:2 SEMA3s-NRPs-PLXNs is required for increasing binding affinity and signalling activation[373].

NRPs lack functional cytoplasmic tyrosine kinase domain and thus they act as co-receptors for plexins. In addition, NRPs can be co-receptors for various RTKs, integrins and other molecules controlling their signalling. The versatility of NRPs allows them to act as co-receptors for different VEGF family members (VEGFs, placenta growth factor –PlGF-), hepatocyte growth factor (HGF), FGFs, PDGFs, TGFβs and their respective receptors[349,350]. Integrins have been also described as NRPs partners and although both lack cytosolic kinase active domain, NRPs have been reported in the intracellular protein clusters where scaffold and/or effector proteins are recruited. Interaction between integrins and NRPs might be essential for regulating cytoskeletal remodelling and cell adhesion to ECM through Src family and FAK[376,377]. These interactions are more commonly found in pathological conditions and will be further discussed.

1.5.2. NRPs, SEMA3s and PLXNs physiological functions

During development, NRP1 is mainly expressed in arteries and NRP2 in veins but both are located on neuronal cells[378,379]. In adult tissues, their expression is widely distributed in different organs where NRP1 is up-regulated in heart and placenta whereas NRP2 shows higher expression in liver and kidney[379]. Similarly, SEMAs and PLXNs are highly expressed in the nervous system although their expression is not restrained to neurons but also present in foetal lungs, liver and kidney and many other adult tissues including mammary, respiratory track and cardiovascular tissues[379]. Their expression is dynamic and age-dependent with the highest levels in developmental embryos where their main functions are the development of the nervous system and the vasculature. Moreover, their expression is also tightly regulated by the spatial localization and temporal expression within a cell where receptor endocytosis, protein transport and intracellular protein degradation are described as the main regulatory mechanisms[361].

1.5.2.1. Axonal guidance

Targeted disruption of genes has highlighted the importance of NRPs and SEMAs in axonal guiding. Expression of a mutant NRP1 with impaired SEMA3A binding but unaffected VEGF-A binding resulted in aberrant sensory nerves but a well-organized cardiovascular system *in vivo*[380]. Similarly, *in vivo* NRP2 knock-down diminished the chemo-repulsive effect of SEMA3F over central NS axonal projections, with different brain areas affected[381]. At the cellular level, SEMAs-mediated repulsion is a result of the modification of the axonal cytoskeleton causing growth cones repulsion and collapse. However, exactly how the axonal cytoskeleton is modulated is not entirely clear. SEMA3s gradient regulates the axonal growth cones towards the targets of innervation. The best characterized guidance molecule is SEMA3A whose levels are abundant in specific regions but more limited in others. After binding NRP1 and PLXNA1, SEMA3A induced F-actin depolymerization at the leading edge where Rac1 plays an important role[382]. The involvement of other Rho GTPases also modulates cell cytoskeleton. The association of Rnd1 to PLXNA1 activates Rnd1 and subsequently induces LIM-kinase[383]. LIM-kinase phosphorylates

and activates the actin-depolymerizing protein cofilin, decreasing the actin filaments turnover and causing filaments unbundling[384]. NRP1-VEGF-A binding similarly promoted neuronal migration and axonal guidance even though via VEGFR2 instead of PLXNA1 [385]. Therefore, this suggests that NRP1 acts either as VEGF-A or SEMA3A receptor, depending on the molecular context of the cell. Several signalling pathways have been described in axonal, dendritic and synaptic development where different ligands, receptors and intracellular molecules are involved[386].

In addition to axonal growth, SEMAs and their receptors also regulate neuronal proliferation, polarity and synapses formation. Therefore, their expression disturbance might be involved in developmental and adult nervous system disorders such as epilepsy, autism and Alzheimer's disease[387,388]. There is not a direct functional relationship but they may aggravate the symptoms.

1.5.2.2. Vasculogenesis

The formation of new vessels during embryo development is similar to axonal growth, where axonal growth cones may act as endothelial tip cells. Hence, many receptors are equally expressed in neuronal and endothelial cells. Consequently, VEGFs and SEMAs can similarly regulate both processes through VEGFRs and PLXNs, respectively, with downstream effectors and signalling pathways overlapping in both processes[361,389]. Interestingly, despite the close interplay between molecules, the effect of SEMAs and VEGFs seems to be opposited[390].

NRPs were initially discovered as essential in the development of cardiovascular system. NRP1 knock-out resulted in poorly organized and missing blood vessels causing severe vascular defects that induced embryonic lethality at E10-E13.5 [391]. NRP2 knock-out generated viable mice with functional blood vessels but deficient lymphatic vessel system [392] whereas in double NRP1-NRP2 knock-out effects were synergistic and embryos dyed at E8.5 due to extreme vascular deformities[391]. Likewise, NRP2 knock-out mice had lower bone density[393] and abnormal cranial nerves development[394].

For vascular development, NRPs act as co-receptors for VEGFRs. NRP1 has been widely described in endothelial cells forming complexes with VEGF-A and VEGFR2 whereas NRP2 is involved in lymph vessels together with VEGF-C/D and VEGFR3 [156,378,395]. The activation of VEGF-C/D-VEGFR3 signalling induces lymphangiogenesis where NRP2 has been shown to play a key role. There are no clear evidences about NRP2 and VEGFR3 complexing but VEGF-C/D binding to NRP2 promotes lymphatic endothelial cells proliferation, polarization remodelling and lymphatic sprouting, suggesting an association between receptors[389,396].

1.5.3. NRPs, SEMA3s and PLXNs in cancer

The importance of NRPs, SEMAs and PLXNs in vasculogenesis and axonal guidance is firmly established. However, their role in cancer is not as clear. NRPs are up-regulated in several tumour types and their expression correlate with worse prognosis and poor survival[397]. Together, they have been described to regulate tumour cells migration and invasion, proliferation and survival (**fig. 13**)[397–399].

Both NRPs are highly expressed in tumour vasculature but their expression by tumour cells varies from weak to strong and is very heterogeneous within cancer types. NRP1 is up-regulated in metastatic breast and non-small-cell lung cancer in comparison to PTs[400]. Meanwhile, colorectal and melanoma samples are usually positive for NRP2 expression[401]. The mechanisms by which NRPs regulate tumours are difficult to elucidate since they interact with many cancer-associated molecules. Besides tumour

cells, stromal cells can also express NRPs to further complicate the insights. In general, NRPs binding to any of their multiple ligands, such as growth factors and integrins, promotes tumour progression. However, the association of SEMA3s prevents the binding of these growth factors and blocks the activation of pro-tumorigenic downstream signalling pathways[398].

The cancer promoting effects of NRPs have often been attributed to VEGF-A-mediated tumour angiogenesis and VEGF-C-mediated lymphangiogenesis through VEGFR2 and VEGFR3, respectively[402] (**fig. 13**). Moreover, NRP1 was shown to be crucial for tip cell phenotype induction inhibiting the canonical TGFβ signalling and activating Notch signalling[403]. However, endothelial cells-derived SEMA3A inhibits angiogenesis via NRP1-PLXNA1/A4 in an autocrine manner[398,402]. Consequently, SEMA3A loss in tumour progression tips the balance in support of the angiogenic switch and tumour development. Blocking NRPs binding site by site-specific anti-NRP monoclonal antibodies reduced tumour-associated vasculature and tumour growth[404,405]. These effects were increased when combining with VEGF blocking antibodies[404]. Consequently, NRPs have been used as anti-angiogenic therapies for cancer treatment even though the expression of NRPs by several cell types hinders the translation of these antibodies to the clinic.

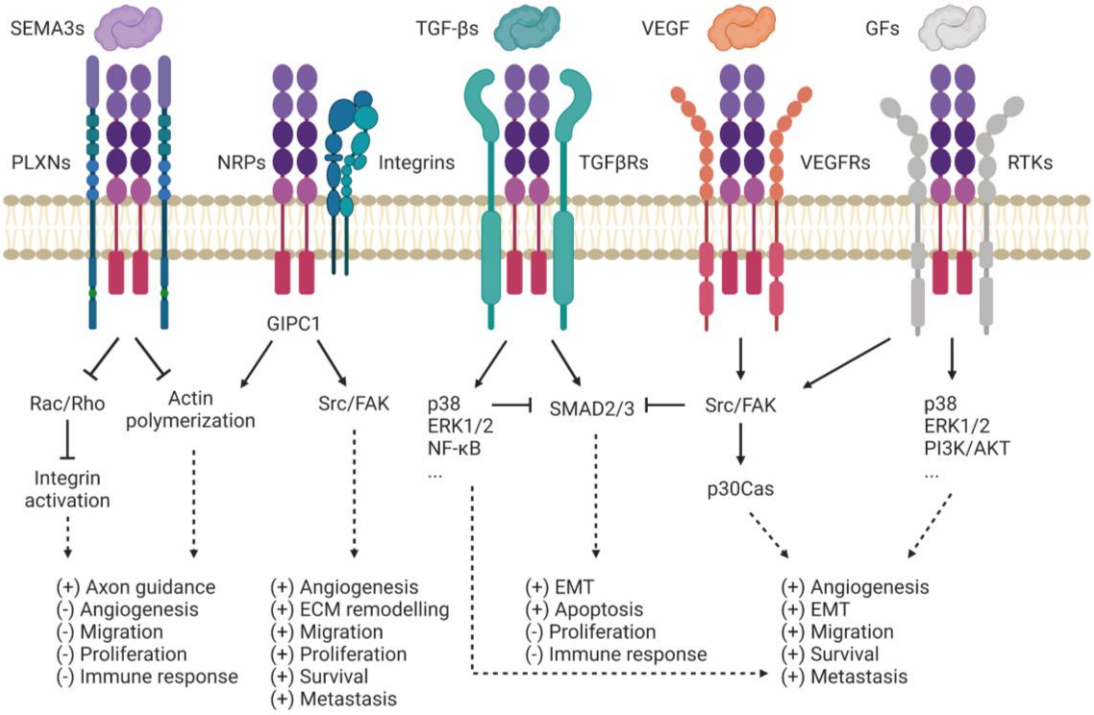

Figure 13. Neuropilins hypothetical model of interaction with multiple growth factors and their receptors. When dimerized ligands (SEMA3s, integrins and several growth factors -GF- such as VEGF or TGFβs) bind to a NRP dimer and PLXNs or RTKs dimer a large number of cellular responses are regulated. Intracellular activated (→) or inhibited (⊢) proteins as well as activated (+) and inhibited (-) cellular effects are indicated. Adapted from Niland & Eble (2019)[399].

NRPs can also regulate angiogenesis and tumorigenesis in a VEGF/VEGFR-independent manner[406]. NRP1 induced endothelial cell migration through the non-receptor tyrosine kinase ABL1 pathway[407] which was also demonstrated to induce BrCa cells proliferation and survival[193]. As many tumour types lack VEGFR expression, NRP-VEGF axis not only might regulate angiogenesis but other tumorigenic steps as well. Several studies correlated VEGFs with cancer cell stemness through NRPs via Wnt/β-

catenin[408] or Hippo signalling pathways[409], contributing to tumour initiation and correlating with poor clinical outcome. VEGF-NRP axis promotes tumour aggressiveness and it might be mediated, in part, by integrins[410]. NRPs can also directly interact with integrins in endothelial and tumour cells modulating their function (**fig. 13**). In pancreatic and BrCa cells, NRP1 and NRP2 interacted with β1-integrins promoting ECM remodelling and conferring growth and survival advantage as well as promoting cell invasiveness[376,411]. A direct role in EMT was also proved where NRP2 was involved in TGFβ1-mediated EMT and cancer progression in several tumour types[398,412].

TGFβ is one of the most studied non-classical NRPs ligands (**fig. 13**). Both NRP1 and NRP2 are able to bind signalling TGFβRs as well as to active and latent TGFβ1 [412,413]. In addition, NRP1 was shown to participate in activation of TGFβ1 in BrCa cell lines[413]. Many studies have demonstrated that NRPs are involved in TGFβ signalling although the exact role remains controversial. NRP1 was shown to bind to TGFβRII inducing canonical signalling in glioblastoma and lung cancer, regulating tumour growth and progression[414,415]. In contrast, although NRP2 was up-regulated after TGFβ1 treatment in a Smad-dependent manner, TGFβ activity was independent of NRP2 in many other models[416,417]. Therefore, whether NRPs are part of the receptor complex activating TGFβ signalling or effectors of already activated TGFβ signalling is still unresolved.

Expression of NRPs, SEMA3s and PLXNs by stromal cells might modulate TME regulating tumour growth. NRP1-expressing fibroblasts associate to soluble fibronectin through α5β1-integrin, inducing fibronectin matrix remodelling promoting tumour growth[418]. Tumour-associated innate and adaptive immune cells express NRPs and have been implicated in pro- or anti-tumour functions[419,420]. NRP2-expressing TAMs have been shown to facilitate tumour progression by engulfing apoptotic tumour cells without triggering immune responses via efferocytosis[419]. Following tumour-derived SEMA3A gradient, NRP1 and PLXNA1/A4 expressing TAMs were recruited to hypoxic areas promoting inflammation and tumour growth[421].

Depending on the tumour type and stage, receptors expressed and growth factors present in the TME, SEMA3s can have a dual role on tumour progression. Some SEMA3s will be mostly anti-tumoral (SEMA3D, 3F, 3G), some will be pro-tumoral (SEMA3C) and others will have dual functions (SEMA3A, 3B, 3E)[398,422]. Since they are secreted, SEMA3s can have either autocrine or paracrine functions as well as they can modulate tumour and/or stromal cells[398,422,423]. In contrast with SEMA3s, the additional SEMAs in vertebrates have been described as angiogenesis and tumour progression promoters being considered feasible targets for cancer treatment[423]. SEMA3A inhibits tumour angiogenesis in many tumour types by competing with $VEGF_{165}$ for NRP1/VEGFR2 binding. Besides, in melanoma and prostate cancer cells SEMA3A inhibited migration and invasion[424,425]. Conversely, it promoted dissemination of cancer cells in glioblastoma and pancreatic cancer[426,427] as well as it regulated T cells inhibition[428] and TAMs-mediated angiogenesis in hypoxic tumours[421]. Little is known about SEMA3B role in tumours where controversial results have demonstrated that although down-regulated in PTs, SEMA3B was increased in disseminated cells[429]. SEMA3C expression is associated with tumour progression and poor prognosis. It induces cell migration, proliferation and metastasis *in vivo*[424,430,431] while its role in angiogenesis remains controversial. SEMA3D has been classically identified as an anti-tumour molecule inhibiting angiogenesis and tumour progression. However, in a recent publication, a pro-metastatic role has been described in pancreatic cancer activating PLXND1 in an autocrine manner[432]. SEMA3E is the only class 3 semaphorin that can bind its receptor, PLXND1, independently of NRPs and thus its role will depend on the availability of PLXND1, since it can also bind other ligands.

Hence, SEMA3E binding to PLXND1 inhibited apoptosis in metastatic BrCa[375]. SEMA3F is the best characterized anti-tumour class 3 semaphorin whose levels are reduced as the tumour progresses. It inhibits tumour growth and metastasis in several cancer types[433,434], likely through lymphangiogenesis inhibition via NRP2 [434,435]. The role of SEMA3G in tumour biology is largely unknown but it is most likely an anti-tumour semaphorin since its over-expression inhibited cell migration and invasion in glial tumours[436].

Although the role of SEMA3 family and NRPs have been implicated in several cancers, the role of PLXNs in tumorigenesis has not yet been deeply studied. There are several potential reasons for explaining the dual role of PLXNs in cancer, which alone or in combination, could make a PLXN either a tumour promoter or a tumour suppressor[437]. It is thought that type-A PLXNs are mainly down-regulated in many cancer types, suggesting tumour suppressor functions[438]. However, oncogenic roles for PLXNA1 and PLXNA4 have been described by regulating cell proliferation and tumour angiogenesis[439–441]. PLXNA2 is up-regulated in aggressive breast [442] and metastatic prostate[443] tumours, regulating cell migration and invasion. Conversely, PLXNA3 expression was observed to be lower in malignant breast[442], endometrial[444] and ovarian[445] cancers. Beyond the correlation of their expression and tumour progression, little is known about their mechanisms of action.

1.5.3.1. NRPs, SEMA3s and PLXNs in metastasis

NRPs are involved in physiological and pathophysiological regulation of angio- or lymphangiogenesis through VEGFs and SEMA3s. Therefore, in addition to tumour growth, they might be involved in tumour cells dissemination and thus metastasis formation. Nevertheless, the mechanisms by which NRPs, SEMA3s and PLXNs regulate cell dissemination and metastatic growth are far from being clear. It would be correct to assume that some of the mechanisms explained above for PTs could also be operational in metastatic tumour growth. In fact, SEMA3E over-expression by metastatic cells triggered PLXND1-dependent HER2 phosphorylation in lung and breast tumour cells inducing pro-invasive and pro-metastatic functions especially via MAPK and phospholipase-Cγ activation[446]. HER2 transactivation was also induced by PLXNB1 in a ligand-independent manner and its inhibition reduced lung metastasis in HER2-positive BrCa[447]. SEMA3E-PLXND1 axis is activated in many metastatic cell types[446] and it inhibited apoptosis in metastatic BrCa[375]. Nevertheless, a recent study demonstrated that osteoblasts-derived SEMA3E might inhibit BrCa bone metastases *in vivo* without affecting bone marrow vasculature[448]. Similarly, SEMA3F reduced colorectal cancer metastasis inhibiting the CXCR4/CXCL12 pathway[433], which is crucial for DTCs homing in bone marrow and secondary organs.

In addition to tumour initiation, tumour cells stemness is also related with tumour relapse. NRPs can activate Wnt/β-catenin and Hedgehog signalling pathways to protect cancer cells from cytotoxic drugs and apoptosis[408,449]. In addition, their expression is regulated in a positive feedback circuit[450]. Knocking down SEMA3F activated Wnt/β-catenin pathway in colorectal cancer cells increasing the expression of stemness-associated genes, tumour growth and metastasis. SEMA3F inhibited Rac1 although the associated PLXN required for the inhibition was not elucidated[451]. NRP2-VEGF-C axis also promotes resistance to therapy in cancer cells promoting autophagy during chemotherapeutic stress[452,453].

There are many evidence about the pro-metastatic functions of NRPs together with PLXNs and specific SEMA3s, above all regulating dissemination through angiogenesis. However, it is unknown

whether they might also regulate DTCs biology promoting survival, quiescence or proliferation in foreign environments. As far as it has been demonstrated, induction of stem-like phenotypes as well as treatments resistance might confer higher survival rates in secondary organs. Once DTCs colonise and adapt to secondary organs, turning on proliferation pathways in which several growth factors and NRPs are involved, might control secondary tumour bulk growth, contributing to the metastatic disease.

1.6. Background of the group

1.6.1. Role of neural mediators in breast cancer

During the last decades, the role of the nervous system on cancer progression has been increasingly recognized suggesting nerves and neural mediators are important elements of the TME. Several groups including ours, have demonstrated the presence of neurotransmitters and neuropeptides receptors in tumour cells[202], which would allow tumour-nerve crosstalk. In the last 10 years, our group has studied the role of substance P (SP) and its receptor neurokinin 1 (NK1), neuropeptides of the tachykinin family, in BrCa progression and treatment resistance. We have evidenced that both are over-expressed in BrCa, promoting the survival of tumour cells and favouring anti-HER2 targeted therapy resistance[454,455]. We have also explored the role of other neural mediators in therapy resistance. For instance, the relevant contribution of the histamine receptor 1 in increasing TNBC cells survival and resistance to trastuzumab[456]. In addition, our group has also focused on analysing the roles of neural mediators, such as glucocorticoids in BrCa initiation and aggressiveness. We have recently reported that physiological stress, through increased glucocorticoid blood levels, promotes the transition from DCIS to IDC, particularly by inducing myoepithelial cell apoptosis[457]. These studies suggest that neural mediators play an important role in BrCa initiation, progression and resistance to therapy. Furthermore, blocking these neural mediators could be a potential and innovative therapy against BrCa.

In an effort to identify putative therapeutic targets, our group has focused on identifying neurogenes associated to BrCa tumorigenesis to use them as biomarkers and/or treatment target candidates. Using bioinformatic tools, our group analysed three different genetic databases of human BrCa patients and identified 7 neurogenes that were differentially expressed among different BrCa subtypes and whose expression correlated with prognosis[458]. Among these genes, NRP2 was found to be over-expressed in basal subtype, the most aggressive BrCa subtype and with lower dormancy periods. In addition, NRP2 expression negatively correlated with patients' survival, patients with higher NRP2 expression having shorter OS[458]. Therefore, these results highlight the potential role of NRP2 in BrCa tumorigenesis and in fact suggest that NRP2 could be used as a prognostic biomarker.

1.6.2. Microenvironmental regulation of tumour dormancy

As mentioned in the *Introduction (section 1.4.3),* dormancy is a crucial trait that allows DTCs and micro-metastases to survive, adapt, and colonize a distant organ. Our previous studies have revealed a "seed and soil" mechanism where TGFβ2 and p38αMAPK regulate DTCs dormancy and define restrictive (bone marrow) and permissive (lung) microenvironments for metastasis[266]. Together with other studies, TGFβ family has been demonstrated to regulate DTCs fate where TGFβ2 regulates DTCs quiescence while TGFβ1 favours DTCs escape from dormancy[266,296]. These studies suggest that the interaction of DTCs with microenvironmental niches are imperative for the reactivation of dormant metastatic cells.

Hypothesis & Aims

Metastasis is the major cause of death associated with solid tumours and despite the improvements in tumour detection and therapies, currently, metastatic disease cannot be cured. Relapses are mainly due to clinically occult DTCs present in secondary organs that years or even decades after treatment of the primary lesion re-activate, proliferate and give rise to metastasis. This pause in tumour progression is due to the acquisition by these DTCs of a dormant behaviour. However, little is known about the signals that induce dormancy in DTCs and the signals that prompt the reprogramming from a dormant to a proliferative behaviour.

Our previous studies have shown that specific microenvironment-driven mechanisms control the growth arrest and survival of dormant DTCs[266]. In addition, we have found that NRP2 is up-regulated in BrCa basal patients (the ones with shorter metastasis-free periods). Furthermore, expression of NRP2 correlates with worse prognosis[458]. NRPs act as co-receptors for SEMA3s, several growth factors and integrins increasing ligand affinity for their receptors, and thus signalling activation, when associated with NRPs. NRPs are not able to transduce SEMA3s signals independently, and associate with type-A plexins (PLXNAs) or with plexin D1 [397,398]. SEMA3s, PLXNs and NRPs have been associated with tumorigenesis although little is known about NRPs, PLXNs and SEMA3s role in dormancy and DTCs regulation. Nevertheless, it is known that NRPs can interact with α5β1 and other integrins[376,377], which have been shown to be key regulators in the switch from cellular dormancy to metastatic growth[311,312,459]. Furthermore, NRPs have also been demonstrated to be involved in TGFβ signalling, which we and others suggest can regulate DTCs proliferation[266,291,296,298].

Therefore, we hypothesize that **NRP2 regulates DTCs biology generating a favourable microenvironment for the survival and proliferation of the DTCs, all stimulating metastases**.

The main objective of this project is to understand the role of NRP2 and its related proteins PLXNs-SEMA3s in BrCa and HNSCC progression, in the regulation of DTCs biology and in the metastatic ability. This would allow the integration of DTCs as a prognostic and predictive tool in advanced tumours treatment.

For that, the specific aims are:

1. To study the role of SEMA3F in tumour progression and tumour dormancy regulation in BrCa and HNSCC.
2. To study the role of PLXNA2 in ER-negative BrCa, focusing on its role in migration/invasion and cancer stem cells properties.
3. To study the role of PLXNA3 in ER-positive breast tumour growth.
4. To study the role of NRP2 in breast and head and neck tumour growth, DTCs biology and metastasis using *in vitro*, 3D and *in vivo* models to:
    4.1. Analyse the role of NRP2 in cell proliferation and quiescence induction, as well as in cell adhesion, migration and invasion *in vitro*.
    4.2. Analyse the role of NRP2 in tumour growth, DTCs fate and metastases development *in vivo*.
    4.3. Analyse the role of the lung microenvironment in the regulation of NRP2 expression in DTCs and in the switch from dormancy to proliferation.

Materials & Methods

3.1. Cell cultures

3.1.1. BrCa cell lines culture

A wide panel of BrCa cell lines was used for the whole study. The following BrCa cell lines were purchased from the American Type Culture Collection (ATCC; Rockville, MD) being classified according to the ER, PR and HER2 status molecular classification[460] in basal, HER2-enriched, luminal A or luminal B as specified in the following **table 4**:

Molecular classification	Cell line	Culture media	Media complementation	
Basal	**BT-549** (ATCC®HTB-122™)	RPMI-1640	10% FBS + 1% Gtx + 1% P/S	10µg/mL Insulin
	MDA-MB-231 (ATCC®HTB-26™)	DMEM-F12	10% FBS + 1% Gtx + 1% P/S	
	MDA-MB-468 (ATCC®HTB-132™)	DMEM-F12	10% FBS + 1% Gtx + 1% P/S	
HER2-enriched	**HCC1954** (ATCC®HTB-2338™)	RPMI-1640	10% FBS + 1% Gtx + 1% P/S	
	MDA-MB-453 (ATCC®HTB-131™)	DMEM-F12	10% FBS + 1% Gtx + 1% P/S	
Luminal B	**BT-474** (ATCC®HTB-20™)	DMEM-F12	10% FBS + 1% Gtx + 1% P/S	10µg/mL Insulin
Luminal A	**MCF7** (ATCC®HTB-22™)	DMEM	10% FBS + 1% Gtx + 1% P/S	10µg/mL Insulin
	T-47D (ATCC®HTB-133™)	RPMI-1640	10% FBS + 1% Gtx + 1% P/S	
	ZR-75-1 (ATCC®HTB-1500™)	RPMI-1640	10% FBS + 1% Gtx + 1% P/S	

Table 4. Molecular classification and culture condition of the breast cancer cell lines used. Cells were grown in DMEM, DMEM-F12 or RPMI-1640 media according to the ATCC indications. These media were supplemented with 10% foetal bovine serum (FBS), 5% Glutamax (Gtx) and 5% Penicillin-Streptomycin (P/S). Moreover, BT-549, BT-474 and MCF7 cell lines media was supplemented with 10µg/mL of human Insulin.

Controversy is found when classifying cell lines into BrCa subtypes following the molecular classification, especially regarding HER2-enriched and Luminal B subtypes. Nevertheless, the best established point is that comparing genomic and transcriptomic profiles, BrCa cell lines can be clearly subdivided in basal and luminal-clusters[461,462], as can PTs. Using this division, Kim and colleagues (2012)[338] generated a dormancy gene signature based on up- and down-regulated gene expression of dormancy regulating genes. They defined a dormancy score and used it to classify commercial BrCa cell lines as low dormancy score (LDS) or high dormancy score (HDS), relating them with higher or lower recurrence risk, respectively. As a result, the abovementioned BrCa cells lines were classified from lower to higher dormancy-score, as shown in **figure 14**.

All cell lines were cultured at 37˚C and in 5% CO_2 atmosphere, as indicated by the ATCC. Cells were grown in Dulbecco's Modified Eagle Medium (DMEM) (#41966-052, Gibco), DMEM-Nutrient Mixture F-12 (DMEM-F12) (#21331-046, Gibco) or Roswell Park Memorial Institute 1640 (RPMI) (#A10491-01, Gibco) culture media supplemented with 10% foetal bovine serum (FBS) (#10082-147, Gibco), 1% Glutamax (Gtx) (#35050-038, Gibco) and 1% Penicillin-Streptomycin mixture (P/S) (#15070-063, Gibco). For the BT-549, MCF7 and BT-474 cell lines the media was supplemented with 10µg/mL of Insulin (#I9278, Sigma-Aldrich) (**table 4**).

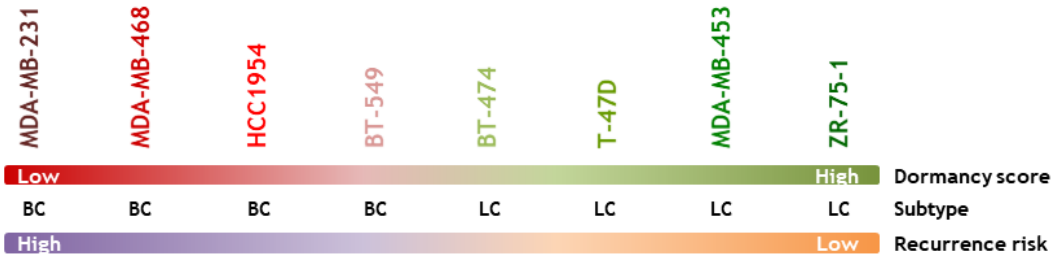

Figure 14. Dormancy score analysis in breast cancer cell lines. Cell lines used in this study are ordered by dormancy score (low to high from left to right) and recurrence risk (high to low from left to right). BC and LC stand for basal-cluster and luminal-cluster molecular classification, respectively. Figure adapted from Kim *et al.* (2012)[338].

3.1.1.1. Lung metastatic MDA-MB-453 cell lines generation

Five-week-old female athymic nude Foxn1^{nu} mice (Janvier, Europe) were used for inoculating $1.5 \cdot 10^6$ MDA-MB-453 cells tagged with mCherry and luciferase[145] in 1:1 ratio in a final volume of 150µL of Phosphate-Buffered Saline (PBS) (#14190-169, Gibco) and matrigel (#354234, Biosciences). The cells were orthotopically inoculated in two mammary fat pads per mouse. After three months of tumour growth, mice were euthanized. Tumours as well as likely metastatic secondary organs (i.e., lungs, bone marrow and brain) were surgically removed and fixed in 4% paraformaldehyde (PFA) for further experiments. In the case of the lungs, one lobule was fixed and the other lobule was used for isolating DTCs for the generation of metastatic lung derived cell lines, using a sterile biosafety cabinet. For that, lungs were minced using sterile razor blades obtaining small fragments, which were enzymatically digested at 37˚C during 30min in 200U/mL collagenase type IV and 100U/mL bovine serum albumin (BSA) solution (#C9891, Sigma-Aldrich). After homogenizing the suspension, collagenase was inactivated by adding complete culture media. Finally, the cell suspension was centrifuged at 1200rpm for 5min and the pellet was cultured in a 100mm Petri dish in complete culture media. After 48h, the adhered cells were treated with 2.5µg/mL of puromycin (#540411, Calbiochem) and mCherry expression was checked (**fig. 15**) for the selection and subsequent expansion of metastatic MDA-MB-453-mCherry-luc cells in complete culture media.

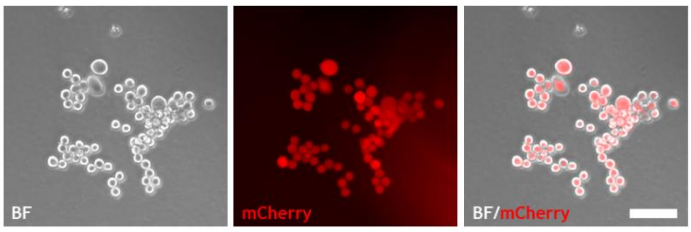

Figure 15. MDA-MB-453-mCherry lung DTCs in culture. Bright field (BF) representative images of mCherry signal (red) in MDA-MB-453 lung DTCs *in vitro*, after isolation and selection. Scale bar: 30µm.

3.1.2. HNSCC cell lines culture

Four different HNSCC cell lines were used for the whole study. All of them derived from the parental patient derived xenograft (PDX) human epidermoid carcinoma HEp3 (T-HEp3) cell line (**fig. 16**)[463], that is always kept *in vivo* either on the chicken embryo model or in mice as will be explained later. T-HEp3 cells were spontaneously reprogrammed by culturing them *in vitro* for 40 generations to create a dormant HEp3 (D-HEp3) cell line[464,465]. In addition, T-HEp3 cells were subcutaneously inoculated in *swiss nude* immunodeficient mice and spontaneous DTCs were isolated from the lung (Lu) and bone-marrow (BM) following their green fluorescent protein (GFP) tag and selected with G418 (#ALX-380-

013-G005, Enzo Life Sciences). These DTCs were cultured *in vitro* generating the proliferative Lu-HEp3 and quiescent BM-HEp3 cell lines, respectively[266].

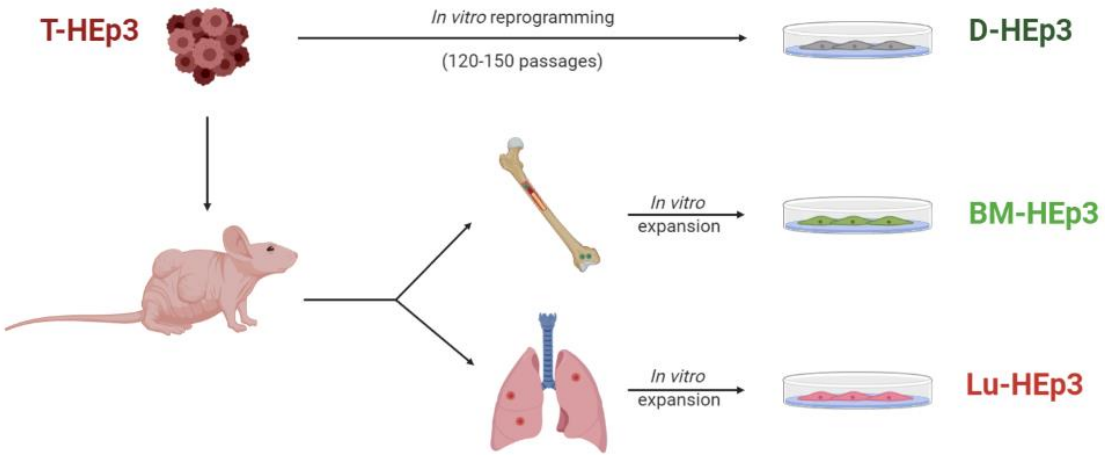

Figure 16. Flowchart of the methodological approach for HEp3 cell lines generation. Parental and primary HEp3 (T-HEp3) cells (obtained from human xenografts) were subcutaneously injected in nude mice. When the tumours reached ~500mm^3 they were surgically removed and cell dissemination was followed by GFP fluorescence. Afterwards, DTCs from the lung and the bone-marrow were isolated for generating stable cell lines *in vitro*[266]. T-HEp3 cells were also the source of D-HEp3 cells by spontaneous *in vitro* reprogramming after 120-150 passages[464, 465].

HEp3 cell lines were cultured at 37˚C and in 5% CO_2 atmosphere in DMEM-F12 media supplemented with 10% FBS, 1% Gtx and 1% P/S. They recapitulate the behaviour of the tumour cells *in vivo* having either a proliferative (T-HEp3, Lu-HEp3) or a dormant phenotype (BM-HEp3, D-HEp3) when inoculated *in vivo*[266]. HEp3 cells phenotype is expressed in response to conditions in the physiological environment but is lost progressively in cell culture[464]. Therefore, these cell lines were maintained as primary cultures and were cultured *in vitro* only up to passage 4. They were maintained *in vivo* using the chicken embryo chorioallantoic membrane (CAM) system (see *Materials & Methods, section 3.8.1* for further details) or inoculating them subcutaneously on nude mice (see *Materials & Methods, section 3.8.2* for further details) and then freezing cell suspensions from tumour collagenase as passage 0.

3.1.3. Other cell lines culture

For some experimental studies, in addition to the previously described BrCa and HNSCC cell lines, the following cell lines were also used:

3.1.3.1. Human bone marrow mesenchymal stromal cells

Human bone marrow mesenchymal stromal cells (hBM-MSC) were used to obtain condition media (CM) to mimic the BM microenvironment *in vitro*[266,466–468]. hBM-MSCs were obtained from BM aspirates of healthy individual donors between 18-25 years old, as previously described[469]. The use of BM aspirates followed the guidelines of a protocol approved by the Institutional Review Board of Hospital Clínic de Barcelona. Primary cultures of hBM-MSCs were established from 3 different donors. At confluence, the non-adherent cells were removed and the adherent cells were sub-cultured in α-MEM (#12571063, Gibco) with 20% FBS, passed at least five times. hBM-MSCs cultures were characterized by common MSC markers[470,471], such as CD45-/CD105+/CD146+, by flow cytometry (**fig. 17A**). In addition, under the right conditions, these primary cultures were capable of differentiating to osteocytes, adipocytes and chondrocytes showing their pluripotent potential (**fig. 17B**).

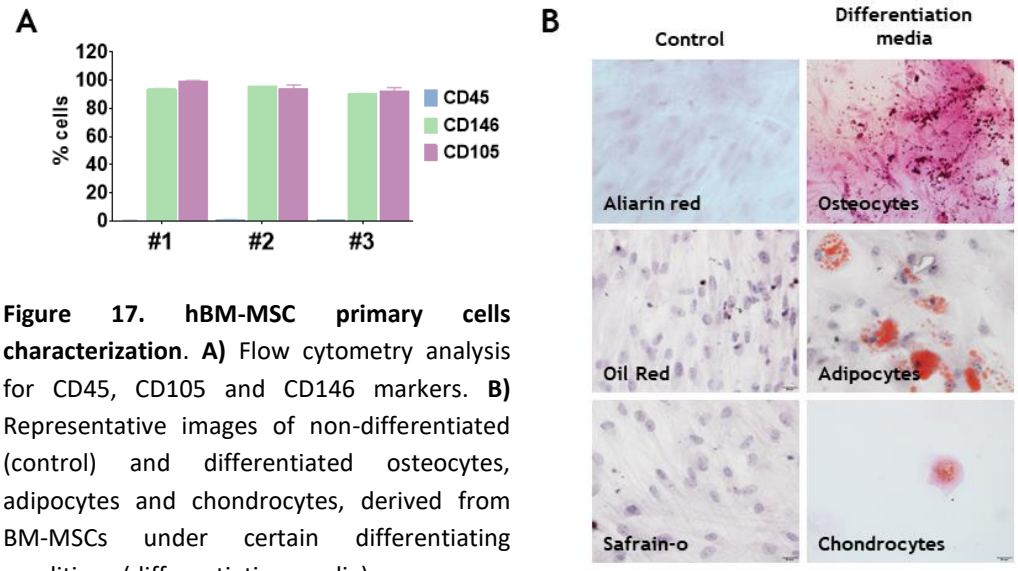

Figure 17. hBM-MSC primary cells characterization. **A)** Flow cytometry analysis for CD45, CD105 and CD146 markers. **B)** Representative images of non-differentiated (control) and differentiated osteocytes, adipocytes and chondrocytes, derived from BM-MSCs under certain differentiating conditions (differentiation media).

3.1.3.2. Macrophages

The human monocyte cell line THP-1 (ATCC®TIB-202™) (kindly provided by Dr. Julve from *Institut de Recerca de l'Hospital de la Santa Creu i Sant Pau*, Barcelona, Spain) were used for studying the effect of macrophages on the behaviour of tumour cells as part of the tumour microenvironment studies. THP-1 cells were cultured at 37˚C and in 5% CO_2 atmosphere in RPMI-1640 supplemented with 10% FBS, 1% Gtx, 1% P/S and 0.05M β-mercaptoethanol. THP-1 cells were differentiated into monocyte-derived macrophages using 50ng/mL of 12-O-tetradecanoylphorbol-l3-acetate (PMA; #P1585, Sigma-Aldrich) for 4 days. Total differentiation of monocyte-derived macrophages was obtained removing the PMA containing media and incubating the cells in fresh culture media for 1-2 days.

3.1.3.3. Fibroblasts

The human lung fibroblast cell line CCD-19Lu (ATCC®CCL-210™) and the immortalised human healthy lung fibroblast P5-C-fibro-Htert (CF5) (kindly provided by Dr. Alcaraz from University of Barcelona, Spain) were used for studying the effect of fibroblasts on tumour cells behaviour as part of the tumour microenvironment studies. CF5 cell line is a primary immortalised lung fibroblasts cell line generated by Dr. Alcaraz group[472]. Both CCD-19Lu and CF5 cells were cultured at 37˚C and in 5% CO_2 atmosphere in DMEM-F12 media supplemented with 10% FBS, 1% Gtx and 1% P/S.

3.1.3.4. HEK293 cell line

The human embryonic kidney cell line HEK293 (ATCC®HTB-1573™) was used for the generation of viruses due to its easy and high efficiency of transformation and protein production[473]. HEK293 cell line derives from transformed human embryonic kidney cells with fragments of human adenovirus type 5 in 1977 [473]. HEK293 cells were cultured at 37˚C and in 5% CO_2 atmosphere in DMEM media supplemented with 10% FBS, 1% Gtx and 1% P/S.

3.1.4. Generation of conditioned media

For the studies of TME effect on tumour cells functions we generated conditioned media (CM) from different stromal cells *in vitro*. For that, THP-1, CCD19, CF5 or hBM-MSC cell were cultured in regular conditions (37˚C and 5% CO_2) until they reached around 80% confluence. Then, after 2 washes with PBS, serum-free culture media was added for 48h. At this point, the culture supernatant was collected,

centrifuged during 5min at 1200rpm to eliminate cell debris and filtered with 0.22µm filter (#GE10462200, GE Healthcare). The obtained CM was aliquoted and stored at -80˚C until its use.

We also generated CM from chicken or mice lungs tissues to analyse whether lung microenvironment modulated cell behaviour. Lung tissues from healthy chicken embryos and healthy young (6 weeks) and old (16 months) C57Black6 mice (kindly donated by Dr. Porras from Complutense University of Madrid) were dissected and placed in a petri dish containing PBS supplemented with 1mM $MgCl_2$ and 0.5mM $CaCl_2$ (PBS++). Single cell suspension of lung tissues was obtained by mincing lungs into small pieces with the help of sterile scissors and razor blades, followed by an enzymatic dissociation by incubation with 200U/mL collagenase type IV and 100U/mL BSA solution for 30min at 37˚C. The tissue cell suspension was homogenized by gentle pipetting during and after the incubation time. After the 30min, collagenase activity was inhibited by adding 10% FBS containing media and after homogenizing, the sample was centrifuged (5min, 1200rpm). Subsequently, cell pellet was resuspended in 10% FBS DMEM-F12 complete media and plated in a 10cm petri dish. After 24h, fresh cell media was added and when 80% confluence was obtained, lung CM was generated as previously described for the stromal cell lines *in vitro*.

3.1.5. 3D cultures

The functional characteristics and the phenotypic features of the tumour cells were analysed by 3D cultures in matrigel. 24 hours before starting the protocol, the BD Matrigel™ Basement Membrane Matrix (#354234, Biosciences) was thawed at 4˚C and all the required material was placed at -20˚C in order to cool it to prevent matrigel gelling while manipulating.

The day of the experiment, 55µL of matrigel were added to each well of an 8-well chamber slide (#354108, BD Falcon CultureSlide), avoiding bubble formation and spreading it throughout the well. The chambers were incubated at 37˚C for no more than 45-60min for matrigel gelling. Meanwhile, cells were detached and prepared for culturing. Briefly, cells were washed twice with PBS and then detached with 25% Trypsin-EDTA (#25200-72, Gibco). Cells were counted using a Neubauer chamber and $1{\cdot}10^3$ MDA-MB-231 or T-HEp3 cells per well were seeded in 400µL of 3D culture media (DMEM-F12 + 5% FBS + 1% P/S + 2% matrigel). Cells were cultured for 7 days and media was changed every 3-4 days. Depending on the experiment, cells were treated every two days with the indicated compound by adding it directly to the well.

For 3D experiments fixation, media was carefully aspirated using a 200µL pipette. Then, 400µL 4% PFA was added through the walls and incubated at room temperature (RT) during 20min. Finally, after eliminating PFA, the wells were washed twice with PBS and the slides were stored at 4˚C with 500µL of PBS until further analysis.

3.1.6. Cell treatments: drugs and inhibitors

In this thesis, diverse treatments were performed to determine the role of NRPs, SEMAs and PLXNs in regulating DTCs survival and phenotype. The following table summarizes the compounds used as well as the treatment doses required for each experiment:

Compound	Brand	Catalogue nº (#)	Working concentration
αNRP2	R&D System	#AF2215	1µg/mL (2D cultures) 10µg/mL (CAM)
Oestradiol (E2)	Sigma-Aldrich	#E8875	1nM
Galunisertib (GNB)	Lilly		5µM
LY294002	Calbiochem	#440202	10µM
PD98059	Tocris Bioscence	#1213/10	20µM
SB-203580	Calbiochem	#559389	10µM
SB-431542	Millipore	#616461	5µM
SEMA3F	R&D System	#3237-S3-025	5ng/mL (2D cultures) 1µg/mL (CAM)
Tamoxifen	Sigma-Aldrich	#H7904	1µM
TGFβ1	R&D System	#240-B	2ng/mL (3D cultures) 5ng/mL (2D and CAM)
TGFβ2	R&D System	#302-B2	2ng/mL (3D cultures) 5ng/mL (2D and CAM)
VEGF-C	R&D System	#9199-VC-025	10ng/mL

Table 5. Treatments used for *in vitro* and *in vivo* experiments. Commercial brand, catalogue number and working final concentration for each compound are specified in the table. Some of the drugs were used at different final concentrations depending on the experiment.

3.2. Gene expression modulation

3.2.1. Small interfering RNA transfection

To study whether the modulation of the expression of several genes could modulate tumour cells behaviour their expression was inhibited through small interfering RNA (siRNA) transfection. For that, siRNA for neuropilin 2 (siNRP2) (ON-TARGETplus Human NRP2 (8828) siRNA; DharmaconTM), siRNA for plexin A2 (siPLXNA2) (ON-TARGETplus Human PLXNA2 (5362) siRNA; DharmaconTM) or siRNA for plexin A3 (siPLXNA3) (ON-TARGETplus Human PLXNA3 (8828) siRNA; DharmaconTM) were used, following the manufacturer's instructions. 50nM of siRNA was used for cell line transfection. siNRP2 and siPLXNA2 treated cell lines were single-transfected whereas siPLXNA3 treated cell lines were double-transfected (the second transfection was performed 24h after the first one).

Total RNA was isolated after 24h (for siNRP2) or 48h (for siPLXNA2 and siPLXNA3) of incubation as well as total protein was extracted after 48h (for siNRP2) or 72h (for siPLXNA2 and siPLXNA3) incubation.

3.2.2. CRISPR-Cas9 system

The Clustered Regularly Interspaced Short Palindromic Repeats (CRISPR) – associated protein 9 (Cas9) system was used as a genome editing technique in order to decipher the role of NRP2 in DTCs biology as well as in tumour progression and metastasis. To efficiently delete NRP2, the CRISPR-Cas9 technology using the double lentiviral system was used, designed by Zhang laboratory[474]. It requires two lentiviral vectors: plentiCas9-Blast plasmid (#52962, Addgene) and pLentiGuide-Puro plasmid (#52963, Addgene) (kindly donated by Dr. Gutierrez-Uzquiza from Complutense University of Madrid). The latest was modified in our laboratory with the single guide RNA of interest, to generate viruses carrying a sgRNA targeting human NRP2 gene. Altogether, the system would induce a double-strand break (DSB) which would be repaired by the non-homologous end joining (NHEJ) system[475,476] generating NRP2-deleted stable cell lines.

Briefly, LentiCas9-Blast lentiviral particles were generated in HEK293T cells (see *Materials & Methods, section 3.2.2.3* for further details). T-HEp3 and MDA-MB-231 parental cells were then infected with these lentiviral vectors to induce the expression of Cas9, and selected with blasticidine (10µg/mL) (#APA3784, PanReac AppliChem). Cas9-positive T-HEp3 and MDA-MB-231 cells were transformed with modified pLentiGuide-Puro lentiviral vectors containing the specific sgRNA for NRP2 (see *Materials & Methods, section 3.2.2.2* for further details) and selected with puromycin (1µg/mL; #P8833, Sigma-Aldrich). In parallel, non-targeting control (NTC) pLentiGuide-Puro plasmid was used for Cas9-positive cells infection in order to generate the Cas9-NTC expressing control cells. Double-infected cells were expanded following a single-cell cloning assay in order to obtain a pure T-HEp3 or MDA-MB-231-Cas9^{+}-NTC or NRP2^{KO} stable cell lines. Cas9 and NRP2 expression levels were checked by western blot and qPCR.

To develop NRP2-deleted (NRP2^{KO}) MDA-MB-231 and T-HEp3 stable cell lines, the following steps were followed:

3.2.2.1. CRISPR design

In order to delete NRP2 genomic sequence, a specific sgRNA was designed. The sgRNA must be specific to the target sequence, targeting a codifying sequence (exon) located at the beginning of the gene sequence (exons 2-4). sgRNAs are 18-20 base-pair length RNA sequences that recognize the target DNA region of interest and direct Cas9 nuclease there to introduce a premature STOP codon inhibiting the expression of the target sequence. Besides, these sgRNAs have a protospacer adjacent motif (PAM) sequence (specific for the used endonuclease; -NGG- for Cas9 endonuclease) at 3' of the 18-20 base-pair target that will allow the recognition and cleavage of the genome.

For sgRNA design, Synthego[477] and Benchling[478] free and online software were used. Combining both bioinformatics systems, sgRNA targeting exon 4 of NRP2 gene sequence was designed and DNA primers coding for that sgRNA (from here refer to them as sgRNAs) were purchased from Thermofisher: 5'-CACCGGACTGCA AGTACGATTGGC-3' (forward) and 5'-AAACGCCAATCG TACTTGCAGTCC-3' (reverse). The sgRNAs were designed to contain BsmBI restriction enzyme compatible sites for the following digestion. They were resuspended in TE buffer (10mM Tris-HCl, pH=8; 1mM EDTA) at a final concentration of 100µM each and stored at -20˚C.

3.2.2.2. Generation of NRP2 cloning vector

After the sgRNAs were designed, they were cloned in a pLentiGuide-Puro (LG; #52963, Addgene) lentiviral plasmid to be able to transfect HEK293 cells to produce recombinant viruses for BrCa and HNSCC cells infection. The puromycin resistance allowed the selection of HEK293 transformed cells.

3.2.2.2.1. Vector digestion and purification

In order to clone the target sequence into the above-mentioned plasmid backbone, it was first digested using BsmBI (#FD0454, ThermoFisher) restriction enzyme. 1µg plasmid was digested in a final volume of 30µL with 10X Fast Digest buffer (#B64, ThermoFisher), 1µL restriction enzymes and RNase-free water. The digestion solution was incubated over-night (ON) at 37˚C for a complete digestion. The digested plasmids were loaded in a 0.75% agarose gel to verify its linearity and integrity as well as to purify the correctly digested plasmid with the GeneJET Gel Extraction kit (#K0691, ThermoFisher).

3.2.2.2.2. sgRNAs annealing and ligation with lentiviral plasmids

Before the ligation, the designed sgRNAs were annealed in the following mix: 25µL of 2X annealing buffer (200mM CH_3CO_2K; 60mM Hepes-KOH, pH=7.4; 4mM $Mg(CH_3COO)_2$), 1µL Forward-sgRNA, 1µL Reverse-sgRNA and 23µL RNase-free water. After 5min of incubation at 95˚C, the annealed sgRNAs were slowly cooled down at RT.

For the sgRNA and plasmid ligation, the annealed sgRNAs were previously diluted 1:10 in RNase-free water) and incubated at RT during 20min in a final volume of 20µL containing 2µL of diluted and annealed sgRNAs, 5µL of purified plasmid (~50ng), 2µL 10X T4 DNA-Ligase buffer (#B69, ThermoFisher) and 1µL T4 DNA-Ligase (#EL0011, ThermoFisher). A negative control for each plasmid was also prepared where no T4 DNA-Ligase was added. This procedure yielded the ligated-NRP2 plasmids and the control ones as well.

3.2.2.2.3. Transformation and plasmid amplification

Finally, the ligated plasmids were used for the transformation of bacterial competent cells that would increase the yield of the cloning vectors.

Before starting the cloning protocol, sterile media and selection plates were prepared. For bacteria recovery and growing the nutrient rich Luria-Bertani (LB) media was prepared with 10% Tryptone, 10% NaCl and 5% Yeast extract in distilled water. After mixing all the components, the media was sterilised by autoclaving the solution on a liquid cycle (20min at 15psi). LB media could be stored either at RT or at 4˚C. In addition, selection Petri dishes were prepared to grow and select the transformed bacteria. Therefore, 15% agarose was added to the LB media before autoclaving it and once it was cooled down (~55˚C), ampicillin (#A9393, Sigma-Aldrich) was added at 100µg/mL. Finally, 10-12mL LB-Agar with ampicillin were added per Petri dish in a sterile environment and incubated at RT until it was totally gelled. Selection plates were stored at 4˚C until used.

After thawing the competent bacteria (#200315, Agilent Technologies) on ice, 4% β-mercaptoethanol was added and tubes were swirled to inactivate RNases and to increase the transformation efficiency. Bacteria were incubated on ice for 10min, swirling gently every 2min. Then, 2µL of the ligation reaction were incubated with 25µL of competent cells during 30min on ice. Right after, a heat shock process was performed to allow the entry of the cloning vector to the competent cells incubating the mix at 42˚C for exactly 30 seconds first, then on ice for 3min and at RT at the end. After adding 250µL of SOC recovery media (#F98226, Lucigen), bacteria were incubated at 37˚C in vigorous movement (300-500rpm) for 1h to allow culture growth. Finally, transformed bacteria were spread and incubated in tempered selection plates (LB-Agar with Ampicillin) ON at 37˚C.

Under the selective environment, only LG lentiviral plasmid containing bacteria survived and formed colonies. One of those colonies was picked and grown in 5mL of selective medium (LB with ampicillin) at 37˚C, 5% CO_2 and vigorous movement during 4h. After adding 25-30mL of selective media, bacteria were incubated at 37˚C and 5% CO_2 ON for plasmid amplification. Finally, isolation and purification of plasmid DNA was performed with Qiagen® Plasmid Midi kit (#12145, Qiagen) following manufacturer's instructions.

3.2.2.2.4. NRP2 CRISPR lentivirus production

For NRP2 CRISPR lentivirus production, a modified protocol from Addgene was used. Briefly, HEK293T packaging cells were seeded in fresh antibiotic free complete medium. When cells reached

60% confluence, half of the media was removed and DNA-Lipofectamine lipid complexes were added drop by drop. For DNA-lipid complexes generation, tube A and tube B contents were mixed in a 1:1 ratio and incubated during 10-20min at RT. Tube A had Lipofectamine 3000 transfection reagent (#15292465, Invitrogen) in Opti-MEM medium (#31985-070, Gibco) while tube B had packaging (psPAX2; #12260, Addgene), enveloping (pMD2-VSVg; #12259, Addgene) and LG-NRP2 plasmids in Opti-MEM medium. Next day, media was changed and replaced with fresh complete media. After 72h incubation, viruses were harvested by centrifuging the culture media at 500g for 5min and filtering the supernatant through a 0.45µm PES filter (#4654, Pall Life Science).

3.2.2.3. Generation of Cas9-positive cell lines

3.2.2.3.1. Generation of Cas9 lentiviral particles

LentiCas9-Blast plasmid (#52962, Addgene) packaging in lentiviral particles was carried out using HEK293T cells. As for LG-NRP2 lentivirus production, DNA-Lipofectamine lipid complexes were used for HEK293T infection. For DNA-lipid complexes generation, tube A and tube B were mixed in a 1:1 ratio and incubated during 10-20min at RT. Tube A had Lipofectamine 3000 transfection reagent in Opti-MEM medium while tube B had packaging (psPAX2), enveloping (pMD2-VSVg) and LG-Cas9 plasmids in Opti-MEM medium. After 24h, fresh media was added and following a 72h incubation, virus were harvested by centrifuging and filtering the culture media at 500g for 5min and filtering the supernatant through a 0.45µm PES filter.

3.2.2.3.2. Cell infection and selection

T-HEp3 and MDA-MB-231 cell lines were transduced with LG-Cas9 lentiviral particles. Briefly, cells were plated in 24 well dishes with fresh complete medium. When cells reached an 80-85% confluence, the medium was removed, a retroviral-enriched supernatant was added, and cells were incubated at 37°C and 5% CO_2 atmosphere. After 24h, media was changed and 48h after transduction cells were split in two wells and treated with 10µg/mL blasticidin. Individual clones were collected and amplified and the genotype was verified by Cas9 western blot (**fig. 18**).

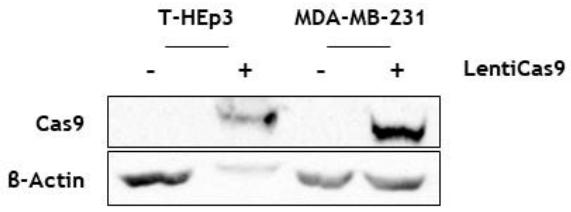

Figure 18. Cas9 protein expression in T-HEp3 and MDA-MB-231 cell lines. Representative western-blot analysis of Cas9 protein levels normalised with β-Actin in control (-) and Cas9-positive (+) T-HEp3 and MDA-MB-231 cells.

3.2.2.4. Generation of NRP2 silenced cell lines

For the generation of stable NRP2-silenced cell lines, Cas9 positive T-HEp3 and MDA-MB-231 cells were plated in 12-well dishes with fresh antibiotic free complete medium. When cells reached a 70-80% confluence, the LG-NRP2 lentiviral stock was diluted 1:4 in 0.5mL of fresh antibiotic free complete medium. The whole volume was added to each MW12 well and the cells were incubated at 37˚C ON. Then, media was changed and complete media was added followed by 48h incubation. Finally, stably transduced cells were submitted to antibiotic selection by adding puromycin (1µg/mL) (for LG-NRP2 selection) and blasticidin (10µg/mL) (for Cas9 selection).

From the CRISPR-Cas9 modified pool of cells, single NRP2-silenced clones were obtained by limited dilution and expansion. Polyclonal cells from the selection step were plated at a density of 15 cells/mL in a 96-well culture plate, adding 100µL of complete media with antibiotics per well. From the wells with only once cell, the total number of colonies per well was assessed assuming each colony as clonal. After the well reached high confluence, selected single-colony wells were initially expanded to 12-well and later to 6-well plates taking a small portion of the cells for checking the expression of the target protein.

3.3. Gene expression studies

3.3.1. Isolation and quantification of RNA

Total RNA from cells in culture or PTs was extracted using TRIzol™ (Invitrogen) according to the manufacturer's instructions. Briefly, 1mL Trizol was added for 0.5-1·10^6 cells lysis and homogenized by pipetting up and down. Then, 200µL chloroform was added per 1mL of Trizol reagent and the tubes were vigorously shaken by hand during 15sec. Samples were centrifuged at 12000g for 15min at 4˚C. Following centrifugation, the mixture separated into a lower phenol-chloroform phase, an interphase and an upper aqueous phase. The aqueous phase was transferred to a fresh tube where isopropyl alcohol was added for RNA precipitation (500µL of isopropyl per 1mL of Trizol). After 1h incubation at -20˚C, samples were centrifuged at 12000g for 10min at 4˚C and the RNA pellet was washed once with 70% Ethanol. Finally, the RNA pellet was dried and dissolved in 20µL RNase-free water. After its extraction, the RNA was quantified using a NanoDrop® spectrophotometer and RNA samples were stored at -80˚C for further analyses.

3.3.2. Reverse transcription

1µg RNA was reverse transcribed to its complementary DNA (cDNA) using a High Capacity cDNA Reverse Transcription Kit (#4368813, ThermoFisher) following the instructions indicated by the manufacturer. Briefly, 1µg RNA was incubated with 1X of reverse transcription master mix composed of the proper volumes of 10X reverse transcription buffer, 10X reverse transcription random primers, 25X dNTP mix (100mM each) and 1X MultiScribe® Reverse Transcriptase (50U/µL) in the needed final volume (10µL/reaction) with RNase-free water. Samples were placed in a thermal cycler where they were first incubated at 25˚C for 10min, then at 37˚C for 120min and finally at 85˚C during 5min for enzyme inactivation. cDNA samples were stored at -20˚C until use.

3.3.3. Quantitative polymerase chain reaction

For gene expression determination, a quantitative polymerase chain reaction (qPCR) was performed using the TaqMan gene expression assay on the 7900HT Fast Real-Time PCR System (Applied Biosystems). The reaction was done in a final volume of 10µL where 0.5µL probe (20X TaqMan® Gene Expression Assay), 5µL MasterMix (2X TaqMan® Gene Expression Master Mix), 2.5µL RNase-free water and 2µL cDNA template were added. Negative controls were prepared using RNase-free water instead of cDNA. The mRNA levels of the gene of interest were normalised with β-actin mRNA levels as endogenous control obtaining the relative expression. Relative expression levels were analysed in triplicates and were calculated using the ΔΔCt method ($2^{-\Delta\Delta Ct}$).

The probes used for each analysed gene were purchased from Applied Biosystems and are listed in the table below:

Gene	Catalogue nº	Gene	Catalogue nº
β-actin	Hs99999903_m1	**SEMA3A**	Hs00173810_m1
ALDH1	Hs02511385_s1	**SEMA3B**	Hs00190328_m1
CD44	Hs01075861_m1	**SEMA3C**	Hs00989373_m1
CD49f	Hs01041011_m1	**SEMA3D**	Hs00380877_m1
Dec2	Hs01036450_g1	**SEMA3E**	Hs00180842_m1
E-cadherin	Hs01023894_m1	**SEMA3F**	Hs00188273_m1
FoxC1	Hs00559473_s1	**SEMA3G**	Hs00220101_m1
NRP2	Hs00187290_m1	**Snail1**	Hs00195591_m1
NRP1	Hs00826128_m1	**TGFβ1**	Hs00998133_m1
PLXNA1	Hs00413698_m1	**TGFβ2**	Hs00234244_m1
PLXNA2	Hs00300697_m1	**TGFβRIII**	Hs01114253_m1
PLXNA3	Hs00250178_m1	**Twist**	Hs01675818_s1
PLXNA4	Hs00297356_m1	**Vimentin**	Hs00185584_m1
PLXND1	Hs00892410_m1		

Table 6. qPCR probes used in this study. All the probes were purchased from Applied Biosystems, with the listed catalogue number.

3.4. Protein analyses

3.4.1. Cell lysis

Cells were washed and detached with trypsin following a subsequent centrifugation at 1200rpm during 5min at 4˚C. Cell pellets were washed once with cold PBS supplemented with a protease and phosphatase inhibitor cocktail (#P8340, Sigma-Aldrich) and 1mM sodium orthovanadate (Na_3VO_4). Then, pellets were lysed for 25min at 4˚C in ice-cold radio-immunoprecipitation assay (RIPA) buffer (50mM Tris-HCl, pH=7.5; NaCl 150mM; 1% Triton X100; 0.5% sodium deoxycholate; 0.1% SDS; 0.2% NaF; 0.25mM EDTA, pH=8) supplemented with protease inhibitors and Na_3VO_4. After centrifuging the samples at 13000rpm during 15min at 4˚C, the supernatant containing the protein fraction was collected and quantified using the Pierce BCA Protein Assay Kit (#23225, Thermo Scientific), following manufacturer's instructions. Cell lysates were stored at -80˚C for further analyses.

3.4.2. Western blotting

For protein expression analysis, equal amounts of total protein were loaded in sodium dodecyl sulphate–polyacrylamide gels (SDS-PAGE) (**table 7**). Protein samples were prepared adding 5X loading buffer (50% glycerol; 10% SDS; 0.1% Bromophenol-Blue; 5% β-mercaptoethanol; 20% Tris-HCl 50mM, pH=6.6). After electrophoresis separation, the proteins were transferred to polyvinylidene difluoride membranes (Immobilon-P Membrane PVDF; #IPVH00010, Merck Millipore). All the transferences were performed in wet conditions, during 1.5h at 4˚C and 350 milliamperes (mA) except from the ones done for studying proteins bigger than 200kDa (such as PLXNs) that were transferred during 1.5h at 4˚C and 400mA. After antigen blocking with 5% milk in TBST solution (150mM NaCl, 20mM Tris-HCl pH=7.4, 0.1% Tween-20) during 1h at RT, membranes were incubated with primary antibodies ON at 4˚C. After three washes with TBST solution, membranes were incubated for 1h at RT with the appropriate secondary antibody conjugated to horseradish peroxidase. **Table 8** and **table 9** lists the primary and secondary antibodies used:

	Separating gel			
Compound	**8% Gel**	**10% Gel**	**12% Gel**	**Stacking gel**
30% Acrylamide/Bisacrylamide	2.7mL	3.3mL	4mL	0.830mL
1.5M Tris-HCl (pH=8.8)	2.5mL	2.5mL	2.5mL	-
1.5M Tris-HCl (pH=6.8)	-	-	-	0.630mL
10% SDS	100µL	100µL	100µL	50µL
10% Ammonium Persulfate	100µL	100µL	100µL	50µL
TEMED	4µL	4µL	4µL	5µL
H_20	4.6mL	4mL	3.3mL	3.4mL

Table 7. SDS-PAGE gels composition. The concentration of acrylamide used in the separation gel was determined depending on the size of the target protein. For small proteins higher concentrations of acrylamide were used (ex.: for p27 detection → 12% acrylamide gels) whereas for big proteins lower concentration acrylamide gels were used (ex.: for PLXNs detection → 8% acrylamide gels).

Primary antibody	Brand	Catalogue nº (#)	Origin	Dilution
α-Tubulin	Cell Signaling	#3873	Mouse	1/2500
β-Actin	Cell Signaling	#4970	Rabbit	1/2500
Bak	Cell Signaling	#12105	Rabbit	1/500
Cleaved Caspase-3 (Asp175)	Cell Signaling	#9661	Rabbit	1/500
Dec2	Santa Cruz	#sc-373763	Mouse	1/500
GAPDH	Cell Signaling	#2118	Rabbit	1/2500
Neuropilin-1	Cell Signaling	#3725	Rabbit	1/500
Neuropilin 2	R&D Systems	#AF2215	Goat	1/500
p21 Waf1/Cip1	Cell Signaling	#2947	Rabbit	1/500
p27 Kip1	Cell Signaling	#3686	Rabbit	1/500
Phospho-p38 MAPK (Thr180/Tyr182)	Cell Signaling	#9211	Rabbit	1/500
Phospho-p44/42 MAPK (Erk1/2) (Thr202/Tyr204)	Cell Signaling	#9101	Rabbit	1/500
Phospho-Smad2 (Ser465/467)	Cell Signaling	#3108	Rabbit	1/250
Plexin A2	Cell Signaling	#5658	Rabbit	1/250
Plexin A3	Cell Signaling	#5512	Rabbit	1/250
Puma	Cell Signaling	#12450	Rabbit	1/500
Total p38 MAPK	Cell Signaling	#9212	Rabbit	1/500
Total p44/42 MAPK (Erk1/2)	Cell Signaling	#9102	Rabbit	1/500
Total Smad2	Cell Signaling	#5339	Rabbit	1/500

Table 8. Primary antibodies used for protein analysis in this study. Commercial brand, catalogue number, origin and conditions used for each antibody are specified in the table. Primary antibodies were diluted in 1% milk in TBST except from the phosphorylated proteins that were diluted in 1% BSA.

Secondary antibody	Brand	Catalogue nº (#)	Dilution
Goat IgG, HRP Linked	Merck Millipore	#AP180P	1/2500
Mouse IgG, HRP Linked	GE HealthCare	#NXA931	1/2500
Rabbit IgG, HRP Linked	GE HealthCare	#NA934V	1/2500

Table 9. Secondary antibodies used for protein analysis in this study. Commercial brand, catalogue number, origin and conditions used for each antibody are specified in the table. Secondary antibodies were diluted in 5% milk in TBST.

Finally, after three washes with TBST solution, proteins were visualised using ECL substrate and a Luminiscent Image Analyzer (LAS4000 Imaging System; Fujifilm, Japan). ImageGauge and Image Studio

Lite software were used for densitometric quantification of the bands. α-Tubulin, β-Actin or GAPDH were used as internal loading controls.

3.4.3. TGFβ1 depletion by immunoprecipitation assay

To deplete TGFβ1 from conditioned culture media, an immunoprecipitation assay was performed using magnetic beads (#10003, Invitrogen). 10mg/mL magnetic beads were incubated with 10µg TGFβ1 antibody (#sc-52893, Santa Cruz) or matched IgG isotype control (#31903, Invitrogen) in a final volume of 200µL with serum-free media. The beads-antibody solution was pre-incubated during 1h at 4˚ºC and rotation movement. After spinning down for 10 seconds at 2000rpm, the magnetics beads were isolated using the magnetic rack. 1mL of the CM was added and incubated ON at 4˚C with rotation movement. The next day, centrifugation and isolation of magnetic beads was performed using the magnetic rack and the supernatant was collected for its immediately use for cell treatment.

Additionally, to ensure that the depletion was correctly performed, TGFβ1 was eluted and the solution was loaded in an acrylamide gel for a protein expression analysis. 40µL Laemmli buffer (1.0M Tris-HCl, pH=6.8; 8%SDS; 40% glycerol; 20% β-mercaptoethanol; 1% Bromophenol Blue) were added following an incubation of 10min at 70˚C for the separation of the TGFβ1 from the magnetic beads. Finally, the magnetic beads were isolated using the magnetic rack while the eluent was separated into a new vial for running a western blot.

3.4.4. Human TGFβ1 immunoassay

For the quantitative determination of activated human TGFβ1 concentrations in cell culture supernatants and CM, the Quantikine ® ELISA kit was used (#DB100B, R&D System), following manufacturer's instructions. This assay uses a monoclonal antibody specific for TGFβ1 previously pre-coated onto a microplate. It will recognize the TGFβ1 present in the media by a sandwich enzyme immunoassay technique. Briefly, cells CM were manipulated to activate latent TGFβ1 to immunoreactive TGFβ1 detectable by the kit. CM were incubated with 1N HCl for 10min at RT. After neutralization with 1.2N NaOH/0.5M HEPES, samples were immediately used. A TGFβ1 standard curve was prepared with known TGFβ1 concentrations (0-2000pg/mL) following 2-fold dilution series.

In order to perform the assay, first 50µL Assay Diluent RD1-21 and 50µL of sample were added to each well. Samples were incubated during 2h at RT. After four washes, 100µL of TGFβ1 conjugate were added to each well, following an incubation for 2h at RT. After repeating the wash steps, 100µL of substrate solution were added and the samples were incubated for 30min at RT, in dark conditions. Finally, optical density at 450nm was determined using a microplate reader (Sinergy, Bio Tek, VE, USA). Wavelength correction measurement was also performed at 540nm. For the calculation of the results, a standard curve was created and the concentration of the TGFβ1 secreted to the media was determined by extrapolation of the absorbance value.

3.5. Cell proliferation and viability assays

3.5.1. Cell proliferation assays: MTT assay

To analyse *in vitro* cell proliferation and viability MTT assay was performed using the Cell Titer 96 Aqueous One Solution Cell Proliferation Assay Kit (Promega, #G3581). Two different MTT assay types were performed. On one hand, to analyse the effect of SEMA3F or NRP2 blocking antibody on cell proliferation, 5000 cells were seeded in a final volume of 100µL per well in MW96 plates. After 24h, cells were treated for 72h with increasing concentrations of SEMA3F (0-3µg/mL) (#3237, R&D System)

or NRP2 blocking antibody (0-10ng/mL) (αNRP2; AF2215, R&D System) or with the corresponding vehicle concentration (PBS). Treatments were prepared in a final volume of 100µL reaching a total volume of 200µL per well during treatment. Different treatment doses were evaluated in sextuplicate.

For developing the colorimetric assay, 80µL of media were removed from each well and 20µL of the tetrazole MTT reagent were added. This process was also performed in three wells with no cells where only culture media was added for developing the blank measurements. After an incubation time of 45-60min at 37˚C (or until the colour become yellowish-reddish brown), absorbance was measured using a microplate reader spectrophotometer (Sinergy, Bio Tek, VE, USA). Measurements were made at 492nm (test wavelength) and at 620nm (reference wavelength), for noise correction. Afterwards, each measurement was normalised with the absorbance in the control situation where no treatment was added.

On the other hand, to determine the effect of NRP2 deletion in MDA-MB-231 and T-HEp3 cells proliferation, a 4-day cell-based proliferation assay was performed. Briefly, 7000 cells were seeded in a final volume of 200µL per well in MW96 plates. Cells were cultured in 2% FBS containing media. After 24h, the colorimetric assay was performed by removing 80µL of media from each well and adding 20µL of the tetrazole MTT reagent. This process was also performed in three wells with no cells where only culture media was added for developing the blank measurements. After 1.5h incubation at 37˚C absorbance at 492nm and 620nm was measured. This procedure was repeated every day during 4 days in a row, with 6 replicates for each condition.

3.5.2. Colony formation assay

For measuring the anchorage-dependent growth ability of the cells, colony formation assays were performed. Briefly, 300 cells were seeded in 60mm diameter dishes in complete culture media. Cell media was changed every 2-3 days and cells were grown at 37˚C between 1-3 weeks until they were able to form independent colonies. Required treatment was added to the media every time it was refreshed. After colonies were formed, media was removed and dishes were washed twice with PBS. Then, cells were stained with crystal violet (HT90132; Sigma-Aldrich) adding 3 drops of the die directly to the plate and incubating it for 1min at RT. The crystal violet was removed and washed with PBS until only the foci were stained. The anchorage-dependent growth capacity of the cells was determined quantifying the area and the number of the colonies using ImageJ software. Experiments were performed in triplicate.

3.5.3. Annexin V assay

For studying cell apoptosis, Annexin-V staining assay was performed. Cells were seeded in 60mm diameter dishes in complete culture media and grown until 70-80% confluence. Later described treatments were performed for the corresponding time and dose for each particular experiment. At the end point, apoptosis was determined using the Annexin V-FITC Apoptosis Detection Kit (#BMS500FI, eBiosciences), according to the manufacturer's instructions. Both attached cells and cells from the supernatant were collected in 15mL Falcon tubes and incubated for 15min at 4˚C in dark conditions with Annexin V-FITC and propidium iodide (PI) solution, diluted in 1X Binding buffer. Then, cells were centrifuged at 2000rpm at 4˚C during 5min and washed once with cold PBS. Finally, cells were resuspended in 1X Binding buffer and analysed by flow cytometry. Control conditions were also performed such as the non-stained (Binding buffer only), Annexin V-FITC only and PI only conditions, in order to determine the proper settings in the FACS Calibur flow cytometer (Fortessa LSR). The results

were analysed by FACSDiva software (Becton-Dickinson). 10.000 cells were analysed for each sample as well as duplicates were performed for each experimental condition.

3.5.4. Cell cycle analysis: PI assay

In order to analyse tumours cell cycle, a cell cycle assay with PI was performed. Cells were seeded in 60mm diameter dishes in complete culture media and grown until 70-80% confluence. Later described treatments were performed for the corresponding time and dose for each particular experiment. Both attached cells and cells from the supernatant were collected in 15mL Falcon tubes. Cells were resuspended in 200µL cold PBS and fixed with cold 70% ethanol added dropwise in slight rotational movement. At this point samples could be stored at 4˚C until they were analysed. Finally, fixed cells were incubated for 15min at 4˚C with PI/RNase Staining Buffer (#550825, BD Pharmingen) adding 500µL of the buffer for every 10^6 cells. After washing once with cold PBS, cells were resuspended in PBS and analysed using flow cytometry (Fortessa LSR). 10.000 cells were analysed for each sample as well as duplicates were performed for each experimental condition.

3.6. Cell adhesion, migration and invasion assays

3.6.1. Cell adhesion assay

For cell adhesion evaluation, 100.000 cells were seeded per well in 12-well tissue culture plates in 10% FBS culture media and incubated at 37˚C and 5% CO_2 during 1.5h. Then, adhered cells were fixed and stained with crystal violet at RT as described in *Materials & Methods, section 3.5.2*. Excess of staining solution was removed with PBS and the number of adhered and stained cell was quantified using ImageJ software.

3.6.2. Wound-healing assay

For determining cell migration capacity, the wound-healing assay was performed. Cells were plated in 24-well tissue culture plates so that at 24h they reach a confluence of ~70-80% as a monolayer. Then, the wound was made scratching the monolayer with a 10µL pipette tip across the centre of the well. After scratching, detached cells were washed with fresh medium and the well was replenished with fresh serum-free medium and the required treatment, when necessary. Cells were allowed to migrate for 24-48h or until the wound was closed, at 37˚C and 5% CO_2. Cell migration was followed over time by a phase-contrast LEICA DFC295/DMIL LED microscope coupled to a digital camera. Photos were taken at different time points (0h, 4h, 8h and 24h/48h) and the migration capacity of the cells was determined quantifying the percentage of the wound closing area using the ImageJ software.

3.6.3. Transwell invasion assay

To analyse the ability of the tumour cells to invade, we performed an invasion assay using 6.5mm Transwell® with 8.0µm pore polycarbonate membrane inserts (#3422, Corning) coated with matrigel. The day before, matrigel was thawed at 4˚C. For generating the extracellular matrix layer that cells must cross depending on their invasion capacity, matrigel was diluted in 1:4 (for SEMA3F experiments) or 1:9 (for $NRP2^{KO}$ experiments) ratio with chilled serum-free culture media prior to the coating. 100µL of diluted matrigel were added directly to the centre of the 24-well transwell inserts. The plate was left in the incubator at 37˚C and 5% CO_2 for 2h to allow matrigel gelling. Meanwhile, tumour cells were detached with 25% Trypsin-EDTA and after collecting them in complete culture media (containing 10% FBS) the cells were centrifuged at 1200rpm at RT for 5min. Between $5{\cdot}10^4$-$1.5{\cdot}10^5$ cells (depending on the experiment) were seeded over the upper matrigel layer in 200µL serum-free media, with the

appropriate treatment when necessary. 600µL of complete culture medium (with 10% FBS as chemoattractant) were added to the lower chamber. The plate was incubated for 24h at 37˚C and 5% CO_2 to allow cell invasion through the matrigel layer. At the end, the inserts were transferred to a new 24-well plate with 4% PFA to fix the cells adhered to the lower part for 20min at RT. The cells were then stained with crystal violet for 30min at RT. To drain off the excess of dye the inserts were washed with water by immersing them in a glass with distilled water until no more dye was released and only the invasive cells remained stained. Finally, the inserts were air-dried before taking photos by a digital camera coupled to a phase-contrast microscope for cell counting.

3.6.4. DQ Collagen invasion assay

The invasion capacity of tumour cells was also analysed performing the DQ Collagen assay where the degradation of the extracellular matrix would determine the invasiveness of the cells. The day before, matrigel was thawed at 4˚C in the refrigerator. First, a lower matrigel layer was generated in an 8 multi-well chamber (#155411, Lab-Tek) adding 25µg/mL DQ™ collagen (#D12052, Invitrogen) with a final volume of 100µL in each well. The plate was left in the incubator at 37˚C and 5% CO_2 for 30min to allow matrigel gelling. Meanwhile, tumour cells were detached with 25% Trypsin-EDTA and after collecting them in complete culture media (containing 10% FBS) cells were centrifuged at 1200rpm at RT for 5min. $3 \cdot 10^4$ cells were seeded per well over the matrigel-collagen layer in 500µL serum-free media, with the appropriate treatment when necessary, supplemented with 4% matrigel. The plate was incubated for 24-96h at 37˚C and 5% CO_2 to allow 3D culture formation. Photos were taken every 24h using an immunofluorescence confocal microscope since the fluorogenic DQ™ collagen allowed us to monitor the collagenase activity of the cells. The invasion capacity was measured by quantifying the emitted GFP signal derived from the degradation of the DQ™ collagen present in the extracellular matrix.

3.7. Immunofluorescence staining

To analyse the expression and the localisation of the proteins either in tumour cells or in tumour tissues, several immunofluorescence (IF) staining were performed. Prior to the staining, cells grown in 2D were fixed with 4% PFA for 20min at 4˚C whereas tumour tissues were fixed with 4% PFA ON at 4˚C. In addition, tissue samples were embedded in paraffin by the biobank facility of the Clinic Hospital-IDIBAPS (Barcelona, Spain). Cells grown in 3D were fixed as previously described in *Materials & Methods, section 3.1.5*.

3.7.1. Immunofluorescence in 2D cultures

For IF staining of cells grown in 2D in coverslips, cells were permeabilised with 0.1 or 0.5% Triton X-100 diluted in PBS for no longer than 10min in a humidified chamber. When analysing membrane or transmembrane proteins no permeabilization was performed. After washing the samples with PBS, cells were blocked with 50µL primary blocking solution (5% normal goat serum –NGS-, 5% normal rabbit serum –NRS- or 5% BSA in IF washing solution) (IF washing solution: 0.02% Tween-20 in PBS) at RT for 1h. Then, cells were incubated ON in a humidified chamber at 4˚C with 30µL of the primary antibody (see **table 10** for the antibodies and dilutions used) diluted in blocking solution. After washing the samples with PBS, the coverslips were incubated with 40µL of appropriate secondary antibodies (**table 11**) diluted in blocking solution for 1h at RT in dark conditions in a humidified chamber. Finally, after three washes with PBS, nuclei were stained with 30µL Hoechst (50ng/mL) (#H3570, Life Technologies) for 15min at RT in dark. After removing the excess of dye washing twice with PBS and

once with distilled water, the coverslips were mounted on glass with Prolong Gold Antifade Mountant reagent (#36930, Thermofisher).

Primary antibody	Brand	Catalogue nº (#)	Origin	Dilution
cErbB2/Her2	Calbiochem	#OP15L	Mouse	1/100
Cleaved Caspase-3 (Asp175)	Cell Signaling	#9661	Rabbit	1/50
Her2	Abcam	#ab214275	Rabbit	1/100
Ki67	Abcam	#15580	Rabbit	1/1000
Ki67	Dako	#M724	Mouse	1/200
Ki67	Invitrogen	#14-5698-82	Rat	1/100
Meca32	Pharmingen	#550563	Mouse	1/50
Neuropilin-1	Cell Signaling	#3725	Rabbit	1/50
Neuropilin-2	R&D Systems	#AF2215	Goat	1/50
p27 Kip1	Cell Signaling	#3686	Rabbit	1/50
Phospho-Histone H3 (Ser10)	Cell Signaling	#9706	Mouse	1/50
Plexin A2	Cell Signaling	#5658	Rabbit	1/50
Plexin A3	Cell Signaling	#5512	Rabbit	1/50
TGFβ1	Santa Cruz	#sc-52893	Mouse	1/50
Vimentin	Abcam	#ab20346	Mouse	1/100
Vimentin	Cell Signaling	#5741	Rabbit	1/100
Vimentin	R&D Systems	#MAB2105	Rat	1/100

Table 10. Primary antibodies used for immunofluorescence staining in this study. Commercial brand, catalogue number, origin and conditions used for each antibody are specified in the table.

Secondary antibody	Brand	Catalogue nº	Dilution
Alexa Fluor 488 Goat anti-mouse IgG	Invitrogen	A-11029	1/1000
Alexa Fluor 488 Goat anti-rabbit IgG	Invitrogen	A-11034	1/1000
Alexa Fluor 488 Donkey anti-goat IgG	Invitrogen	A-11055	1/1000
Alexa Fluor 555 Goat anti-mouse IgG	Invitrogen	A-32727	1/1000
Alexa Fluor 555 Goat anti-rabbit IgG	Invitrogen	A-21428	1/1000
Alexa Fluor 568 Goat anti-rabbit IgG	Invitrogen	A-11011	1/1000
Alexa Fluor 568 Goat anti-rat IgG	Invitrogen	A-11077	1/1000
Alexa Fluor 568 Donkey anti-goat IgG	Invitrogen	A-21432	1/1000
Alexa Fluor 647 Goat anti-rat IgG	Invitrogen	A-21247	1/1000
Alexa Fluor 647 Donkey anti-goat IgG	Invitrogen	A-32849	1/1000
APC conjugated Goat anti-mouse IgG1	Invitrogen	A-10541	1/1000

Table 11. Secondary antibodies used for immunofluorescence staining in this study. Commercial brand, catalogue number, origin and conditions used for each antibody are specified in the table.

3.7.2. Immunofluorescence in 3D cultures

For IF staining of cells grown in 3D, cells were permeabilised for no longer than 10min with 0.5% Triton X-100 diluted in PBS. After washing the samples with 0.75% Glycine-PBS, cells were blocked with 200µL of primary blocking solution (5% NGS, 5% NRS or 5% BSA in IF washing solution as in *Materials & Methods, section 3.7.1*) at RT for 1-1.5h. Then, cells were incubated ON at 4˚C with 100µL primary antibody solution (**table 10**). After washing the samples with PBS-Glycine, an incubation of 1h at RT and dark conditions was performed with 100µL of secondary antibodies (**table 11**). Finally, after three washes with PBS-Glycine, nuclei were stained incubating the samples with 30µL Hoechst (50ng/mL) for 15min at RT in dark conditions. After washing the samples with PBS-Glycine once and with PBS twice, the plastic chamber of every slide was lifted from the glass by cutting in between with a razor blade. The coverslips were mounted on glass with an excess of Prolong Gold Antifade Mountant

reagent to avoid bubble formation. The slides were sealed with nail polish after they were completely dry.

3.7.3. Immunofluorescence in tissue samples

For IF staining of tissue samples, after tissue fixation and paraffin embedding the obtained blocks were used to construct slides with tissue cuts of 4µm thickness. Samples were deparaffinised incubating the slides at 65˚C for 30min and hydrated following a xylene and decreasing ethanol gradient (100-70%). After, slides were incubated in a steamer containing citrate buffer (10mM Citric Acid, 0.05% Tween-20, pH=6.0) for antigen retrieval for 45min. When cooled down, all the samples were permeabilised with 0.1% or 0.5% Triton X-100 in PBS (when required) for 5min at RT and blocked with 3% BSA-1.5% NGS in PBS, 3%BSA-1.5% NRS in PBS or 5%BSA in PBS for 30min at RT. Then, the samples were incubated ON at 4˚C with subsequently specified primary antibodies in 3% BSA-PBS in a humidified chamber (**table 10**). After washing with PBS, the secondary antibodies diluted in 3% BSA-PBS were added for 1h at RT in dark conditions in a humidified chamber (**table 11**). Finally, the samples were incubated with Hoechst for 15min at RT in dark conditions and after washing twice with PBS and once with distilled water, they were mounted in Prolong Gold Antifade Mountant reagent and kept at -20˚C.

All the samples were visualised using either an inverted epifluorescence microscope (Leica SP2) or a confocal microscope (Zeiss 880). Image assembly and processing was performed using the ImageJ and Leica-Zen3.2 (blue) software.

3.8. *In vivo* experiments

3.8.1. Chicken embryo chorioallantoic membrane assay

For the *in vivo* experiments using the chicken embryo chorioallantoic membrane (CAM) model (**fig. 19**) we used premium specific pathogen-free (SPF), fertile, 11-day incubated embryonated chicken eggs supplied by Gibert farmers (Tarragona, Spain). After arrival, embryonated eggs were incubated for two days at 37˚C in a humidified chamber and in rotation to increase their survival rate. At day 11, tumour cells were grafted *in vivo* introducing 50µL of the cell suspension through a small window made in the shell and above the lowered CAM. For the CAM to be dropped, an air pocket between the shell egg and the CAM was performed. HNSCC cells diluted in PBS++ (supplemented with 1mM $CaCl_2$ and 0.5mM $MgCl_2$) were inoculated on the CAM after being either pre-treated for 24h or transfected with a specific siRNA. BrCa cells were diluted in a 1:1 relation matrigel:PBS++ solution in order to increase their engraftment and survival. 50µL of the cell suspension were inoculated per egg, whereas the number of inoculated cells varied depending on the cell line: $3 \cdot 10^5$cells/egg for T-HEp3 and Lu-HEp3, $1 \cdot 10^6$cells/egg for MDA-MB-231 and $1.5 \cdot 10^6$cells/egg for ZR-75-1. When necessary, while incubating at 37˚C but without rotation, tumours were treated daily and from the day after the inoculation, preparing the treatment in a final volume of 50µL PBS++. The number of days (4 to 6 days) the experiments lasted depended on the experiment and it is specified further for each experiment in the *Results* and *Discussion* sections. At the end, the PTs were excised, weighed, measured and fixed in 4% PFA for 20min at 4˚C. In addition, chicken embryos lungs and liver were also isolated for cell dissemination analysis fixing both with 4% PFA for 20min at 4˚C. All the tissue samples were embedded in paraffin after PFA fixation for further IF studies.

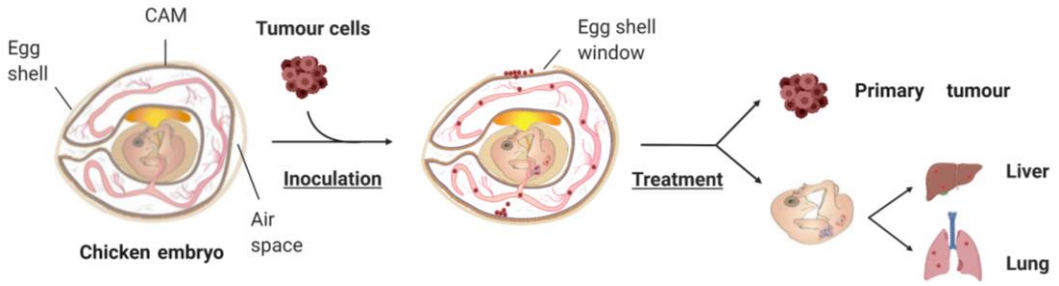

Figure 19. *In vivo* chicken embryo CAM model. Tumour cells were inoculated in 11-day old chicken embryo CAM. After 4 to 6 days of incubation, where daily tumour treatment could be performed, primary tumour growth was analysed. In addition, cell dissemination to secondary organs was also studied by isolating and fixing chicken embryos liver and lungs.

Besides IF studies, PTs and chicken livers and lungs could be enzymatically dissociated for RNA analysis or DTCs counting, respectively. Tissues were dissociated and minced with sterile scissors and razor blades and transferred to a new 15mL Falcon tube. Samples were incubated with type 1A Collagenase (#C9891, Sigma-Aldrich) at 37˚C for 30-60min. After homogenizing the suspension, collagenase was inactivated with complete culture media. Then, the suspension was centrifuged at 1200rpm at RT for 5min and the pellet resuspended in PBS++ for washing. For PT samples, the cell pellet was stored at -80˚C for RNA extraction and gene expression analysis by performing a qPCR. For lungs and livers, the total number of DTCs was counted detecting the number of GFP-positive cells using a haemocytometer under the fluorescence microscope.

3.8.2. *In vivo* 1: xenograft mouse model, orthotopic inoculation

Five-week-old female NOD-SCID mice (CB17/IcrHanHsd-PrKdc Scid) were obtained from Janvier Labs (France, Europe). Xenograft tumours were obtained by orthotopic inoculation of 1:1 ratio mixture of matrigel and PBS++, in a final volume of 100µL per mouse. Either $8{\cdot}10^5$ of T-HEp3-NTC or T-HEp3-NRP2^{KO} cells were inoculated in mice neck area. Mice weight and tumour growth were measured twice per week using a calliper, where tumour volume (V) was calculated as $V=(D*d)^2/2$ (D: long diameter; d: short diameter). Once tumours volumes mean was around of 1000mm^3 (in NTC group) or 300mm^3 (in NRP2^{KO} group), PTs were surgically removed and mice were left for 4 additional weeks. Surgically removed PTs were measured, weighted and stored at -80˚C for protein and RNA extraction or fixed in 4% PFA for further immunohistochemical analyses. After 4 weeks growth, mice were anesthetized and euthanized in accordance with the regulations of the institution's ethics commission. At the end point, potential metastatic organs such as the lungs were surgically removed and fixed in 4% PFA for the analysis of the presence of DTCs (**fig. 20**).

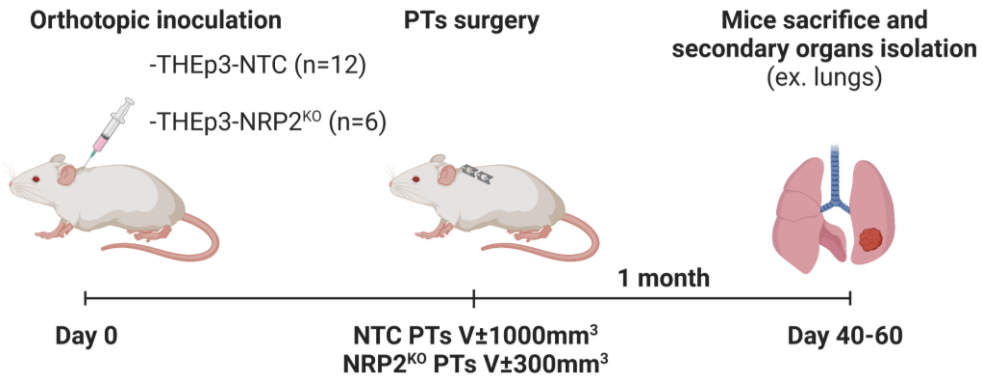

Figure 20. Tumour xenograft *in vivo* assay in mice. $8{\cdot}10^5$ of T-HEp3-NTC or T-HEp3-NRP2^{KO} cells were inoculated in mice neck area, in a 1:1 matrigel:PBS++ mixture. 12 mice were inoculated with T-HEp3-NTC cells whereas 6 mice were inoculated with T-HEp3-NRP2^{KO} cells. Mice weight and PTs volume was measured every 3-4 days and when PTs volume reached 1000mm^3 (in NTC group) or 300mm^3 (in NRP2^{KO} group) they were surgically removed. 4 weeks after surgery, mice were euthanized and potential metastatic organs were removed (ex. lungs) as well as tumour relapses, when grown. All tissue samples were either fixed in 4% PFA or enzymatically dissociated with type 1A collagenase for further analyses.

3.8.3. *In vivo* 2: tail vein injection

Five-week-old female NOD-SCID mice (CB17/IcrHanHsd-PrKdc Scid) were obtained from Janvier Labs (France, Europe). $2{,}5{\cdot}10^5$ of T-HEp3-NTC or T-HEp3-NRP2^{KO} cells or $5{\cdot}10^5$ of MDA-MB-231-Cas9 or MDA-MB-231-NRP2^{KO} cells were inoculated into the lateral caudal tail vein. 5 mice per group were inoculated for each condition. The cells were inoculated in a final volume of 100µL per mouse, diluted in PBS++. Mice weight was measured twice per week. 2 weeks and 4 weeks after inoculation, mice were anesthetized and euthanized in accordance with the regulations of the institution's ethics commission. At the end point, lungs were removed for metastasis analysis, by fixing them in 4% PFA for the analysis of the presence of DTCs by immunocytochemistry (**fig. 21**).

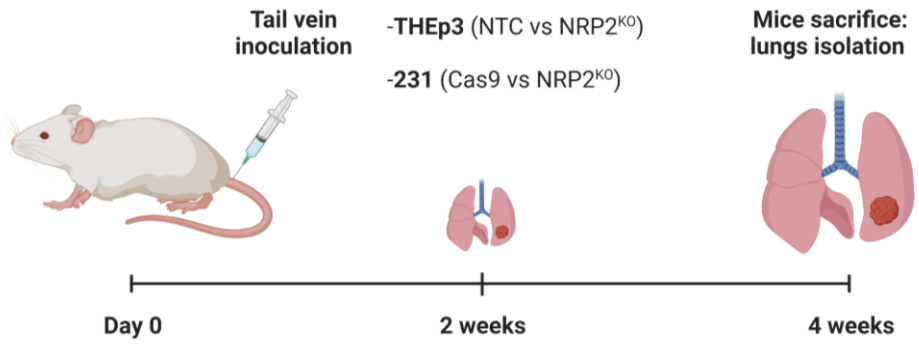

Figure 21. *In vivo* tail vein mouse model. $2{,}5{\cdot}10^5$ of T-HEp3-NTC or T-HEp3-NRP2^{KO} cells or $5{\cdot}10^5$ of MDA-MB-231-Cas9 or MDA-MB-231-NRP2^{KO} cells diluted in PBS++ were inoculated into the lateral caudal tail vein. 2 weeks and 4 weeks after inoculation, mice were euthanized and lungs were isolated for cell dissemination analyses.

3.9. Studies with patients

NRPs, SEMA3s and PLXNs mRNA or protein expression was analysed in BrCa or HNSCC patients' data using GOBO[479,480], Kaplan-Meier plotter[481], GEPIA (Gene Expression Profiling Interactive Analysis)[482] and CANCERTOOL[483] public databases. GOBO[479,480] consists of 1881 BrCa tumour samples where gene expression levels, identification of co-expressed genes and association with outcome for single genes analyses can be performed. Kaplan-Meier plotter[481] includes data from GEO (Gene Expression Omnibus), TCGA (The Cancer Genome Atlas) and EGA (European Genome-phenome Archive) to analyse 7830 human BrCa samples and determine the relapse free and overall survival. GEPIA[482] was used for analysing the RNA sequencing expression data in HNSCC patients from the TCGA and the GTEx (Genotype-Tissue Expression) projects. CANCERTOOL[483] was used to perform gene expression comparative analyses between different groups of BrCa patients, where different datasets can be used for the analyses. In addition, in collaboration with Dr. Camacho and Dr. Leon from Sant Pau Hospital (Barcelona, Spain), NRP2 mRNA expression was analysed by qPCR in PT samples in a cohort of 92 HNSCC patients and correlated with distant metastases-free survival (DMFS).

3.10. Statistical analysis

The results were graphically plotted and statistically analysed using GraphPad Prism7 software. Graphs represent the mean value of the samples ± standard error of the mean (S.E.M.). To compare two experimental groups the unpaired *t*-Student's test was used whereas one-way ANOVA or two-way ANOVA test were used to compare more than two groups, with one or two variables, respectively. Multiple comparison tests were performed after. Statistical significance was considered when the p-value was lower than 0.05, following the next annotation: *p-value ≤ 0.05, **p-value ≤ 0.01, ***p-value ≤ 0.001 and ****p-value ≤ 0.0001.

Results

4.1. NRPs, SEMA3s and PLXNs expression characterization in BrCa and HNSCC cell lines

Neuropilins are transmembrane glycoproteins widely expressed in several cancer types that have been related with tumour progression. Although they lack active cytoplasmic domain, they act as co-receptors for several ligand-receptor partners, such as SEMA3s and PLXNs, forming an heterotetrameric complex[349,397]. Despite the fact that they have been related to metastasis, little is known about the mechanisms and the role of NRPs regulating DTCs fate once they reach secondary organs such as lungs. Therefore, we wanted to determine whether NRP2 regulates DTCs phenotype at secondary organs.

4.1.1. Characterization of NRPs expression in BrCa and HNSCC cell lines

In order to determine the role of NRP2 in tumour progression and metastasis development, we first determined the expression of NRPs in a wide variety of BrCa cell lines (**fig. 22**). The BrCa cell lines used can be classified either by their molecular subtypes (basal, HER2-enriched, luminal A or luminal B)[25] or by a dormancy-signature score based on the expression of dormancy regulating genes[338]. According to the latest, BrCa cell lines can be classified as low dormancy-score (LDS) or high dormancy-score (HDS) cell lines considering the ratio between the expression of positive dormancy genes (ex. *BHLHE41* -Dec2-, *NR2F1*, *TGFβ2*) and negative dormancy genes (ex. *ATF4*, *EGFR*, *PIK3CB*). Therefore, the proliferation rate and risk of recurrence will be higher in LDS than in HDS cell lines[338]. In this way, MDA-MB-231, MDA-MB-468, HCC1954 and BT-549 are considered LDS cell lines whereas BT-474, T-47D, MDA-MB-453 and ZR-75-1 are classified as HDS cells (**fig. 22A**).

Having all of this into account, we analysed NRPs mRNA levels by qPCR in different human BrCa cell lines and also in the human healthy mammary epithelial cell line MCF10A. We found that NRP1 and NRP2 were up-regulated in LDS cell lines compared to HDS. NRP2 gene expression was down-regulated in HDS when compared to MCF10A cells as well (**fig. 22B**). Next, we studied NRPs protein levels by western blot, where both NRPs protein expression corresponded with mRNA levels. We found that NRP1 and NRP2 protein levels were up-regulated in LDS cells, above all in MDA-MB-231 and BT-549, in contrast with their lower levels in HDS cell lines (**fig. 22C**). Moreover, we also performed an immunofluorescence staining to determine NRPs localization and we detected no differences in NRPs distribution between BrCa cell lines with proliferative or dormant-like phenotypes (**fig. 22D**).

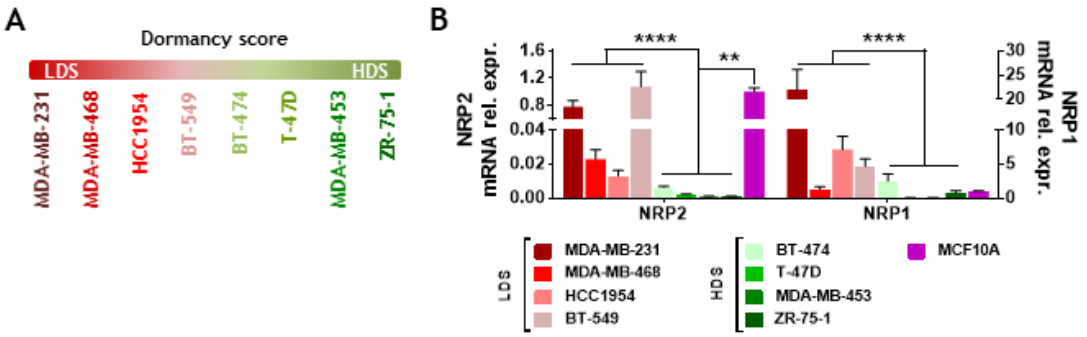

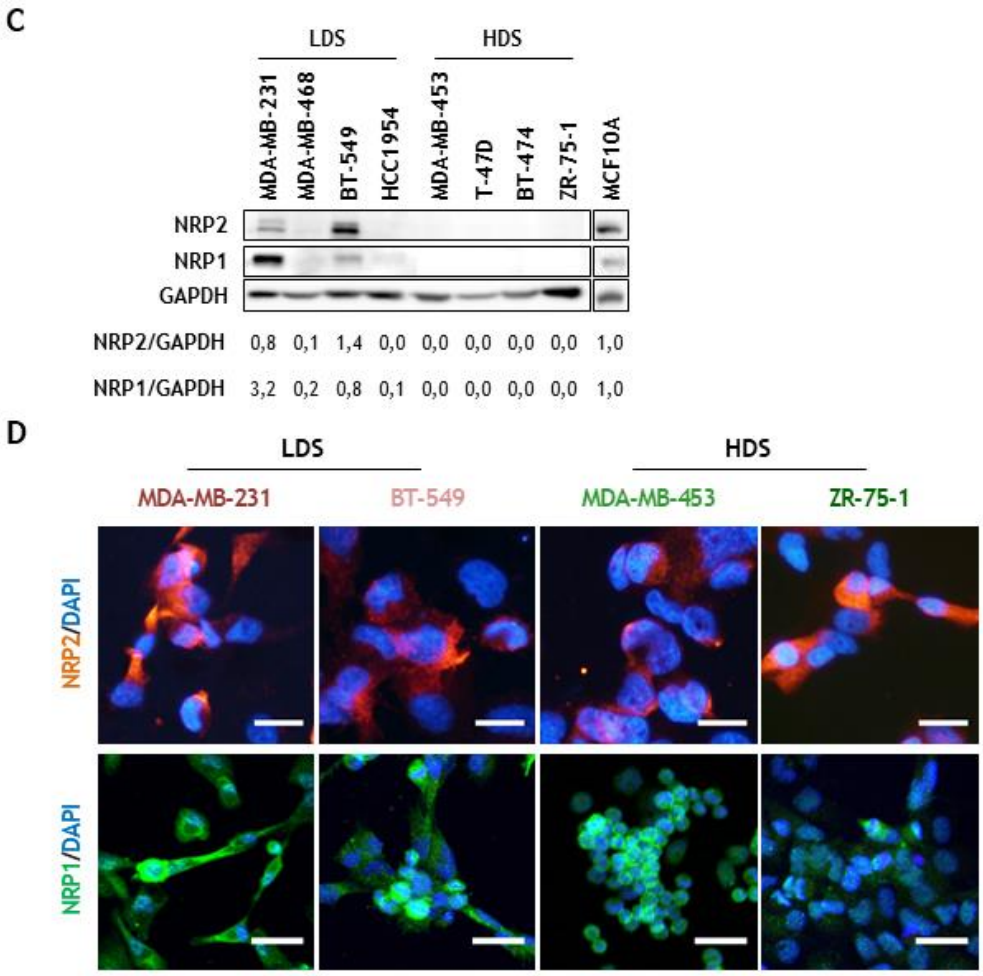

Figure 22. Characterization of neuropilins expression in BrCa cell lines. **A)** Schematic representation of the dormancy score of BrCa cell lines. LDS, low dormancy-score (MDA-MB-231, MDA-MB-468, HCC1954 and BT-549 cell lines); HDS, high dormancy-score (BT-474, T-47D, MDA-MB-453 and ZR-75-1 cell lines). **B)** Analysis of NRPs mRNA relative expression in human healthy mammary epithelial and BrCa cell lines. The graph shows relative quantification (RQ) values referred to MCF10A cells (n=3). The graph represents RQ mean values ± S.E.M.; **P < 0.01, ****P < 0.0001 comparing LDS *vs* HDS cell lines by *t*-Student's test. **C)** Representative western-blot analysis of NRPs protein levels normalized with GAPDH. Protein quantifications are referred to MCF10A (n>3). **D)** Representative immunofluorescence (IF) images of NRPs expression in LDS (MDA-MB-231, BT-549) and HDS (MDA-MB-453, ZR-75-1) cell lines. Scale bar: 20µm (NRP2 images, top panel) and 40µm (NRP1 images, lower panel) (n=2).

These results suggested that NRP2 and NRP1 expression is inversely correlated with a dormant phenotype. To confirm this, we tested the expression of NRPs in a panel of HNSCC proliferative and dormant cell lines[266] (**fig. 23A**). As described in *Materials & Methods, section 3.1.2*, DTCs were isolated from lung (Lu) and bone marrow (BM) from a HNSCC patient derived xenograft (PDX) model (T-HEp3) and expanded into cell lines that mimic the behaviour of lung DTCs and BM DTCs *in vivo* respectively (**fig. 16**)[266]. The lung DTCs derived cells (Lu-HEp3) are proliferative, meanwhile the BM DTCs derived cell line (BM-HEp3) has a dormant phenotype[266]. We have validated these cell lines as a good model to study DTCs biology, since the mechanisms we have discovered using these models were later found to be also operative in patient-derived DTCs[293,339,340]. In addition, we have also used an *in vitro* derived dormant variant of HEp3 (D-HEp3)[266]. When we analysed NRPs levels, we found that NRP1 and NRP2 were up-regulated in proliferative HNSCC cell lines, both at mRNA (**fig.**

23B) and protein levels measured by western blot (**fig. 23C**). NRPs protein localization analysis determined by IF staining showed no differences in their cellular distribution between HNSCC cell lines with proliferative or dormant phenotypes (**fig. 23D**).

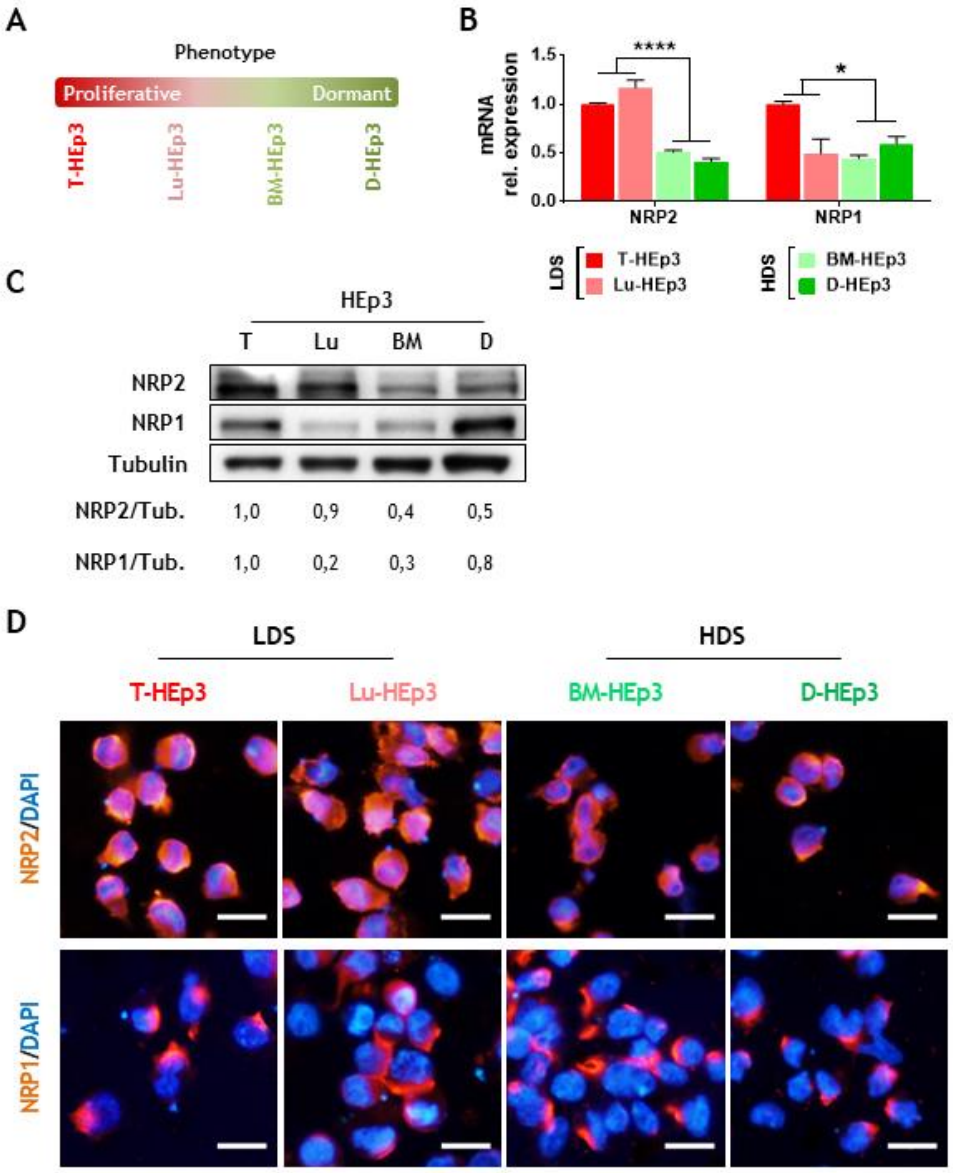

Figure 23. Characterization of neuropilins expression in HNSCC cell lines. **A)** Schematic representation of the dormancy phenotype of HNSCC cells. Proliferative, T-HEp3 and Lu-HEp3; dormant, BM-HEp3 and D-HEp3. **B)** Analysis of NRPs mRNA relative expression in our panel of HNSCC cell lines. The graph shows RQ mean values ± S.E.M. referred to T-HEp3 cells (n>3); *P < 0.05, ****P < 0.0001 comparing proliferative *vs* dormant cell lines by *t*-Student's test. **C)** Representative western-blot analysis of NRPs protein levels normalized with β-Tubulin. Protein quantifications are referred to T-HEp3 cells (n>3). **D)** Representative IF images of NRP2 (upper panel) and NRP1 (lower panel) expression. Scale bar: 20µm (n=2).

Consequently, these results showed that NRPs expression is down-regulated in dormant cells lines, both in BrCa and HNSCC cell lines and hence, correlates with a more proliferative phenotype.

4.1.2. Characterization of PLXNs expression in BrCa and HNSCC cell lines

In view of the significative increase in the expression of NRPs in more proliferative BrCa and HNSCC cell lines, we decided to analyse PLXNs expression as well in both models as they are the NRPs classically described receptor partners in the nervous system[367].

In BrCa cell lines, PLXNs mRNA levels analysis showed that PLXNA2 was significantly over-expressed in LDS cell lines whereas PLXNA3 expression was up-regulated in HDS cells (**fig. 24A**). However, the difference was not that clear for PLXNA2 protein levels when we analysed them by western blot where it was mainly up-regulated in HCC1954 cells (LDS) (**fig. 24B**). On the contrary, PLXNA3 protein levels concurred with mRNA levels since they seemed to be up-regulated in HDS cells (MDA-MB-453, ZR-75-1) compared to LDS cells when analysed by western blot (**fig. 24B**). Nevertheless, when we analysed PLXNAs protein localization by IF we found that there were no differences in their cellular distribution between BrCa cell lines with proliferative or dormant phenotypes (**fig. 24C, D**).

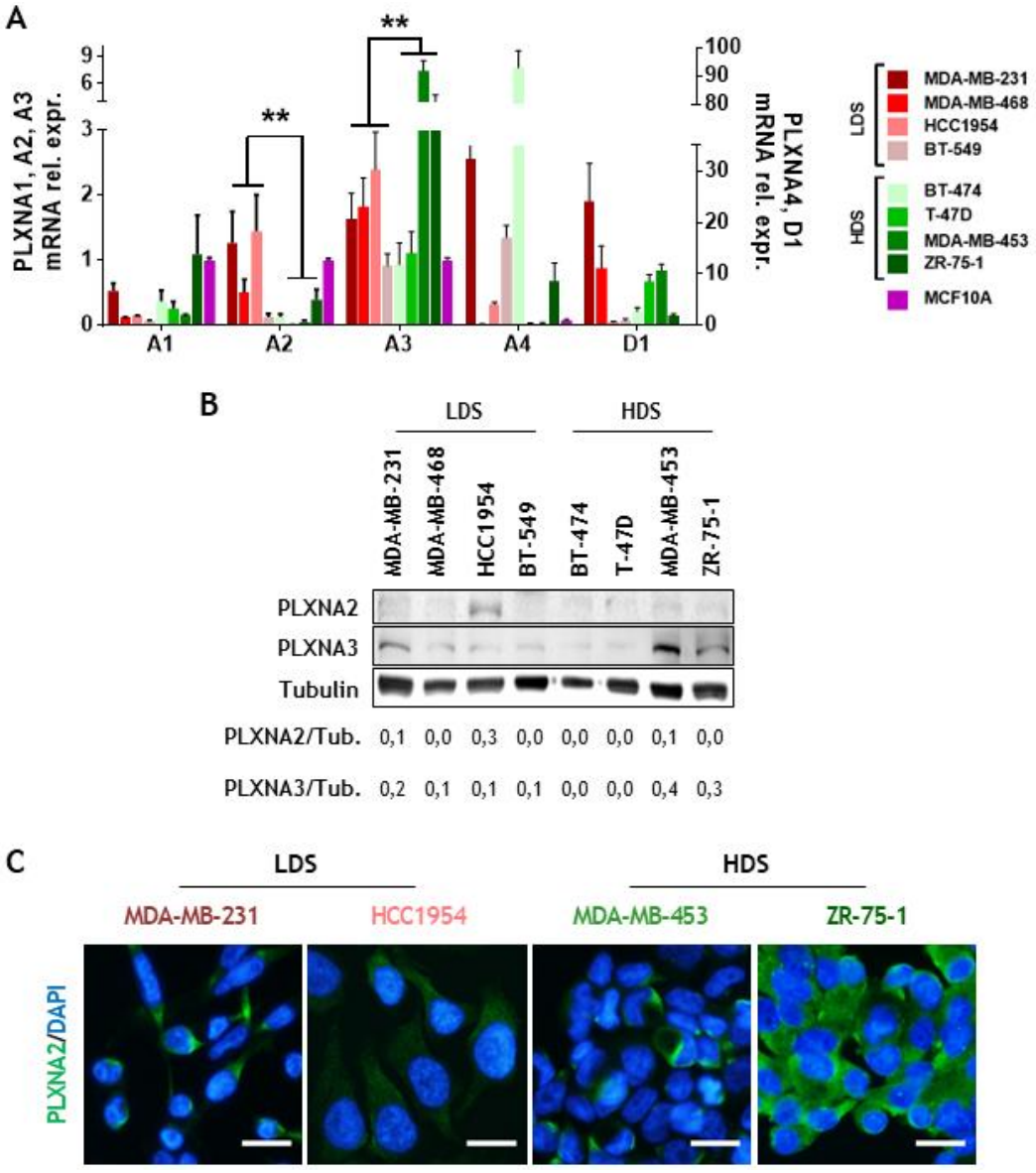

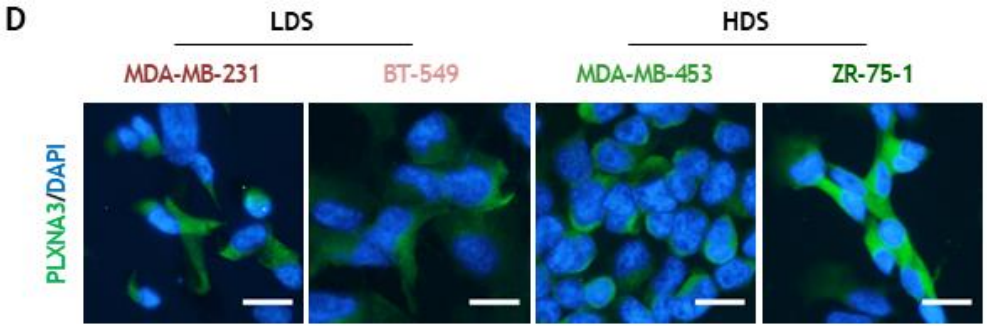

Figure 24. Characterization of plexins expression in BrCa cell lines. **A)** Analysis of PLXNs mRNA relative expression in human healthy mammary epithelial and BrCa cell lines. The graph shows RQ mean values ± S.E.M. referred to MCF10A cells (n>3); **P < 0.01 comparing LDS *vs* HDS cell lines by *t*-Student's test. **B)** Representative western-blot analysis of PLXNA2 and PLXNA3 protein levels normalized with β-Tubulin (n=3). **C, D)** Representative IF images of PLXNA2 (**C**) and PLXNA3 (**D**) expression in LDS (MDA-MB-231, HCC1954 or BT-549) and HDS (MDA-MB-453, ZR-75-1) cell lines. Scale bar: 20µm (n=2).

On the other hand, analysis of PLXNs in the HNSCC cell lines revealed that their expression levels are lower than in BrCa cells, being more challenging to determine their role in this model. PLXNA2 seemed to be slightly up-regulated in Lu-HEp3 and BM-HEp3 cells both at mRNA and protein levels (**fig. 25A, B**). Both Lu-HEp3 and BM-HEp3 cells derived from DTCs suggesting a potential role in DTCs biology. In agreement with the results of our BrCa cell lines, we found that PLXNA3 was over-expressed in dormant HEp3 cell lines at mRNA level as did PLXNA4 and PLXND1 genes (**fig. 25A**). Nevertheless, PLXNA3 expression could not be detected by western blot. However, we were able to detect it when analysing PLXNs protein distribution by IF, where no differences in plexins distribution were observed between proliferative and dormant phenotype HEp3 cells, neither in PLXNA2 nor in PLXNA3 (**fig. 25C**).

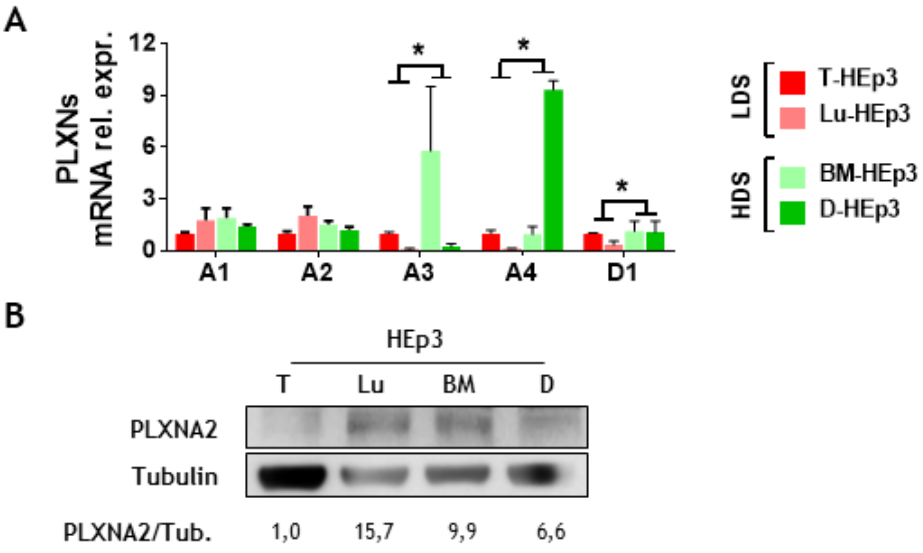

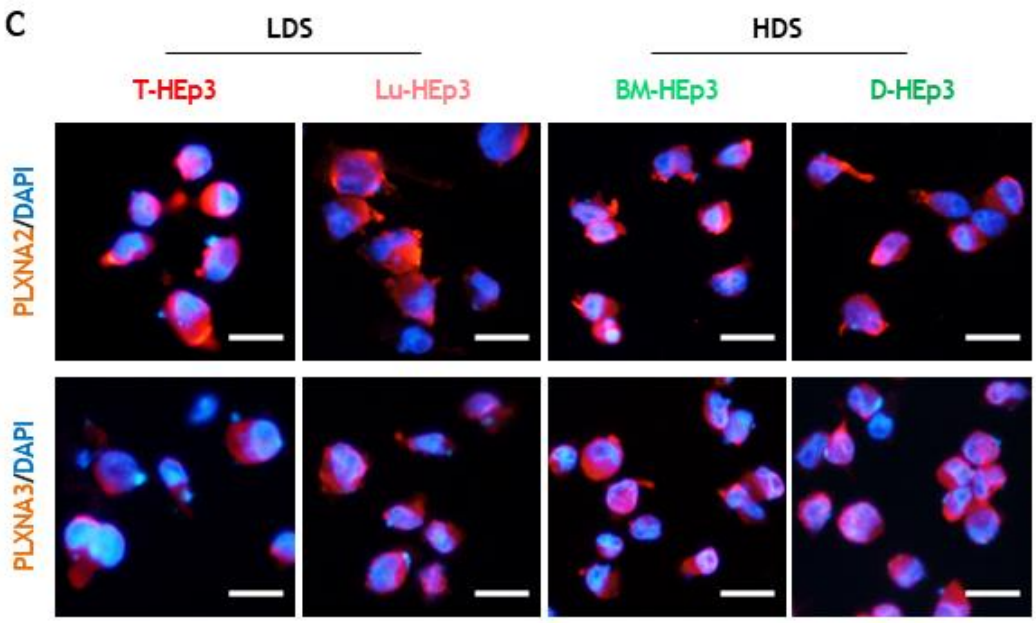

Figure 25. Characterization of plexins expression in HNSCC cell lines. **A)** Analysis of PLXNs mRNA relative expression in our panel of HNSCC cell lines. The graph shows RQ mean values ± S.E.M. referred to T-HEp3 cells (n=3); *P < 0.05 comparing proliferative *vs* dormant cell lines by *t*-Student's test. **B)** Representative western-blot analysis of PLXNA2 protein levels normalized with β-Tubulin. Protein quantifications are referred to T-HEp3. **C)** Representative IF images of PLXNA2 (upper panels) and PLXNA3 (lower panels) expression. Scale bar: 20µm (n=2).

As shown in **figure 24** and **figure 25**, we studied all the members of the PLXN family that can participate in the formation of the heterotetrameric receptor complex with NRPs but we mainly found statistically significant differences between proliferative/LDS and dormant/HDS cell lines in PLXNA2 and PLXNA3 expression. For that reason, we decided to continue studying the role of these two proteins in our models of study.

4.1.3. Characterization SEMA3s expression in BrCa and HNSCC cell lines

Finally, to further characterize the role of NRPs and their receptor partners in tumorigenesis, we analysed the expression of SEMA3s that are the main ligands of NRP-PLXN axis. SEMA3s are the only members of the semaphorin family that can be released and act as an autocrine or paracrine regulatory signal[398].

In this context, we found that of all the members of the family, only SEMA3A, SEMA3C and SEMA3F had statistically significant expression differences in the BrCa cell lines panel (**fig. 26A**). SEMA3A is described as a dual-function semaphorin, which could act as a pro-tumoral or anti-tumoral protein depending on the tumour type and the receptor complexes present on tumour cells[422,423]. In our BrCa cell lines, SEMA3A was down-regulated in HDS compared to LDS and MCF10A cell lines (**fig. 26A**) which made us consider SEMA3A as a pro-tumoral protein. SEMA3C is widely described as a pro-tumoral protein promoting tumour growth and cell dissemination[422,423]. Surprisingly, it was up-regulated in HDS cell lines (**fig. 26A**) making us consider it as a pro-dormancy gene in our model. Finally, SEMA3F which is commonly classified as an anti-tumoral protein in diverse tumour types[422,423], was shown to be clearly over-expressed in HDS cell lines (**fig. 26A**). Thus, we considered SEMA3F as a pro-dormancy gene in our BrCa model. Regarding SEMA3s expression in HNSCC, we observed a statistically significant over-expression of SEMA3B and SEMA3F in

dormant cell lines (**fig. 26B**) while there were no significant differences in any of the other members of the family.

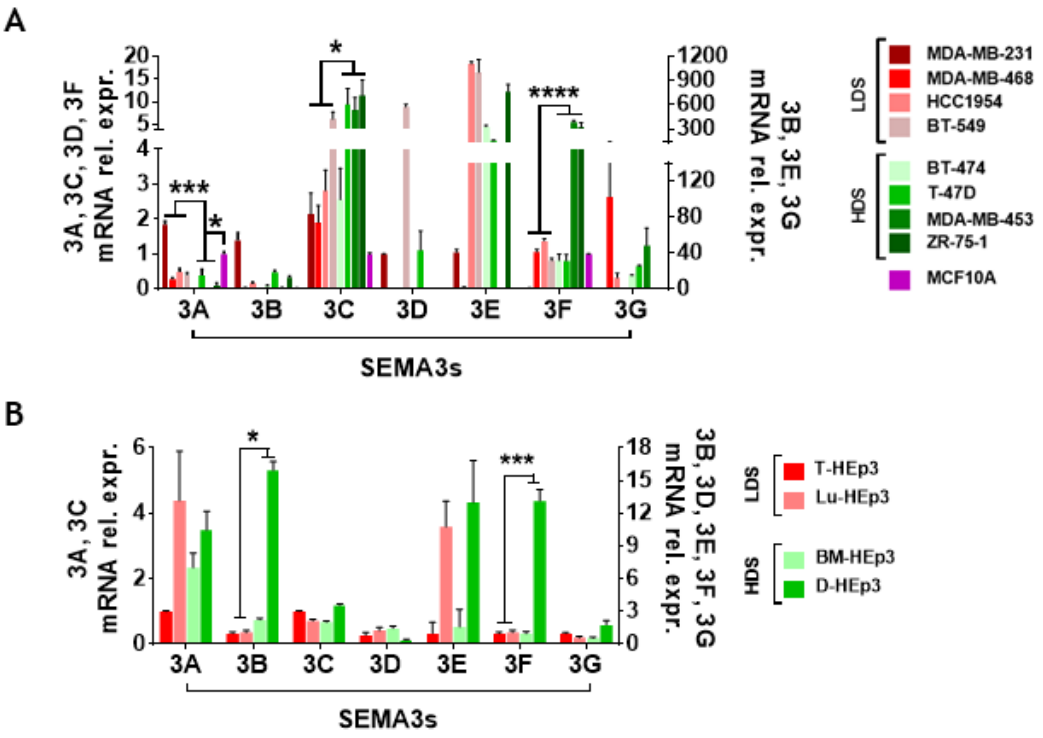

Figure 26. Characterization of semaphorins gene expression in breast and head and neck cancer cell lines. Analysis of SEMA3s mRNA relative expression in BrCa (**A**) and HNSCC (**B**) cell lines. The graphs represent RQ mean values ± S.E.M referred to MCF10A (**A**) or T-HEp3 cells (**B**) (n=3); *P < 0.05, ***P<0.001, ****P<0.0001 comparing LDS *vs* HDS or proliferative *vs* dormant cell lines by *t*-Student's test.

Taking all the results of the characterization together, we described a proliferative or dormant expression profile in our models of study. Although similar for both cancer types, each model needs to be considered as independent since gene and protein expression patterns slightly differ from BrCa to HNSCC. Considering this, we grouped as pro-proliferative molecules those highly expressed in LDS/proliferative cells or down-regulated in HDS/dormant cells while those down-regulated in LDS/proliferative cells or highly expressed in HDS/dormant cells were classified as pro-dormancy molecules. Having this into account, we defined NRP2, NRP1, PLXNA2 and SEMA3A as pro-proliferative in BrCa whereas PLXNA3, SEMA3C and SEMA3F were considered pro-quiescent (**fig. 27, left**). Conversely, only NRP2 and NRP1 were considered as pro-proliferative in HNSCC whereas PLXNA3, PLXNA4, PLXND1, SEMA3B and SEMA3F were considered as pro-dormancy (**fig. 27, right**). When combining the expression profiles from BrCa and HNSCC, we observed that some of them matched in both models as did also their proliferative or quiescent classification. Thus, NRP2 and NRP1 were globally classified as pro-proliferative molecules while PLXNA3 and SEMA3F were catalogued as pro-quiescence. PLXNA2 was classified as pro-proliferative in BrCa while being interestingly up-regulated in both HNSCC cell lines derived from DTCs, with higher levels in proliferative cells (Lu-HEp3). A recent study in lung cancer has showed that global chromatin alterations driven by Nfib promoted a neuronal gene expression program on metastatic DTCs[484]. Interestingly, one of the genes regulated by Nfib and up-regulated in metastatic lung DTCs was

PLXNA2. This study suggests that expression of plexins might regulate the metastatic capacity of DTCs. Hence, we decided to include PLXNA2 in the experimental body of this thesis, as well.

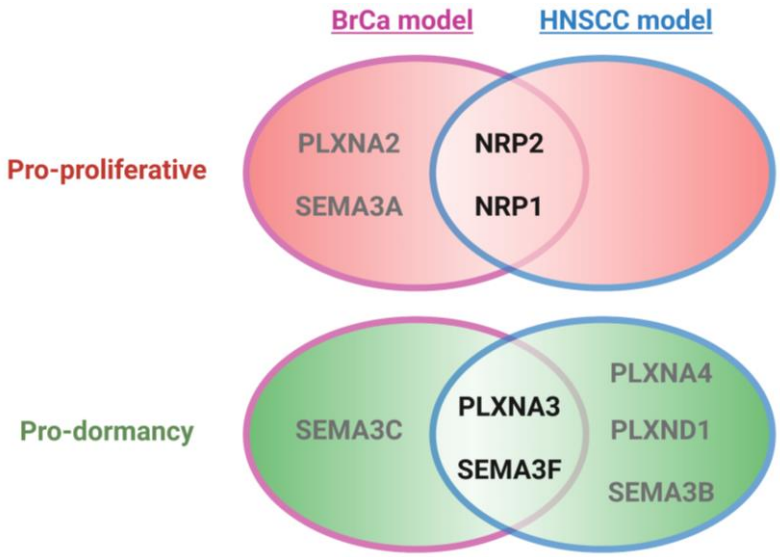

Figure 27. Classification of NRPs, PLXNs and SEMA3s as proliferation or dormancy cues in BrCa and HNSCC. Pro-proliferative gene/proteins (upper panel) are those highly expressed in LDS/proliferative cells or down-regulated in HDS/dormant cells while pro-dormancy gene/proteins (lower panel) are those down-regulated in LDS/proliferative cells or highly expressed in HDS/dormant cells.

4.2. Role of SEMA3F as a dormancy-inducer in BrCa and HNSCC models

Our preliminary data from the characterization determined that SEMA3F was down-regulated in LDS BrCa and proliferative HNSCC cell lines (**fig. 26**), such as MDA-MB-231 and BT-549 in BrCa and T-HEp3 and Lu-HEp3 in HNSCC cell lines, which suggested that SEMA3F could be a tumour suppressor. In accordance with our *in vitro* results, using data from the GOBO database where 1881 human BrCa samples were analysed, we found that SEMA3F is down-regulated in the basal BrCa subtype while being up-regulated in luminal subtypes (**fig. 28A**). Luminal subtypes comprise less aggressive tumours, with longer periods of MRD where relapses could appear months or even decades after PT diagnosis[254,270], suggesting these patients undergo a longer phase of dormancy prior to developing metastasis. In agreement with this, when we analysed SEMA3F in the METABRIC database using CANCERTOOL, we found that SEMA3F expression positively correlates with ER expression, being up-regulated in ER-positive tumours in several studies (**fig. 28B**). It has previously been shown that ER expression correlates with longer metastasis-free periods and longer dormancy periods[338]. Moreover, SEMA3F expression negatively correlated with tumour grade where lower SEMA3F levels were found in more aggressive and advanced tumours (**fig. 28C**).

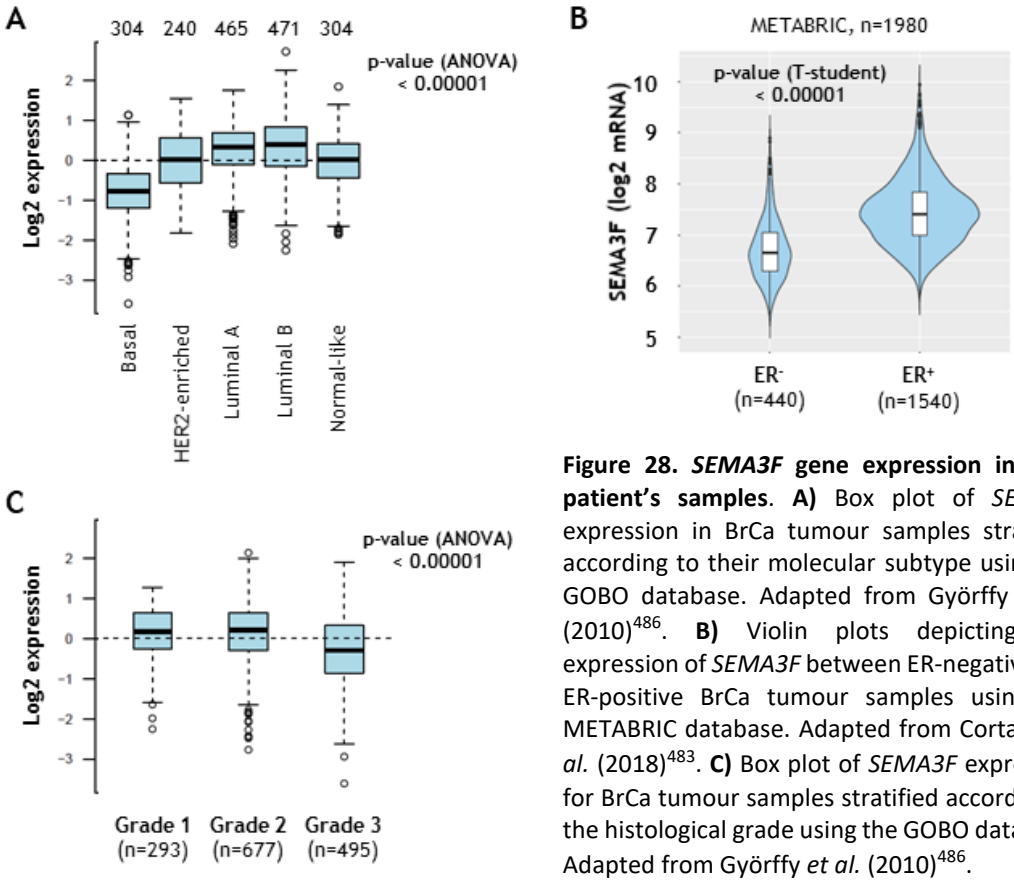

Figure 28. *SEMA3F* gene expression in BrCa patient's samples. **A)** Box plot of *SEMA3F* expression in BrCa tumour samples stratified according to their molecular subtype using the GOBO database. Adapted from Györffy *et al.* (2010)[486]. **B)** Violin plots depicting the expression of *SEMA3F* between ER-negative and ER-positive BrCa tumour samples using the METABRIC database. Adapted from Cortazar *et al.* (2018)[483]. **C)** Box plot of *SEMA3F* expression for BrCa tumour samples stratified according to the histological grade using the GOBO database. Adapted from Györffy *et al.* (2010)[486].

In relation with HNSCC, using the GEPIA web server we did not find any differences in SEMA3F expression between tumour and normal HNSCC patient samples (**fig. 29A**). When we analysed its expression in different HNSCC stages we found that, although not reaching statistical significance, *SEMA3F* expression also tends to negatively correlate with tumour stage, in agreement with the BrCa data (**fig. 29B**).

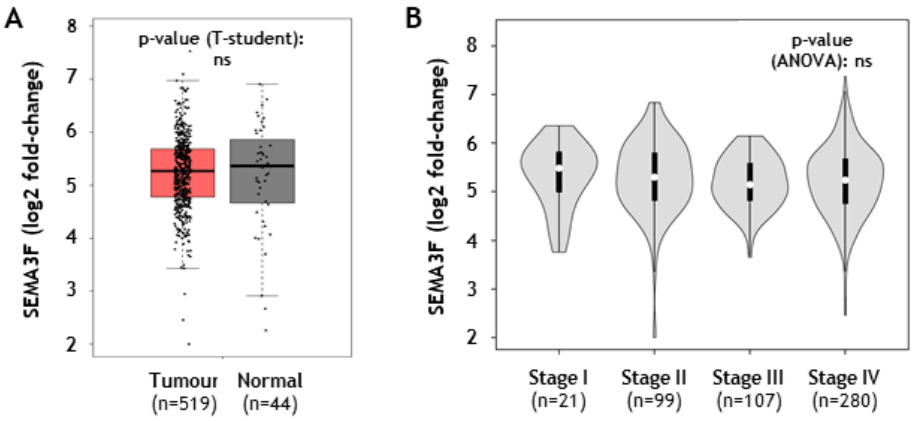

Figure 29. *SEMA3F* gene expression in HNSCC patient's samples. **A)** Box plot of *SEMA3F* expression in head and neck tumours (red; n=519) or healthy/normal (grey; n=44) samples. The method for differential analysis is *t*-Student's test, using disease state (tumour or normal) as variable for calculating differential expression. **B)** Box plot of *SEMA3F* expression for HNSCC tumour samples stratified according to the histological grade. The method for differential analysis is one-way ANOVA, using tumour stage as variable for calculating differential expression. Adapted from Tang *et al.* (2017)[482].

4.2.1. SEMA3F treatment increases p27 quiescence marker expression *in vitro*

Taking into account that SEMA3F was up-regulated in HDS BrCa and dormant HNSCC cell lines, and that its expression negatively correlates with tumour grade in patient samples, our next step was to analyse the potential dormancy inducer role of SEMA3F. For that, we treated highly proliferative cell lines from both models (MDA-MB-231, BT-549 and T-HEp3) with SEMA3F. In a preliminary dose-curve experiment, we tested different doses of SEMA3F and determined 5ng/mL as the SEMA3F working concentration for our *in vitro* experiments (data not shown). Then, we treated the cells with 5ng/mL SEMA3F and analysed dormancy markers expression by western blot and qPCR. As shown in **figure 30A**, we observed a clear increase in the protein levels of the quiescence protein marker p27 after 24h of treatment with SEMA3F. No differences were observed either in phosphorylated (p)-p38 or p-ERK levels (**fig. 30A**). Dec2 and TGFβR3 mRNA levels were also studied as dormancy markers, where TGFβR3 is considered as so due to its requirement for TGFβ2-dependent dormancy induction[266]. Treatment with SEMA3F showed little effect in the mRNA levels of both molecules (**fig. 30B**). Hence, our results suggest that SEMA3F could up-regulate the expression of the quiescence marker p27.

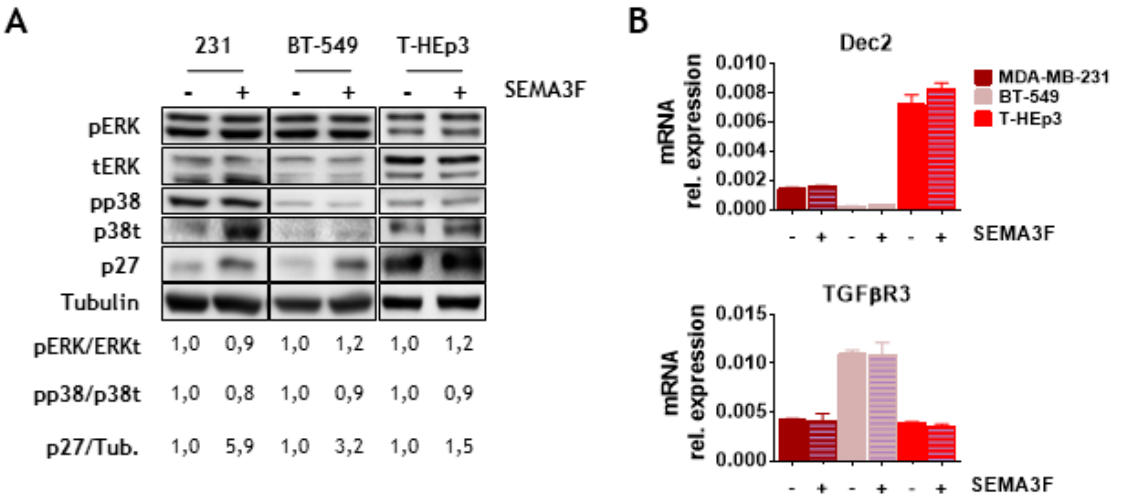

Figure 30. SEMA3F treatment increases p27 quiescence marker expression in human BrCa and HNSCC cell lines. **A)** Representative western blot analysis of phosphorylated (p)-ERK, p-p38 and p27 protein levels normalized with β-Tubulin after 24h treatment with SEMA3F (5ng/mL) in BrCa (MDA-MB-231 -231-, BT-549) and HNSCC (T-HEp3) cell lines. Protein quantifications are referred to the non-treated control condition (-) (n=3). **B)** Analysis of Dec2 and TGFβR3 mRNA levels after 24h treatment with SEMA3F (5ng/mL) in BrCa (MDA-MB-231 -231-, BT-549) and HNSCC (T-HEp3) cell lines. Graphs represent RQ mean values ± S.E.M. (n=1, triplicates); *t*-Student's test between control (-) and SEMA3F treated (+) was performed and revealed non-significant differences.

4.2.2. SEMA3F has no effect on cell proliferation, clonogenicity and cell cycle regulation *in vitro*

In order to study the potential inhibitory role of SEMA3F in human BrCa and HNSCC cells, we performed several functional *in vitro* experiments. We first performed a proliferation assay treating the cells with increasing doses of SEMA3F for 72h, where we found that SEMA3F neither modulated the proliferation rate of BrCa (MDA-MB-231, BT-549) nor that of HNSCC (T-HEp3) cells *in vitro* (**fig. 31A**). Since the increase in the CDK inhibitor p27 expression after SEMA3F treatment (**fig. 30**) suggested that SEMA3F could be a quiescence inductor, we treated BrCa cell lines with SEMA3F chronically (ch. 3F) for 14 days, and then analysed the cell cycle. Under these conditions, no changes

in cell cycle were observed in treated cells, except for a slight increase in the percentage of cells in G2 phase in BT-549 cells (**fig. 31B**).

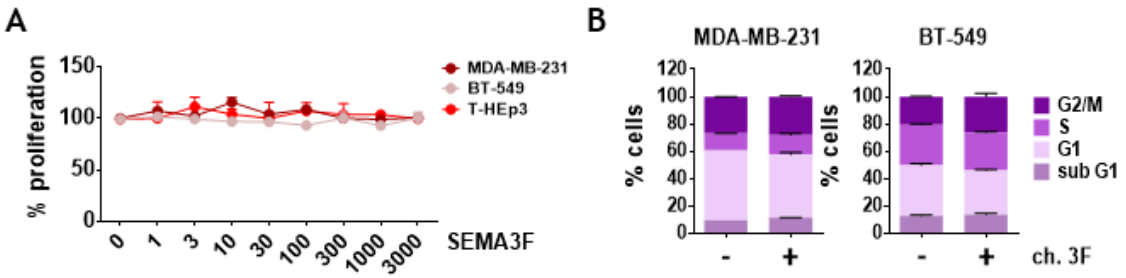

Figure 31. SEMA3F effect on cell proliferation and cell cycle *in vitro*. A) Cell proliferation quantification for MDA-MB-231, BT-549 and T-HEp3 cells treated for 72h with increasing doses of SEMA3F (0-3000ng/mL). The graph shows the percentage of cell proliferation (mean ± S.E.M.; n=1). **B)** Cell cycle analysis in MDA-MB-231 and BT-549 after chronic SEMA3F treatment (ch.3F) (5ng/mL SEMA3F in 5% FBS containing media) for 14 days. Graphs represent the percentage of cells in each cell cycle phase (mean ± S.E.M.; n=1). *t*-Student's test between control (-) and SEMA3F treated (+) was performed and revealed non-significant differences.

In addition, we also evaluated the ability of these cells to grow in an anchorage-dependent manner following a clonogenic assay. We treated the cells with SEMA3F for 6 days prior to the experiment seeding, mimicking a semi-chronic treatment and then let the cells grow for 10-15 days. We observed no change either in the number or in the size of the foci between treated and non-treated cells (**fig. 32**). Altogether, our findings indicate that although SEMA3F up-regulates p27 expression, it is not enough for triggering a phenotype change *in vitro* by itself. This could be explained by the fact that these cells have a high proliferation rate that might require stronger anti-proliferative stimuli to modulate their proliferative and growth capacities *in vitro*.

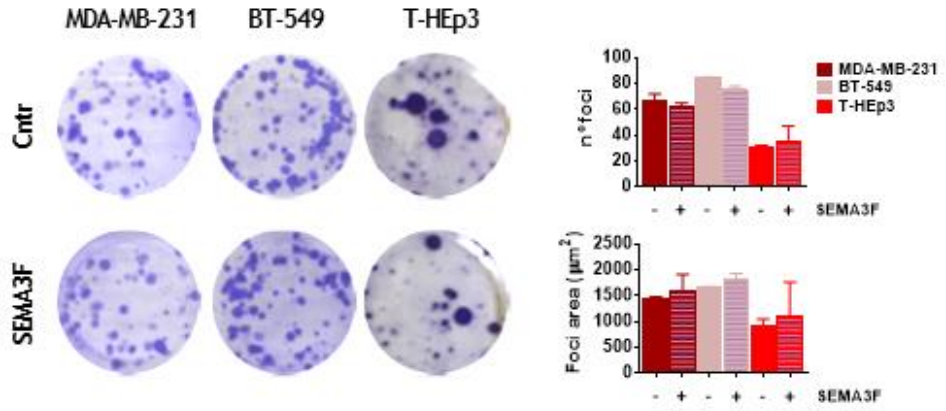

Figure 32. SEMA3F effect on anchorage-dependent growth *in vitro*. Representative images (left panels) and quantification of the total number of cell foci (right upper graph) and foci area (right lower graph) from anchorage-dependent growth assay. Cells were treated for 6 days with SEMA3F (5ng/mL) in 5% FBS containing media before performing the assay. The graph represents mean ± S.E.M. (n=1, triplicates); *t*-Student's test between control (-) and SEMA3F treated (+) was performed and revealed non-significant differences.

4.2.3. SEMA3F does not regulate cell migration and invasion *in vitro*

SEMA3s are axon guide molecules and they have been previously shown to regulate cancer cells migration and invasion. Thus, the effect of SEMA3F treatment was further studied in our cell lines by investigating whether SEMA3F could modify the migration and/or invasion properties of these cells *in vitro*. Cells were pre-treated for 24h with SEMA3F (5ng/mL) before performing the wound-healing assay in serum-free conditions, where cells were also treated with SEMA3F. We found that there were no differences in the ratio of the total wound area between treated and non-treated cells. Hence, treatment with SEMA3F had little effect on the wound-closure in MDA-MB-231 (**fig. 33A**) and BT-549 (**fig. 33B**) cell lines. The same pattern was observed in T-HEp3 cells where SEMA3F had no effect on cell migration either (**fig. 33C**).

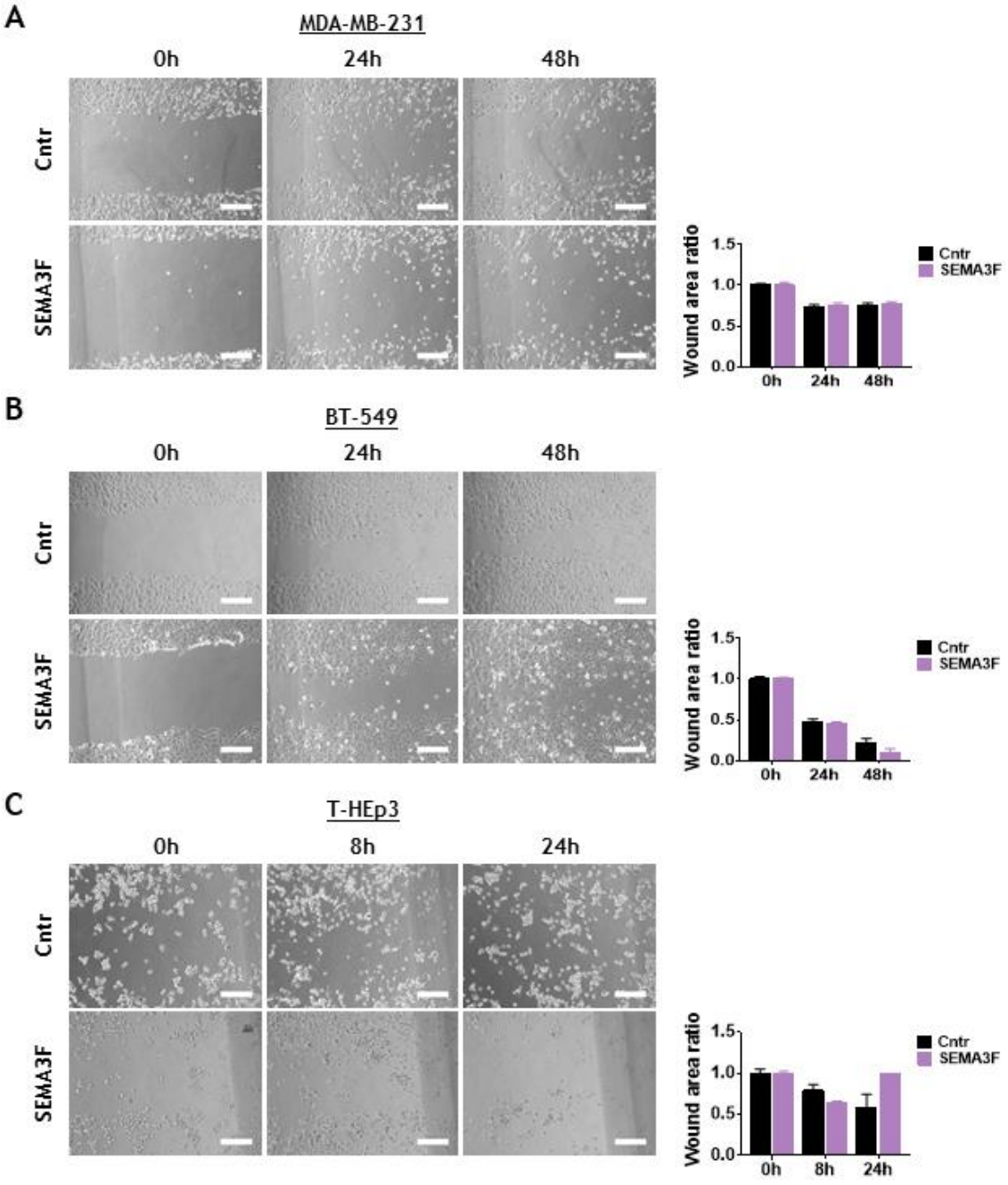

Figure 33. SEMA3F treatment effect on cell migration *in vitro*. Representative images from phase-contrast microscopy (left panels) and quantification of the ratio of the wound area (right graphs) after 0, 8, 24 and 48h migration in non-treated (upper panels) and SEMA3F treated (5ng/mL) (lower panels) MDA-MB-231 (**A**), BT-549 (**B**) and T-HEp3 (**C**) cells. Scale bar: 300µm. Graphs represent mean ± S.E.M. (n=1, triplicates); two-way ANOVA, Sidak's test between control and SEMA3F treated cells was performed and revealed non-significant differences.

As in previous sections, we also performed a chronic SEMA3F treatment to evaluate its effect on BrCa cell migration (**fig. 34**). We found that chronic SEMA3F treatment slightly reduced wound closure in MDA-MB-231 at 24h although the differences were non-significant (**fig. 34A**) while no differences were observed in BT-549 cells (**fig. 34B**). Hence, our results suggest that SEMA3F has no effect on cell migration.

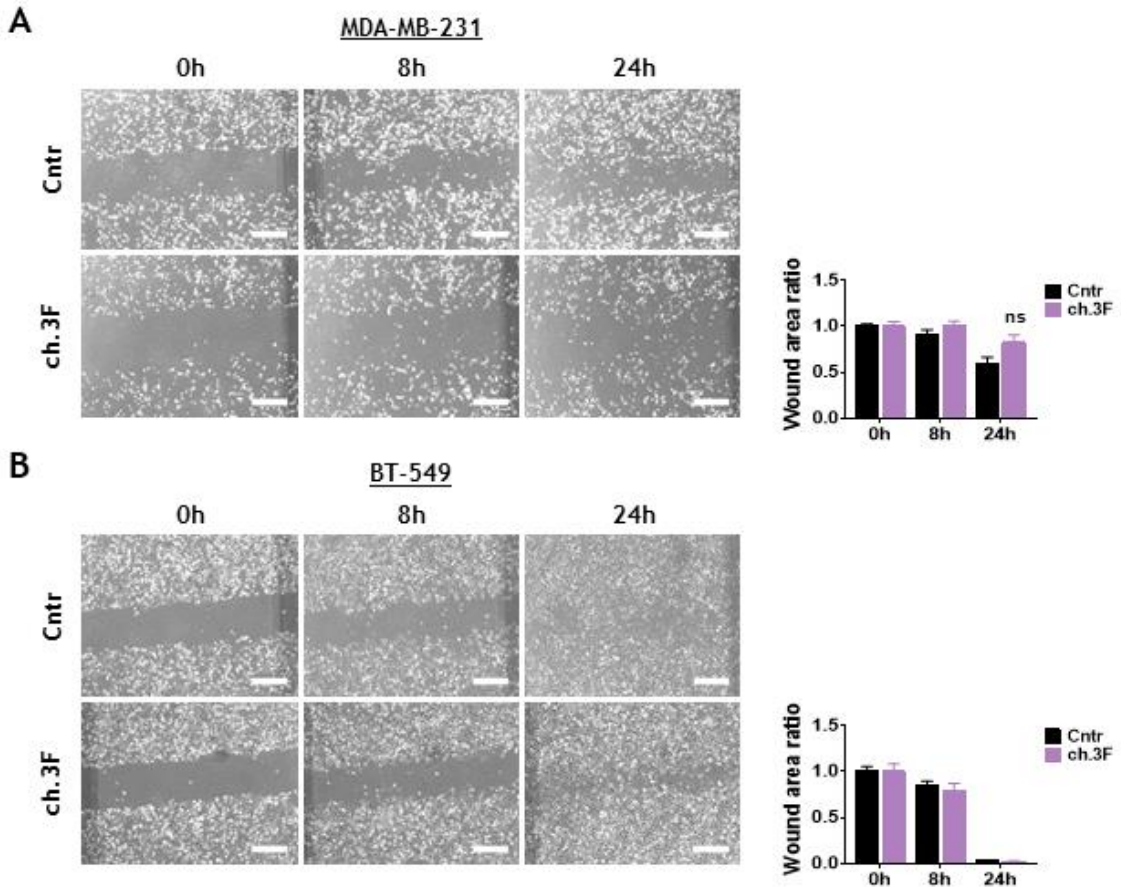

Figure 34. SEMA3F chronic treatment effect on cell migration ability *in vitro*. Representative images from phase-contrast microscopy (left panels) and quantification of the ratio of the wound area (right graphs) after 0, 8 and 24h migration in MDA-MB-231 (**A**) and BT-549 (**B**) cells. Cells were previously treated with SEMA3F (5ng/mL) for 14 days (ch.3F) in 5% FBS containing media. 5ng/mL SEMA3F was also added during the wound healing assay. Scale bar: 300µm. Graphs represent mean ± S.E.M. (n=1, triplicates); two-way ANOVA, Sidak's test between control and SEMA3F treated was performed and revealed non-significant (ns) differences.

To test the effect of SEMA3F on invasion we performed an invasion assay on transwells coated with a matrigel layer. Cells were previously treated with SEMA3F for 6 days in 5% FBS containing media and then seeded on top of the matrigel layer, where cells were also treated with 5ng/mL

SEMA3F for 48h. 10% serum containing media was used as a chemoattractant. Here either, no effects were noticed after 48h in the number of MDA-MB-231 or BT-549 cells that were able to pass through and form cell colonies (**fig. 35**). Taken together, these results indicate that SEMA3F does not alter the migration and invasion features of proliferative BrCa and HNSCC cell lines *in vitro*.

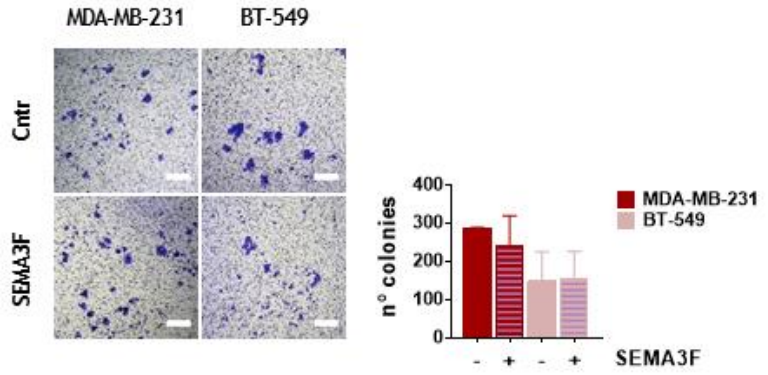

Figure 35. SEMA3F treatment effect on cell invasion *in vitro*. Invasion through matrigel using 10% FBS as chemoattractant. Representative phase contrast microscopy images of invading cells (left panel) and the histogram showing the total number of invading colonies (right panel). Cells were previously treated with SEMA3F (5ng/mL) for 6 days in 5% FBS containing media. 5ng/mL SEMA3F was also added during the invasion assay. Scale bar: 300µm. Graphs represent mean ± S.E.M. (n=1, duplicates); *t*-Student's test between control (-) and SEMA3F treated (+) was performed and revealed non-significant differences.

4.2.4. SEMA3F induces dormancy genes expression on primary tumours and reduces tumour cell dissemination to secondary organs *in vivo*

In the previous sections we have found that SEMA3F treatments increased p27 expression, suggesting SEMA3F could induce quiescence in LDS BrCa and proliferative HNSCC cells. Although we did not see any effect on cell proliferation *in vitro*, we next explored whether SEMA3F treatment was able to affect tumour growth *in vivo*. We used the chicken embryo CAM assay as a quick preliminary approximation in tumour growth and biology (see *Materials & Methods, section 3.8.1* for further details). Briefly, we inoculated breast or head and neck tumour cells in the CAMs of day 11 chicken embryos and let them grow for 5-6 days while locally treating them every day with SEMA3F (1µg/mL). At end point, we removed, measured and fixed PTs. Furthermore, potential secondary organs (i.e., liver, lungs) were isolated for tumour cell dissemination analyses as well.

Regarding MDA-MB-231 cells, although a trend to form smaller PTs was detected, no statistically significant effects in tumour weight and volume were observed in SEMA3F treated tumours (**fig. 36A**). In agreement with this, no differences were found in Ki67 protein levels between treated and non-treated MDA-MB-231 PTs (**fig. 36B**). However, when we analysed Dec2 and TGFβR3 dormancy markers expression on the tumours by qPCR, we found that TGFβR3 mRNA levels were significantly higher on SEMA3F treated tumours (**fig. 36C**). These results suggest that although SEMA3F does not affect MDA-MB-231 tumour growth, it induces an up-regulation of some dormancy markers, which could affect tumour cells adaptation to secondary organs, in the sense that these tumour cells might be more prone to enter dormancy when they reach a new microenvironment.

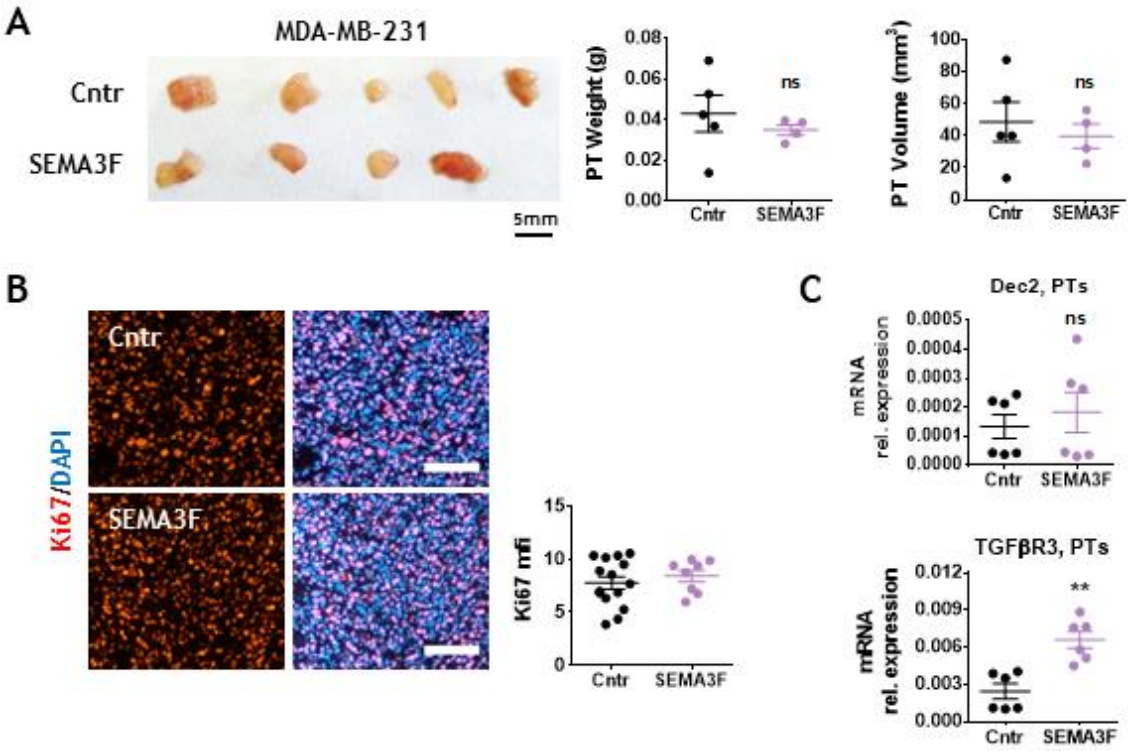

Figure 36. SEMA3F increases TGFRβ3 expression in BrCa tumours *in vivo*. A) $2 \cdot 10^6$ MDA-MB-231 cells were inoculated in day 11 chicken embryo CAMs, treating half of the PTs with PBS (Cntr) or SEMA3F (1µg/mL) for 5 days. Left panel, representative images of MDA-MB-231 tumours at end point. Middle and right panels, graphs showing tumour weight (g) (middle) and volume (mm^3) (right) at end point. **B)** Left panel, Ki67 IF representative images in MDA-MB-231 PTs. Scale bar: 50µm. Right panel, Ki67 mfi quantification. **C)** Dec2 (upper graph) and TGFRβ3 (lower graph) mRNA levels in MDA-MB-231 PTs. Graphs represent mfi or RQ mean values ± S.E.M. (n=1, with 6 inoculated eggs per group); ns, non-significant, **P < 0.01 comparing Cntr *vs* SEMA3F by *t*-Student's test.

In the same way, after T-HEp3 cells inoculation and SEMA3F treatment for 6 days, we did not detect a reduction in tumour weight and volume (**fig. 37A**). Indeed, we found that tumours treated with SEMA3F were slightly bigger than non-treated tumours. Nevertheless, when we analysed dormancy and quiescence markers expression in these tumours using either qPCR or IF we found that SEMA3F treated tumours had significantly higher Dec2 and TGFβR3 mRNA levels (**fig. 37B**). Interestingly, SEMA3F treated tumours also showed significant up-regulation of p27 protein expression (**fig. 37C**) and a decrease in Ki67 expression (**fig. 37D**). These *in vivo* results corroborated our previous observations *in vitro*, which postulate that SEMA3F might boost tumour cells entrance to quiescence. Hence, these results suggest that SEMA3F could act as a dormant phenotype promoter, making proliferative tumour cells more quiescent and thus less likely to proliferate when they arrive to secondary organs and thus render them less metastatic.

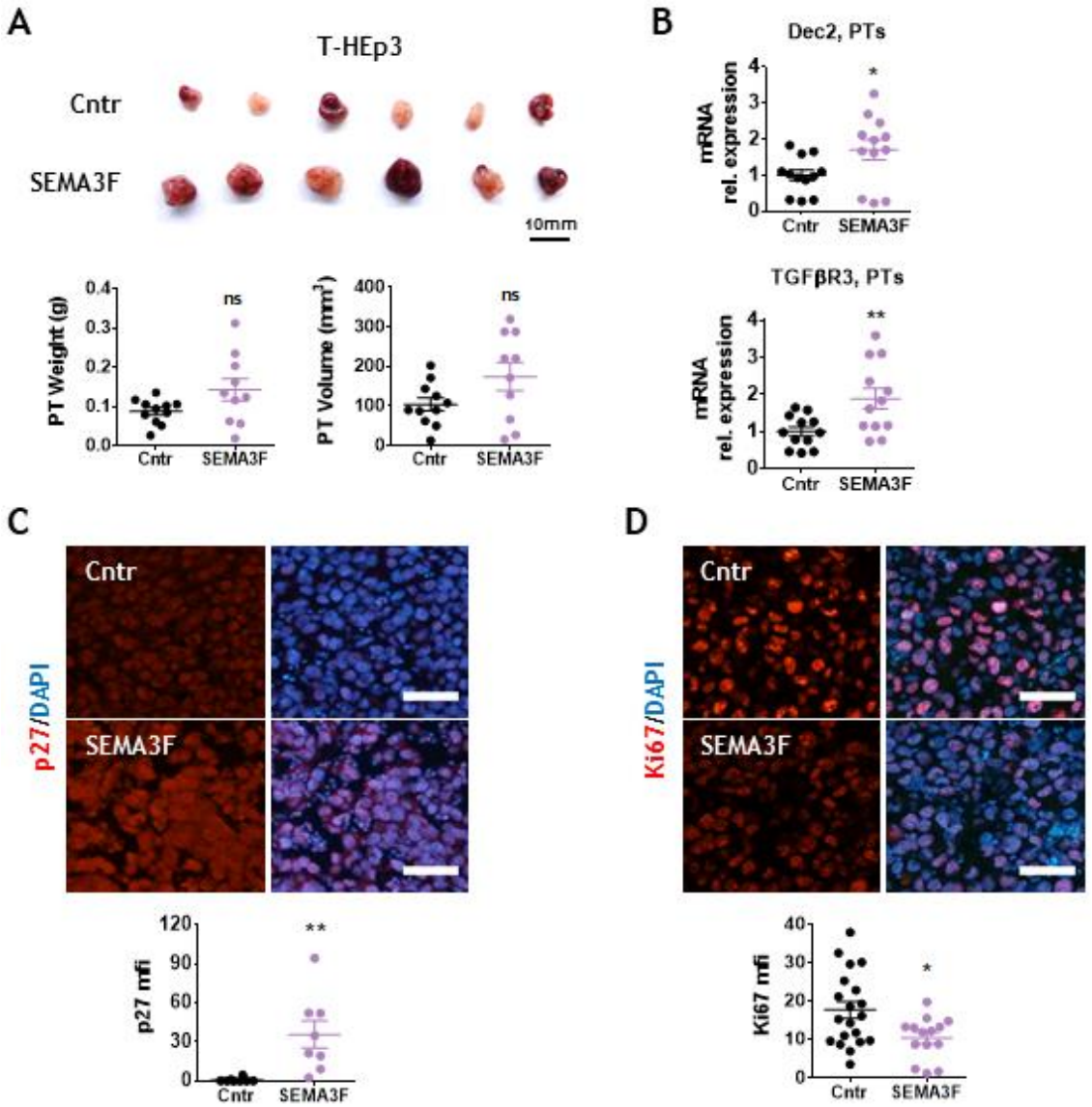

Figure 37. SEMA3F decreases Ki67 cell proliferation marker while inducing quiescence markers expression in HNSCC tumours *in vivo*. A) $3 \cdot 10^5$ T-HEp3 cells were inoculated in day 11 chicken embryo CAMs, treating half of the PTs with PBS (Cntr) or SEMA3F (1µg/mL) for 6 days. Upper panel, representative images of T-HEp3 tumours. Lower panels, graphs showing tumour weight (g) (left) and volume (mm^3) (right) at end point. **B)** Dec2 (upper graph) and TGFRβ3 (lower graph) mRNA RQ levels in T-HEp3 PTs. **C, D)** Representative IF images (upper panel) and mfi quantification (lower panel) of p27 (**C**) and Ki67 (**D**) in T-HEp3 PTs. Scale bar: 50µm. Graphs represent RQ or mfi mean values ± S.E.M. (n=2 experiments, with 6 inoculated eggs per group); ns, non-significant, *P < 0.05, **P < 0.01 comparing Cntr *vs* SEMA3F by *t*-Student's test.

Our results suggest that SEMA3F could promote PTs switch from a proliferative to a dormant phenotype, as suggested by the up-regulation of some quiescence markers (p27, Dec2, TGFβR3) together with a down-regulation of proliferative markers (Ki67) in the HNSCC model (**fig. 37**). Besides studying its effects over PTs, we also wanted to explore whether SEMA3F affects tumour cell dissemination and adaptation to secondary organs. To that end, potential secondary target organs such as liver and lungs were isolated and analysed looking for disseminated T-HEp3 cells by GFP or vimentin expression. After 6 days of tumour growth, we detected a significant lower number of disseminated T-HEp3 cells in the livers from the chickens whose tumours were treated with

SEMA3F (detected by GFP expression) (**fig. 38A**). We also observed a clear trend to have a lower number of disseminated T-HEp3 cells in the lungs isolated from chickens with SEMA3F treated tumours (detected by vimentin expression) (**fig. 38B**). Therefore, our results indicate that treatment of PTs with SEMA3F might reduce tumour cell dissemination to lungs and livers in HNSCC by mechanisms that are still unclear.

Additionally, we wanted to analyse the proliferative or dormant phenotype of the lungs DTCs to test if SEMA3F might be also regulating DTCs fate at secondary organs. To this end, an immunostaining of vimentin (as a mesenchymal marker, for DTCs detection) and Ki67 (as a proliferation marker, for determining DTCs phenotype) was performed in lung tissues. Therefore, vimentin^{+}/Ki67^{+} cells were considered proliferative DTCs whereas vimentin^{+}/Ki67^{-} cells were considered dormant DTCs. We found that in the lungs from the chickens with non-treated tumours there was a higher proportion of proliferative lung DTCs as compared to the lungs from the chicken with SEMA3F treated tumours (**fig. 38C**). These evidence support the idea that SEMA3F might be turning-off the proliferative phenotype of BrCa and HNSCC disseminated cells by stimulating a more dormant phenotype, which predispose tumour cells to enter quiescence at secondary organs leading to a reduction in the number of DTCs at secondary organs and a DTC switch from proliferative to dormant phenotype.

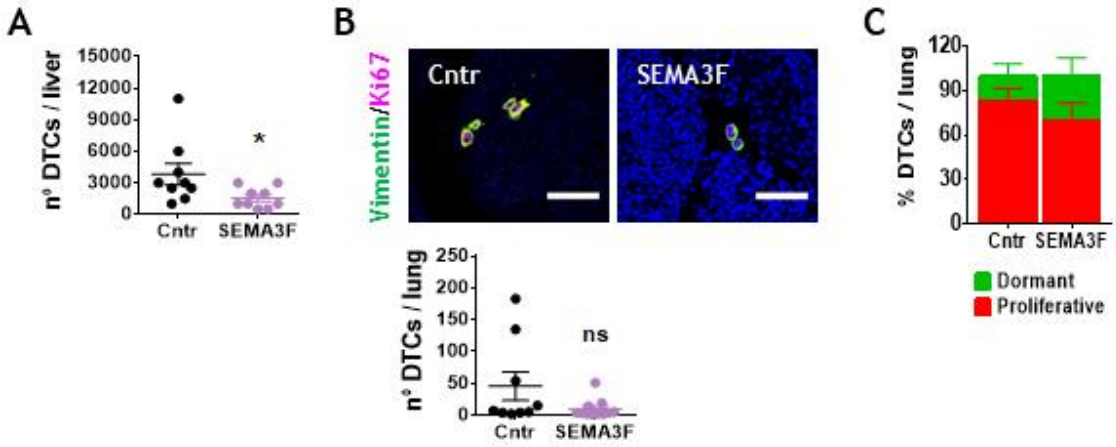

Figure 38. SEMA3F reduces T-HEp3 cells dissemination to secondary organs *in vivo*. A) Quantification of the number of disseminated T-HEp3 cells to the chicken liver after 6 days of SEMA3F (5ng/mL) treatment. Liver DTCs were quantified as the total number of GPF-positive cells per liver. **B)** Quantification of the number of disseminated T-HEp3 cells to the chicken lung after 6 days of SEMA3F (5ng/mL) treatment. Upper panel, representative IF images of vimentin (green) and Ki67 (pink) in chicken lung sections. Scale bar: 50µm. Lower panel, quantification of the total number of vimentin-positive cells per lung. **C)** Graph showing the percentage (%) of proliferative (Ki67^{+}) and dormant (Ki67^{-}) T-HEp3 lung DTCs per chicken lung. Graphs represent mean ± S.E.M. (n=2 experiments, with 6 inoculated eggs per group); ns, non-significant, *P < 0.05 comparing Cntr *vs* SEMA3F by by *t*-Student's test.

4.3. Role of PLXNA2 and PLXNA3 in BrCa

The formation of a receptor complex composed of PLXNs and NRPs is required for SEMA3s signal transduction. Type-A PLXNs act as the main receptors for SEMA3s not only in neural cells, but also in endothelial and tumour cells[423]. Our previous results have shown that dormant BrCa cell lines over-expressed PLXNA3 (**fig. 24**). PLXNA2 was down-regulated in HDS BrCa cell lines (**fig. 24**), while being up-regulated in HNSCC DTCs-derived cell lines (**fig. 25**).

When we analysed PLXNA3 and PLXNA2 expression in HNSCC patient samples using GEPIA, we found that PLXNA3 is over-expressed in tumour samples (**fig. 39A**). However, its expression does not correlate with patients' OS (**fig. 39B**). In the case of PLXNA2, there are no differences in its expression between tumour and normal samples (**fig. 39C**) and it did not correlate with OS either (**fig. 39D**).

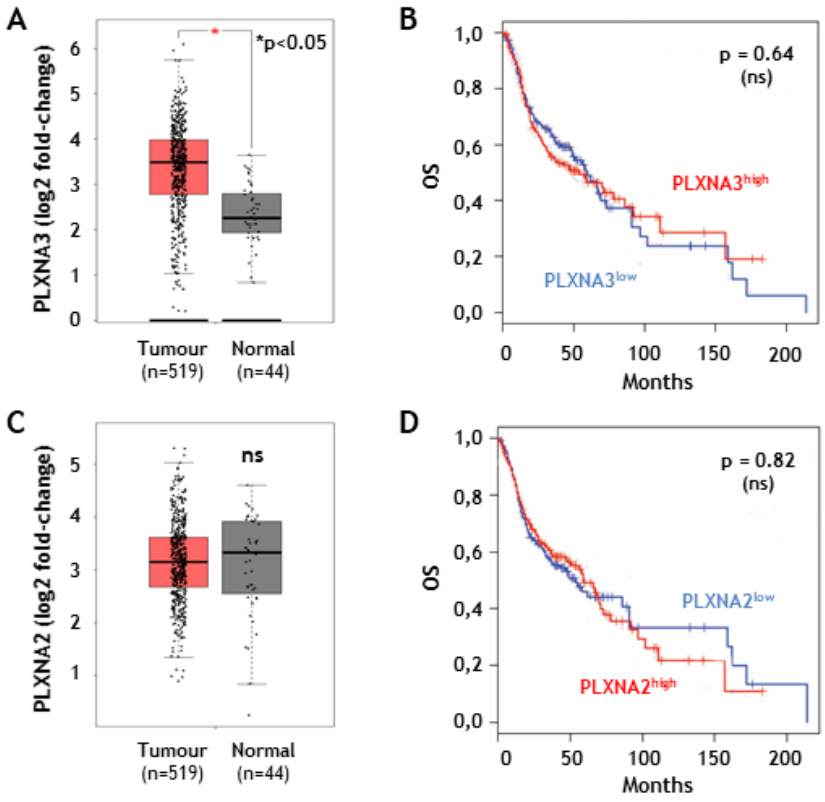

Figure 39. *PLXNA2* and *PLXNA3* gene expression in HNSCC using GEPIA web server. **A)** Box plot of *PLXNA3* expression in head and neck tumours (red; n=519) or healthy/normal (grey; n=44) samples. **B)** Kaplan-Meier curve for overall survival (OS) of a cohort of 517 HNSCC patients with high (red; n=258) or low (blue; n=259) levels of *PLXNA3*. **C)** Box plot of *PLXNA2* expression in head and neck tumours (red; n=519) or healthy/normal (grey; n=44) samples. **D)** Kaplan-Meier curve for OS of a cohort of 517 HNSCC patients with high (red; n=259) or low (blue; n=259) levels of *PLXNA2*. The method for differential analysis is one-way ANOVA, using disease state (tumour *vs* normal or high *vs* low) as variable for calculating differential expression. Adapted from Tang *et al.* (2017)[482].

When analysing PLXNs expression in BrCa databases, we found that PLXNA3 is over-expressed in ER-positive breast tumours (**fig. 40A**)[483,485] which, as mentioned before, show longer dormancy periods. Moreover, its over-expression correlates with good prognosis (**fig. 40B**)[486], suggesting it could be a tumour suppressor or a dormancy inducer. When studying PLXNA2, we found that it is up-regulated in ER-negative BrCa patients (**fig. 40C**)[483], which show lower dormancy periods. Regarding PLXNA2 protein expression and OS, Kaplan-Meier curves differentiated two subpopulations of ER-negative BrCa patients according to PLXNA2 expression. Contrary to what we expected, patients with higher PLXNA2 expression seem to have longer OS although there was no statistical significance (**fig. 40D**)[486].

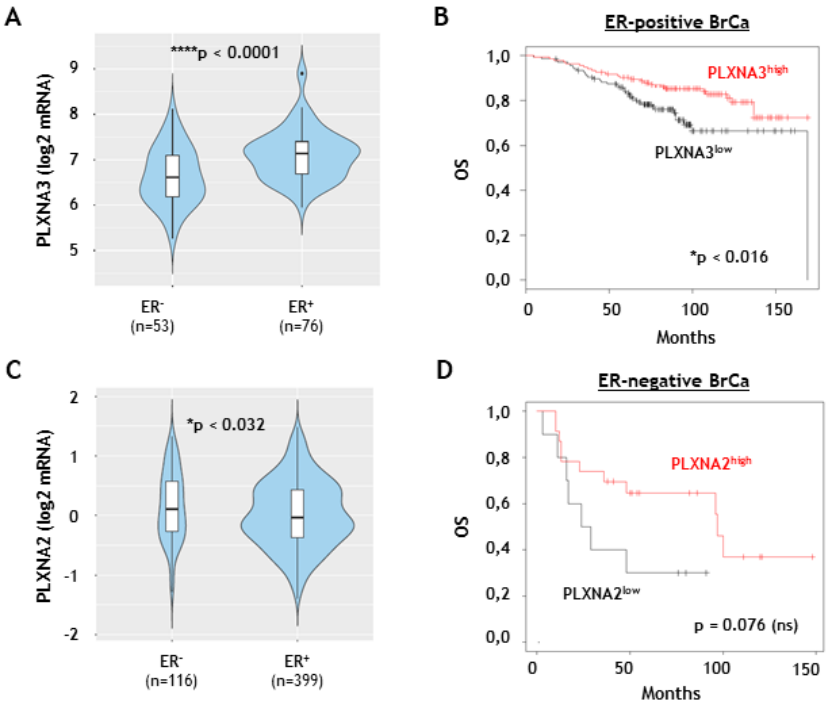

Figure 40. *PLXNA3* and *PLXNA2* gene expression in BrCa patient samples. **A)** mRNA expression for PLXNA3 in a cohort of 129 ER-negative (n=53) *vs* ER-positive (n=76) BrCa patients. Database from Lu *et al.* (2008)[485]. Adapted from Cortazar *et al.* (2018)[483]. **B)** Kaplan-Meier curve for OS in a cohort of 554 ER-positive BrCa patients with high (red; n=277) or low (black; n=277) levels of *PLXNA3*. Adapted from Györffy *et al.* (2010)[486]. **C)** mRNA expression for PLXNA2 in a cohort of 522 ER-negative (n=116) *vs* ER-positive (n=399) BrCa patients. TCGA database. Adapted from Cortazar *et al.* (2018)[483]. **D)** Kaplan-Meier curve for OS in a cohort of 33 ER-negative BrCa patients with high (red; n=23) or low (black; n=10) levels of PLXNA2 protein. Adapted from Györffy *et al.* (2010)[483].

Having into account the lack of OS predictive value and the fact that PLXNs expression was very low in our HNSCC cell lines, we focused on studying the role of PLXNA2 and PLXNA3 in BrCa.

4.3.1. Regulation of PLXNA2 and PLXNA3 expression by signals present in the tumour microenvironment *in vitro*

Taking into account the results obtained in the characterization and the patient data, we initially defined PLXNA2 as a potential pro-tumourigenic protein since it was up-regulated in more proliferative and ER-negative BrCa cell lines and tumours (**fig. 24, 40C**), although it could also predict high OS (**fig. 40D**). We also classified PLXNA3 as a plausible pro-quiescence molecule due to its higher expression in more dormant-like cell lines (**fig. 24**), ER-positive BrCa patients (**fig. 40A**) and high OS prediction (**fig. 40B**). Previous studies from our laboratory have shown that TGFβ2 and TGFβ1 regulate DTCs fate in opposite directions[266]. Moreover, since PLXNS are co-receptors for NRPs, which have been described to interact with TGFβ receptors[412,487], we wondered whether the expression of PLXNs could be modulated by signals present in the TME that have been shown to modulate DTCs behaviour, such as the TGFβ family members.

First, we treated the cells with the pro-proliferative signal TGFβ1 and we detected an up-regulation of PLXNA2 mRNA (**fig. 41A**) and protein levels (**fig. 41B**) in MDA-MB-231 cells but not in HCC1954, classified as LDS cells. On the contrary, PLXNA3 was clearly down-regulated upon TGFβ1

treatment in HDS cells and HCC1954 (LDS) as well (**fig. 41B**). As the expression of both PLXNs might be inversely regulated by TGFβ1 in LDS and HDS cells, we next studied whether they could also be regulated by dormancy-inducing signals.

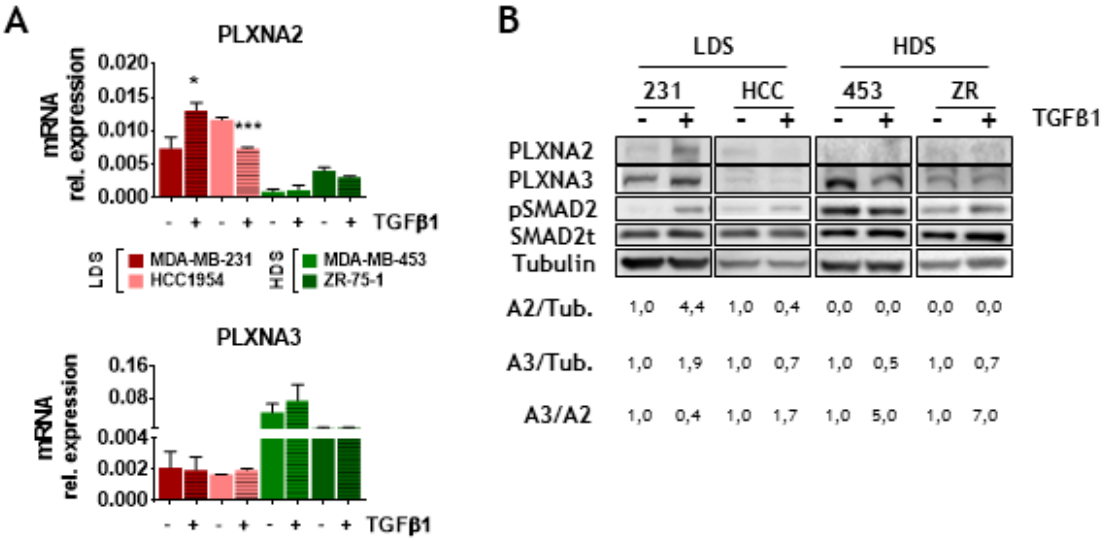

Figure 41. TGFβ1 regulates PLXNA2 and PLXNA3 expression in BrCa cells. **A)** Analysis of PLXNA2 (upper graph) and PLXNA3 (lower graph) mRNA levels after 24h treatment with TGFβ1 (5ng/mL). Graphs represent RQ mean values ± S.E.M. (n=1, triplicates); *P < 0.05, ***P < 0.001 comparing control (-) *vs* TGFβ1 (+) by *t*-Student's test. **B)** Representative western blot analysis of PLXNA2 and PLXNA3 protein levels normalized with β-Tubulin after 4h treatment of BrCa (MDA-MB-231 -231-, BT-549 -BT-, MDA-MB-453 -453- and ZR-75-1 -ZR-) cells with TGFβ1 (5ng/mL). Protein quantifications are referred to the non-treated control condition (-) (n=2).

For this end, we used the bone marrow conditioned media (BMCM) obtained from hBM-MSCs (see *Materials & Methods, section 3.1.3.1* for further information), described as a quiescence inducing stroma[306]. After 48h treatment, we found that PLXNA3 expression was up-regulated in LDS cells at protein (**fig. 42A**) and mRNA levels (**fig. 42B**) and in the HDS MDA-MB-453 cell line at the protein level as well (**fig. 42A**). Although no significant changes were detected in PLXNA2 mRNA levels (**fig. 42B**), a down-regulation of PLXNA2 protein level was observed in MDA-MB-231 (LDS) and ZR-75-1 (HDS) cells treated with the BMCM (**fig. 42A**). These results suggested that dormancy inducing signals could induce PLXNA3 expression and decrease PLXNA2 expression in some cases, increasing PLXNA3/PLXNA2 ratio in LDS and ZR-75-1 (HDS) (**fig. 42A**). Thus, our results indicate that dormant-like BrCa cells might express high levels of PLXNA3 while low levels of PLXNA2.

Taken all together, our results showed that both PLXNs might be regulated in opposite ways by pro- or anti-proliferative signals suggesting that microenvironmental signals, TGFβ family members among them, can regulate PLXNs expression.

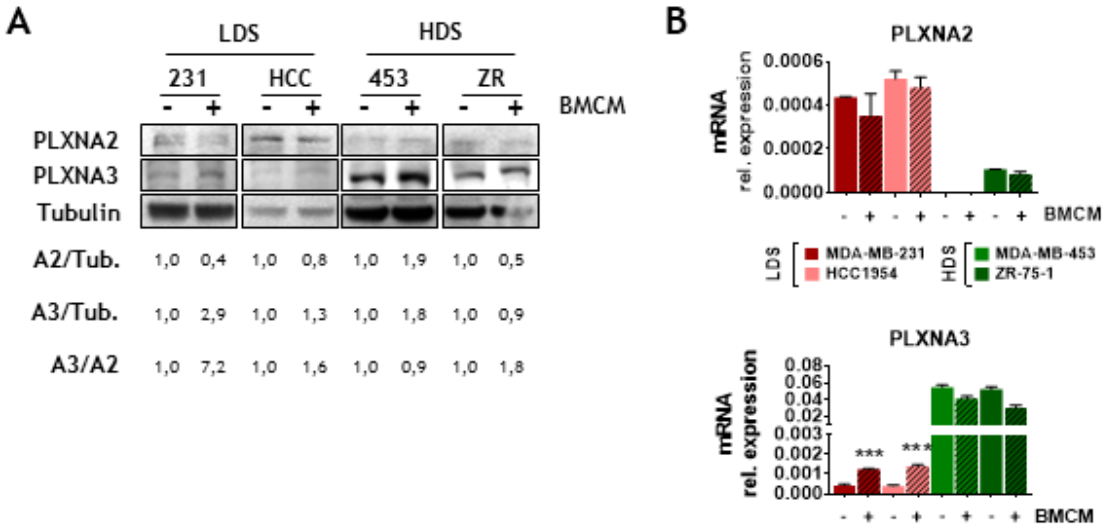

Figure 42. Bone marrow conditioned media increases PLXNA3 levels while reduces PLXNA2 expression levels in BrCa cells. **A)** Representative analysis of PLXNA2 and PLXNA3 protein levels normalized with β-Tubulin after 48h treatment with BMCM. Protein quantifications are referred to the non-treated control condition (-) (n=2). **B)** Analysis of PLXNA2 (upper graph) and PLXNA3 (lower graph) mRNA levels after 48h treatment with BMCM. Graphs represent RQ mean values ± S.E.M. (n=1, triplicates); ***P < 0.001 comparing control (-) *vs* BMCM (+) treatment by *t*-Student's test.

4.3.2. PLXNA2 regulates breast tumour growth by inhibiting cell migration, invasion and stemness

Beyond being the receptor for SEMA3s and co-receptor for NRPs, little is known about the role of PLXNA2 in tumorigenesis. Hence, we studied the functional consequences of PLXNA2 inhibition in MDA-MB-231 cells, where it is highly expressed.

4.3.2.1. PLXNA2 inhibition does not regulate quiescence markers expression

Previous results have showed that PLXNA2 was regulated by microenvironmental signals described as DTCs phenotype modulators (TGFβ1 and BMCM) (**fig. 41, 42**). In addition, PLXNA2 was up-regulated in lung and bone-marrow DTCs in our HNSCC model (**fig. 25C**) as well as in lung cancer DTCs[484]. Based on the above, we analysed if PLXNA2 could regulate dormancy/quiescence markers expression. We used a small-interfering RNA against PLXNA2 (siA2) to inhibit its expression and then tested the activation of several dormancy-driver pathways. PLXNA2 silencing increased TGFβR3 but not Dec2 mRNA levels (**fig. 43A**) as well as it slightly activated p38 signalling pathway (**fig. 43B**). Finally, we evaluated whether PLXNA2 could be modulating cell cycle progression in proliferative BrCa cells. For this, we inhibited PLXNA2 expression for 48h and then cultured the cells in serum-free media for 24h. As expected from qPCR and western blot results, the inhibition of PLXNA2 did not alter MDA-MB-231 cell cycle progression (**fig. 43C**).

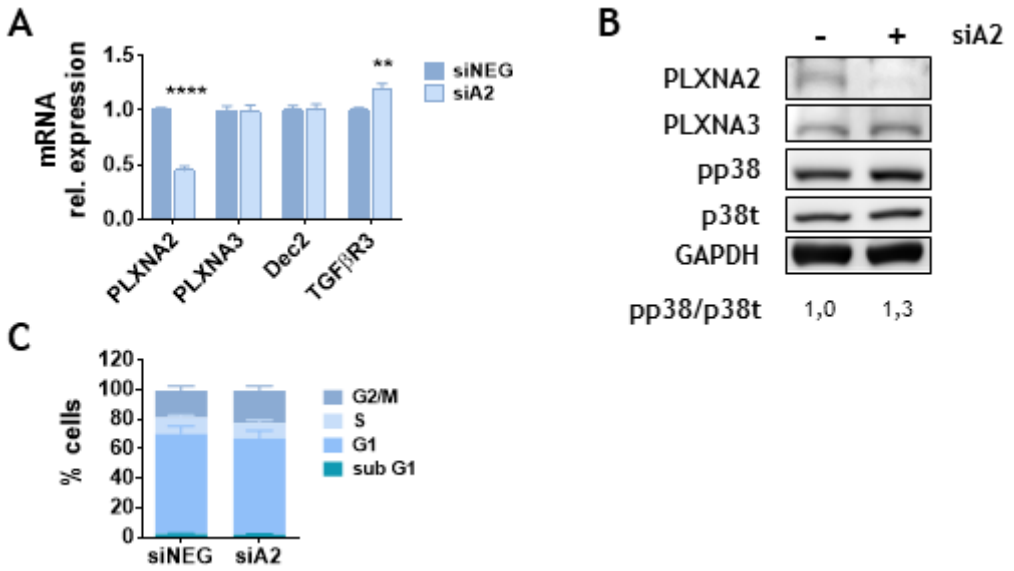

Figure 43. PLXNA2 inhibition does not modulate MDA-MB-231 quiescence and cell cycle *in vitro*. A) Analysis of PLXNA2, PLXNA3 and the dormancy markers Dec2 and TGFβR3 mRNA levels after 48h treatment with siA2. Graphs represent mRNA RQ mean values normalized to siNEG (n=3, triplicates). **B)** Representative western blot analysis of PLXNA2, PLXNA3 and pp38/p38 protein levels normalized with GAPDH after 48h of siA2 treatment. pp38/p38 protein levels are referred to siNEG (-) (n=2). **C)** Cell cycle analysis in siNEG and PLXNA2 silenced (siA2) MDA-MB-231 cells (n=2, duplicates). Graphs represent the percentage of cells in each cell cycle phase. All the graphs represent mean ± S.E.M.; **P < 0.01, ****P < 0.0001 comparing siNEG *vs* siA2 by *t*-Student's test.

4.3.2.2. PLXNA2 inhibition enhances cell migration and invasion in BrCa cells

PLXNA2 and its ligand SEMA6A are widely described as master regulators of neural cells migration[488,489]. However, only one study has related PLXNA2 expression with tumour cell migration and invasion, associating its up-regulation with metastatic prostate cancer progression[443]. To study if PLXNA2 plays a role in BrCa migration, we inhibited PLXNA2 and then studied cell migration using wound healing assays. Interestingly, we observed that PLXNA2-silenced cells migrated more than non-silenced cells (**fig. 44A**). However, there were no differences regarding cell invasion using 10% serum containing media as a chemoattractant (**fig. 44B**). Nevertheless, we also measured the effect of PLXNA2 inhibition in ECM proteolytic degradation. For this, a DQ Collagen assay was performed where cells were grown in the presence of a fluorescent dye-quenched DQ-collagen IV mixed with matrigel. Therefore, high enzymatic activity of pro-invasive cells, mainly by MMPs, results in a green fluorescence signal. We found that PLXNA2-silenced cells resulted in higher detectable fluorescence signal, hence, inhibition of PLXNA2 increased ECM degradation (**fig. 44C**). With all, our data suggest that PLXNA2 may restrain ECM degradation and cell migration.

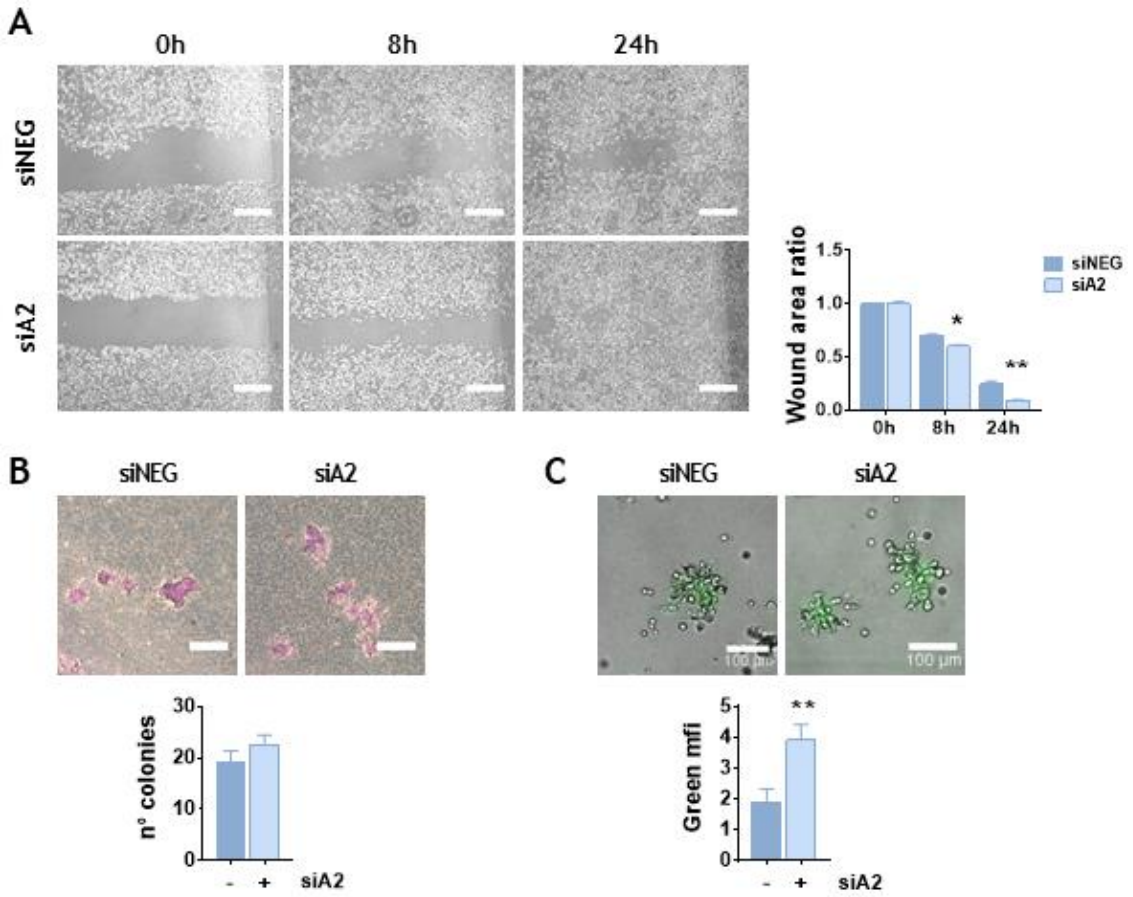

Figure 44. PLXNA2 inhibition promotes cell migration and ECM degradation. **A)** Left panels, representative images from phase-contrast microscopy after 0, 8 and 24h migration of siNEG (upper panels) and PLXNA2 silenced (siA2) (lower panels) MDA-MB-231 cells. Scale bar: 150µm. Right panel, graph showing the quantification of the ratio of the wound area (n=2, triplicates). **B)** Invasion through matrigel using 10% FBS as chemoattractant. Upper panel, representative phase contrast microscopy images of siNEG or siA2 invading cells (48h). Scale bar: 50µm. Lower panel, graph showing the mean value ± S.E.M. of the number of invading colonies (n=1, duplicates). **C)** Upper panel, representative images of the DQ Collagen degradation, detected by green signal, 96h after cell seeding. Cells were previously treated with siA2 for 48h. Scale bar: 100µm. Lower panel, graph showing the quantification of the green mfi (n=1, duplicates). All the graphs represent mean ± S.E.M.; *P < 0.05, **P < 0.01 comparing siNEG (-) *vs* siA2 (+) by *t*-Student's test (**B, C**) or by one-way ANOVA, Sidak's test (**A**).

For cell migration to occur, the acquisition of mesenchymal features from epithelial cells is required[490]. Therefore, to further study the role of PLXNA2 on cell migration, we analysed the expression of EMT program markers by qPCR. PLXNA2 inhibition revealed no changes in the expression of some EMT markers (**fig. 45**), likely since MDA-MB-231 cells are highly mesenchymal cells (low E-cadherin/vimentin ratio) and thus, it might be hard to detect an increase in these features towards an even more mesenchymal phenotype. With all, our results on migration and invasion suggest that in BrCa cells PLXNA2 prevents ECM degradation and cells migration.

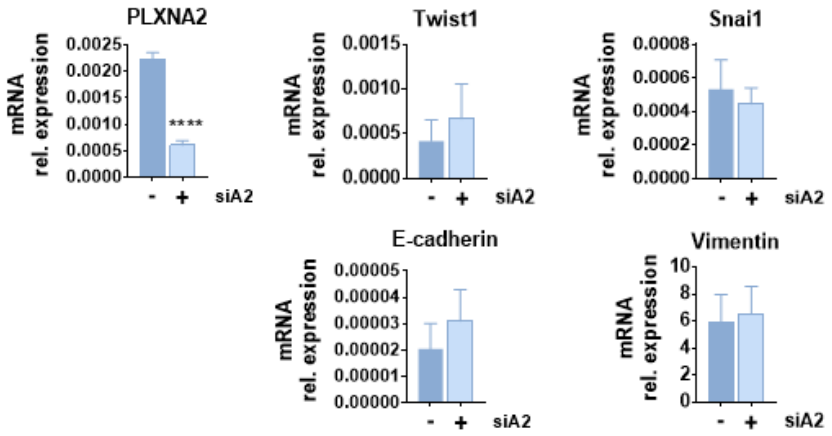

Figure 45. PLXNA2 inhibition regulates EMT markers expression. Analysis of EMT markers mRNA levels after 48h siA2 treatment. Graphs represent RQ mean values ± S.E.M. (n=4, triplicates); ****P < 0.0001 comparing siNEG (-) *vs* siA2 (+) by *t*-Student's test.

4.3.2.3. PLXNA2 negatively regulates BrCa stemness and tumour-initiation capacity

Following with our studies, we tested the role of PLXNA2 in tumour initiating capacity *in vitro*. For that, we performed anchorage-dependent growing assays and found that PLXNA2-inhibited cells were able to form a higher number and bigger foci (**fig. 46**). These results indicate that PLXNA2 might be determinant in tumour-initiation capacity.

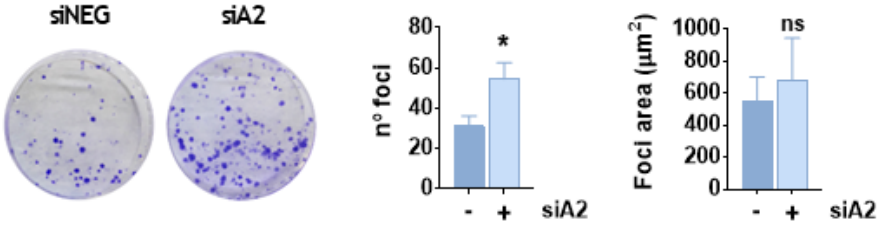

Figure 46. PLXNA2 inhibition increases clonogenicity. Representative images (left panel) and quantification of the total number of cell foci (middle graph) and foci area (right graph) of the colonies from anchorage-dependent growth assay. Cells were previously treated with siA2 for 48h and cultured during 10-15 days in 5% FBS containing media. Graph represents mean ± S.E.M. (n=3, duplicates); ns, non-significant, *P < 0.05 siNEG (-) *vs* siA2 (+) by *t*-Student's test.

Therefore, to further investigate the potential function of PLXNA2 in tumorigenesis, we analysed its association with cancer cell stemness. CSCs are responsible of the generation, reconstitution and propagation of the disease and thus, of tumour initiation and metastasis[19,20]. The stemness properties of the cells were analysed by testing the mRNA expression of some stem cell markers. We detected a slight upward trend on the expression of CD44, CD49f and FoxC1 as well as a prominent ALDH1 induction upon PLXNA2 inhibition (**fig. 47A**). To confirm these results, we analysed CD44 and CD49f expression using flow cytometry. We found that CD44 levels were slightly increased when PLXNA2 was inhibited although it did not reach statistical significance (**fig. 47B**). According to our results, PLXNA2 might restrict breast cancer cells stemness and thus reduce breast tumour initiation.

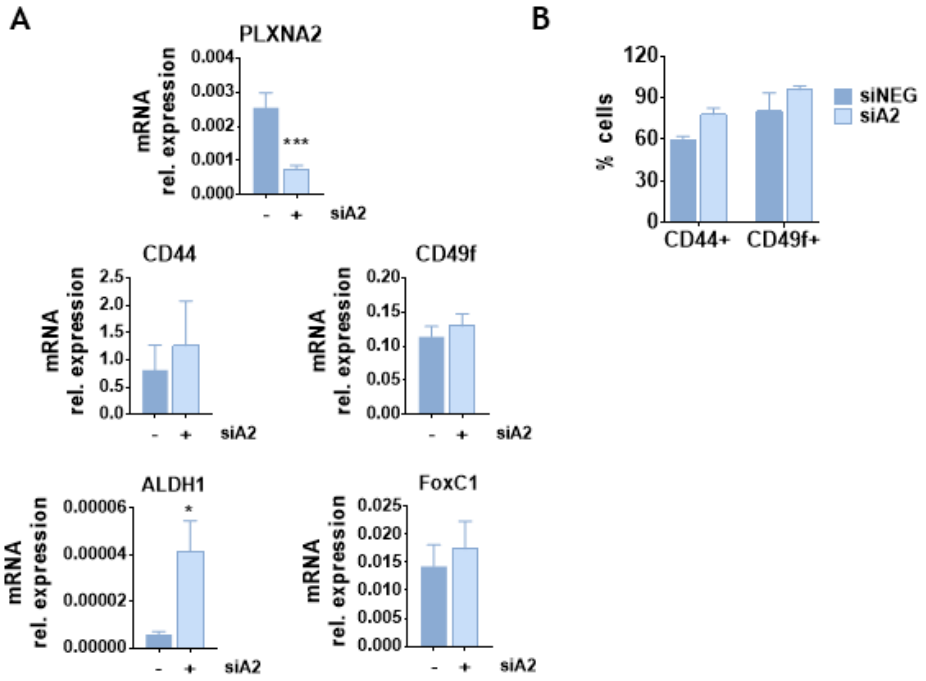

Figure 47. PLXNA2 inhibition effect on stemness markers expression. **A)** Analysis of stem cell markers mRNA levels in siNEG and siA2 cells (48h). Graphs represent mRNA RQ mean values (n=4, triplicates). **B)** Flow cytometric analysis of cell surface CD44 and CD49f levels in siNEG and siA2 cells (48h). Graphs represent the percentage of cells expressing CD44 or CD49f in each condition (n=2, duplicates). All the graphs represent mean ± S.E.M.; *P < 0.05, ***P < 0.001 comparing siNEG (-) *vs* siA2 (+) by *t*-Student's test.

3.2.4. PLXNA2 regulates tumour growth *in vivo*, likely inducing cell quiescence

To confirm the inhibitory role of PLXNA2 in breast cancer initiation, we finally examined whether PLXNA2 inhibition affects tumour growth *in vivo*. To test this, we used the chicken embryo CAM assay (see *Materials & Methods, section 3.8.1* for further details) where PLXNA2-inhibited (siA2) or control (siNEG) MDA-MB-231 cells were inoculated and let the PTs grow for 4 days. We found that the tumours formed by the PLXNA2-silenced cells tend to be bigger than the control tumours (**fig. 48A**), suggesting that PLXNA2 might inhibit tumour growth. Analysing the histological features of these tumours, we observed that the proliferation marker Ki67 was not modulated (**fig. 48B**). Nevertheless, the quiescence marker p21 was down-regulated when PLXNA2 was inhibited (**fig. 48C**), suggesting that PLXNA2 might regulate the size of the tumours by inducing cell quiescence *in vivo*.

Altogether, the results obtained from the inhibition of PLXNA2 in the MDA-MB-231 cells suggested that PLXNA2 could have a potential role as an anti-tumour protein. Our results suggest that PLXNA2 might inhibit BrCa cells growth and dissemination by blocking cell migration and invasion and regulating stem-cell associated properties.

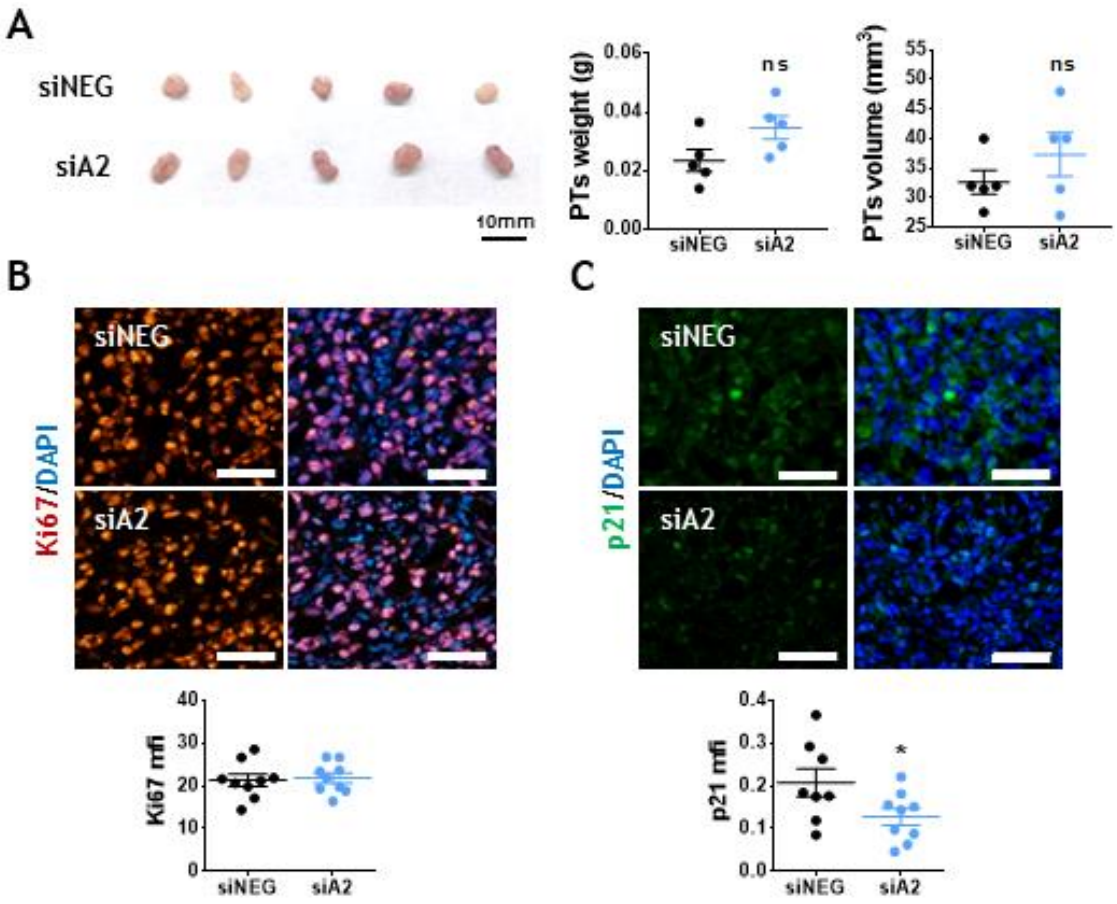

Figure 48. PLXNA2 inhibition effects on tumour growth in CAM *in vivo* assays. **A)** $1.5 \cdot 10^6$ control (siNEG) or PLXNA2 inhibited (siA2) (48h) MDA-MB-231 cells were inoculated in day 11 chicken embryo CAMs and let them grow for 4 days. Left panel, representative MDA-MB-231 tumour images. Middle and left panels graphs showing tumour weight (g) (middle) and volume (mm^3) (right) at end point. **B, C)** Representative IF images of Ki67 (**B**) and p21 (**C**). Scale bar: 50µm. Lower graphs, Ki67 and p21 mfi quantification in MDA-MB-231 PTs. Graphs represent mean ± S.E.M. (n=1, with 5 inoculated eggs per group); ns, non-significant, *P < 0.05 comparing siNEG *vs* siA2 by *t*-Student's test.

4.3.3. PLXNA3 might restrain tumour growth in ER-positive breast tumours

Regarding PLXNA3, little is known about its role in tumourigenesis beyond the fact that it is down-regulated in tumour samples as compared to healthy tissues[442,444,445]. Our initial characterization revealed that PLXNA3 is up-regulated in ZR-75-1 cells (**fig. 24**). This cell line is classified as luminal A BrCa subtype, whose relapses usually develops after very long periods of quiescence[69]. Interestingly, luminal BrCa patients expressing high levels of PLXNA3 have better prognosis (**fig. 40B**), suggesting PLXNA3 can be a tumour suppressor. Moreover, we found that dormancy-inducing signals (ex. BMCM) increased PLXNA3 expression in LDS cells (**fig. 42**). Therefore, we wondered whether PLXNA3 could regulate dormancy induction in luminal BrCa subtypes.

4.3.3.1. PLXNA3 down-regulation enhances luminal A breast tumours growth *in vivo*

To characterize the role of PLXNA3 in BrCa tumorigenesis, we first analysed whether PLXNA3 regulated cell cycle. For that, we inhibited its expression using a siRNA specifically designed against PLXNA3 (siA3). The HDS ZR-75-1 cells were transfected with siA3 and treated with serum-free media

for 24h before cell cycle analysis. No differences in cell cycle were observed in PLXNA3-inhibited cells as compared to control cells (**fig. 49A**). Tumorigenic capacities were further studied by performing clonogenic assays and we detected no changes in the number and size of foci between control and inhibited cells (**fig. 49B**). Nevertheless, PLXNA3 inhibition induced an up-regulation in some stem cell markers expression, such as CD44 and FoxC1, when analysed by qPCR (**fig. 49C**). Moreover, PLXNA3 inhibition significantly increased *Twist1* and *Snai1* gene expression (**fig. 49D**), both EMT markers. These results suggest that PLXNA3 inhibition does not affect BrCa cells cell cycle progression or tumour initiation capacity *in vitro*, whereas it might activate some stem cell-like and EMT programs.

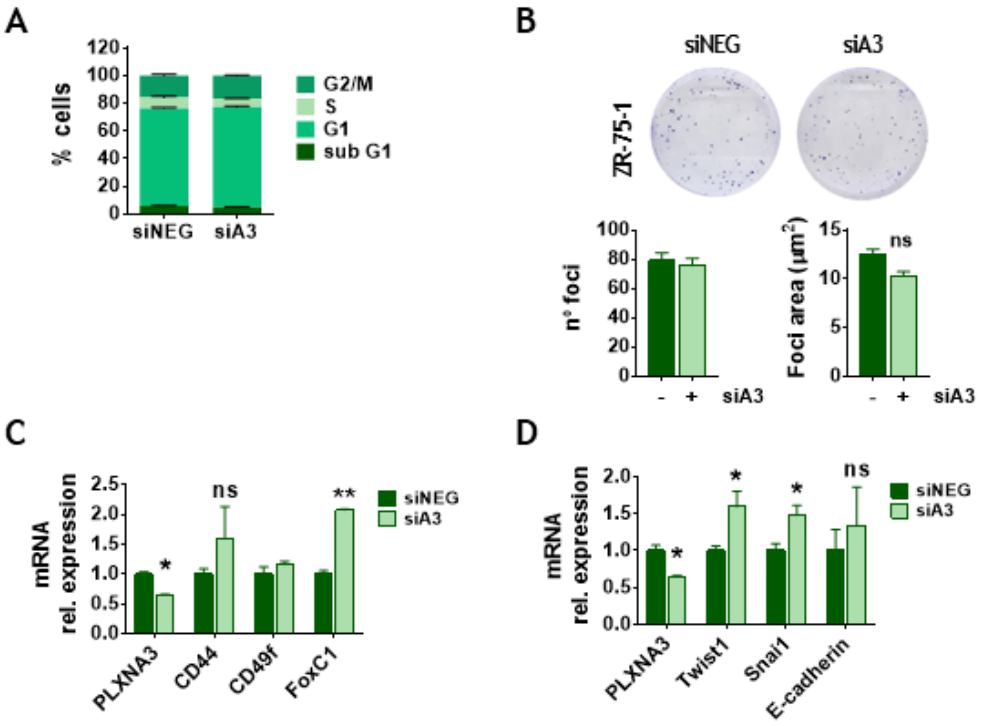

Figure 49. PLXNA3 inhibition does not regulate cell cycle and clonogenicity but it might increase cells stemness. **A)** Cell cycle analysis in control (siNEG) and PLXNA3 silenced (siA3) ZR-75-1 cells. Graphs represent the percentage of cells in each cell cycle phase (n=1, duplicates). **B)** Representative images (upper panel) and quantification of the total number of cell foci (lower left graph) and foci area (lower right graph) of the colonies from anchorage-dependent growth assay in siNEG siA3 cells. Graphs represent mean values ± S.E.M. (n=1, triplicates). **C)** Analysis of stem cell markers mRNA levels in siNEG siA3 cells (n=2, triplicates). **D)** Analysis of EMT markers mRNA levels in siNEG and siA3 cells (n=2, triplicates). All the graphs represent mean ± S.E.M.; ns, non-significant, *P < 0.05; **P < 0.01 comparing siNEG *vs* siA3 by *t*-Student's test.

To evaluate whether PLXNA3 could be implicated in breast tumours growth, we inoculated PLXNA3-inhibited ZR-75-1 cells in day 11 chicken embryo CAM (see *Materials & Methods, section 3.8.1* for further details). After 4 days growing, tumours formed by the inhibited cells were bigger and with more than one nodule, although it did not reach statistical significance (**fig. 50A**). Ki67 expression was slightly decreased in siA3 tumours (**fig. 50B**) while PLXNA3-inhibited tumours tend to express lower levels of the dormancy marker, p21 (**fig. 50C**). With all, these results suggest that PLXNA3 may inhibit tumour growth, at least in this luminal A BrCa subtype cell line.

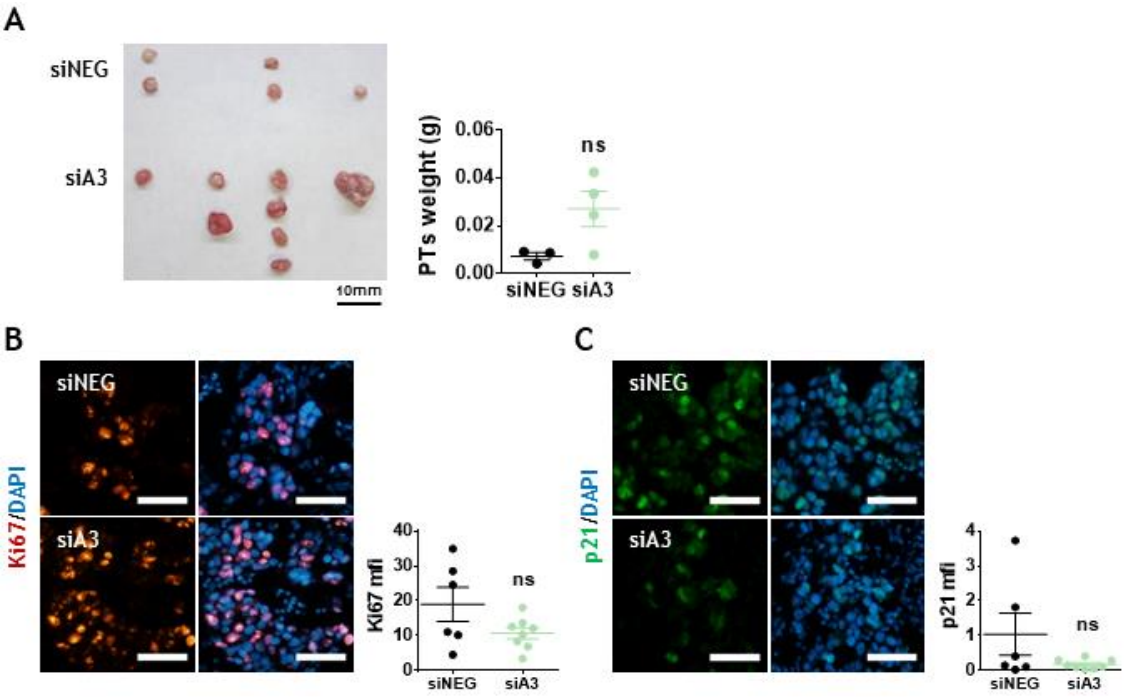

Figure 50. PLXNA3 down-regulation effects on tumour growth in CAM *in vivo* assays. **A)** $1.5 \cdot 10^6$ control (siNEG) or PLXNA3 inhibited (siA3) (48h) ZR-75-1 cells were inoculated in day 11 chicken embryo CAMs where they grew for 4 days. Left panel, representative ZR-75-1 tumour images. Right panel, graph showing tumour weight (g) at end point. **B, C)** Left panels, representative IF images of Ki67 (**B**) and p21 (**C**). Scale bar: 50µm. Right panels, graphs showing Ki67 and p21 mfi quantification in ZR-75-1 PTs. Graphs represent mean ± S.E.M. (n=1, with >3 inoculated eggs per group); *t*-Student's test between siNEG and siA3 was performed and revealed non-significant (ns) differences.

4.3.3.2. Oestrogens regulate PLXNA3 expression in ER-positive BrCa cells

Patients' data revealed that PLXNA3 is up-regulated in ER-positive breast tumours (**fig. 40A**) where higher *PLXNA3* gene expression correlates with higher OS (**fig. 40B**). In this regard, we wondered whether PLXNA3 could be regulated by oestrogens in BrCa as it has been described previously for other hormone-dependent tumour types, such as ovarian cancer[491]. Therefore, we treated ZR-75-1 cells with β-oestradiol (E2) and we found no changes in PLXNA3 mRNA levels (**fig. 51A**). However, upon treatment with β-oestradiol PLXNA3 protein expression was up-regulated (**fig. 51B**), suggesting that E2 exerts a post-transcriptional regulation of PLXNA3 expression.

As explained, ER-positive tumours are clinically treated with ER inhibitors, which increase patients' OS[63,68]. Hence, in parallel, cells were treated with the widely used ER inhibitor tamoxifen. After 48h of treatment, no differences in PLXNA3 mRNA levels were detected (**fig. 51C**) whereas conversely to E2 treatment, PLXNA3 protein levels were clearly down-regulated when treated with the ER inhibitor tamoxifen (**fig. 51D**). These results suggest that oestrogen signalling pathway might be involved in PLXNA3 up-regulation in dormant-like BrCa cells.

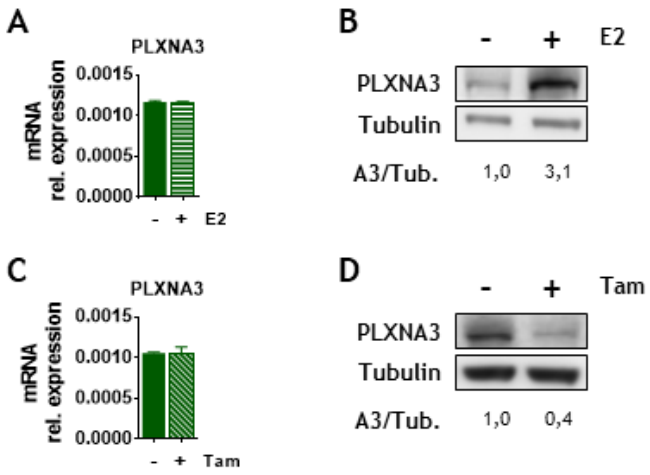

Figure 51. PLXNA3 expression is regulated by ER signalling. **A, C)** Analysis of PLXNA3 mRNA levels in ZR-75-1 cells after 48h treatment with oestradiol (E2) (1nM) (**A**) or tamoxifen (Tam) (1µM) (**C**). Graphs represent RQ mean values ± S.E.M. (n=2, triplicates); *t*-Student's test between control (-) and oestradiol or tamoxifen (+) treatment was performed and revealed non-significant differences. **B, D)** Representative western blot analysis of PLXNA3 protein levels normalized with β-Tubulin in ZR-75-1 cells after 48h treatment with oestradiol (E2) (1nM) (**B**; n=2) or tamoxifen (Tam) (1µM) (**D**; n=1). PLXNA3 quantifications are referred to the non-treated control (-) condition.

4.4. NRP2 induces tumour growth and DTCs proliferation promoting lung metastases development

NRP2 is a coreceptor for PLXNs and SEMA3s. It plays an important role in tumour biology regulating multiple tumourigenic processes such as cell proliferation, survival, migration and dissemination. Altogether, NRP2 has been shown to promote tumour growth and metastasis in different tumour types[389,397]. Even though its malignant nature is well demonstrated, little is known about the mechanisms regulated by NRP2 which will lead to tumour development. Furthermore, NRP2 role in DTCs biology has not been explored before.

4.4.1. NRP2 expression negatively correlates with metastatic risk and BrCa and HNSCC patients' survival

The initial characterization of NRPs expression in our models highlighted the up-regulation of NRP1 and NRP2 in more aggressive BrCa and HNSCC cell lines (**fig. 22, 23**). In addition, previous data from our group has previously shown that NRP2 expression correlates with worse prognosis in BrCa patients[458]. Furthermore, using data from Kaplan-Meier plot database where 2765 human BrCa samples were analysed, we found that patients with high NRP2 expression have lower DMFS)(61.2 months) than patients with low NRP2 expression (116 months) (**fig. 52A**)[481,486]. To analyse the role of NRP2 in head and neck cancer, in collaboration with Dr. Camacho and Dr. Leon at Sant Pau Hospital (Barcelona, Spain), we analysed *NRP2* gene expression in the PTs of a cohort of 92 HNSCC patients and detected that high levels of *NRP2* positively correlated with higher risk of developing metastasis and worse patients' DMFS (**fig. 52B**). These results suggest that NRP2 expression correlates with a higher risk of metastasis development and hence, might be a good biomarker of metastasis risk.

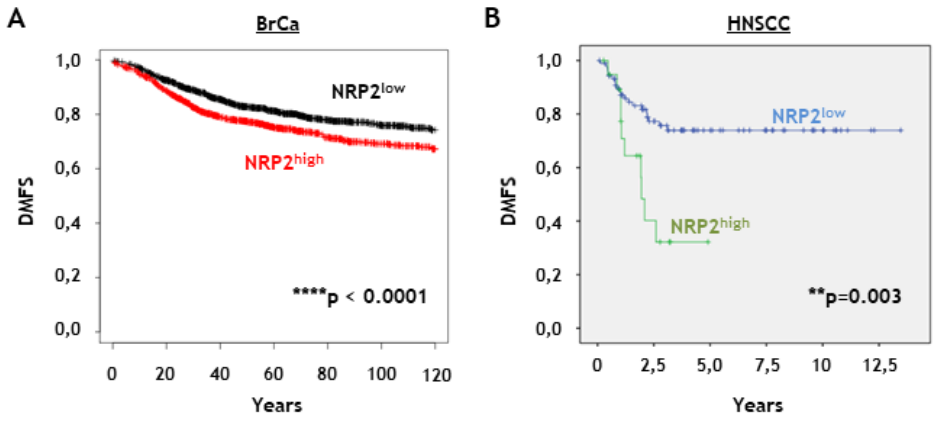

Figure 52. High levels of NRP2 negatively correlate with BrCa and HNSCC patients' survival. **A)** Kaplan-Meier curve for distant metastases-free survival (DMFS) in a cohort of 2765 BrCa patients with high (red; n=1437) or low (black; n=1328) levels of NRP2. Adapted from Györffy *et al.* (2010)[486]. **B)** Kaplan-Meier curve for DMFS in a cohort of 92 HNSCC patients with high (green; n=20) or low (blue; n=72) levels of NRP2. Analysis performed in collaboration with Dr. Camacho and Dr. Leon from Sant Pau Hospital (Barcelona, Spain).

4.4.2. NRP2 regulates cell proliferation while reducing p27 expression, triggering tumour growth *in vivo*

Analysis of NRPs expression in BrCa cell lines classified according to their expression of dormancy inducing genes showed that dormant-like BrCa cells down-regulated NRP2 and NRP1 (**fig. 22**). Furthermore, NRP2 expression was down-regulated in head and neck dormant cell lines (**fig. 23**). These results suggested that NRP2 expression inversely correlated with a dormant/quiescent phenotype. Therefore, we decided to characterize NRP2 role in BrCa and HNSCC proliferation.

4.4.2.1. NRP2 deletion inhibits cell proliferation and cell cycle progression

To analyse NRP2 function, we modulated NRP2 expression using three different strategies: transient inhibition using a small-interfering RNAs specifically designed against NRP2 (siNRP2), blocking its activity with a NRP2-blocking antibody (αNRP2) which was previously shown to prevent ligands binding to NRP2 [405,492,493] and permanent deletion of NRP2 expression using CRISPR-Cas9 system ($NRP2^{KO}$). We first performed MTT assays using different doses of the NRP2 blocking antibody for 72h. Although NRP2 has been related with cell proliferation, increasing doses of the antibody did not reveal any modulation in the proliferation rate of the cells *in vitro* (**fig. 53**).

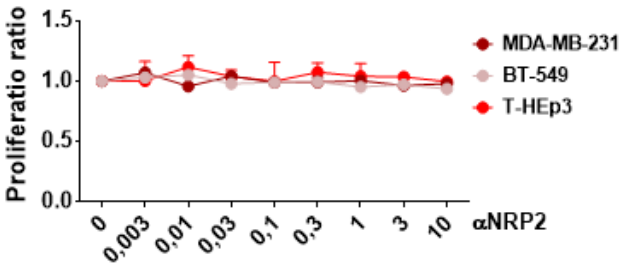

Figure 53. Blocking NRP2 activity does not modulate cell proliferation *in vitro*. Cell proliferation quantification for MDA-MB-231, BT-549 and T-HEp3 cells treated for 72h with increasing doses of NRP2 blocking antibody (αNRP2) (0-10µg/mL). The graph represents the ratio of proliferation mean value ± S.E.M. (n=1); two-way ANOVA, Dunnett's test between control (no treatment; 0) and each concentration of αNRP2 treatment was performed and revealed non-significant differences.

Then, our next step was to study the role of NRP2 in proliferation by generating stable NRP2-kock out cell lines. Permanent NRP2 knock-out ($NRP2^{KO}$) in MDA-MB-231 and T-HEp3 cell lines was achieved through the CRISPR-Cas9 technology, where complete mRNA (**fig. 54A, C**) and protein (**fig. 54B, D**) inhibition was obtained. Interestingly, total NRP2 deletion notably increased p27 protein expression in MDA-MB-231 and T-HEp3 cells (**fig. 54B, D**).

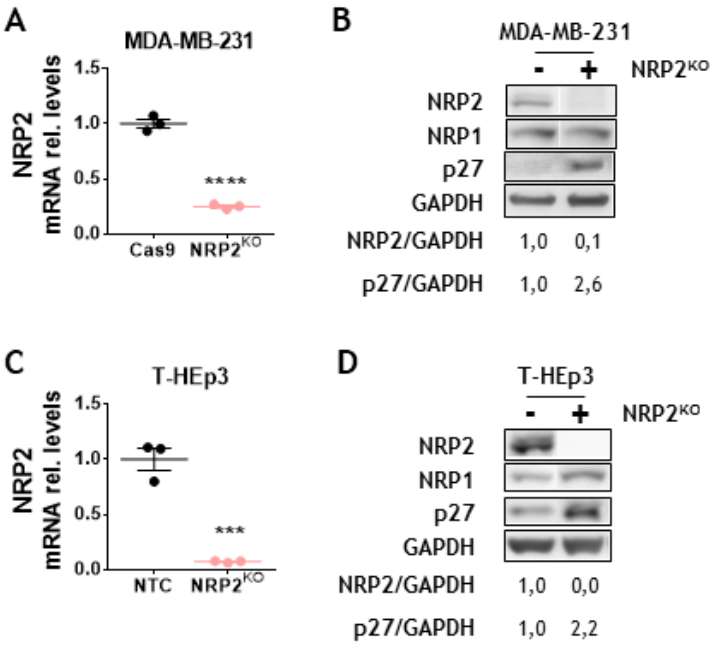

Figure 54. NRP2 deletion by CRISPR-Cas9 system. A, C) Analysis of NRP2 mRNA levels in Cas9 or Cas9-NTC (NTC; non-targeted cells) controls and $NRP2^{KO}$ MDA-MB-231 (**A**) and T-HEp3 (**C**) cells. Graphs represent RQ mean values ± S.E.M. (n≥3); ***P < 0.001, ****P < 0.0001 comparing Cas9/NTC *vs* $NRP2^{KO}$ by *t*-Student's test. **B, D)** Representative western blot analysis of NRP2, NRP1 and p27 protein levels normalized with GAPDH in Cas9/NTC and $NRP2^{KO}$ MDA-MB-231 (**B**) and T-HEp3 (**D**) cells. Protein quantifications are referred to the control (-) condition.

Cell cycle progression relies on protein complexes composed by cyclins and CDKs. To prevent abnormal proliferation, nuclear Cip/Kip proteins, such as p21 and p27, act as catalytic inhibitors of CDKs[494,495]. Due to the key role of p27 in cell cycle progression and the observed p27 induction after NRP2 deletion, we next analysed whether NRP2 knock-out induced cell cycle arrest. After culturing the cells for 24h in serum-free media, we found that $NRP2^{KO}$ cells had their cell cycle arrested although the arrest was uneven in both cell lines. While MDA-MB-231 $NRP2^{KO}$ cells were arrested in G2/M phase (**fig. 55A**), T-HEp3 $NRP2^{KO}$ cells were arrested in G1 as compared to NTC control cells (**fig. 55B**).

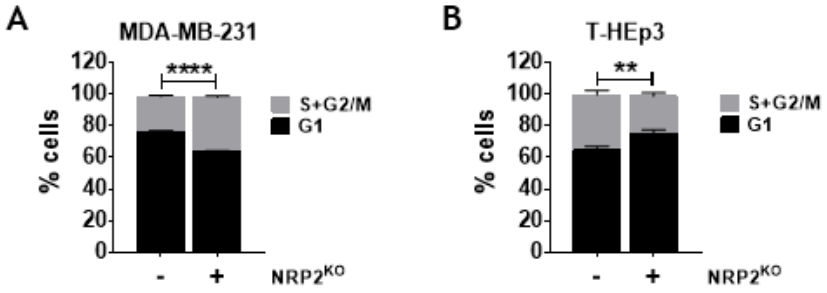

Figure 55. NRP2 deletion induces cell cycle arrest. MDA-MB-231 (**A**) and T-HEp3 (**B**) cell cycle in control (NTC) *vs* NRP2-deleted cells ($NRP2^{KO}$). Cells were seeded and cultured with serum-free culture media for 24h before performing the cell cycle analysis. Graphs show the percentage (%) of cells in each phase. Both graphs represent mean ± S.E.M. (n=2 in MDA-MB-231 and n=3 in T-HEp3); **P < 0.01, ****P < 0.0001 comparing NTC *vs* $NRP2^{KO}$ by two-way ANOVA, Sidak's test.

These results suggested that NRP2 deletion promotes cell cycle arrest and might induce quiescence by p27 up-regulation. Cell proliferation clearly reflects the activity of cell cycle. Therefore, we next evaluated whether tumour cells proliferation rate was modulated by NRP2 deletion. We performed MTT proliferation assays for 4 days in a row and observed that NRP2^{KO} cells had significantly lower proliferation than control cells, both in MDA-MB-231 (**fig. 56A**) and T-HEp3 cells (**fig. 56B**).

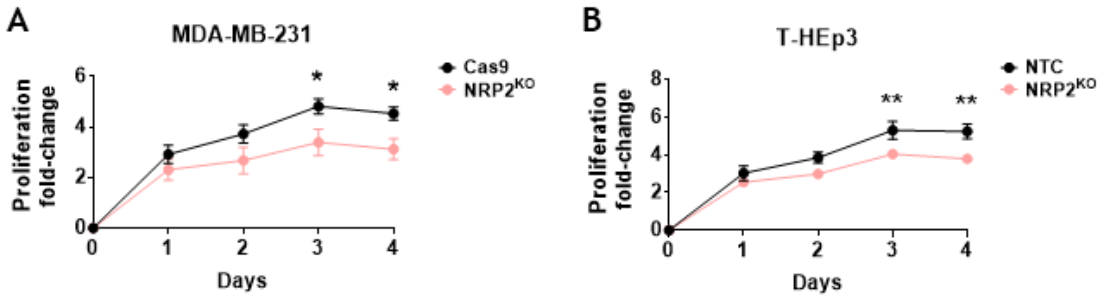

Figure 56. NRP2 deletion reduces cell proliferation. MDA-MB-231 (**A**) and T-HEp3 (**B**) cells proliferation in control (Cas9, NTC) *vs* NRP2-deleted cells (NRP2^{KO}). Cells were seeded and culture with 2% FBS culture media and proliferation was assessed with MTT assays every day, for 4 days after seeding. Graphs represent the fold-change of proliferation mean ± S.E.M. referred to day 0 (n=2); *P < 0.05, **P < 0.01 comparing Cas9/NTC *vs* NRP2^{KO} by one-way ANOVA, Sidak's test.

Taking together, our results indicate that knocking out NRP2 expression in BrCa and HNSCC cells reduces cell proliferation while promoting cell cycle arrest in different cell cycle phases. This could be a consequence of the p27 up-regulation observed in cells with NRP2 deletion.

4.4.2.2. NRP2 inhibition up-regulates p27 levels in BrCa and HNSCC cell lines

To confirm that NRP2 can modulate p27 expression, we either treated the cells with the NRP2 blocking antibody or inhibited NRP2 expression with the siRNA and analysed p27 expression. Interestingly, we found that, in agreement with the previous mentioned results, NRP2 expression modulation increased p27 levels (**fig. 57**). Either by blocking NRP2 activity (**fig. 57A**) or inhibiting NRP2 expression by siNRP2 (**fig. 57B**), p27 protein levels were clearly up-regulated in BrCa and HNSCC proliferative cell lines. Taken together, these results suggest that NRP2 inhibits the expression of the cell cycle inhibitor p27, which in turn could be related to the pro-tumorigenic role of NRP2.

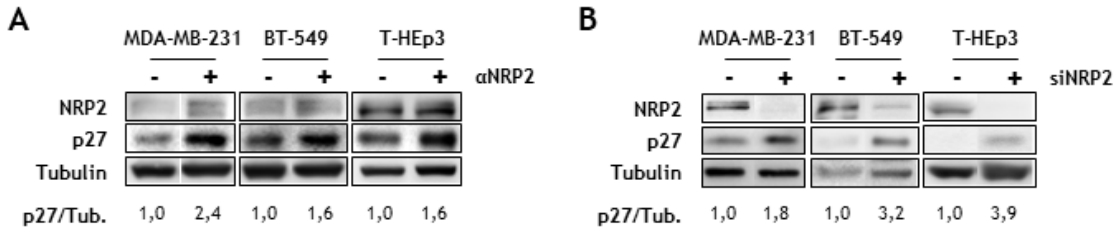

Figure 57. NRP2 down-regulation increases p27 expression. A) Representative western blot analysis of NRP2 and p27 protein levels normalized with α-tubulin after 24h treatment with αNRP2 (1µg/mL) (n≥3). **B)** Representative western blot analysis of NRP2 and p27 protein levels normalized with α-tubulin after 48h transfection with siNEG (-) or siNRP2 (+). p27 quantifications are referred to the non-treated (**A**) or non-inhibited (**B**) control (-) conditions (n≥3).

Our previous data have shown that NRP2 inhibits p27 expression. To assess the mechanisms by which NRP2 regulates p27 expression we first inhibited NRP2 using siRNAs and 24h after we inhibited several signalling pathways. We inhibited PI3K/AKT pathway using a selective AKT inhibitor (LY294002), the MEK/ERK pathway with a MEK inhibitor (PD98059) and the p38α/β MAPK pathway with a selective p38α inhibitor (SB203580). LY294002 and PD98059 treatments increased p27 levels in non-inhibited cells, suggesting p27 expression could be regulated by PI3K/AKT and ERK signalling pathways, whereas p38α inhibition induced p27 expression only in BT-549 cells (**fig. 58**). Moreover, we found that the up-regulation of p27, derived from the inhibition of NRP2, was slightly reverted in MDA-MB-231 cell line upon AKT inhibition (**fig. 58**). Nevertheless, ERK and AKT induction of p27 was attenuated upon NRP2 inhibition, at least in BT-549 cells (**fig. 58**).

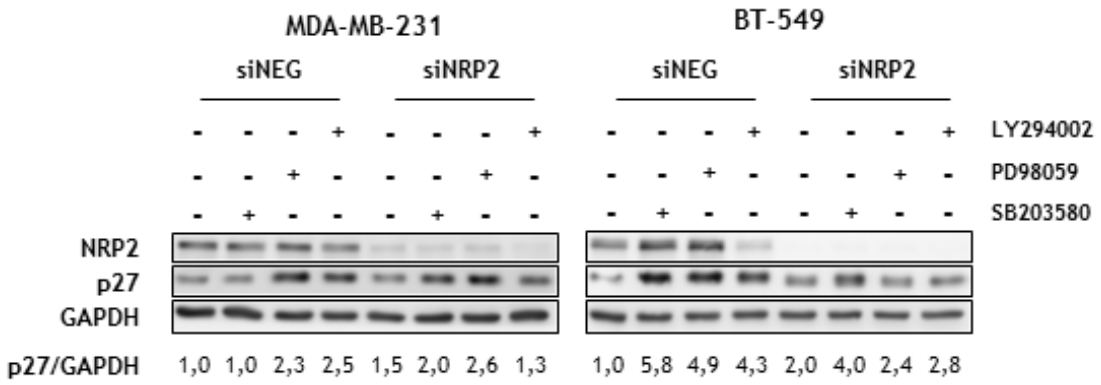

Figure 58. p27 expression regulation by NRP2, AKT, ERK and p38α in BrCa cells. Analysis of NRP2 and p27 protein levels normalized with GAPDH after 48h treatment with siNRP2 and 24h treatment with inhibitors in MDA-MB-231 (left panel) and BT-549 (right panel) cells. LY294002 (10μM), PD98059 (20μM) and SB203580 (10μM) were added in 10% FBS containing media for 24h after the first 24h of siNRP2 transfection. Inhibitors were directly added to the culture media. p27 quantifications are referred to the non-treated (-) and non-inhibited (siNEG) control condition (n=3).

4.4.2.3 NRP2 inhibition decreases the *in vitro* tumour-initiation capacity of BrCa and HNSCC cells

To study whether NRP2 inhibition modulated the tumour-initiation capacity of the cells we performed colony formation assays in NTC and NRP2-depleted cells. After 15 days, complete deletion of NRP2 tend to decrease the number of foci in T-HEp3 cells (**fig. 59A**) and more clearly in MDA-MB-231 cells, where NRP2 deletion completely abrogated foci formation (**fig. 59B**). These results suggest that the malignant role of NRP2 might be also associated to the tumour-initiation capacity enhancement in BrCa and HNSCC cells.

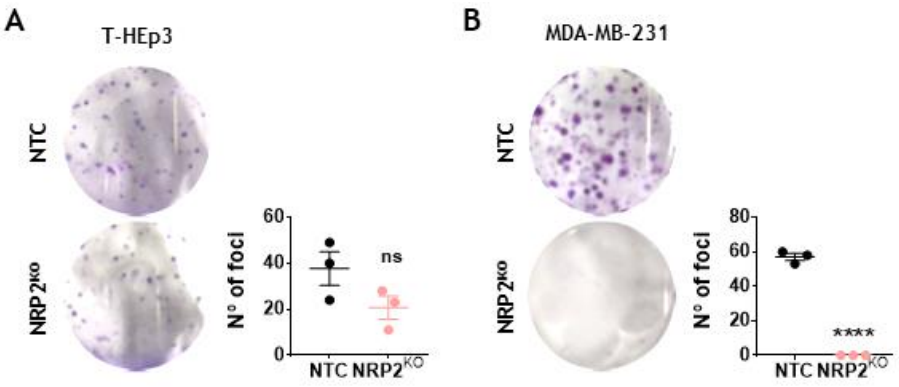

Figure 59. NRP2 deletion reduces the number of foci in T-HEp3 and MDA-MB-231 cells. A, B) Left panels, representative images of colonies from anchorage-dependent growth assay in T-HEp3 (**A**) and MDA-MB-231 (**B**) cells. Right graphs, quantification of the total number of colonies. Graphs represent mean ± S.E.M. (n=1, triplicates); ns, non-significant, ****P < 0.0001, comparing NTC *vs* NRP2^{KO} by *t*-Student's test.

4.4.2.4. NRP2 expression modulation might induce cell apoptosis by the intrinsic signalling pathway

Recent studies have associated NRP2 with cell death in tumour cells, where a decrease in its expression induces apoptosis[449,496–498]. To study if NRP2 could regulate apoptosis, we studied whether the intrinsic apoptotic signalling pathway was modulated after NRP2 inhibition with siRNA. We found that the pro-apoptotic protein Puma was induced after NRP2 knock-down, mainly in MDA-MB-231 cells (**fig. 60**).

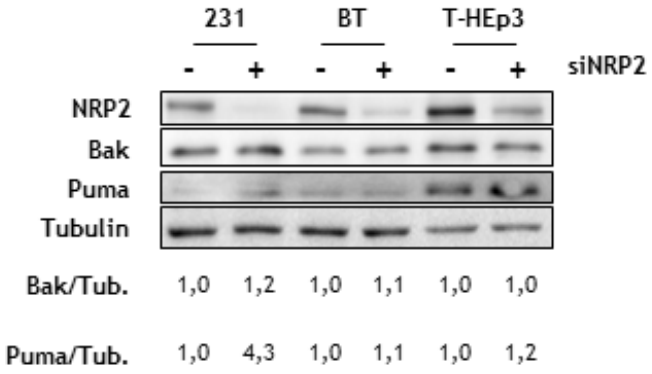

Figure 60. Transient NRP2 silencing increases the expression of the pro-apoptotic protein Puma in MDA-MB-231 cells. Representative western blot analysis of NRP2, Bak and Puma protein levels normalized with α-tubulin after 48h transfection with siNEG (-) or siNRP2 (+). Protein quantifications are referred to the non-inhibited (-) condition (n=2).

To examine the effect of NRP2 on BrCa cell viability, we performed an Annexin V/PI assay in NRP2 silenced cells. Here, Annexin V-positive cells were classified as early apoptotic cells, Annexin-V/PI-double positive cells as late apoptotic cells whereas PI-positive cells were considered necrotic cells. After 48h siNRP2 transfection and 24h culture in serum-free media, we found that transient NRP2 inhibition was not able to modulate BrCa cell death *in vitro* (**fig. 61**), where only a slight increase in the percentage of necrotic cells was observed in MDA-MB-231 and BT-549 cells.

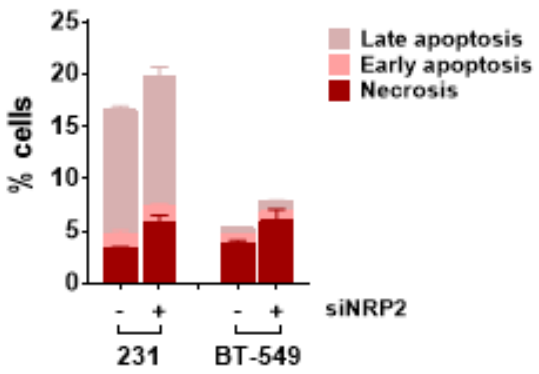

Figure 61. Transient NRP2 inhibition does not increase BrCa cell death *in vitro*. Apoptosis analysis in MDA-MB-231 (231) and BT-549 cell lines after 48h transfection with siNEG or siNRP2. Cells were treated with serum-free culture media for 24h before performing the Annexin V/PI protocol. Late apoptosis (Annexin V^+/PI^+); early apoptosis (Annexin V^+); necrosis (PI^+). The graph represents the mean of the percentage (%) of cells in each group ± S.E.M. (n=1, duplicates); two-way ANOVA, Tukey's test between siNEG (-) and siNRP2 (+) cells was performed and revealed non-significant differences.

4.4.2.5 NRP2 deletion reduces cell adhesion, inhibits migration and blocks invasion of BrCa and HNSCC cells

NRP2 has been implicated in cell adhesion by regulating integrins expression in cancer as well as in endothelial cells[376,499], promoting cell migration[499]. Thus, to further characterize the role of NRP2 in tumorigenesis, we next evaluated whether NRP2 regulates the migration capacity of the cells. For that, we tested the effect of NRP2 depletion using CRISPR-Cas9 in BrCa and HNSCC cells migration and adhesion. We found that NRP2 deletion reduced the adhesion capacity of the cells after 1.5h (**fig. 62A, B**). Moreover, this decrease was accompanied by a reduction in MDA-MB-231 cells migratory ability. We found that $NRP2^{KO}$ MDA-MB-231 cells migrate less than Cas9 control cells (**fig. 62C**). However, in T-HEp3, NRP2 deletion had no effect on cell migration capacity, likely related to the lesser migratory ability of these cells (**fig. 62D**).

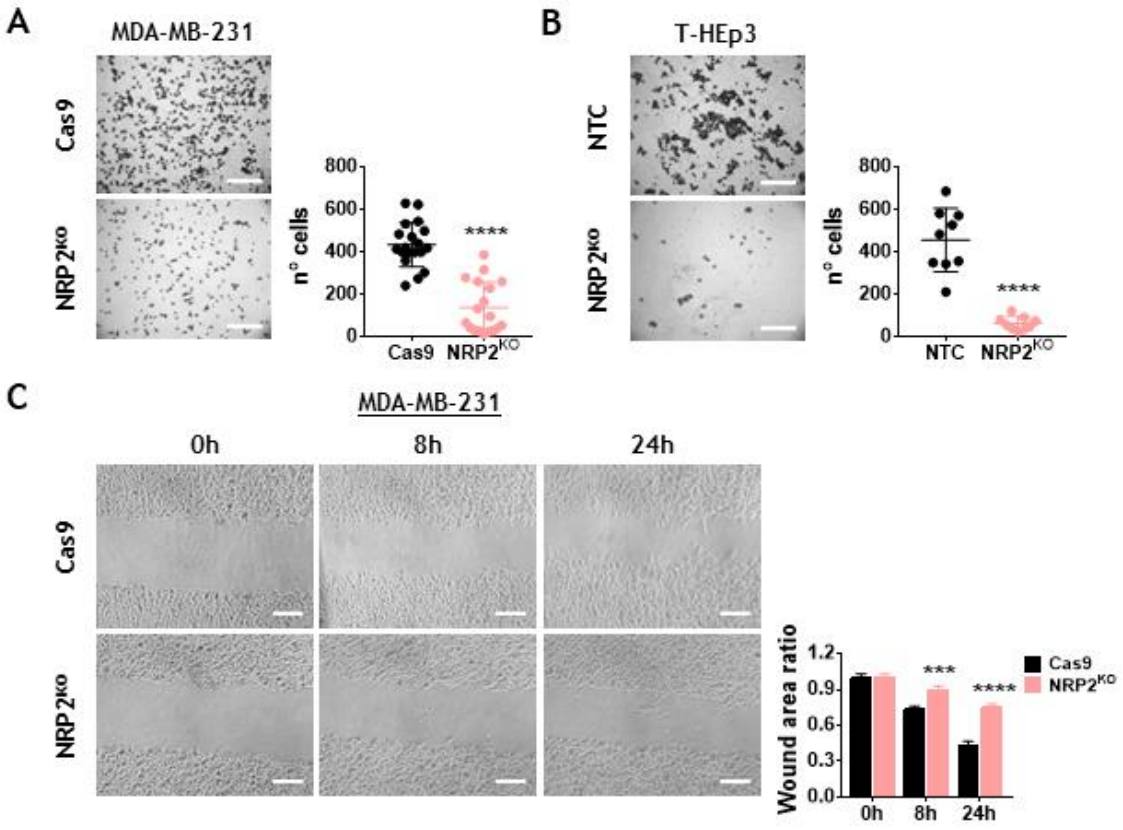

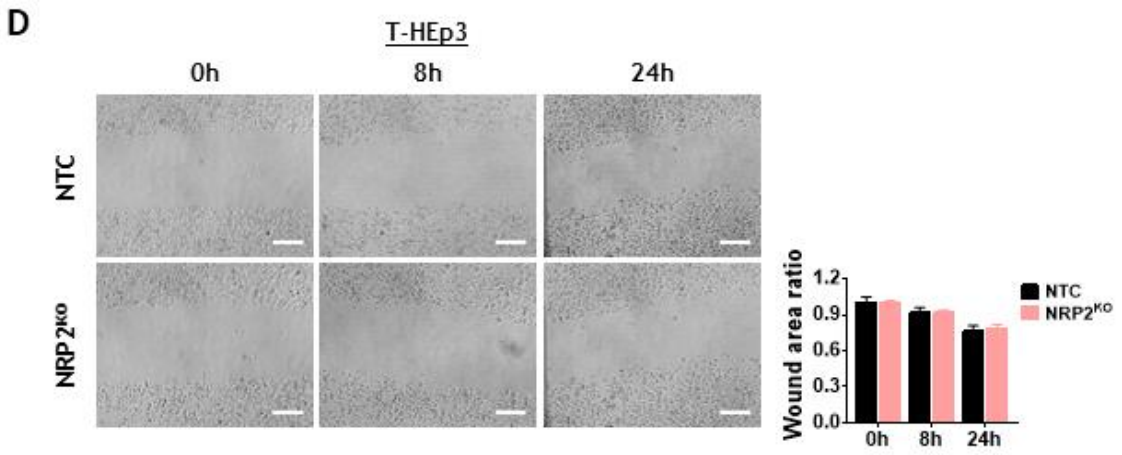

Figure 62. NRP2 deletion decreases cell adhesion and migration. A, B) Left panels, representative images from phase-contrast microscopy. Right panels, quantification of the number of cells 1.5h after seeding in the absence of ECM in Cas9/NTC and NRP2^{KO} MDA-MB-231 (**A**) and T-HEp3 (**B**) cells. Scale bar: 200µm. **C, D)** Left panels, representative images from phase-contrast microscopy. Right panels, quantification of the wound area ratio after 0, 8 and 24h migration in control (Cas9/NTC) and NRP2^{KO} MDA-MB-231 (**C**) and T-HEp3 (**D**) cells. Scale bar: 150µm. Graphs represent mean ± S.E.M. (n≥2); ***P < 0.001, ****P < 0.0001, comparing Cas9/NTC *vs* NRP2^{KO} by *t*-Student's (**A, B**) or two-way ANOVA, Sidak's test (**C, D**).

Furthermore, to assess the effect of NRP2 deletion in cell invasion, we performed an invasion assay through a matrigel layer. The invasion capacity of the NRP2-depleted cells was significantly reduced as compared to non-silenced cells in MDA-MB-231 (**fig. 63A**) and in T-HEp3 (**fig. 63B**) cells.

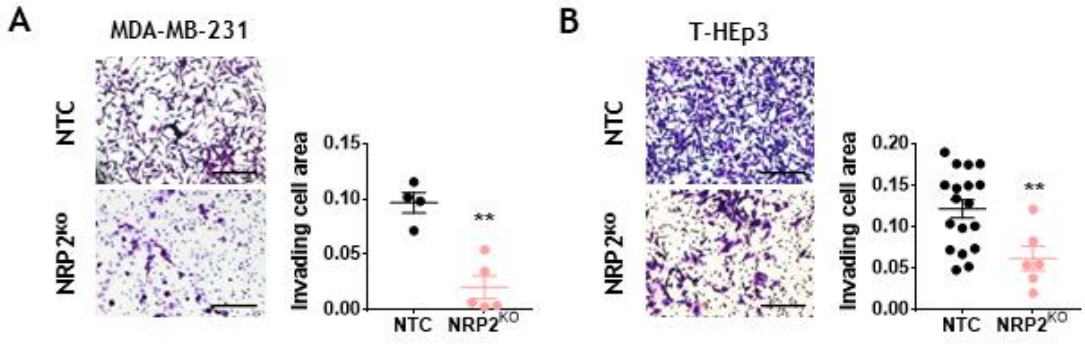

Figure 63. NRP2 deletion decreases cell invasion. Invasion assay through matrigel using 10% FBS as chemoattractant after 24h where 5·10^4 MDA-MB-231 (**A**) and 7.5·10^4 T-HEp3 (**B**) NTC and NRP2^{KO} cells were seeded. Left panels, representative images from phase-contrast microscopy. Scale bar: 200µm. Right panels, quantification of the invading cells area. Graphs represent mean ± S.E.M. (n=2); **P < 0.01 comparing Cas9/NTC *vs* NRP2^{KO} by *t*-Student's test.

Altogether, the previously described data indicate that NRP2 depletion in aggressive BrCa and HNSCC cells inhibited proliferation, induced p27 up-regulation and decreased tumour-initiation capacity. Moreover, NRP2 depletion also reduced cell adhesion, migration and invasion.

4.4.2.6. NRP2 expression modulation increases p27 expression and induces cleaved caspase 3 in the chicken embryo CAM *in vivo* model

As explained in the introduction and demonstrated by our *in vitro* results, NRP2 regulates diverse tumorigenic functions such as cell proliferation, migration and invasion. Consequently, in

an effort to define the role of NRP2 in BrCa and HNSCC progression, we inoculated the transient genetically modified T-HEp3 and MDA-MB-231 cell lines in the chicken embryo CAM *in vivo* model (**fig. 19**) (see *Materials & Methods, section 3.8.1* for further details). This model would allow us to do an initial evaluation about whether the microenvironment enhances the effect of NRP2 inhibition in the tumourigenic properties of the cells. Cells were transfected with siNRP2 48h before inoculation and no treatment was performed during the days that the experiment lasted. Due to the transient inhibition, we let the tumours grow only for 4 days. At the end, we found no differences in PTs weight and volume between silenced and non-silenced cells in T-HEp3 tumours (**fig. 64A**). However, Ki67 expression was higher in NRP2-inhibited T-HEp3 tumours (**fig. 64B**). Here, we thought that this was due to the non-inhibited cells that were masking the effect of the NRP2 down-regulated cells. In addition, since our previous results underline the possibility that NRP2 could regulate cell death, we also tested the expression of the apoptotic marker cleaved-caspase 3 (cc3) by immunofluorescence staining in T-HEp3 tumours. According to our *in vitro* results where little changes were observed in Bak and Puma expression in T-HEp3 cells (**fig. 60**), cc3 protein levels were also maintained constant in T-HEp3 PTs (**fig. 64C**).

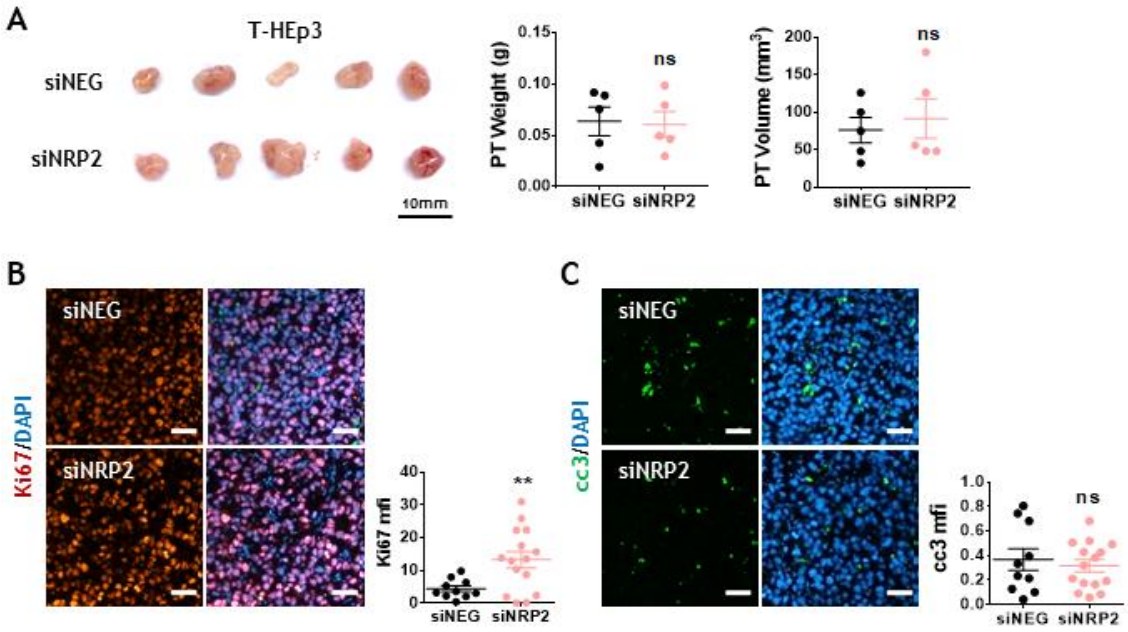

Figure 64. Transient NRP2 inhibition increases the cell proliferation marker Ki67 in T-HEp3 primary tumours in CAM *in vivo* model. A) Control (siNEG) or NRP2-inhibited (siNRP2) $3{\cdot}10^5$ T-HEp3 cells were inoculated in day 11 chicken embryo CAMs. Left panels, representative T-HEp3 tumour images. Middle and right panels, graphs showing tumour weight (g) (middle) and tumour volume (mm^3) (right) at end point. **B, C)** Representative IF images (left panels; scale bar: 50µm) of Ki67 (**B**) or cleaved caspase 3 (cc3) (**C**) and mfi quantification (right panels) in T-HEp3 PTs. Graphs represent mean ± S.E.M. (n=1, with 5 inoculated eggs per group); ns, non-significant, **P < 0.01, comparing siNEG *vs* siNRP2 by *t*-Student's test.

Regarding MDA-MB-231 growth, as in HNSCC model, we did not detect differences in PTs weight and volume when NRP2 was inhibited (**fig. 65A**). Tumour tissue analyses revealed a tendency to higher Ki67 expression (**fig. 65B**). Nevertheless, we found that NRP2 inhibition in MDA-MB-231 PTs up-regulated cc3 expression (**fig. 65C**), in accordance with the increase in Puma expression *in vitro* (**fig. 60**), suggesting that NRP2 might regulate tumour cells survival, at least in breast tumour cells.

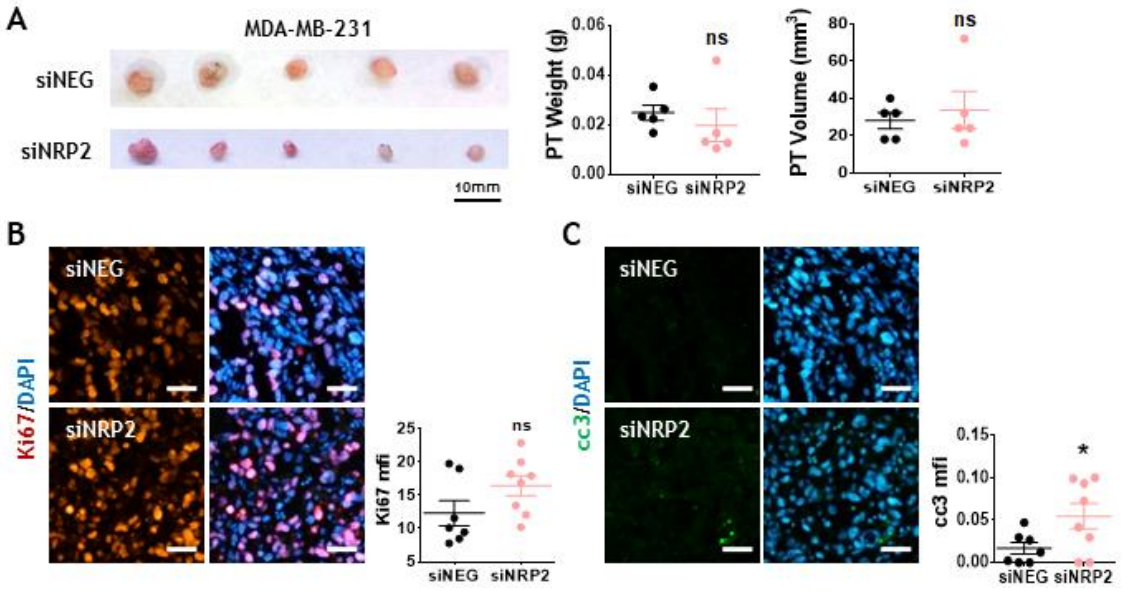

Figure 65. Transient NRP2 inhibition increases the apoptosis marker cc3 expression in MDA-MB-231 primary tumours in CAM *in vivo* model. A) Control (siNEG) or NRP2-inhibited (siNRP2) $5 \cdot 10^5$ MDA-MB-231 cells were inoculated in day 11 chicken embryo CAMs. Left panels, representative MDA-MB-231 tumour images. Middle and right panels, graphs showing tumour weight (g) (middle) and tumour volume (mm^3) (right) at end point. **B, C)** Representative IF images (left panels; scale bar: 50µm) of Ki67 (**B**) or cleaved caspase 3 (cc3) (**C**) and mfi quantification (right panels) in MDA-MB-231 PTs. Graphs represent mean ± S.E.M. (n=1, with 5 inoculated eggs per group); ns, non-significant, *P < 0.05 comparing siNEG *vs* siNRP2 by *t*-Student's test.

Since transient NRP2 inhibition did not have a great effect on tumour growth *in vivo*, we decided to use the NRP2 blocking antibody to test if blocking NRP2 activity had an effect on tumour growth. For that purpose, we inoculated wild-type T-HEp3 cells and treated them with the blocking antibody (αNRP2; 10µg/mL) each day for 6 days. In addition, cells were pre-treated *in vitro* with the NRP2 blocking antibody (1µg/mL) 24h before the inoculation. In agreement with the *in vivo* results obtained with the transient genetic inhibition, we found no differences in PTs size between treated and non-treated tumours (**fig. 66A**). Moreover, the histological analysis of CAM-derived tumours showed no differences in Ki67 expression between treated and non-treated tumours (**fig. 66B**). Nevertheless, we also analysed the expression of the apoptotic marker cc3 in T-HEp3 tumours and we detected that blocking NRP2 activity significantly increased cc3 expression as compared to non-treated tumours (**fig. 66C**). Interestingly, when we analysed the expression of the dormancy marker p27, we found that, in agreement with our *in vitro* results, tumours treated with the NRP2 blocking antibody had significantly higher p27 levels (**fig. 66D**).

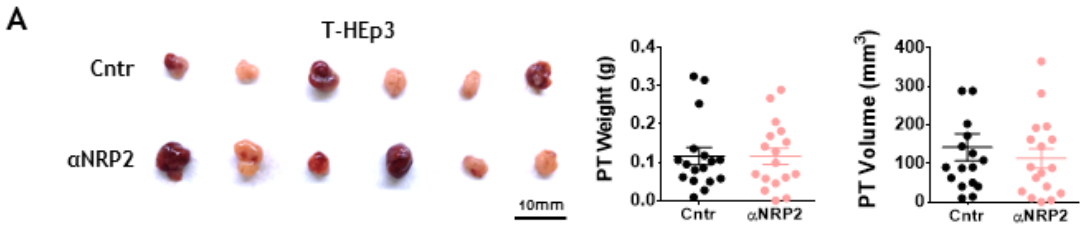

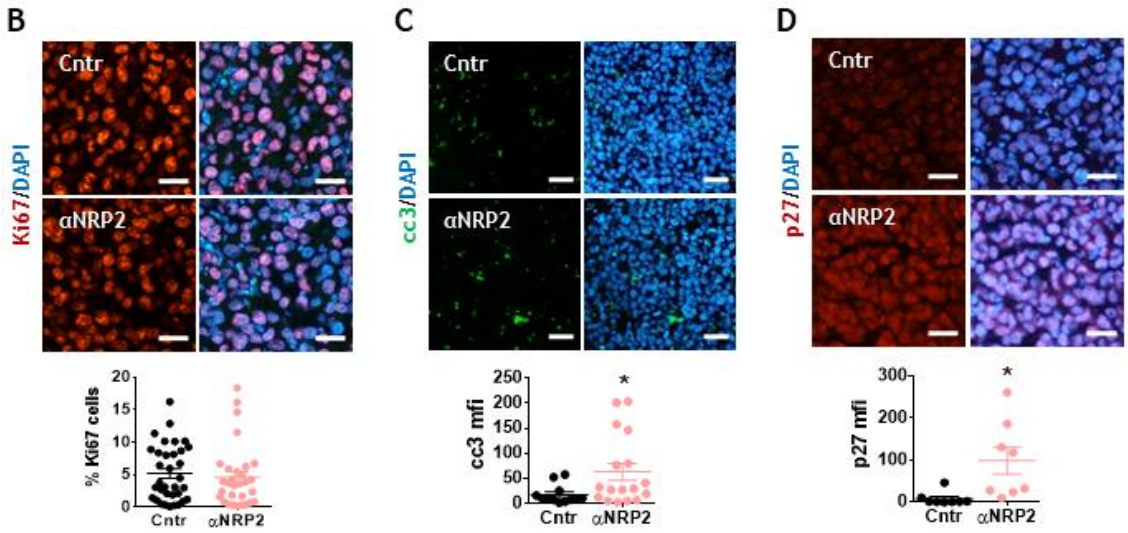

Figure 66. Blocking NRP2 activity increases p27 and cc3 expression in T-HEp3 primary tumours in CAM *in vivo* model. A) $3 \cdot 10^5$ T-HEp3 cells were inoculated in day 11 chicken embryo CAMs. 24h before, cells were pre-treated with a NRP2 blocking antibody (αNRP2) (1µg/mL). Then, PTs were treated with PBS (Cntr) or with αNRP2 (10µg/mL) for 6 days. Left panel, representative T-HEp3 tumour images. Middle and right panels, graphs showing tumour weight (g) (middle) and tumour volume (mm^3) (right) at end point. **B, C, D)** Representative IF images (upper panels) of Ki67 (**B**; scale bar: 100µm), cleaved caspase 3 (cc3) (**C**; scale bar: 50µm) or p27 (**D**; scale bar: 100µm) and mfi quantification (lower panels). Graphs represent mean ± S.E.M. (n=3, with 6 inoculated eggs per group); *P < 0.05 comparing Cntr *vs* αNRP2 by *t*-Student's test.

These results suggest that blocking NRP2 activity induces a phenotypic switch in tumour cells that up-regulates the quiescence marker p27 and the apoptotic marker cc3 although this is not enough to prevent tumour growth. Therefore, we decided to test whether depleting NRP2 expression had a stronger effect on tumour growth. We inoculated T-HEp3 and MDA-MB-231 Cas9-NTC and $NRP2^{KO}$ in day 11 chicken embryo CAMs for 6 days. Interestingly, we found that depleting NRP2 had a tendency to inhibit tumour growth in HNSCC (**fig. 67A**) while having little effect on MDA-MB-231 (**fig. 67B**). Nonetheless, there was a decrease in the incidence of tumours in T-HEp3 $NRP2^{KO}$ cells with fewer tumours being able to grow (**fig. 67C**), suggesting NRP2 deletion might decrease cell engraftment and prevent HNSCC growth initiation.

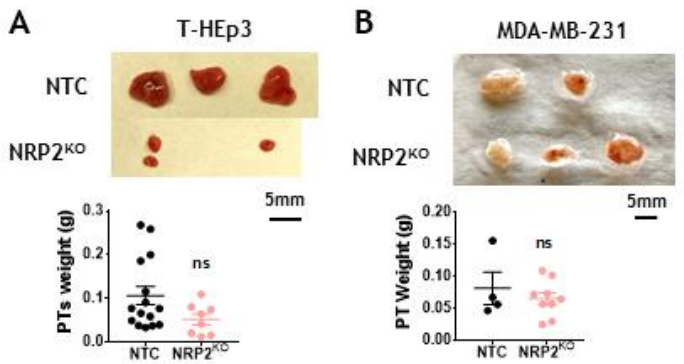

C

Growth incidence	T-HEp3	MDA-MB-231
NTC	22 / 28	7 / 8
$NRP2^{KO}$	8 / 18	12 / 14

Figure 67. NRP2 deletion reduces tumour growth incidence in T-HEp3 cells CAM *in vivo* model. $3{\cdot}10^5$ T-HEp3 (**A**) or $5{\cdot}10^5$ MDA-MB-231 (**B**) NTC or $NRP2^{KO}$ cells were inoculated in day 11 chicken embryo CAMs for 6 days. Upper panels, representative tumour images. Lower panels, graphs showing tumour weight (g) at end point. Graphs represent mean ± S.E.M. (n=3, with >3 inoculated eggs per group); *t*-Student's test (for PTs weight) or two-way ANOVA, Sidak's test (for growth incidence) between NTC *vs* $NRP2^{KO}$ was performed and revealed non-significant (ns) differences. **C)** Quantification of T-HEp3 cells engraftment and growth incidence: the table shows the number of tumours at end point and the total number of chicken embryos CAMs inoculated with T-HEp3 NTC or $NRP2^{KO}$ cells.

4.4.2.7. NRP2 deletion completely blocks T-HEp3 tumour growth in xenograft models

Our previous results suggest that NRP2 plays a role in BrCa and HNSCC tumorigenesis regulating cell proliferation, survival, adhesion, migration and invasion *in vitro* and *in vivo*. To further validate our results, we analysed *in vivo* tumour growth by performing xenograft assays in NOD-SCID mice with NRP2-deleted and non-deleted T-HEp3 cells (**fig. 20**) (see *Materials & Methods, section 3.8.2* for further information). Interestingly, control tumours derived from NTC cells grew vigorously as compared to $NRP2^{KO}$ cells derived tumours. In fact, they had to be surgically removed 16 days after inoculation. Surprisingly, $NRP2^{KO}$ cells derived tumours had a delay of 1 month in growth in comparison with the control group (**fig. 68A**). Moreover, NTC tumours were bigger than $NRP2^{KO}$ tumours regarding PTs weight and volume (**fig. 68B**), which support our previous results and suggest that NRP2 has a key role in promoting tumour growth.

Next, we evaluated some of the characteristics of the tumours using tumour sections. First, we confirmed that NRP2 deletion was maintained in $NRP2^{KO}$ cells derived tumours (**fig. 68C**). In agreement with *in vitro* and *in vivo* experiments, deletion of NRP2 increased p27 levels in tumour samples as well, although not reaching statistical significance (**fig. 68D**). In addition, a significant up-regulation of the apoptotic marker cc3 expression was observed in $NRP2^{KO}$ tumours (**fig. 68E**). These results suggest that NRP2 deletion reduces *in vivo* HNSCC tumour growth more likely by promoting quiescence and apoptosis, validating our *in vitro* results. Hence, low levels of NRP2 might induce a more dormant phenotype in HNSCC tumour cells together with a reduction in cell proliferation and survival in the PT bulk.

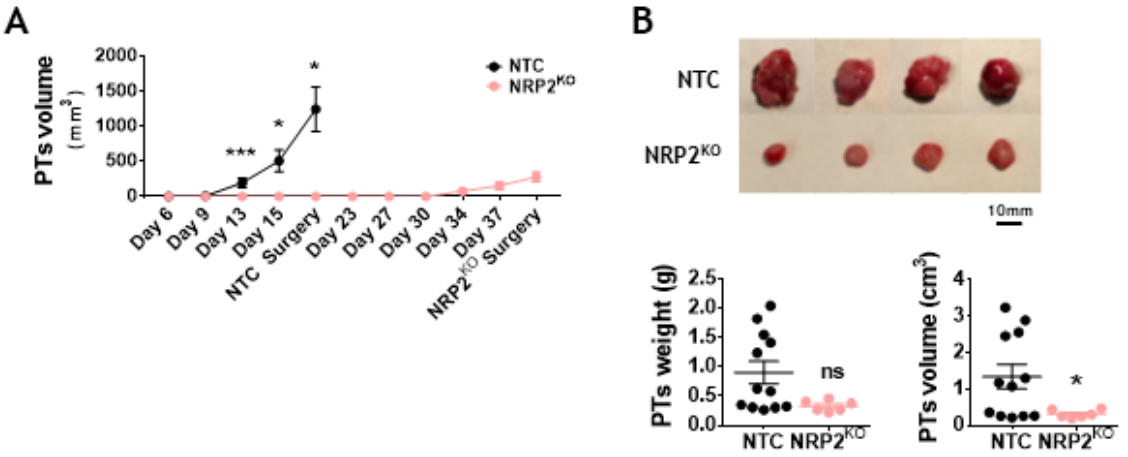

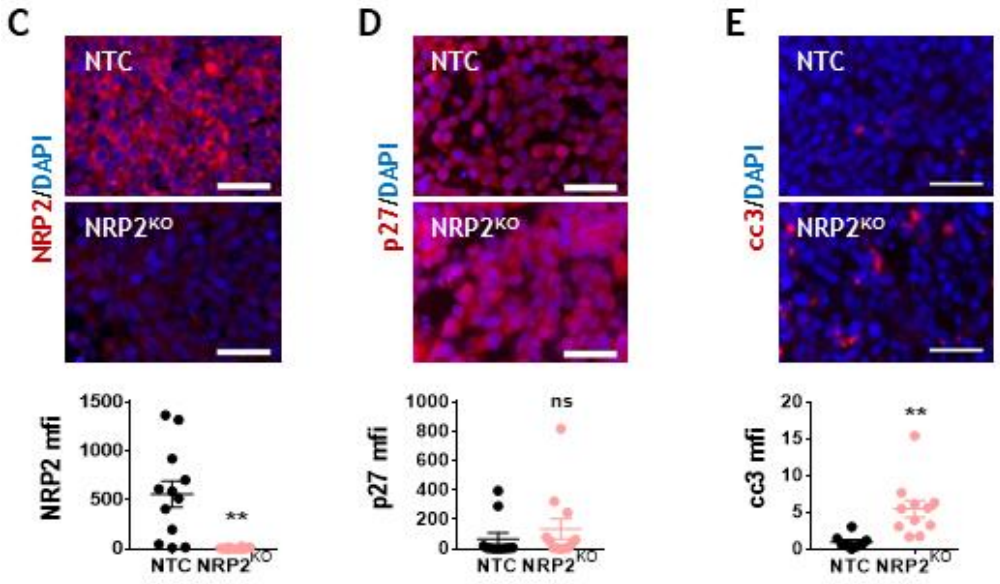

Figure 68. NRP2 deletion inhibits T-HEp3 tumour growth *in vivo*. $5 \cdot 10^5$ NTC or NRP2^{KO} cells were orthotopically inoculated per mouse (n=12 for NTC and n=6 for NRP2^{KO}). Mice were weighted and PTs measured twice per week. When the mean of PTs volume was around 1000mm^3 (for NTC) and 300mm^3 (for NRP2^{KO}), they were surgically removed. 1 month after the surgery, mice were sacrificed and lungs were isolated for further cell dissemination analysis (**fig. 20**). **A)** Graph representing T-HEp3 tumours volume (mm^3) over time for each group. **B)** Upper panel, representative T-HEp3 tumour images at the time of surgery. Lower panels, graphs showing PTs weight (g) (left) and volume (cm^3) (right) at the time of surgery. **C, D, E)** Upper panels, representative IF images of NRP2 (**C**), p27 (**D**) and cc3 (**E**) in T-HEp3 mice tumours. Scale bar: 50µm. Lower panels, mfi quantification of NRP2, p27 and cc3. Graphs represent mean ± S.E.M. (n=1, with 12 mice for NTC and 6 mice for NRP2^{KO}); *P < 0.05, **P < 0.01, ***P < 0.001 comparing NTC *vs* NRP2^{KO} by *t*-Student's test.

4.4.3. NRP2 induces proliferation in lung DTCs and promotes lung metastases development *in vivo*

As reported in previous sections, we have shown that NRP2 negatively regulates the expression of the cell cycle inhibitor p27, an event associated with a more proliferative phenotype. We next investigated whether NRP2 has a role in regulating DTCs phenotype promoting their proliferation in secondary organs.

4.4.3.1. NRP2 blocking reduces lung DTCs derived cell lines proliferation *in vivo*

To analyse if NRP2 could regulate lung metastases, we used the lung DTCs derived HNSCC cell line (Lu-HEp3). These cells derive from tumour cells that were able to escape from T-HEp3 PTs and disseminate to the lung. These lung DTCs were isolated and expanded *in vitro*, generating the proliferative Lu-HEp3 cell line (**fig. 16**)[266]. Therefore, these cells were used as an *in vitro* model that mimic lung DTCs behaviour *in vivo*. As shown in **figure 23**, Lu-HEp3 cells have high levels of NRP2.

To test if NRP2 regulated lung DTCs growth, we inoculated Lu-HEp3 cells in day 11 chicken embryos CAMs and treated them with the NRP2 blocking antibody for 6 days. Similar to what we found in the *in vivo* experiments with T-HEp3 cells, Lu-HEp3 cells treatment with NRP2 blocking antibody had little effect on PTs weight and volume (**fig. 69A**). However, in the histological characterization of the tumours we detected lower levels of the proliferation marker Ki67 in the tumours treated with the NRP2 blocking antibody (**fig. 69B**), suggesting that blocking NRP2 activity

decreases Lu-HEp3 cells proliferation. In addition, blocking NRP2 activity increased the apoptotic marker cc3 levels in Lu-HEp3 tumours (**fig. 69C**), relating NRP2 to lung DTCs survival too. Consequently, these results go in line with our previous findings and suggest that NRP2 might regulate lung DTCs growth and survival.

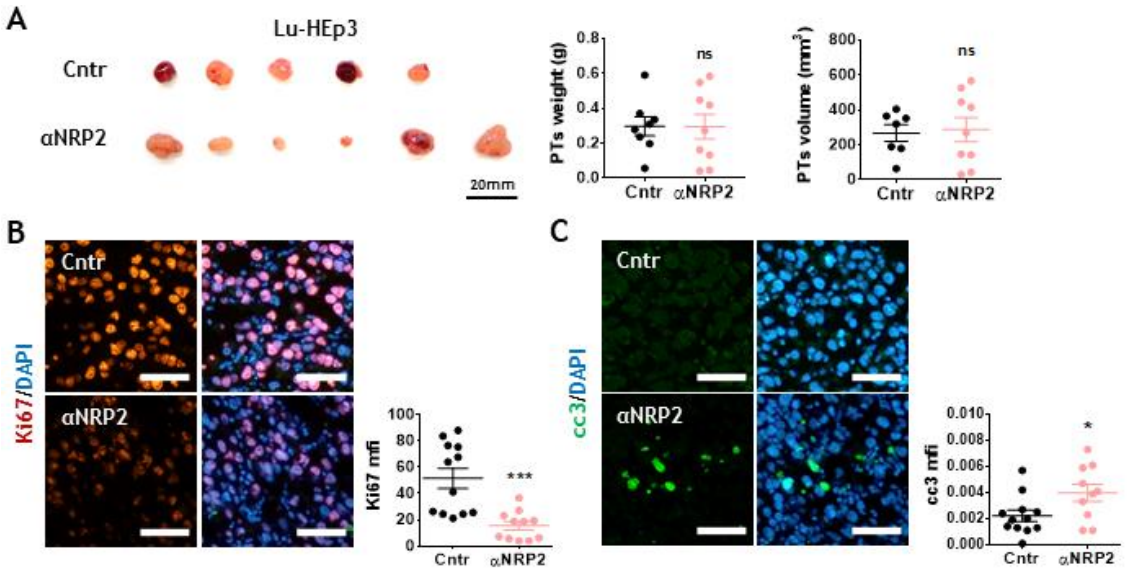

Figure 69. NRP2 blocking reduces Lu-HEp3 tumour proliferation and increases apoptosis *in vivo*. A) $3{\cdot}10^5$ Lu-HEp3 cells were inoculated in day 11 chicken embryo CAM. 24h before, cells were pre-treated with the NRP2 blocking antibody (αNRP2) (1µg/mL). Then, PTs were treated with PBS (Cntr) or with the NRP2 blocking antibody (αNRP2) (10µg/mL) for 6 days. Left panel, representative tumour images. Middle and right panels, graphs representing tumour weight (g) (middle) and tumour volume (mm^3) (right) at end point. **B, C)** Representative IF images (left panels; scale bar: 50µm) and Ki67 (**B**) or cleaved caspase 3 (cc3) (**C**) mfi quantification (right panels). Graphs represent mean ± S.E.M. (n=2, with 5 inoculated eggs per group); ns, non-significant, *P < 0.05, ***P < 0.001 comparing Cntr *vs* αNRP2 by *t*-Student's test.

4.4.3.2. Lung DTCs up-regulate NRP2 expression to form micrometastases

To demonstrate that NRP2 exerts a determinant role in lung DTCs biology, we next studied whether we were able to detect NRP2 expression in lung DTCs *in vivo*. First, we stained chicken and mice lungs from control animals in the experiments described in **figure 66** and **figure 68** in order to detect T-HEp3 lung DTCs (by vimentin-positive staining) (**fig. 70A, top and middle panel**). We also used the MMTV-Neu mice model for BrCa where multifocal breast carcinomas with lung metastases are developed after 12-16 weeks of growth[500] to detect HER2-positive BrCa lung DTCs (by Her2 staining) (**fig. 70A, bottom panel**). Tissue samples of this model were kindly donated by Dr. Aguirre-Ghiso, from the Icahn School of Medicine at Mount Sinai (New York, USA). Here, we found that vimentin in T-HEp3 DTCs and Her2 in BrCa DTCs were co-expressed with NRP2 (**fig. 70A**), manifesting that NRP2 is expressed in PTs-derived lung DTCs.

Interestingly, in a single cell analysis that we performed in collaboration with Dr. Aguirre-Ghiso, we found that not only BrCa lung DTCs expressed NRP2 (**fig. 70A**) but also that they up-regulated its expression as compared to primary tumours (PT) and pre-malignant mammary gland lesions (PMMG) (**fig. 70B**). Moreover, in a lung metastasis *in vivo* experiment performed by Dr. Aguirre-Ghiso's laboratory where wild-type T-HEp3 cells were inoculated through the tail vein, we observed that DTCs in early lungs (isolated 1 week after inoculation) expressed NRP2 which was increased in

late lung macrometastases (isolated 3 weeks after inoculation), where statistically significant higher number of NRP2-positive T-HEp3 cells were detected as compared to early lungs (**fig. 70C**).

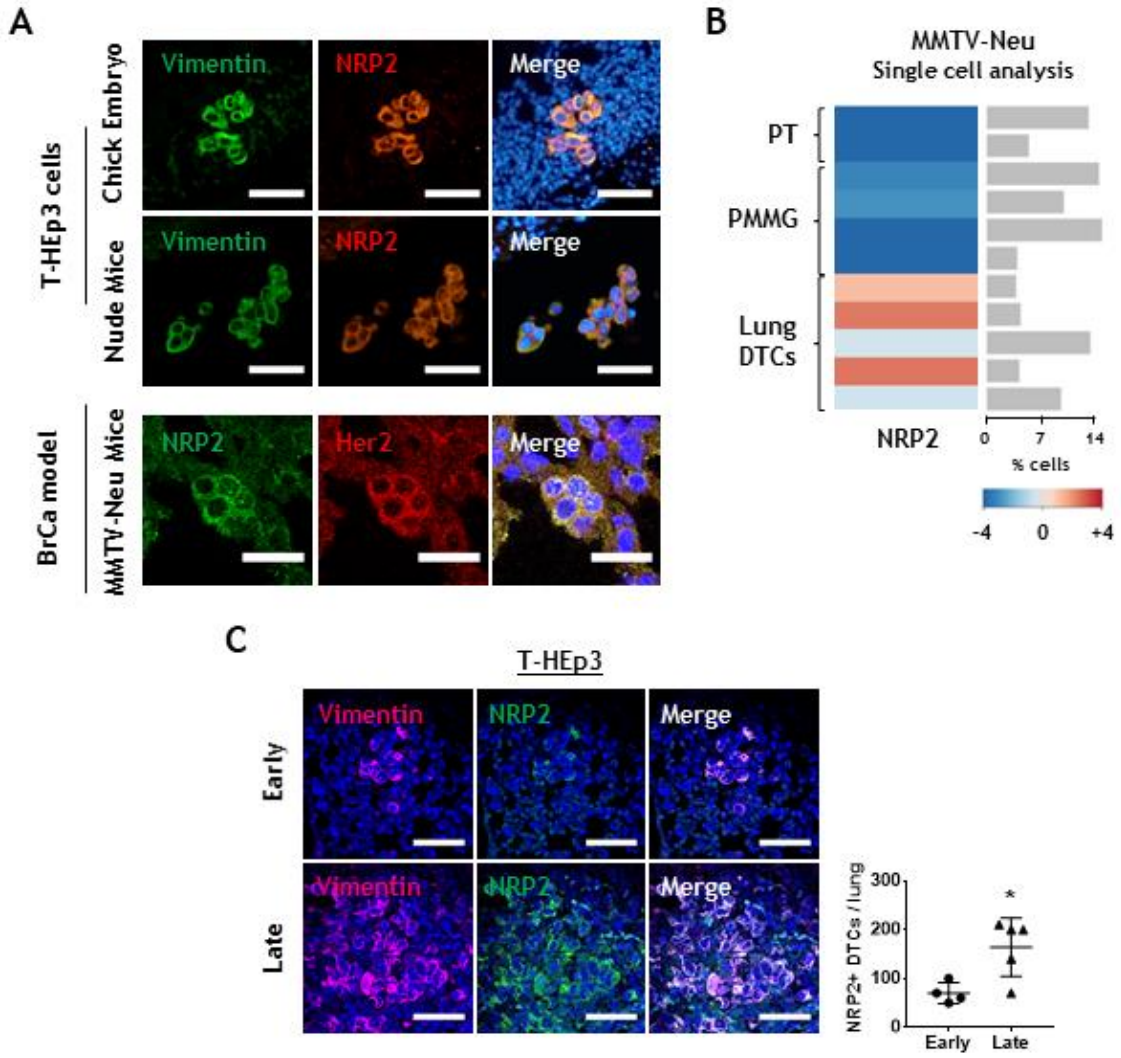

Figure 70. Lung DTCs express NRP2 *in vivo*. A) Top and middle panels, representative IF images of vimentin (green) and NRP2 (red) staining of lung T-HEp3 DTCs in chicken (top; scale bar: 50µm) and mice (middle; scale bar: 50µm) lung sections. Bottom panel, representative IF images of NRP2 (green) and HER2 (red) staining in MMTV-Neu lung sections. Scale bar: 20µm. **B)** Heatmap showing *NRP2* gene expression analysis based on single tumour cell gene expression in BrCa MMTV-Neu mice model. PT, primary tumour; PMMG, pre-malignant mammary gland lesions. The colour legend depicts an enrichment score [log2(expression/mean)], where relative *NRP2* expression goes from -4 to 4. **C)** Representative IF images of vimentin (pink) and NRP2 (green) T-HEp3 lung DTCs in early (isolated 1 week post-inoculation) and late (isolated three weeks post-inoculation) mice tail vein *in vivo* models. Scale bar: 50µm. The graph represents the number of NRP2-positive lung DTCs mean ± S.E.M.; *P < 0.05 comparing early *vs* late by *t*-Student's test. These experiments were performed in collaboration with Dr. Aguirre-Ghiso from the Icahn School of Medicine at Mount Sinai (New York, USA).

T-HEp3 cells express high levels of NRP2. Therefore, to test if NRP2 expression in lung DTCs could be regulated by the lung microenvironment, we studied NRP2 expression in MDA-MB-453 (HDS, low NRP2 expression) (**fig. 23**) lung DTCs and metastasis. We inoculated MDA-MB-453 mCherry^{+}

cells orthotopically into mice mammary fat pad and let tumours grow for 12 weeks. At end point, lungs were isolated and cell dissemination was analysed by detecting lung DTCs by HER2 staining (**fig. 71A**) (see *Materials & Methods, section 3.1.1.1* for further information). Surprisingly, we found that while single DTCs were still negative for NRP2 expression (**fig. 71B, upper panel**), NRP2 was found up-regulated in MDA-MB-453 DTCs-derived lung micrometastases (**fig. 71B, lower panel**). This suggests that up-regulation of NRP2 was necessary for lung metastasis outgrowth. It also suggests that the lung microenvironment can up-regulate NRP2 expression. Taken all together, these results highlight the key role of NRP2 in lung metastases development both in HNSCC and BrCa cells, even in HDS BrCa cells with low levels of NRP2.

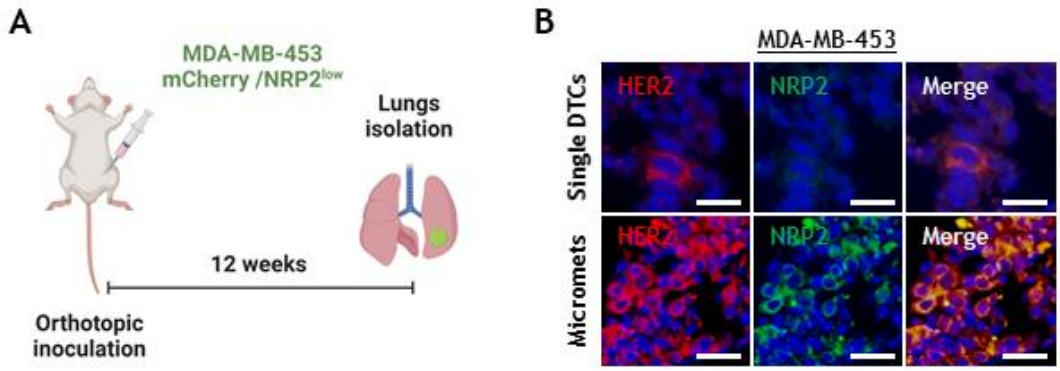

Figure 71. Lung DTCs up-regulates NRP2 in lung metastases *in vivo*. A) Diagram of the mice *in vivo* experiment using MDA-MB-453 mCherry+ cells. $1.5 \cdot 10^6$ MDA-MB-453 cells tagged with mCherry and luciferase were orthotopically inoculated into mice mammary fat pad and tumours grew for 12 weeks. At end point, lungs were isolated for lung DTCs analysis (see *Materials & Methods, section 3.1.1.1* for further information). **B)** Representative IF images of HER2 (red) and NRP2 (green) staining in lung MDA-MB-453 single DTCs and micrometastases (micromets). Scale bar: 50µm.

Following with our study, we next compared NRP2 levels in cells derived from the PTs and lung DTCs from the MDA-MB-453 *in vivo* model. For that purpose, primary MDA-MB-453 cell lines derived from the PT or from the isolated lung DTCs were generated by our laboratory (**fig. 72A**)[145]. The analyses of NRP2 expression either at mRNA or protein levels confirmed our previous results. We observed that cells that were able to disseminate and colonize the lung had significative higher NRP2 protein expression than PT cells (**fig. 72C**) although significant differences in NRP2 mRNA levels were observed (**fig. 72B**). Altogether, these results suggest that NRP2 might be required for DTCs growth in the lung.

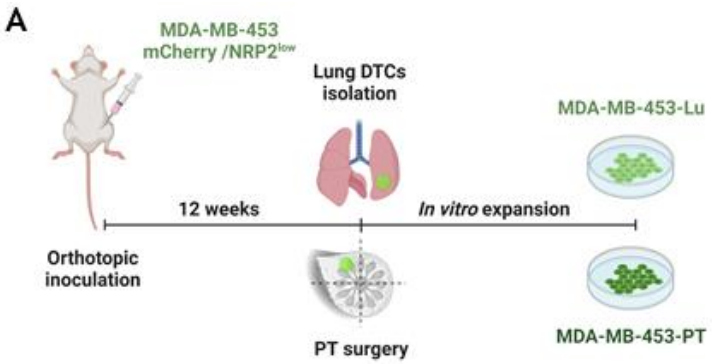

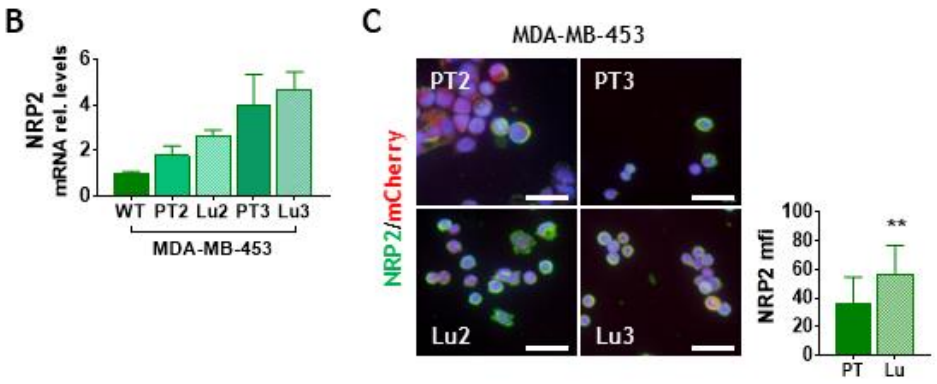

Figure 72. HDS BrCa lung DTCs derived cell lines up-regulate NRP2 expression. A) Diagram of the mice *in vivo* experiment using MDA-MB-453 cells. $1.5 \cdot 10^6$ MDA-MB-453 mCherry$^+$/luciferase$^+$ cells were orthotopically inoculated into the mice mammary fat pad. After 12 weeks, PTs and lungs containing DTCs were minced and enzymatically digested. Then, MDA-MB-453-mCherry$^+$ cells were selected and expanded *in vitro* for MDA-MB-453-PT and MDA-MB-453-Lu primary cell lines generation (see *Materials & Methods, section 3.1.1.1* for further information). **B)** Analysis of NRP2 mRNA levels comparing PT and lung DTCs (Lu) with wild-type (WT) MDA-MB-453 cell lines. **C)** Left panels, representative IF images of NRP2 (green) and mCherry (red) in MDA-MB-453 PT and lung cell lines from the *in vivo* experiment in A. Scale bar: 50µm. Right panel, NRP2 mfi quantification. 2 and 3 refer to different mice. Graphs represent mean ± S.E.M. (n=3, triplicates); **P < 0.01 comparing PT *vs* Lu by *t*-Student's test.

4.3.3. NRP2 promotes lung DTCs proliferation resulting in a higher number and bigger lung metastases

Based on the fact that NRP2 is up-regulated in lung DTCs and it promotes cell proliferation while inhibiting the dormancy marker p27, we wondered whether NRP2 inhibition would induce quiescence in lung DTCs, reprograming them to become dormant, causing a decrease in lung metastases development. To prove this hypothesis, we considered studying cells that had disseminated to the lung in our *in vivo* experiments (**fig. 64, 66**). Tumour cells were identified by vimentin expression as a mesenchymal tumour cell marker whereas DTCs phenotype was determined by the proliferation marker Ki67 signal. In our preliminary chicken CAM *in vivo* experiments we found that neither NRP2 inhibition (**fig. 73A, left graph**) nor blocking NRP2 activity (**fig. 73B, left graph**) diminished the number of DTCs detected in lungs. However, when we analysed DTCs phenotype we found that NRP2 inhibition induced a switch in lung DTCs phenotype. Although not in a significative manner, NRP2 inhibition increased the percentage of dormant DTCs present in chicken lungs (**fig. 73A, right graph**). In a similar way, while the total amount of T-HEp3 DTCs was not affected when NRP2 activity was blocked (**fig. 73B, left graph**), the percentage of dormant DTCs also tend to increase (**fig. 73B, right graph**).

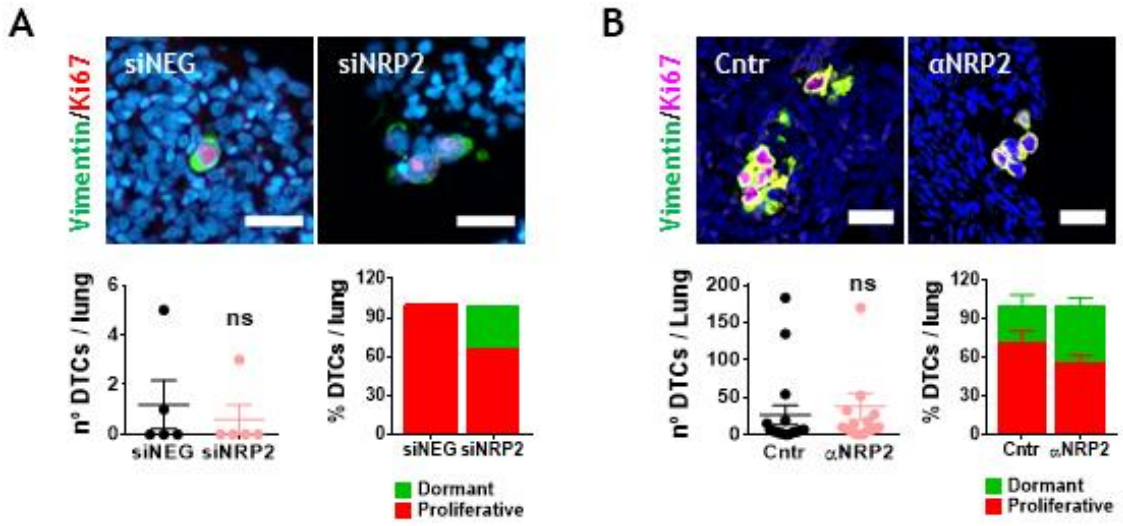

Figure 73. NRP2 induces lung T-HEp3 DTCs quiescence *in vivo*. CAM *in vivo* experiments using T-HEp3 cells transfected with siNRP2 (**A**) or treated with αNRP2 (10µg/mL) (**B**) (see *Materials & Methods, section 3.8.1* for further information). **A, B)** Upper panels, representative IF images of vimentin (green) and Ki67 (red or pink) in chicken lung sections. Lower left panels, quantification of total number of vimentin-positive cells per lung. Lower right panels, quantification of the percentage (%) of Ki67-positive (proliferative) or Ki67-negative (dormant) cells per lung. Scale bar: 50µm. Graphs represent mean ± S.E.M. (n=1 for siNRP2 and n=2 for αNRP2, with 5 inoculated eggs per group); *t*-Student's test between siNEG *vs* siNRP2 or cntr *vs* αNRP2 was performed and revealed not significant differences.

To confirm the role of NRP2 regulating DTCs dormancy we next studied the effect of complete NRP2 depletion in lung DTCs. To perform this experiment, in the T-HEp3 xenograft model, we performed PTs surgery and then wait 4 weeks before euthanizing the mice to study NRP2 role in spontaneous metastasis formation (**fig. 20**). Analyses of the lungs showed a downward trend to decrease the total amount of lung micro- and macrometastases in $NRP2^{KO}$ mice as compared to the control (NTC) mice (**fig. 74A**). There were no differences on the incidence of single, double and cluster DTCs (**fig. 74B**), suggesting both NTC and $NRP2^{KO}$ tumour cells disseminate and colonize lungs. However, lungs from mice inoculated with $NRP2^{KO}$ cells have higher incidence of micrometastases but lower of macrometastases (**fig. 74B**), suggesting that there is a delay in the evolution of metastases in mice inoculated with $NRP2^{KO}$ cells. Furthermore, we also observed that the size of these metastases was also modulated by NRP2 depletion. While effects on macrometastases were not evident, micrometastases developed from $NRP2^{KO}$ cells were significantly smaller than the control micrometastases (**fig. 74C**). Moreover, when we analysed the phenotype of single and double lung T-HEp3 DTCs we found that NRP2 deletion significatively increased the percentage of dormant single DTCs (**fig. 74D**). Therefore, our results suggest that inhibition of NRP2 reprograms DTCs into dormant DTCs, which delays lung metastases development.

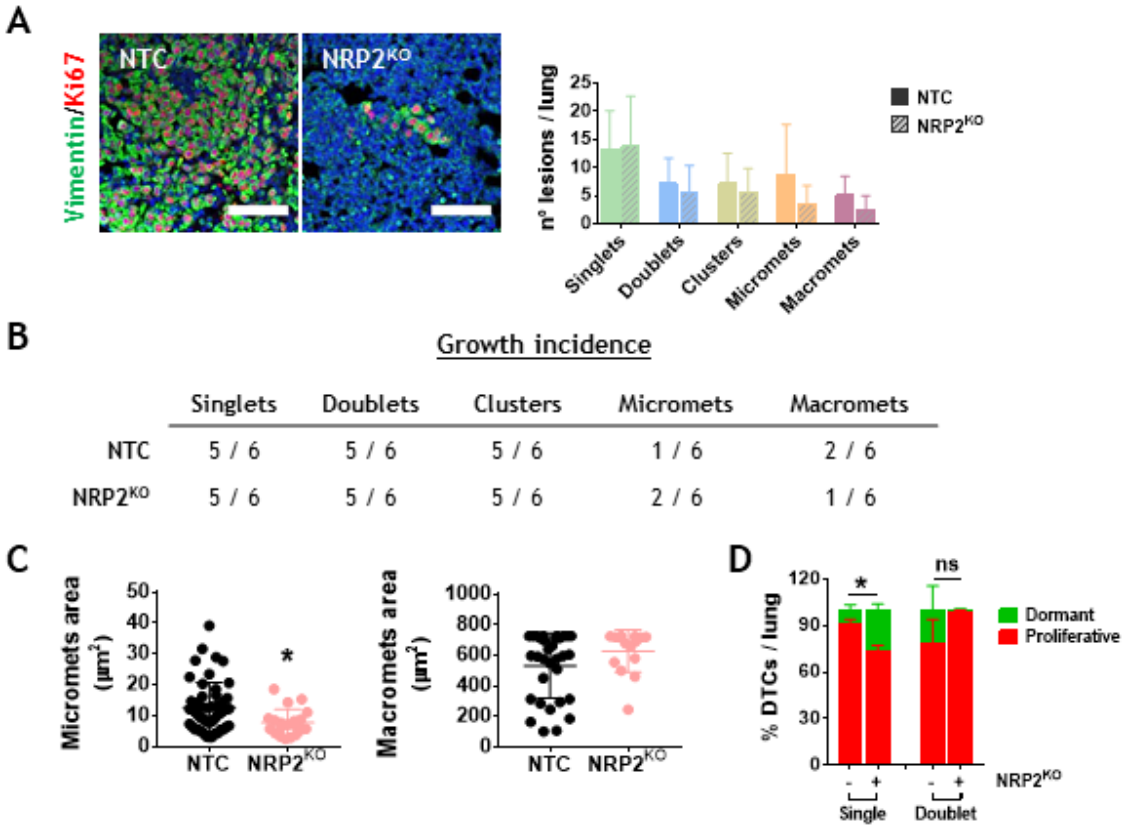

Figure 74. NRP2 induces T-HEp3 cells-derived lung metastasis development and enlargement *in vivo*. **A)** Left panel, representative IF images of vimentin (green) and Ki67 (red) staining of T-HEp3 lung DTCs. Scale bar: 100µm. Right panel, quantification of the number of vimentin-positive T-HEp3 lung lesions in the lung from mice in the T-HEp3 *in vivo* experiment from **figure 68** (see *Materials & Methods, section 3.8.2* for further information). The graph shows the total number of singlets, doublets, clusters (3-8 cells), micrometastases (9-100 cells; <100µm^2) and macrometastases (>100 cells; >100µm^2) per lung. **B)** Quantification of the lung metastatic lesions incidence. The numbers represent the number of mice with lung lesions related to the total number of mice in each group. **C)** Quantification of lung micrometastases (left) and macrometastases (right) area (µm^2). ImageJ software was used for the quantification. **D)** Quantification of the percentage (%) of Ki67-positive (proliferative) or Ki67-negative (dormant) single and doublet T-HEp3 cells per lung. Graphs represent mean ± S.E.M. (n=6 lungs per group); *P < 0.05 comparing NTC *vs* NRP2^{KO} by *t*-Student's test.

Taking into account our previous results, NRP2 clearly regulates lung DTCs proliferative phenotype and thus promotes lung metastases development. However, to rule out that the decrease in the size of the micrometastases and the delay in lung metastases progression in the lungs from the mice inoculated with NRP2^{KO} cells was caused by defects in NRP2^{KO} cells dissemination, invasion and colonization of secondary organs we performed a tail vein *in vivo* experiment. In this experiment, we used both BrCa and HNSCC cells that were directly inoculated into the bloodstream. MDA-MB-231 or T-HEp3 NTC or NRP2^{KO} cells were inoculated in the tail vein and after 2 and 4 weeks of growth, lungs were isolated and cell dissemination was studied (**fig. 21**) (see *Materials & Methods, section 3.8.3* for further information). As in the previous *in vivo* experiments, DTCs were detected by vimentin staining whereas Ki67 signal was used for DTCs phenotype determination.

An increasing trend in the total number of metastatic lesions per mice was found in MDA-MB-231 NRP2^{KO} mice at 4 weeks (**fig. 75A**) whereas, as we expected, NRP2^{KO} macrometastases were

statistically significantly smaller than Cas9 macrometastases (fig. 75B). Moreover, phenotypic characterization of the metastatic lesions revealed that NRP2^{KO} derived DTCs were transformed towards a more dormant phenotype, a prominent effect clearly observed in doublets lung DTCs (fig. 75C).

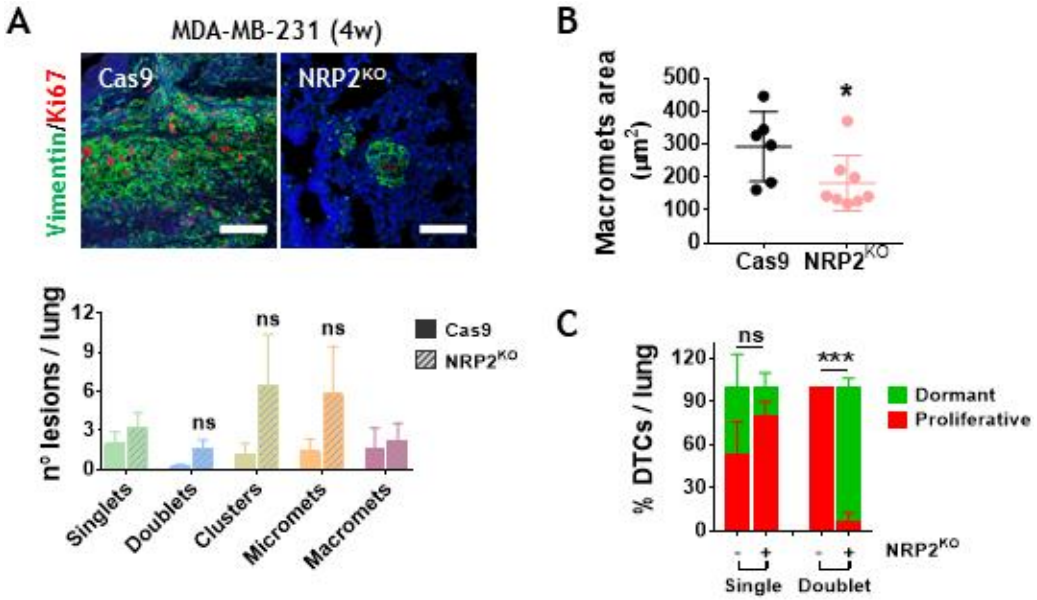

Figure 75. NRP2 deletion decreases MDA-MB-231 lung metastases size as well as triggers quiescence in lung DTCs *in vivo*. $5{\cdot}10^5$ Cas9 or NRP2^{KO} MDA-MB-231 cells were inoculated into the lateral tail vein of the mous. 4 weeks after inoculation, lungs were isolated for lung DTCs analysis (see *Materials & Methods, section 3.8.3* for further information). **A)** Upper panel, representative IF images of vimentin (green) and Ki67 (red) in MDA-MB-231 lung sections. Scale bar: 50µm. Lower panel, quantification of the number of MDA-MB-231 lung lesions. Lung BrCa lesions were quantified as the total number of vimentin-positive cells per lung: singlets, doublets, clusters (3-8 cells), micrometastases (9-100 cells; <100µm^2) and macrometastases (>100 cells; >100µm^2). **B)** Quantification of lung macrometastases area (µm^2) in mice inoculated with MDA-MB-231 Cas9 or NRP2^{KO} cells after 4 weeks. **C)** Quantification of the percentage (%) of Ki67-positive (proliferative) or Ki67-negative (dormant) MDA-MB-231 single and doublet DTCs per lung. Graphs represent mean ± S.E.M. (n=1, with 5 mice per group); ns, non-significant, *P < 0.05, ***P < 0.001 comparing Cas9 (-) *vs* NRP2^{KO} (+) by *t*-Student's test.

To confirm the role of NRP2 in metastasis in the HNSCC model, NTC or NRP2^{KO} T-HEp3 cells were inoculated through the lateral tail vein. 2 weeks after the inoculation, no macrometastases were found whereas similar number of metastatic lesions were detected in the NRP2-deleted group as compared to the control group (**fig. 76A**). Interestingly, the number of single DTCs increased (**fig. 76A**). Furthermore, by characterizing the phenotype of these cells, we observed that those single and double DTCs derived from the NRP2-depleted cells were clearly more dormant in comparison to control mice (**fig. 76B**). The phenotypic switch from proliferative to dormant phenotype was found in more than 50% of the detected metastatic lesions (**fig. 76B**). Thus, these results validate our previous results that clearly indicate that deletion of NRP2 reprograms lung DTCs into dormancy. NRP2 depletion effects in lung metastases were also evidenced after 4 weeks. Here, lower numbers of singlets, doublets, clusters and micrometastases were detected in NRP2^{KO} mice (**fig. 76C**). In addition, a significant reduction in the size of macrometastases was found in NRP2^{KO} mice as compared to NTC control mice (**fig. 76D**). Moreover, in agreement with the results from 2

weeks growth *in vivo*, single and double lung DTCs derived from NRP2^{KO} cells were significatively more dormant (**fig. 76E**).

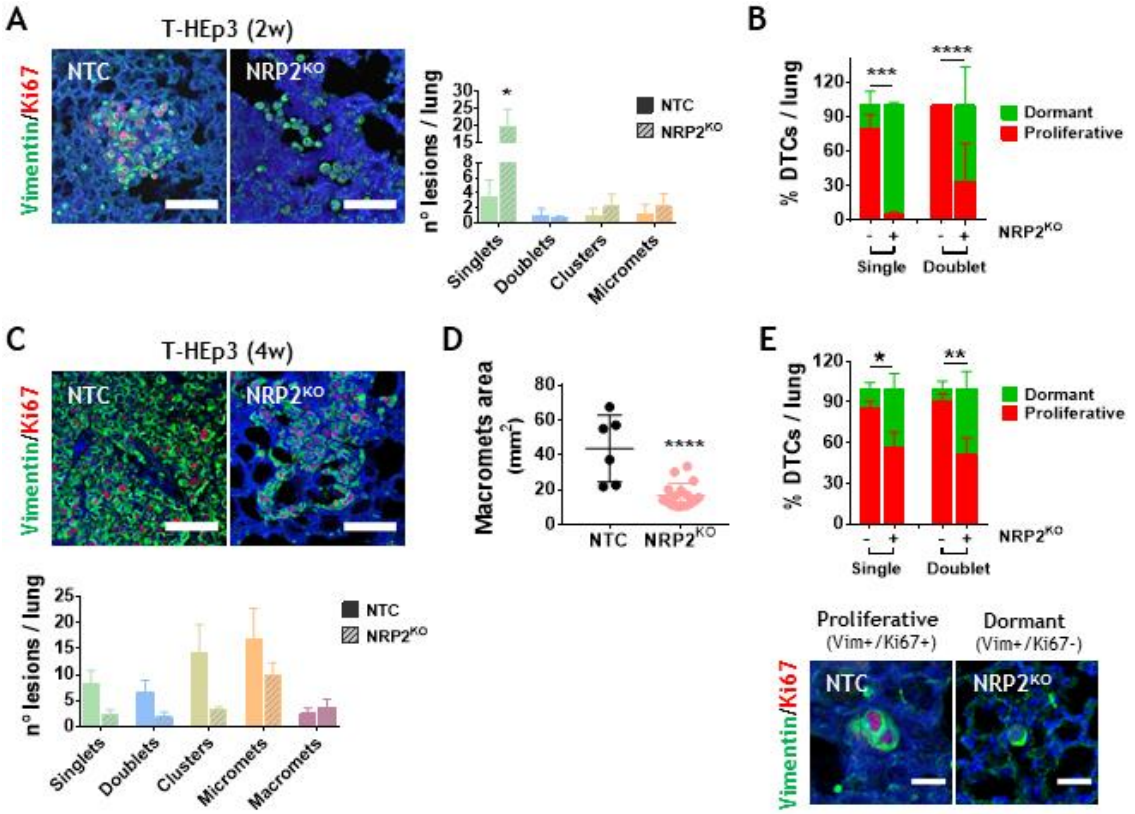

Figure 76. NRP2 deletion decreases T-HEp3 lung metastases number and size as well as triggers quiescence in lung DTCs *in vivo*. 2.5·10^5 Cas9 or NRP2^{KO} T-HEp3 cells were inoculated into the lateral tail vein of the mouse. 2 and 4 weeks after inoculation, lungs were isolated for lung DTCs analysis (see *Materials & Methods, section 3.8.3* for further information). **A)** Left panel, representative IF images of vimentin (green) and Ki67 (red) in T-HEp3 lung DTCs. Scale bar: 50µm. Right panel, quantification of the number of T-HEp3 lung lesions. **B)** Quantification of the percentage (%) of Ki67-positive (proliferative) or Ki67-negative (dormant) T-HEp3 single and double DTCs per lung after 2 weeks. **C)** Upper panel, representative IF images of vimentin (green) and Ki67 (red) in T-HEp3 lung DTCs after 4 weeks. Scale bar: 50µm. Lower panel, quantification of the number of T-HEp3 lung lesions after 4 weeks. **D)** Quantification of lung macrometastases size in mice inoculated with T-HEp3 NTC or NRP2^{KO} cells after 4 weeks. **E)** Quantification of the percentage (%) of Ki67-positive (proliferative) or Ki67-negative (dormant) T-HEp3 single and double DTCs per lung after 4 weeks. Lung DTCs were quantified as the total number of vimentin-positive cells per lung: singlets, doublets, clusters (3-8 cells), micrometastases (9-100 cells; <100µm^2) and macrometastases (>100 cells; >100µm^2). DTCs phenotype was determined by Ki67 expression (Ki67$^+$ as proliferative DTCs; Ki67$^-$ as dormant DTCs). Graphs represent mean ± S.E.M. (n=1, with 5 mice per group); *P < 0.05, **P < 0.01, ***P < 0.001, ****P < 0.0001 comparing NTC (-) *vs* NRP2^{KO} (+) by *t*-Student's test.

Taken all together, these data support the hypothesis that NRP2 has a determinant role in triggering lung metastases development by regulating DTCs proliferative phenotype. Our results show that NRP2 exerts an important function in lung metastases development by maintaining the proliferative phenotype of DTCs and thus, favouring the development and enlargement of lung metastases.

4.4.4. Microenvironmental signals regulate NRP2 expression *in vitro*

We have certainly demonstrated that NRP2 regulates lung DTCs proliferation as well as lung metastases formation. Moreover, our previous results using the MDA-MB-453 model suggest that factors or signals in the lung microenvironment can regulate NRP2 expression and promote metastasis (**fig. 71**). Hence, we first evaluated whether NRP2 expression could be regulated by factors present in the TME. Published data have described NRP2 as a main regulator of lymphangiogenesis, promoting tumour cell dissemination and metastasis[396]. Together with VEGFR3, NRP2 acts as the main co-receptor for VEGF-C, inducing lymphatic endothelial cells proliferation and favouring cell migration and invasion[396]. Moreover, VEGF-C also acts on tumour cells favouring tumour cells malignant properties through NRPs signalling among others[410,501,502]. To this end, we first analysed whether NRP2 expression was up-regulated after VEGF-C treatment in our models. We found no clear differences in NRP2 levels in cells treated with the vasculogenic factor (**fig. 77A**). Hence, we next explored whether NRP2 might be regulated by other factors present in the TME such as TGFβ1. Both NRPs have been shown to participate in TGFβ1 signalling in several cancer types[412–414,416], which induces a more malignant phenotype. In addition, TGFβ1 activates proliferation of dormant HEp3 cell lines as well as dormant bone marrow DTCs variants[266]. In this case, we observed that TGFβ1 treatment clearly up-regulated NRP2 expression while NRP1 levels were differently regulated depending on the cell line (**fig. 77B**). BrCa and HNSCC cell lines doubled their NRP2 expression after 4h of treatment with TGFβ1, suggesting a post-transcriptional TGFβ1-derived NRP2 regulation since we did not detect any changes in NRP2 mRNA levels upon treatment with TGFβ1 (**fig. 77C**).

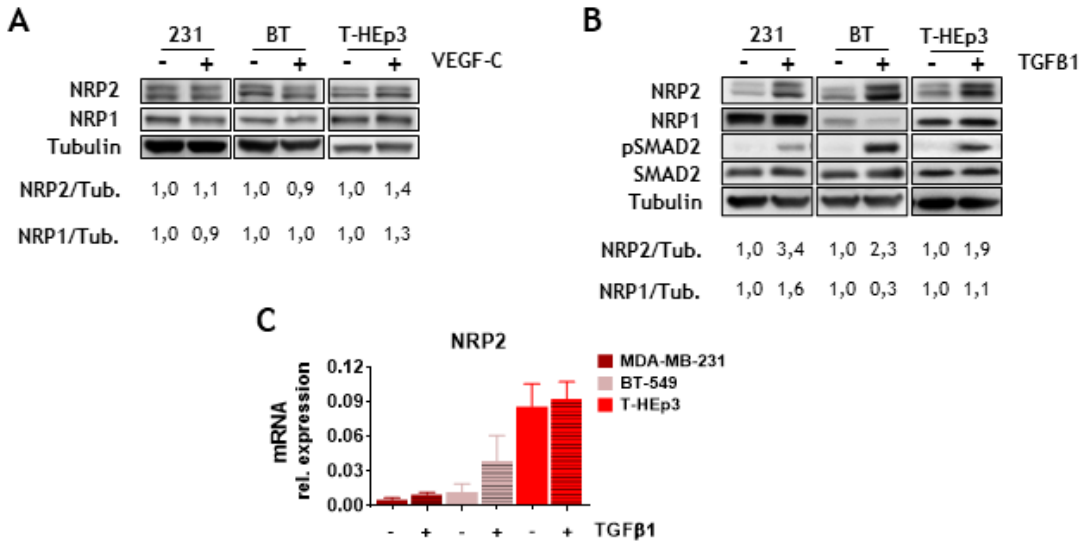

Figure 77. NRP2 expression is post-transcriptionally up-regulated by TGFβ1. Representative western blot analysis of NRP2 and NRP1 protein levels normalized with β-Tubulin after 4h treatment with VEGF-C (10ng/mL) (**A**; n=1) and TGFβ1 (5ng/mL) (**B**; n≥3) in BrCa (MDA-MB-231 -231-, BT-549 -BT-) and HNSCC (T-HEp3) cell lines. Protein quantifications are referred to the non-treated (-) condition. **C)** Analysis of NRP2 mRNA levels after 24h treatment with TGFβ1 (5ng/mL). Graphs represent RQ mean values ± S.E.M. (n≥3, triplicates); *t*-Student's test between control (-) and TGFβ1 treatment (+) was performed and revealed non-significant differences.

Following with our study, we next analysed the effect of TGFβ1 treatment in 3D cultures, which resembles the complex extracellular microenvironment and thus better mimics the physiological conditions of the cells. After 7 days treatment with TGFβ1, no quantitative differences were detected in the size of MDA-MB-231 colonies (**fig. 78A, lower panel**). However, higher percentage of T-HEp3 colonies with more than 8 cells were found in TGFβ1-treated cells (**fig. 78B, lower panel**). Moreover, IF staining of these colonies revealed that NRP2 expression had an upward trend in TGFβ1-treated cells as compared to the control cells, both in MDA-MB-231 (**fig. 78C, upper panel**) and T-HEp3 cells (**fig. 78D, upper panel**). Consistent with the size of the colonies, we also found an up-regulation in the number of Ki67-positive cells not only in T-HEp3 3D cultures (**fig. 78D, lower panel**) but also in MDA-MB-231 colonies (**fig. 78C, lower panel**). Altogether, our results suggest that TGFβ1 up-regulates NRP2 expression and that NRP2 up-regulation might correlate with proliferation induction in 3D models.

Since our results suggest that proliferative signals such as TGFβ1 could positively regulate NRP2 expression, we wondered whether TME dormancy-inducing signals could inhibit NRP2 expression. As explained before, the bone marrow can act as a restrictive-microenvironment where dormant DTCs can be found in patients showing no clinical symptoms[268]. BM-MSC suppressed BrCa cell proliferation and invasion when co-cultured together[466,467], which induced reversible cell cycle arrest[467]. Furthermore, we have previously shown that BMCM can be used to mimic bone marrow niche conditions and effects on DTCs[266]. Therefore, we first treated BrCa and HNSCC cell lines for 48h with BMCM obtained from human BM-MSC (see *Materials & Methods, section 3.1.3.1* for further information). However, BMCM treatment did not modify NRP2 protein levels (**fig. 79A**).

TGFβ2 is one of the factors highly present in the BM able to induce dormancy in DTCs[266,291,292]. Hence, we wanted to determine whether treating with TGFβ2 could down-regulate NRP2 expression. These experiments were performed in 3D colonies, similar to the previously described TGFβ1 experiments. The quantification of the number and size of the colonies showed that treatment with TGFβ2 reduced the number of bigger colonies in MDA-MB-231 3D cultures (**fig. 79B**) while we observed no significant effects in T-HEp3 colony size (**fig. 79C**). When we analysed NRP2 expression on the colonies, opposite to TGFβ1 effects, NRP2 levels tend to be lower after TGFβ2 treatment in BrCa cells (**fig. 79D, upper panel**). In T-HEp3 cells there was an unexpected tendency to increase NRP2 levels (**fig. 79E, upper panel**). Furthermore, we also analysed Ki67 expression in the 3D cultures treated with TGFβ2. We found no significant differences in Ki67 staining in either MDA-MB-231 cultures (**fig. 79C, lower panel**) or in T-HEp3 cultures (**fig. 79E, lower panel**). Our results suggest that TGFβ family members might differentially regulate NRP2 expression, being the activated downstream signalling pathways likely different between TGFβ1 and TGFβ2 and thus their effects on the cells as well. Taken these results together, we concluded that NRP2 expression is up-regulated by TGFβ1 in aggressive BrCa and HNSCC cell lines.

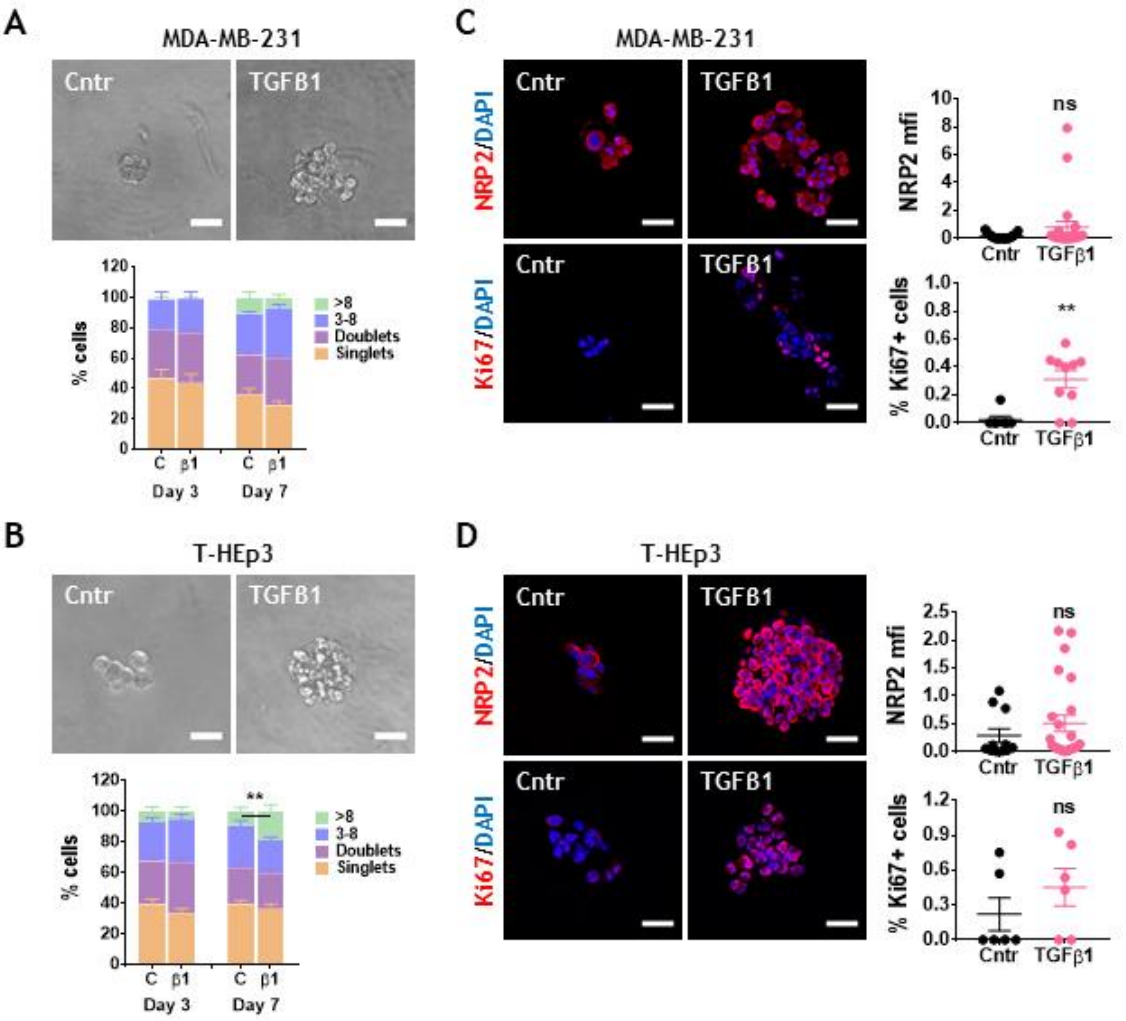

Figure 78. TGFβ1 induces the expression of Ki67 favouring cell growth and up-regulates NRP2 expression in 3D experiments. **A, B)** Upper panels, representative bright field images of MDA-MB-231 (**A**) and T-HEp3 (**B**) colonies after 7 days growing in 3D. Cells were treated with TGFβ1 (2ng/mL) every two days. Scale bar: 800µm. Lower panels, quantification of the percentage (%) of cells in singlets (orange), doublets (purple), colonies from 3 to 8 cells (blue) and colonies of more than 8 cells (green). **C, D)** Left panels, representative IF images of NRP2 (upper panel) and Ki67 (lower panels) in MDA-MB-231 (**C**) and T-HEp3 (**D**) cells grown in 3D for 7 days. Scale bar: 50µm. Right panels, NRP2 and Ki67 mfi quantification. Graphs represent mean ± S.E.M. (n≥3); ns, non-significant, **P < 0.01 comparing Cntr (C) *vs* TGFβ1 (β1) by *t*-Student's test.

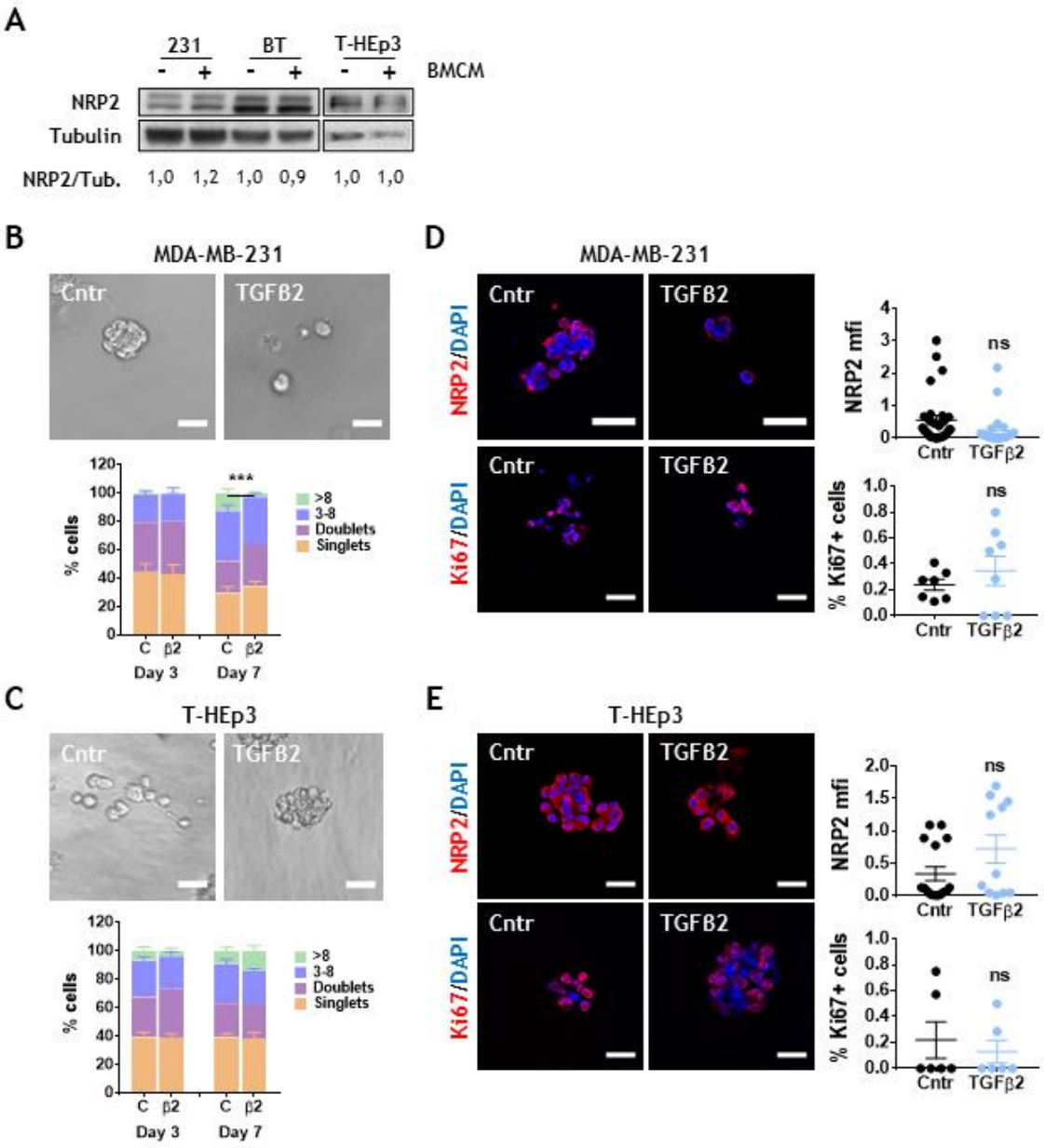

Figure 79. Dormancy-inducing signals effect on the expression of Ki67 and NRP2 in BrCa and HNSCC cells grown in 3D. **A)** Representative western blot analysis of NRP2 protein levels normalized with β-Tubulin after 48h BMCM treatment. NRP2 quantifications are referred to the non-treated (-) condition (n>3 for BrCa cells, n=1 for T-HEp3). **B, C)** Upper panels, representative bright field images of MDA-MB-231 (**B**) and T-HEp3 (**C**) colonies after 7 days growing in 3D. Cells were treated with TGFβ2 (2ng/mL) every two days. Scale bar: 800µm. Lower panels, quantification of the percentage (%) of cells in singlets (orange), doublets (purple), colonies from 3 to 8 cells (blue) and colonies of more than 8 cells (green). **D, E)** Left panels, representative IF images of NRP2 (upper panel) and Ki67 (lower panels) in MDA-MB-231 (**D**) and T-HEp3 (**E**) cells grown in 3D for 7 days. Scale bar: 50µm. Right panels, NRP2 and Ki67 mfi quantification. Graphs represent mean ± S.E.M. (n≥3); ns, non-significant, ***P<0.001 comparing Cntr (C) *vs* TGFβ2 (β2) by *t*-Student's test.

4.4.4.1. Canonical TGFβ1 signalling pathway up-regulates NRP2 expression

In the previous section, we have demonstrated that TGFβ1 regulates NRP2 expression in a post-transcriptional manner, with a significative up-regulation after 4h of treatment (**fig. 77B**). TGFβ regulates gene expression mainly through the canonical pathway using SMAD proteins[503]. To better

understand the regulation of NRP2 by TGFβ1, we inhibited the canonical TGFβ signalling pathway with two different inhibitors. First, we used the SB431542 inhibitor which inhibits the canonical pathway by preventing the type I TGFβ receptor ALK5 activation. Hence, SB431542 avoids the TGFβ1-induced phosphorylation and subsequent activation of SMAD2/3 [472]. Cells were first pre-treated with SB431542 for 2h to ensure the inhibition of the canonical pathway, before treating the cells with TGFβ1 for 24h. SB431542 treatment was repeated when TGFβ1 was added. We found that the TGFβ1-induced activation of NRP2 was mostly reverted when the type I TGFβ receptor was inhibited. Indeed, NRP2 levels returned to the basal levels both in BrCa and in HNSCC cell lines (**fig. 80A**). Interestingly, inhibition of TGFβ1 also inhibited NRP2 up-regulation in lung DTCs derived cell line (**fig. 80A**). In parallel, we used another type I TGFβ receptor inhibitor, Galunisertib (termed as GNB) (LY2157299), produced by Eli Lilly and investigated in various clinical trials for hepatocellular, lung and pancreatic cancers (NCT01246986; NCT02423343; NCT02734160). In a similar way, GNB treatment prevented the TGFβ1-induced NRP2 up-regulation, decreasing NRP2 levels to the levels of the non-treated control cells in all the cell lines (**fig. 80B**). Consequently, these results verify that TGFβ1 regulates NRP2 expression in proliferative cell lines as well as in lung DTCs derived cell lines by the classical canonical signalling pathway.

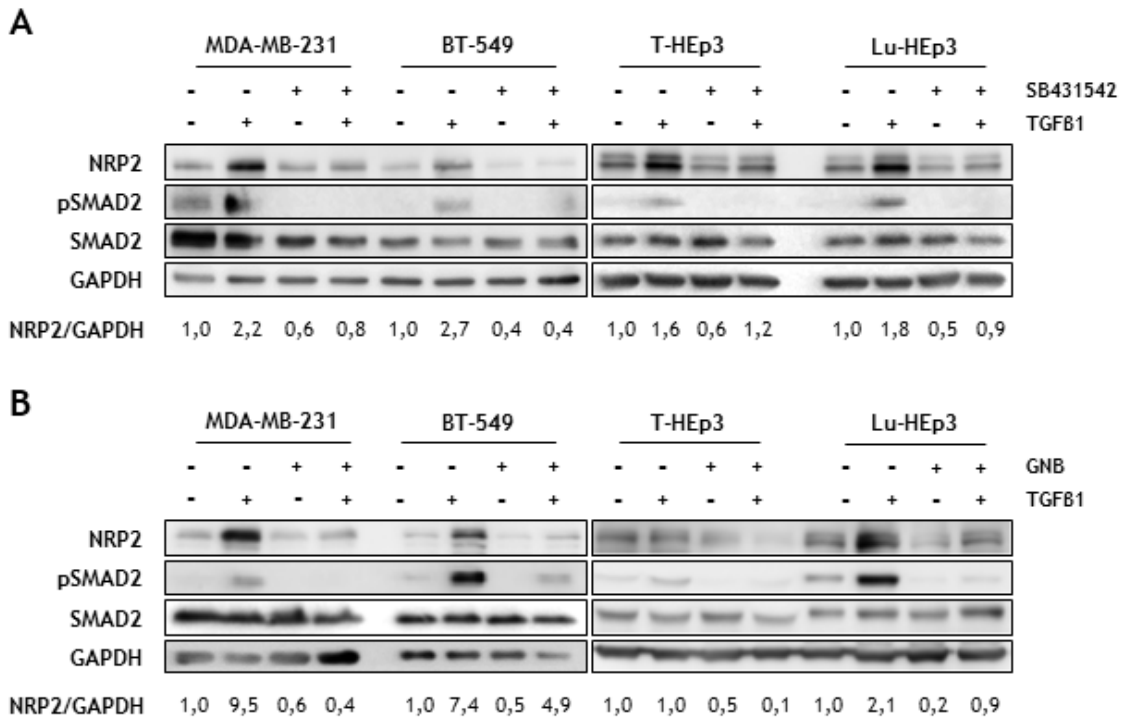

Figure 80. NRP2 expression is up-regulated by the TGFβ canonical signalling pathway. **A)** Representative western blot analysis of NRP2 and pSMAD2/SMAD2 protein levels normalized with GAPDH after 24h treatment with SB431542 (5μM) and/or TGFβ1 (5ng/mL). Cells were previously pre-treated with SB431542 for 2h and then again together with the TGFβ1 treatment. NRP2 protein quantification is referred to the non-treated control condition (n=3). **B)** Representative western blot analysis of NRP2 and pSMAD2/SMAD2 protein levels normalized with GAPDH after 24h treatment with GNB (5μM) and/or TGFβ1 (5ng/mL). Cells were previously pre-treated with GNB for 2h and then again together with the TGFβ1 treatment. NRP2 protein quantifications are referred to the non-treated control condition (n=2).

4.4.5. Lung fibroblasts and macrophages-secreted TGFβ1 increases NRP2 expression

Tumour microenvironment regulates tumour growth and dissemination as well as metastasis development in secondary organs[121,257]. Our previous results have demonstrated that NRP2 is up-regulated by TGFβ1 (**fig. 77, 79, 80**), which is highly present in tumour microenvironments. Moreover, we have verified that NRP2 directly controls the proliferative phenotype of lung DTCs and thus lung metastases development (**fig. 73-76**). With this context, our final step was to investigate how NRP2 could be regulated in the lung microenvironment.

4.4.5.1. Lung-derived TGFβ1 up-regulates NRP2 expression by the canonical signalling pathway

To mimic the lung microenvironment *in vitro* we first obtained chicken embryo lung CM to treat the cells (see *Materials & Methods, section 3.1.4* for further information). Then, we treated the cells with the lung CM for 24h and found, as expected, that NRP2 was highly up-regulated in BrCa and HNSCC proliferative cells (**fig. 81A**). To test if the factor in the lung CM that was increasing NRP2 was TGFβ1, we depleted TGFβ1 from the lung CM (**fig. 81B**) and then treated the cells with these TGFβ1-depleted lung CM. Here, we found that the NRP2 up-regulation derived from the non-depleted lung CM was partially reverted when TGFβ1 was removed (**fig. 81C**). Altogether, these results suggest that lung-derived TGFβ1 could be one of the factors up-regulating NRP2 expression in the lung microenvironment.

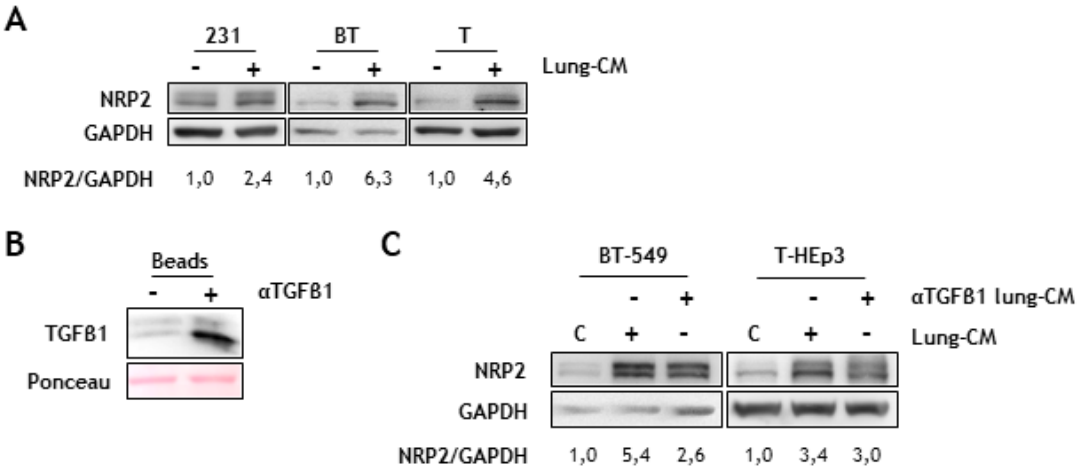

Figure 81. Lung-derived TGFβ1 increases NRP2 expression. **A)** Representative western blot analysis of NRP2 protein levels normalized with GAPDH after 24h treatment of BrCa (MDA-MB-231 -231-, BT-549 -BT-) and HNSCC (T-HEp3 -T-) cell lines with chicken embryo lung CM. NRP2 protein quantification is referred to the control condition (C) (n=2). **B)** Representative western blot analysis of TGFβ1 protein levels released from the beads used for lung CM depletion used in C. Beads (-) refers to the control condition where control IgG has been used for the depletion whereas beads (+) refers to those beads with linked TGFβ1 antibody. After the depletion, depleted TGFβ1 has been released by an incubation of 10min at 70°C and the sample has been analysed by western blot for TGFβ1 detection. Ponceau has been used as a loading control. **C)** Representative western blot analysis of NRP2 protein levels normalized with GAPDH after 24h treatment with lung CM or TGFβ1-depleted lung CM. NRP2 protein quantifications are referred to the non-treated control condition (C) (n=1).

Finally, we inhibited the canonical TGFβ1 signalling pathway while treating with the lung CM. We observed that the up-regulation of NRP2 expression derived from lung CM treatment was

partially reverted in proliferative cells when the type I TGFβ receptor was inhibited (**fig. 82A**). Furthermore, as NRP2 was found to be determinant for lung metastases development in NRP2 low expressing cells (**fig. 72, 73**), we also studied the effect of lung CM treatment in dormant-like BrCa (ZR-75-1) and dormant HNSCC (D-HEp3) cells. Although they express low NRP2 basal levels, ZR-75-1 and D-HEp3 cells showed an increase in NRP2 after the lung CM treatment (**fig. 82B, C**). Here, NRP2 activation was also down-regulated when the canonical TGFβ pathway was suppressed (**fig. 82B, C**). Taken all together, these results clearly indicate that TGFβ1 is one of the factors present in the lungs up-regulating NRP2 not only in proliferative, but also in dormant tumour cells, suggesting it can reprogram dormant DTCs to a more proliferative phenotype through NRP2 up-regulation.

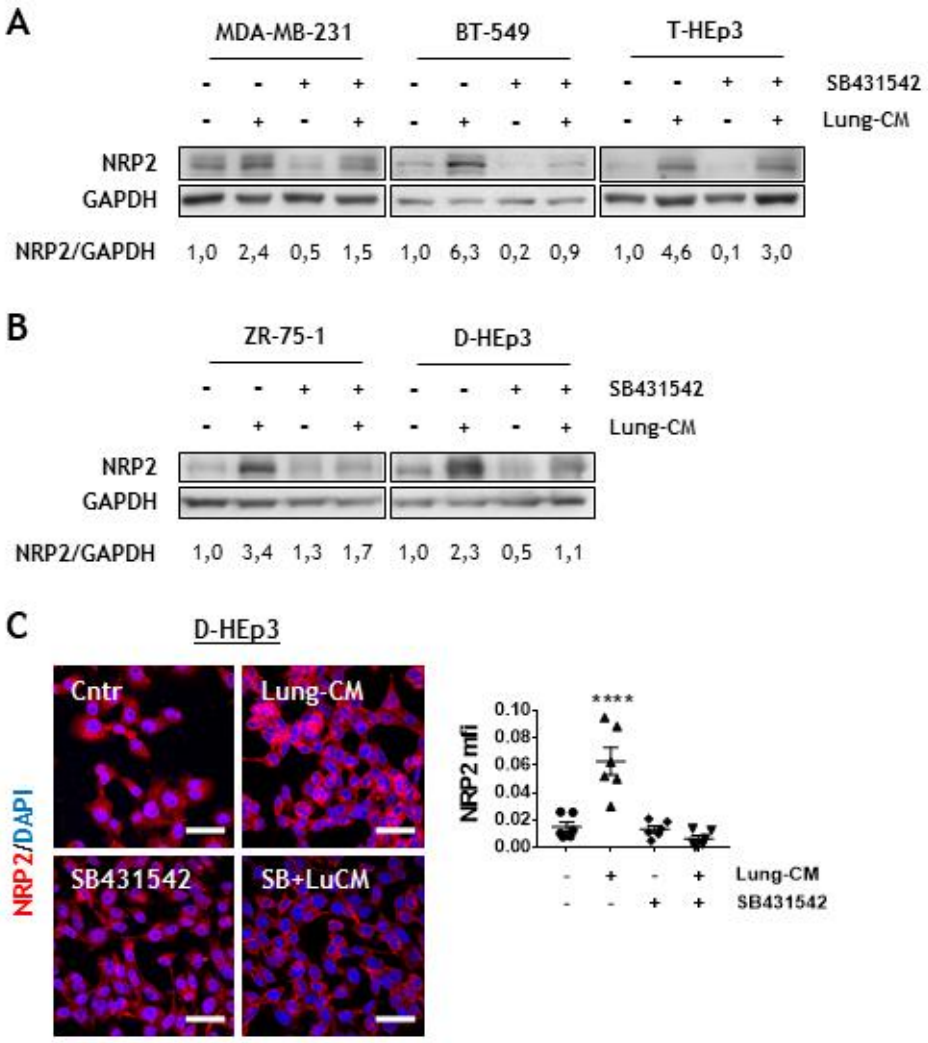

Figure 82. Lung-derived type I TGFβ receptor ligands increase NRP2 expression in proliferative and dormant BrCa and HNSCC cell lines. **A, B)** Representative western blot analysis of NRP2 protein levels normalized with GAPDH after 24h treatment with chicken embryo lung CM and/or SB431542 (5μM) in LDS-proliferative (**A**; n=2) and HDS-dormant (**B;** n=1) cell lines. NRP2 protein quantifications are referred to the control condition. **C)** Left panel, representative IF images of NRP2 in D-HEp3 cells after 24h treatment with chicken embryo lung CM and/or SB431542 (5μM; SB). Scale bar: 50μm. Right panel, graph representing NRP2 mfi mean values ± S.E.M. (n=1); ****P < 0.0001 comparing Cntr *vs* lung CM, SB or SB + LuCM by one-way ANOVA, Dunnett's test. In all the experiments cells were previously pre-treated with SB431542 for 2h and then again together with the lung CM treatment.

4.4.5.2. Macrophages and fibroblasts-released TGFβ1 might be responsible of NRP2 up-regulation in lung DTCs

As our results indicate that TGFβ1 is one of the factors activating NRP2 in the lung microenvironment, we next wanted to determine which could be the source of this TGFβ1. As previously described, the TME is composed by many cellular and extracellular elements that altogether regulate tumour biology and thus its progression[120,163,176,198]. In pathological conditions, the lung microenvironment might support tumour development by changing anatomical and cellular features[504]. Macrophages and fibroblasts have been demonstrated to be some of the tumour-promoting cells in the lung[504]. Hence, we hypothesized both might be source of the TGFβ1 responsible of NRP2 activation. To test this, we first analysed whether they synthetized and released TGFβ1 to the media. Differentiated human THP-1 macrophages had high TGFβ1 mRNA levels while expressing low levels of TGFβ2 (**fig. 83A**). Regarding fibroblasts, we worked with the commercial CCD19 and the primary CF5 human lung fibroblasts cell lines. Both fibroblasts cell lines had similar levels of TGFβ1 and TGFβ2 mRNA levels, but much lower expression than macrophages (**fig. 83A**). TGFβ1/TGFβ2 ratio suggests that macrophages synthetised higher amount of TGFβ1 than lung fibroblasts, as did T-HEp3 cells as well (**fig. 83A, lower panel**). Besides TGFβ1 mRNA expression, we also analysed TGFβ1 secretion by performing an ELISA in chicken embryo lung, lung fibroblasts and macrophages CM, as well as in T-HEp3 and MDA-MB-231 conditioned media. We found that all the cell lines produced TGFβ1 (**fig. 83B**). Nevertheless, lung fibroblasts and macrophages secreted higher levels of TGFβ1 than tumour cell lines (**fig. 83B**), suggesting lung fibroblasts and macrophages secreted TGFβ1 might have a paracrine role on tumour cells.

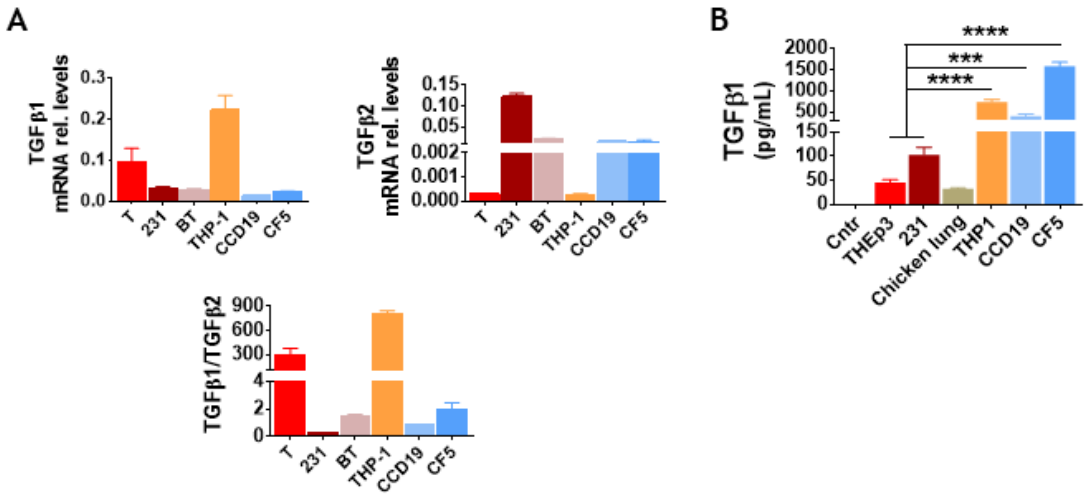

Figure 83. Lung fibroblasts and macrophages secrete high levels of TGFβ1. A) Analysis of TGFβ1 and TGFβ2 mRNA levels in tumour (T-HEp3 -T-, MDA-MB-231 -231- and BT-549 -BT-), macrophages (THP-1) and lung-derived fibroblast (CCD19, CF5) cell lines. Graphs represent RQ mean values ± S.E.M. (n=2, triplicates). **B)** Quantification of TGFβ1 levels by ELISA (pg/mL), in tumour cells (T-HEp3 -T-, MDA-MB-231 -231-), chicken lung and TME cells CM (macrophages, THP-1; fibroblasts, CCD19 and CF5). The graph represents the TGFβ1 pg/mL mean values ± S.E.M (n=1, triplicates); ***P < 0.001, ****P < 0.0001 comparing tumour cells (T-HEp3 and 231) *vs* THP-1, CCD19 or CF5 by one-way ANOVA, Sidak's test.

To test if macrophages and fibroblasts-derived TGFβ1 could activate NRP2, we first treated proliferative cells with THP-1 macrophages CM and NRP2 protein levels were analysed. Here, we found that in response to stimulation with THP1-CM, NRP2 expression was markedly increased in

BrCa and HNSCC cell lines (**fig. 84A**). As TGFβ1 levels were also detected in lung fibroblasts, we treated tumour cells with fibroblasts CM as well. In a similar way to the macrophages CM, both commercial CCD19 (**fig. 84B**) and primary CF5 (**fig. 84C**) lung fibroblasts CM induced NRP2 activation. These results suggest that macrophages and fibroblasts can induce NRP2 activation. Then, to study whether this was dependent on TGFβ1 production, in parallel, we inhibited the type I TGFβ receptor using the SB431542 inhibitor. A pre-treatment of 2h was performed with SB431532 before treating with the CM, where the SB431542 treatment was again repeated. As shown in **figure 84**, either with macrophages or with both lung fibroblasts CM treatment the activation of NRP2 was diminished when the CM treatment was combined with the SB431542. Therefore, these results suggest that lung fibroblasts and macrophages secrete TGFβ1 which will in turn activate NRP2 expression in tumour cells, partly by the TGFβ canonical signalling pathway.

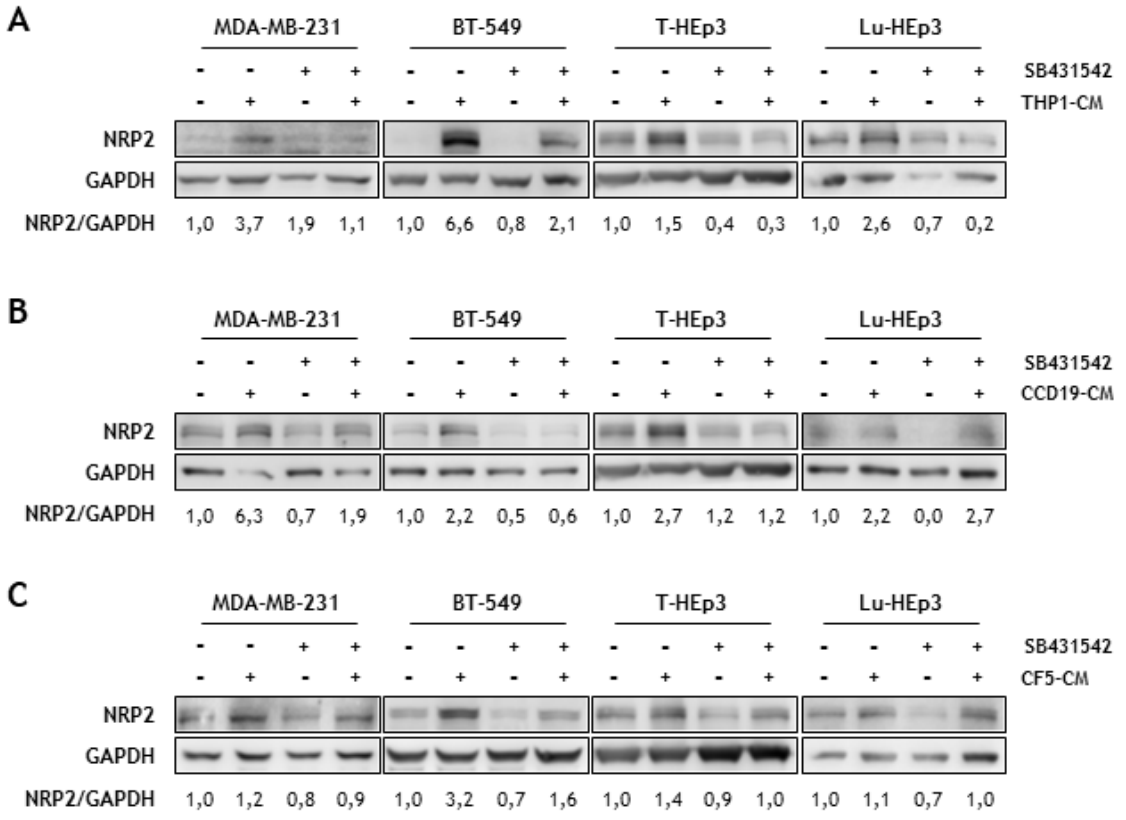

Figure 84. Lung fibroblasts and macrophages conditioned media increase NRP2 expression by TGFβ1 secretion. A) Representative western blot analysis of NRP2 protein levels normalized with GAPDH after 24h treatment with THP1-CM. **B)** Representative western blot analysis of NRP2 protein levels normalized with GAPDH after 24h treatment with CCD19-CM. **C)** Representative western blot analysis of NRP2 protein levels normalized with GAPDH after 24h treatment with CF5-CM. In all the experiments, cells were pre-treated with SB431542 (5μM) 2h before and together with the CM treatments. NRP2 protein quantifications are referred to the non-treated control condition (n=2).

4.4.5.3. Lung fibrosis is associated with NRP2 up-regulation

Pulmonary fibrosis, characterized by an excess of myofibroblasts that are permanently activated, is associated to lung cancer as well as to lung metastases development[505]. Many growth factors and cytokines have been related with lung fibrosis development, TGFβ1 among them[506]. In fact, TGFβ1-driven lung fibrosis promoted dormant lung DTCs re-awakening and generation of overt lung metastases[300]. Pulmonary fibrosis is related with ageing, where older patients have higher

incidence of the disease[507]. Therefore, we wondered whether lung fibrosis induced cell proliferation could be regulated by NRP2. To address this hypothesis, we used young (6 weeks) and old (16 months) healthy mice (kindly donated by Dr. Porras from Complutense University of Madrid) lungs CM and analysed NRP2 expression. To corroborate that old lungs were fibrotic, we evaluated the expression of αSMA (α-smooth muscle actin), a marker of activated fibroblasts or myofibroblasts. Here, we found that old lungs were more fibrotic, with higher levels of αSMA protein (**fig. 85A, upper panel**). Moreover, old lungs had higher levels of TGFβ1 (**fig. 85A, B**). As shown in **figure 85C**, both young and old lungs CM up-regulated NRP2 although the effect of old lungs was more marked. Interestingly, inhibition of type I TGFβ receptor using the SB431542 inhibitor reverted NRP2 induction by the old lung CM, while had little effect on NRP2 induction by young lung CM (**fig. 85C**). These results suggest that NRP2 induction might be age-dependent where TGFβ1, that is more abundant in fibrotic old lungs, could be associated both with NRP2 up-regulation and dormant lung DTCs re-awakening.

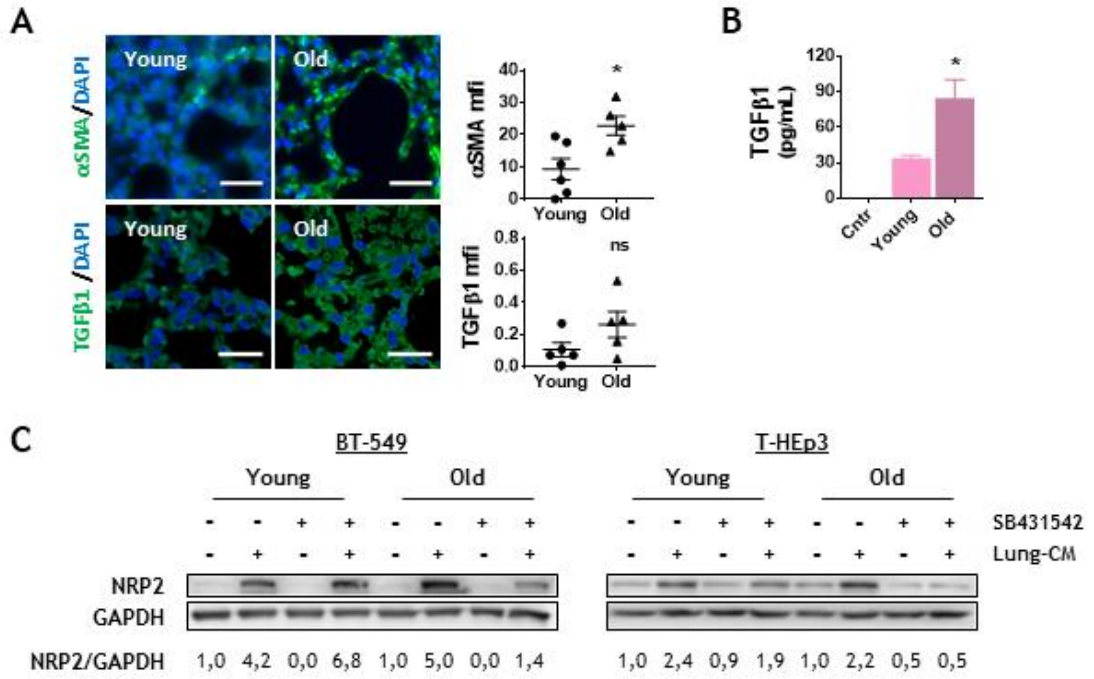

Figure 85. Lung fibrosis up-regulates NRP2 expression. A) Left panel, representative IF images of αSMA (upper panels; scale bar: 3μm) and TGFβ1 (lower panels; scale bar: 25μm) in young and old mouse lungs. Right panels, αSMA (top panel) and TGFβ1 (bottom panel) mfi quantifications (n=1). **B)** TGFβ1 quantification by ELISA (pg/mL), in young and old mouse lung CM (n=1, triplicates). Graphs represent mean ± S.E.M.; ns, non-significant, *P < 0.05 comparing young *vs* old by one-way ANOVA, Sidak's test. **C)** Representative western blot analysis of NRP2 protein levels normalized with GAPDH after 24h treatment with young or old mouse lung-CM in BT-549 and T-HEp3 cell lines. Cells were pre-treated with SB431542 (5μM) 2h before and together with the CM treatment. NRP2 protein quantifications are referred to the non-treated control condition (n=1).

Discussion

Metastasis is the most advanced stage of a tumour that without available effective treatments is considered non-curable and causes the vast majority of cancer-related deaths[231]. Metastasis derives from DTCs that following a well-orchestrated but very inefficient multi-step process, escape from the PT and colonize distant organs promoting secondary tumours growth[208,229]. From the invasion to the colonization, the complexity of the mechanisms followed by tumour cells have hampered the understanding of such lethal disease and thus have prevented an effective cancer management.

A successful metastatic cell must not only be able to invade and survive within the circulation, but also to survive and adapt to the new microenvironment. Getting to the target organ will not always lead to metastasis growth. Indeed, DTCs usually enter a reversible quiescence phase (dormancy) during the adaptation to new microenvironments[270,279,280]. At some later stage, these dormant DTCs might become re-activated and proliferative extending into a metastasis. However, not all dormant DTCs will progress to proliferative DTCs and in fact some will be kept dormant forever[270,280,508]. Still, the mechanisms governing cell quiescence as well as the signals regulating the reawakening of DTCs remain unclear.

In recent years, it has become clear that the relationship between DTCs and the colonized microenvironment is crucial for metastatic success. The microenvironment has a pivotal role in determining whether DTCs will grow in unexplored areas or whether they will not be able to overcome the selective pressure imposed on them. Factors present in secondary organs microenvironments, including TGFβ family members[266,291,292,296–298], BMPs[264,265] and several cytokines[290,297], might also be responsible for inducing and maintaining dormancy while DTCs adapt to the colonized organ. Identifying the microenvironment properties or signals that confer DTCs adaptive and survival abilities would provide enough notions to start thinking about therapeutically targetable events.

In view of the above considerations, the main objective of this thesis has been to decipher some of the mechanisms regulating DTCs fate in secondary organs. Understanding the biology of DTCs and the mechanisms regulating their quiescence state and survival will allow the integration of DTCs as a prognostic and predictive tool in the management of cancer. Therefore, we would be a step closer to inhibit metastasis development by generating new target therapies specifically designed against these DTCs.

With all, our results highlight the **role of SEMA3F and NRP2 in regulating quiescence and proliferation in lung DTCs respectively and thus, in the development of lung metastases**. In addition, they support the idea that **NRP2 is up-regulated by the lung microenvironment derived TGFβ1**, produced by lung fibroblasts and macrophages. Moreover, once NRP2 is activated, it induces DTCs re-awakening through p27 inhibition and promotes metastases formation in the lung.

5.1. SEMA3F is a dormancy-inducer protein in BrCa and HNSCC prompting dormancy in lung DTCs

Semaphorins were initially found as axon guidance cues involved in the development of the NS whereas their functions have been tangled in several homeostatic and malignant conditions at present. In fact, the plasticity of tumour cells required for tumour progression might be explained by the role of SEMAs in cell morphology, cell adhesion and cytoskeletal rearrangements[509]. SEMAs have also been associated to tumour angiogenesis by regulating endothelial cells movement towards or against a specific stimulus, which promote cancer cells migration, invasion and metastasis[395,398,510].

From all semaphorins family members, we have focused on understanding the role of class 3 semaphorins as they bind to receptor complexes composed by NRPs and PLXNs[365,422]. Being secreted, SEMA3s can signal in an autocrine or a paracrine manner acting as tumour inducer or tumour suppressor molecules depending on the context[423,510,511]. Therefore, in order to determine whether SEMA3s act as attractive signals inducing tumour growth or as repulsive cues inhibiting tumour development, we have first characterized their expression in our models. Our preliminary data suggest an anti-tumoural role for SEMA3F in our models based on its lower expression in aggressive BrCa and HNSCC cells (**fig. 26**). Moreover, public databases analyses have revealed that SEMA3F levels are decreased in BrCa and HNSCC patients' advanced tumours (**fig. 28, 29**), suggesting its expression is lost as tumour aggressiveness increases. As in our models, in the literature SEMA3F is mainly described as a tumour suppressor protein that inhibits tumour growth and dissemination[434,512] when binding to its main receptor NRP2 [513,514]. However, no direct association has been published between SEMA3F and DTCs dormancy, increasing our interest about studying this neural factor. In addition, the increased SEMA3F expression in HDS BrCa cells (ex. MDA-MB-453, ZR-75-1) and dormant HEp3 cells lead us to hypothesize that SEMA3F could induce tumour dormancy in aggressive BrCa and HNSCC tumours. Hence, since it is up-regulated in less aggressive cells, SEMA3F could be defined as a good prognostic factor, increasing its potential clinical value.

The lack of information in recent publications regarding quiescence modulation by SEMA3F have encouraged us to delve deeper in this topic. The SEMA3F-dormancy crosstalk has been confirmed when SEMA3F treatment increases dormancy protein markers expression (**fig. 30**). The positive regulation of p27 *in vitro* by SEMA3F indicates that SEMA3F might induce a switch towards a more dormant-like phenotype in BrCa and HNSCC models. This pro-dormancy effect has also been supported by the *in vivo* data derived from the inoculation of MDA-MB-231 and T-HEp3 cells in chicken embryo CAMs (**fig. 36, 37**), where besides p27, mRNA levels of Dec2 and TGFRβ3, both dormancy inductor genes, are also up-regulated. This goes in agreement with SEMA3F being a plausible good prognosis marker in HNSCCs[515], correlating with lower metastases and patients' outcome[434].

We have not analysed how SEMA3F regulates p27 expression in our models. Nevertheless, SEMA3F has been found to be directly regulated by the major tumour suppressor gene *p53* [516], mutated in many cancer types[517,518]. When activated, p53 initiates a transcriptional program that altogether will prevent the neoplastic transformation of a cell[518]. A major player in the p53-mediated cell cycle arrest is p21 [519], whose expression was also found to be increased after the p53-derived SEMA3F up-regulation[516]. Therefore, similar to p21 regulation, the SEMA3F-derived p27 up-regulation seen in our models might also be regulated by *TP53.* Furthermore, published data indicate that SEMA3F negatively regulates PI3K/AKT/mTOR pathway in glioblastoma, gastro-intestinal and lung cancer[520–522]. p27 cellular

localization determines p27 function, acting as a cell cycle inhibitor when localized in the nucleus[523]. AKT phosphorylation of p27 was shown to induce cytoplasmic translocation of the nuclear p27 inducing cell proliferation[523–525]. Therefore, a plausible explanation could be that SEMA3F might be protecting p27 from the proteasome degradation by inhibiting PI3K/AKT and thus the nuclear export of p27, favouring the anti-proliferative role of p27.

SEMA3F treatment does not affect migration or invasion of our cells *in vitro* (**fig. 33-35**). However, HEK293-secreted SEMA3F induced repulsion of BrCa cells, where the implication of other secreted proteins might also be considered in the regulation of cell movement[513]. Treatment of lymphatic endothelial cells with SEMA3F-depleted colorectal cancer cells CM treatment activated tubule formation, where the presence of IL-6 was also required to promote cell migration[526]. Therefore, the lack of notorious changes in our functional *in vitro* experiments where SEMA3F treatment is used as the only potential modulator displays the importance of the TME. The fact that cell phenotype variations are mainly observed *in vivo* corroborate the idea that there may be other environmental factors regulating cell biology together with SEMA3F, which would promote the inhibition of cell proliferation, migration and invasion in BrCa and HNSCC.

The results derived from the *in vivo* experiment demonstrate that SEMA3F treatment reduces the number of liver and lung DTCs (**fig. 38**). This could be related with the role of SEMA3F as a chemorepulsive molecule. SEMA3F is an axonal guidance molecule that through NRP2 binding regulates the wiring and patterning of neurons in the nervous system[394,527]. In this sense, SEMA3F has been described as inhibitor of cell migration and invasion in breast[512,513], head and neck[434,528] and lung cancer[529], although in a NRP2-independent manner. This is in agreement with our results, since NRP2 seems to induce cell migration and invasion as well as DTCs proliferation in our models. Hence, SEMA3F effect seem to be independent of NRP2 in our system. Accordingly, several studies have shown evidence of the lower metastatic capacity of SEMA3F over-expressing tumours[514,521,528,530], although no clear mechanisms have been described regarding SEMA3F inhibition of cell dissemination and metastasis. Integrins might be involved in SEMA3F inhibition of cell dissemination, where SEMA3F expressing cells down-regulated α5β3-[530] and β1-integrins[514] resulting in less liver metastases *in vivo*[530].

In relation with this data, we have found that not only cell dissemination but also DTCs proliferative phenotype is reduced after PTs treatment with SEMA3F (**fig. 38**). In agreement with this, recent studies have demonstrated that SEMA3F over-expression reduces lung and liver metastases[433,530], most likely through PI3K/AKT pathway inhibition[433]. The mechanisms by which lung DTCs become more dormant in our model need to be further investigated. While no changes in ERK and p38α signalling pathways are observed following SEMA3F treatment *in vitro* (**fig. 30**), the SEMA3F-regulated inhibition of PI3K/AKT pathway, which in turn would increase p27 expression (likely by protein stabilization) and thus induce cell cycle arrest, could be a good starting point of study.

In summary, our results suggest that SEMA3F can induce DTCs dormancy through up-regulation of the quiescence marker p27 (**fig. 86**).

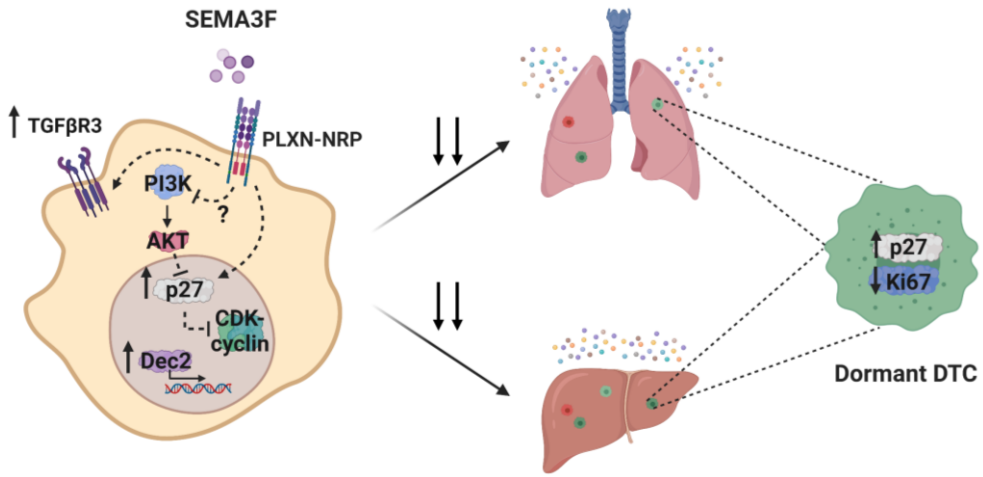

Figure 86. SEMA3F induces dormant DTCs phenotype and reduces cell dissemination to secondary organs. According to our data, SEMA3F treatment up-regulates dormancy markers expression (ex. p27, Dec2, TGFβR3) while decreases proliferation markers (ex. Ki67). Together with other factors present in the microenvironment (coloured balls) which will enhance SEMA3F effect, SEMA3F reduces cell dissemination to the liver and lungs and triggers a dormant phenotype in DTCs.

We have not studied how SEMA3F expression is regulated in cancer progression. However, understanding how SEMA3F expression is inhibited in cancer cells is also important. As in embryo development where SEMA3F exhibits distinct, spatiotemporally changing expression patterns[531,532], we believe SEMA3F expression might also be temporally regulated in tumour presenting lower levels in more advanced tumours. Zeb1, a transcription factor that promotes tumour invasion and metastasis[533,534], has been found to be involved in SEMA3F down-regulation in lung cancer[529]. Zeb1 can directly bind to SEMA3F promoter, down-regulating its expression and inhibiting its anti-tumour activity[529]. Therefore, the higher expression of Zeb1 in more advanced tumours could be responsible for the decreasing levels of SEMA3F and thus, for the activation of EMT-programs, cell dissemination and metastases.

5.2. PLXNA2 inhibits tumorigenic cell properties in ER-negative BrCa cells

Plexins are involved in numerous cellular activities related to cell proliferation, adhesion, cellular motility and invasive capability and thus, their expression is often dysregulated in cancers[367,535].

When we have analysed PLXNs expression in HDS and LDS cells, we have found that PLXND1 and PLXNA2 are up-regulated in LDS BrCa cells, while PLXNA3 expression was down-regulated (**fig. 24**). Interestingly, PLXND1 is the most studied plexin and it has been described to act as a dependence receptor[446] that inhibits BrCa growth and dissemination in the absence of its ligand, the SEMA3E[375]. However, the role of PLXNA2 or PLXNA3 in cancer is still unclear. Moreover, although there are only few studies associating PLXNA2 expression with tumour progression, such as in neuroblastoma[536] or prostate cancer[443], we have also showed that PLXNA2 may be involved in regulating tumour cell proliferation due to its differential expression between proliferative and dormant-like BrCa cells (**fig. 24**). Interestingly, we have found it is up-regulated in head and neck DTCs derived cell lines as compared to parental cells (**fig. 25**), indicating PLXNA2 expression might also be associated to tumour cell dissemination. In agreement with this, a recent study has associated PLXNA2 with lung cancer metastasis where it was shown to be up-regulated in metastatic DTCs[484].

The initial characterization prompted us to consider PLXNA2 as a key protein in BrCa progression. Being up-regulated in the aggressive and low dormancy-score MDA-MB-231 cells (**fig. 24**), we have used them as the preliminary experimental model. First, we have analysed whether PLXNA2 expression could be modulated by factors present in the TME. Here, we have found that pro-proliferative signals such as TGFβ1 increase its expression (**fig. 41**) whereas quiescence inducer signals such as BMCM oppositely down-regulate it (**fig. 42**). Resulting in a contention, the regulation of PLXNA2 by TGFβ family has been previously observed. Some studies have shown that the TGFβ1-driven EMT process suppressed the activity of PLXNA2 and PLXND1 [537] while EMT induced PLXNA2 activation in other models[538]. Moreover, other TGFβ family members such as BMP2 increased PLXNA2 expression, which promoted non-canonical, AKT and p38α signalling pathways activation to induce osteoblasts differentiation[539].

Then, we have studied whether its inhibition using siRNAs modulated the tumorigenic properties of the cells. Interestingly, we have found that PLXNA2 inhibition induces MDA-MB-231 cells migration and invasion (**fig. 44**). In relation with this, PLXNA2 down-regulation in glioblastoma cells induced actin cytoskeleton reorganization[540], a critical step for inducing cell migration and invasion. Further analysis of cell cytoskeleton should be done in order to determine whether PLXNA2 in MDA-MB-231 cells might follow the same functional pattern as in glioblastoma cells. Conversely, many studies have described that PLXNA2 is required for the migration of neural cells[541] as well as tumour cells[443], where its inhibition down-regulated cells movement in 20-30% [443,538]. The EMT-promoter microRNA-27 triggers endothelial cells migration, required for angiogenesis and the subsequent cell dissemination, while decreasing PLXNA2 levels[537]. Hence, PLXN2 role in migration might be cell type dependent and it may block cell migration in MDA-MB-231 cells.

Our results also suggest that PLXNA2 might inhibit tumour-initiating capacity and cell stemness in MDA-MB-231 cells (**fig. 46**). There are no published studies demonstrating the role of PLXNA2 in regulating stem cell properties in tumour cells. However, the aberrant expression of SOX4, a recently identified cancer stemness promoter in colorectal[542] and gastric cancer[543], modulated the expression of SEMA3-PLXNs family members, including PLXNA2, inhibiting cell proliferation and tumour growth *in vivo*[544]. Hence, although we have not been able to test it yet, we propose that PLXNA2 might be regulated by SOX family proteins, such as SOX4 and SOX11, that have been associated with PLXNA2 regulation in limb bud development in the NS[545], suggesting SOX4-PLXNA2 crosstalk might occur not only in tumour cells but also in neural cells. Results obtained in PLXNA2-inhibited breast tumours where the expression of proliferation markers (ex. Ki67) is maintained while the expression of cell quiescence markers (ex. p21) is decreased (**fig. 48**) support the potential relevance of PLXNA2 in inhibiting breast tumorigenesis and it deserves further studies.

According to BrCa patients' database, PLXNA2 is up-regulated in ER-negative BrCa patients (**fig. 40C**), classified as the most aggressive BrCa subtype. In addition, PLXNA2 is commonly defined as a potential oncogene as it is up-regulated in some cancer types[442,443,540]. However, there is controversy about the exact role of this protein since PLXNA2 inhibition does not have functional effects in some tumour models[536,540]. Our results suggest that PLXNA2 inhibits tumour cell dissemination and tumour initiation in MDA-MB-231 cells and thus, it might be considered a metastasis suppressor gene candidate for some BrCa subtypes (**fig. 87**).

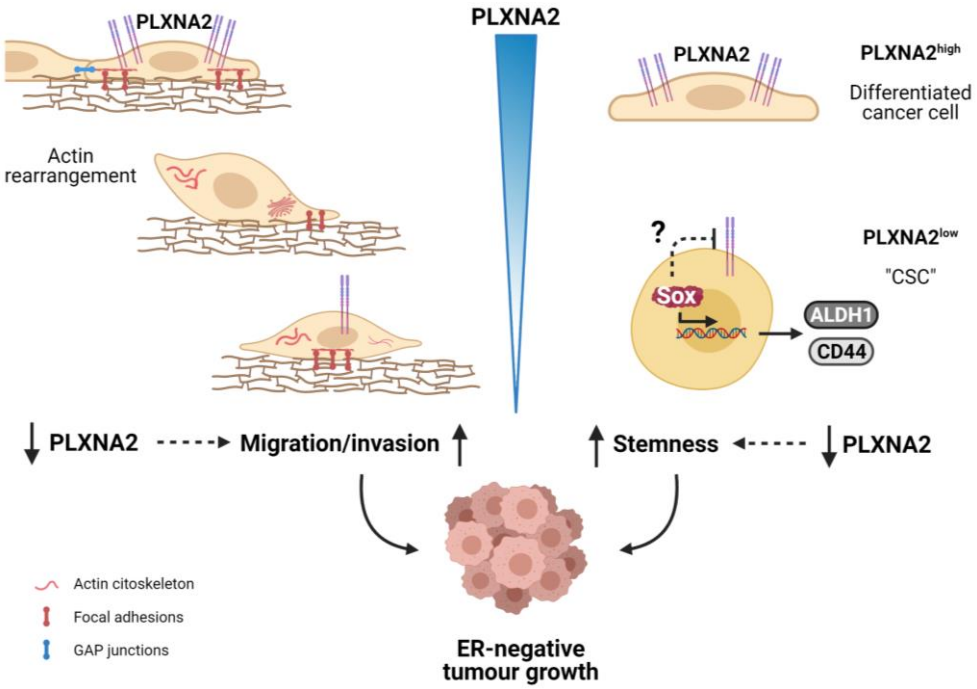

Figure 87. PLXNA2 down-regulation might promote ER-negative breast tumour growth by inducing cells migration and invasion while enhancing stemness. PLXNA2 inhibits MDA-MB-231 tumour growth by reducing cell migration and invasion (left panel). According to literature, this could be promoted by actin cytoskeleton reorganization when PLXNA2 expression is down-regulated[540]. We also observe an increased stem cell capacity in PLXNA2-inhibited cells (right panel), associating PLXNA2 with tumour initiation. PLXNA2^{high} cells would be more differentiated whereas PLXNA2^{low} cells would be CSC-like. SOX family members could be negatively regulating PLXNA2 expression while activating stem-cell markers expression[544].

5.3. PLXNA3 expression is regulated by oestrogens and it might be inducing dormancy in ER-positive breast tumours

PLXNA3 is an important regulator of cell migration and survival of neural cells in response to SEMA3s[546–548]. Despite its relevance in the NS, almost nothing is known about the role of PLXNA3 in tumorigenesis. In accordance to published data where PLXNA3 expression is higher in normal endometrial and ovarian healthy tissue compared to tumour samples[444,491], we have found that PLXNA3 is up-regulated in less aggressive BrCa and HNSCC cell lines (**fig. 24, 25**). Our results emphasize the potential role of PLXNA3 in promoting DTCs dormant phenotype since it is differentially up-regulated in dormant-like cells (**fig. 24, 25**), suggesting it could contribute to cell quiescence.

The higher expression of PLXNA3 in ZR-75-1 cells, classified as HDS cells (**fig. 24**), leads us to believe that it could be involved in cell quiescence. Moreover, our data suggest that PLXNA3 could be inhibiting luminal A BrCa subtype cell proliferation and tumour growth *in vivo*, by inducing cell quiescence based on the smaller PTs volume together with the up-regulation of p21 (**fig. 50**). One of the main distinctive features of the luminal BrCa subtypes is the ER expression and the delayed relapses in ER-positive BrCa patients[254]. Besides, 50% of patients recur after adjuvant anti-oestrogen therapy or menopause[254]. Losing the ER expression also seems to be a molecular differentiation process in dormant metastatic BrCa implying worst prognosis[549]. The ER status affects the time to distant recurrence and thus ER might be somehow regulating DTCs quiescence. Interestingly, our analyses of public databases have revealed that PLXNA3 is over-expressed in ER-positive tumours (**fig. 40A**) and its expression correlates

with survival in ER-positive BrCa patients, which show higher OS when PLXNA3 levels are up-regulated (**fig. 40B**). This has led us to believe that PLXNA3 expression might be regulated by oestrogens. Accordingly, we have found that PLXNA3 expression is up-regulated when treating with oestradiol whereas its expression is down-regulated when the cells are treated with the ER inhibitor tamoxifen (**fig. 51**). Interestingly, in agreement with our results, PLXNA3 expression has been previously associated with oestrogens in ovarian cancer[491]. For the moment, we do not know the mechanisms by which oestrogens might regulate PLXNA3. Nevertheless, analyses of PLXNA3 promoter show that there are response elements for oestrogen receptor (data not shown), suggesting that PLXNA3 expression could be transcriptionally modulated by oestrogens. More studies are still needed to clearly analyse the mechanisms behind PLXNA3 regulation by oestrogen signalling.

There is an urgent need to better understand the pathways and mechanisms contributing to tumour dormancy and metastasis. More studies are needed to correctly describe the role of PLXNA3 to make it a targetable protein, but our preliminary results suggest that ER-related dormancy could be partially regulated by PLXNA3. Hence, endorsed by future experiments, PLXNA3 might be described as a good prognosis marker in luminal A BrCa subtypes.

In summary, our results suggest that PLXNA3 can act as a tumour suppressor in ER-positive BrCa subtypes and that its expression is up-regulated by oestrogen signalling (**fig. 88**).

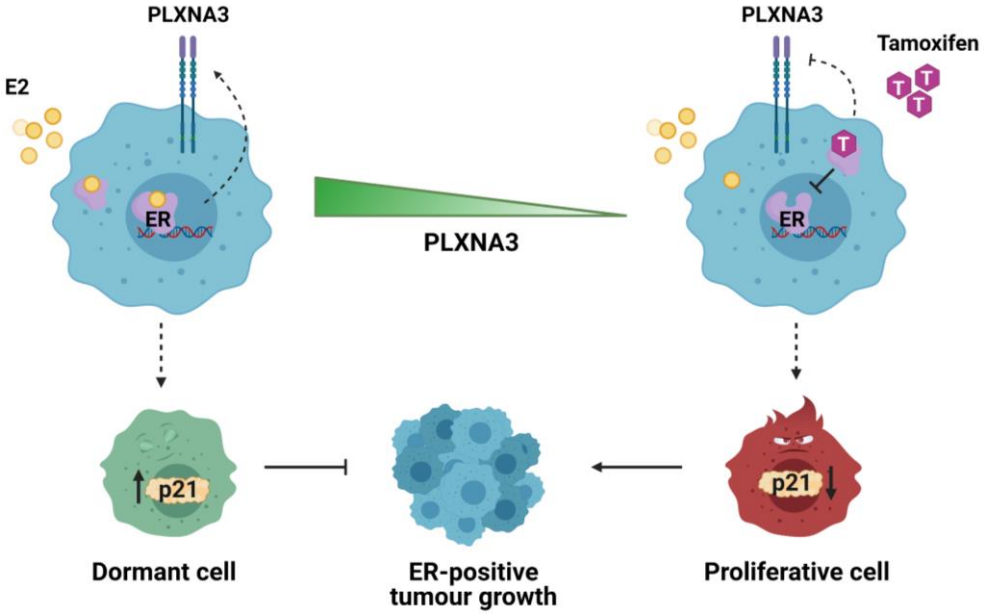

Figure 88. Oestrogens signalling pathway up-regulates PLXNA3 expression, whose down-regulation triggers ER-positive BrCa growth. PLXNA3 might inhibit ER-positive breast tumour growth *in vivo*, which could be implicated in longer dormancy periods of these tumour subtypes. Oestrogen (E2) up-regulates PLXNA3 protein levels whereas tamoxifen (T) down-regulates it while inhibiting the ER. This suggests that oestrogen signalling pathway might be involved in PLXNA3 up-regulation in dormant-like BrCa cells and unveils a potential adverse effect of tamoxifen treatment, inducing proliferative phenotype of ER-positive BrCa cells.

5.4. NRP2 enhances tumour growth and promotes lung DTCs proliferation triggering lung metastases development

NRPs are essential cell surface co-receptors that act in multiple cellular and molecular systems. Functional studies have revealed the pleiotropic functions regulated by NRPs within biological processes including cardiovascular, neuronal, immune and tumorigenic functions[349,389]. Widely described in NS development and physiological angiogenesis, NRPs act in multiple steps of the tumour formation process[349,350]. Both NRP1 and NRP2 are aberrantly expressed in tumour cells inducing malignant cell properties such as cell proliferation, migration and invasion[396,397,400,405].

Our data corroborate higher NRPs expression in more aggressive BrCa and HNSCC cell lines, both at mRNA and protein levels (**fig. 22, 23**). Moreover, when comparing their expression according to the dormancy-like phenotype, we observe that NRP2 is down-regulated in HDS BrCa cells and dormant HEp3 cells (**fig. 22, 23**). Our results go in accordance with the well-demonstrated malignant functions of NRPs in different tumour types[405,416,418,550]. Nevertheless, very little is known regarding NRPs role in DTCs regulation in the metastatic niche. NRP2 is a co-receptor for several growth factors, such as VEGF-C regulating lymphangiogenesis[396,405] and TGFβ regulating cell migration and proliferation[412,416,551], but it can also be associated to integrins acting as a co-receptor for ECM components, modulating cell cytoskeleton and inducing cell movement[376,397,410]. Together with PLXNs, NRPs transduce SEMA3s signal modulating axonal guidance in the NS[361,365] and regulating several tumour properties, which depending on the SEMA3 ligand, tumour type and/or microenvironment could be pro- or anti-tumoral[398,422,510].

NRPs are aberrantly expressed in tumour tissues in comparison with healthy epithelial tissues highlighting their potential role as oncogenic proteins[349,389]. Previous results from our group have shown that NRP2 is over-expressed in basal-like BrCa subtype and its expression correlated with worse prognosis[458]. Moreover, our analysis of public databases shows that high expression of NRP2 correlates with lower DMFS in BrCa patients (**fig. 52A**). In addition, in collaboration with Sant Pau Hospital, we have analysed NRP2 mRNA levels in PT biopsies from HNSCC patients and correlated with DMFS. Our results show that those patients with high NRP2 expression have lower DMFS (**fig. 52B**). Altogether, patients' data underline the malignant role of NRP2 in BrCa and HNSCC, since NRP2 higher expression in metastases negatively correlates with patients' survival (**fig. 52**).

5.4.1. NRP2 induces proliferation and inhibits quiescence in cancer cells, promoting tumour growth

Our results suggest that NRP2 promotes cell proliferation. Transient NRP2 inhibition or blocking NRP2 activity show no effect on cell proliferation *in vitro* (**fig. 53**) and no clear differences in tumour size *in vivo* (**fig. 64-66**). The latter might be explained by the masking effect of non-inhibited cells, where NRP2 expression would induce cell proliferation reducing the anti-proliferative effect of NRP2 inhibition in down-regulated cells. Hence, in a pull of inhibited and non-inhibited cells, NRP2 gives tumour cells a proliferative advantage and thus, fosters PT growth. Nevertheless, when complete deletion of NRP2 using CRISPR-Cas9 was performed, we observe a significative reduction in the proliferation rate of $NRP2^{KO}$ cells *in vitro* as compare to the wild-type cells (fig. **56**). Our data also reveal a clear cell proliferation inhibition *in vivo* (**fig. 68**), where NTC tumours had to be surgically removed 2 weeks after the inoculation whereas $NRP2^{KO}$ tumours were surgically removed 6 weeks after inoculation. Moreover, PTs size was evidently bigger in NTC tumours (**fig. 68C**) despite the shorter growing time, emphasizing the correlation between high proliferation rate and active NRP2. Hence,

our results indicate that NRP2 promotes proliferation and tumour growth. As previously mentioned, NRP2 has been described to play a key role in tumour growth, regulating several tumorigenic processes such as cell proliferation[389,397]. High levels of NRP2 have been associated with more proliferative breast[552], lung[487], melanoma[550], colorectal[412], hepatic[416] and head and neck[553] tumours, which goes in agreement with our results. The mechanisms by which NRP2 induces cell proliferation are not well understood and in fact, some models have unaffected cell proliferation when modulating NRP2 expression *in vitro*[498]. Nevertheless, in the vast majority of the studies NRP2 inhibition implies a reduction in tumour growth *in vivo*.

Cell proliferation depends on cell cycle progression, which is tightly controlled to ensure complete and precise DNA replication and cell division. Therefore, the one month delay in $NRP2^{KO}$ tumours growth as compared to NTC tumours could be due to cell cycle arrest, since we have shown that MDA-MB-231 $NRP2^{KO}$ cells were arrested in G2/M while T-HEp3 $NRP2^{KO}$ cells were arrested in G1 (**fig. 55**). These results denote that NRP2 promotes proliferation in BrCa and HNSCC by allowing cells to overcome cell cycle checkpoints. In some tumours, NRP2 might regulate the G0/G1 checkpoint (restriction checkpoint) as it does in T-HEp3 cells. The cell cycle restriction checkpoint is largely controlled by the Rb/E2F signalling pathway, which impedes cell cycle progression in front of adverse situations (ex. DNA damage, lack of nutrients…)[554]. The phosphorylation and inactivation of Rb protein was shown to be driven by keratinocyte growth factor in adipose-derived stem cells, with NRP1 as a co-receptor mediating its action[555]. Moreover, while NRP1 promoter contains a transcriptional activator E2F1 binding site[556], Rb/E2F pathway was shown to negatively regulate NRP1 expression under hypoxic circumstances by the suppressor E2F7 [557]. Due to the lack of information about NRP2 role in regulating cell cycle and the homology between NRP1 and NRP2, we propose that NRP2 might also be negatively regulated by Rb/E2F pathway. However, we have not tested this hypothesis yet. Therefore, upon damage induction, Rb/E2F could inhibit NRP2 expression and thus block the oncogenic benefits it provides, such as an uncontrolled cell cycle. In other tumour types such as BrCa, NRP2 might induce cell proliferation by allowing dividing cells to go beyond G2 checkpoint. NRP2-mediated cell cycle activation has been previously described in cervical cancer[558], where G2/M cell cycle arrest was induced in NRP2-inhibited cells. Those cells with NRP2 expression inhibited, besides being arrested in G2/M phase, they had higher expression of the dormancy marker p16 [558]. Therefore, the observed stop in cell proliferation after NRP2 inhibition might be induced by the activation of CDK inhibitors. To study the mechanisms by which NRP2 inhibition could induce cell cycle arrest in our models, we have analysed NRP2 regulation of CDKs inhibitors, such as p21 or p27 that negatively regulate CDKs activity in the cell cycle checkpoints[554]. Our results unveil a novel function of NRP2 controlling the expression of p27 (**fig. 89**), which represents one of the CDK inhibitors regulating cell cycle[494,495]. The results show that p27 is directly inhibited by NRP2, whose blocking or inhibition (either transient or permanent) clearly up-regulates p27 levels *in vitro* (**fig. 57**) and *in vivo* (**fig. 66, 68**). Therefore, we suggest that NRP2 inhibition induces cell cycle arrest through p27 up-regulation (**fig. 89**).

In agreement with our data, in gastric cancer, NRP1 depletion mediated cell proliferation inhibition by Ki67 down-regulation, together with p27 levels up-regulation and cell cycle arrest in the G1/S phase[559], suggesting NRPs modulate tumour phenotype stimulating proliferative properties. However, the precise mechanisms involved in NRP2-mediated p27 inhibition need to be characterized in detail. p27 can be regulated by ERK or AKT pathways[494]. Nevertheless, our preliminary results suggest that NRP2 inhibition of p27 is independent of both AKT and ERK pathways (**fig. 58**). p27 function is regulated through phosphorylation that controls its binding to and inhibition of cyclin-Cdk complexes, its

localization and its ubiquitin-mediated proteolysis[494,495]. It is possible that NRP2 inhibits p27 either by accelerating its degradation or by affecting its localization. Future studies should be done to determine the localization of p27 when NRP2 is inhibited to decipher whether it might be acting as a tumour suppressor protein. Mutations in the *p27* gene in cancer are rare, so p27 role usually depends on its intracellular localization. Nuclear p27 negatively regulates cell proliferation whereas when mislocated in the cytoplasm, p27 might exert pro-tumorigenic functions[494]. As a consequence, the localization of p27 should be analysed in order to elucidate the role of the increased levels of p27 in our NRP2-depleted cells. However, although we have not analysed it in detailed, we have not observed a change in the localization of p27 in the staining of the tumours with NRP2 blocking or inhibition. Nevertheless, the switch in PTs phenotype from proliferative to quiescence together with the reduction in NRP2-depleted tumours volume suggest that p27 may be inducing cell cycle arrest in our model.

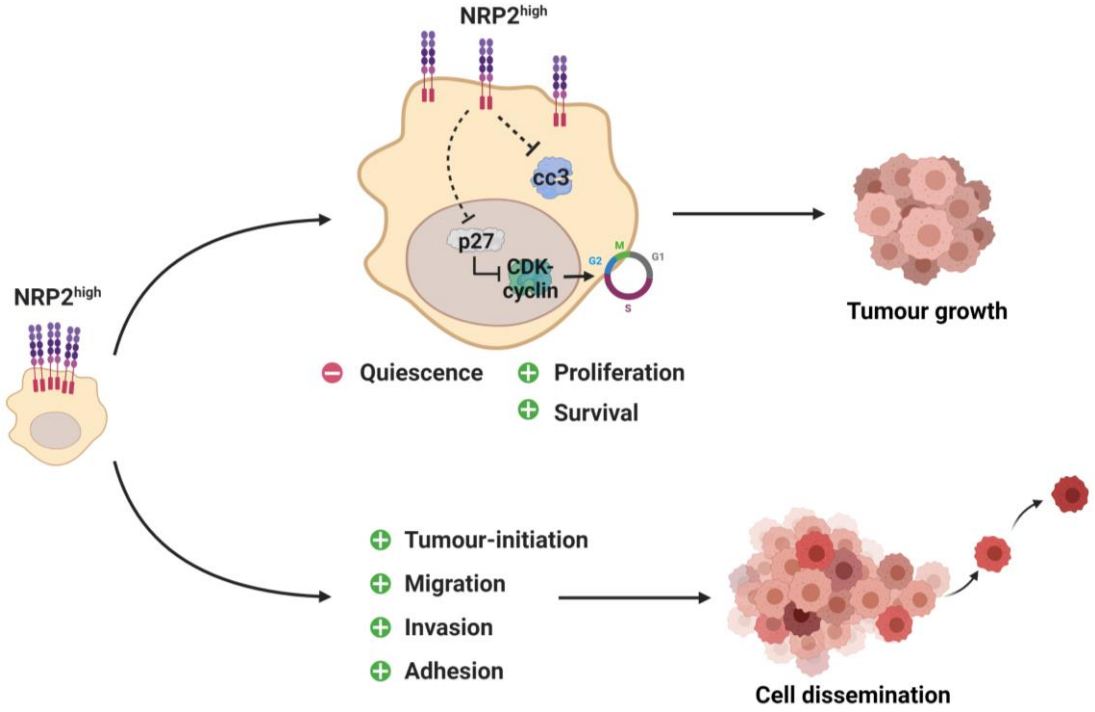

Figure 89. NRP2 induces tumour growth and cell dissemination. Upper diagram, NRP2 regulates cell cycle progression by inhibiting CDK inhibitors expression (ex. p27). This will impede quiescence entrance and thus will activate cell proliferation in NRP2^{high} tumour cells. Moreover, NRP2 somehow inhibits cleaved caspase 3 (cc3), promoting cell survival. Altogether, promoting cell proliferation and survival, NRP2^{high} cells will promote tumour growth. Lower diagram, NRP2 induces cell migration, invasion and adhesion to the ECM, which will in turn foster cell dissemination and tumour progression, all enabling metastasis development.

5.4.2. NRP2 regulates cell survival

According to the results derived from the *in vivo* assays, the observed increase of cell proliferation prompted tumour growth. Nevertheless, our results suggest that besides promoting proliferation, NRP2 might also be controlling cell survival, both contributing to tumour progression. In fact, we observe that NRP2 inhibition activates cell apoptosis by increasing cleaved caspase 3 levels in chicken and mouse *in vivo* models (**fig. 64C, 65C, 66C, 68E**). Interestingly, in agreement with our results, recent studies have shown that NRP2 targeting by microRNAs regulates cell proliferation by inducing cell quiescence and apoptosis[496,558,560], more likely inhibiting the activity of viral E7 oncogene[558,560]. Moreover, Wnt/β-Catenin signalling pathway has also been targeted by microRNAs decreasing cell

proliferation in a NRP2-dependent manner[561]. NRPs expression is positively regulated by Wnt/β-Catenin pathway causing tumour growth and metastases development *in vivo*[560,562,563]. Furthermore, there might be a feedback loop as NRP2 down-regulation reduces β-Catenin levels in gastric cancer cells[561]. In agreement, β-Catenin is degraded by cleaved, and thus active, caspase 3 during apoptosis[564]. Consequently, NRP2 might be promoting cell survival by stabilizing β-Catenin levels, inhibiting its proteasomal degradation and favouring β-Catenin translocation to the nucleus where it will activate oncogenic gene transcription. Hence, it would be interesting to test whether this positive NRP2/β-Catenin crosstalk may contribute to tumour cells survival in our models.

5.4.3. NRP2 induces tumour initiation

Our results also indicate that NRP2 promotes tumour-initiating capacity *in vitro*, since we observe a lower number of cell foci in NRP2-deleted MDA-MB-231 and T-HEp3 cells in anchorage-dependent growth assays (**fig. 59**). Furthermore, our *in vivo* assays show a delay of four weeks in PT growth between NTC and $NRP2^{KO}$ T-HEp3 cells (**fig. 68**), suggesting that NRP2 deletion inhibits tumour initiation ability (**fig. 89**). This indicates that NRP2-deleted cells might have a repressed stem cell phenotype, with lower tumourigenic properties, and hypothetically an enhanced differentiated phenotype. In agreement with our results, several studies have revealed the up-regulation of NRP2 in breast[565], brain[566] and prostate CSCs[502] as well as in HNSCC tumour-initiating cells[567]. Moreover, NRP1 targeting resulted in decreased self-renewal activity in medulloblastoma cells, more likely by inhibiting PI3K/AKT and ERK signalling pathways[566].

The mechanisms by which NRP2 signalling promotes tumour initiation are poorly understood and we have not explored them in depth. Given that NRPs lack active intracellular domains and act as co-receptors, it is assumed that it will require a functional receptor for stemness stimulation. VEGFR/NRP1 complexes have been described as essential for the survival of glioma CSCs[568] whereas VEGF/NRP2 have been described to regulate Bmi-1 expression[502], a transcription factor that controls the expression of many stem genes[569]. Bmi-1 was also activated when NRP2 had α6β1-integrin as a working partner promoting mammosphere formation and thus, tumour initiation in TNBC[565]. Here, the hedgehog pathway effector and stemness activator, GLI1, induced Bmi-1 expression when activated by VEGF/NRP2 and α6β1-integrin signalling, altogether contributing to tumour-initiation capacity[565]. VEGF/NRP2 and integrins connection has also been related with the transcription factor TAZ, promoting CSC-like behaviour and a more mesenchymal phenotype in BrCa cells[409].

Besides tumour initiation, CSCs are also associated to therapy resistance as well as to tumour recurrence, contributing to metastases[20,570]. Therefore, NRP2 expression regulation by stem programs and its implication in providing cells with higher tumour initiation abilities reinforce our hypothesis that NRP2 is an oncogenic protein implicated in tumour growth and metastases development.

5.4.4. NRP2 promotes cell adhesion, migration and invasion

The metastatic cascade is a multi-step process where a tumour cell might pass through all the stages to become a successful metastatic cell. The very first step is characterized by the invasion of the local stroma in the PT location[208,229]. Of particular significance during migration and invasion is the EMT process, which modulates cell plasticity acquiring a more mesenchymal phenotype and providing cells with more malignant features that include increased cell migration and invasiveness[490,571]. Using CRISPR-Cas9 as a NRP2 modulation strategy, we have found that NRP2-deletion in MDA-MB-231 cells decreases cell migration (**fig. 62C**) whereas no changes are observed in T-HEp3 cells that have low

migration capacity *in vitro* (**fig. 62D**). The association of NRP2 with cell migration and invasion has been broadly studied during the last years. NRP2 increasing levels promote cell movement[416,499,552,572], mainly modulating integrins expression[376,499,552] and cytoskeletal rearrangement[572]. Cell migration is promoted by the EMT through many transcription factors, such as Twist1, Snail and Zeb1 when they are activated by different signalling pathways, such as TGFβ pathway[490,571]. Related to this, Wittmann *et al*. (2015) demonstrated that the higher migration and invasion properties in hepatocellular cancer cells derived from the TGFβ1 treatment was partially dependent of NRP2 expression. NRP2-inhibited cells had less motility, which was accentuated when the TGFβ canonical pathway was inhibited[416]. Recently it has been shown that constitutive expression and activation of mutated p53 induced cell migration, proliferation and metastasis by up-regulating NRP2 expression in lung cancer[573]. Interestingly, both T-HEp3 and MDA-MB-231 cells have mutant p53, that might be regulating NRP2 to promote migration and invasion. Further analyses might be required to study effects on cell morphology and cytoskeletal organization after NRP2 deletion in our models.

During the EMT process, the adhesion molecules expressed by the cells are modified to adopt a migratory and invasive phenotype in response to pleiotropic signals. The expression of these molecules is altered in non-homeostatic conditions, being associated with tumour progression and metastasis[238,574]. Adhesion to the ECM is given by focal adhesions where integrins are the predominant receptors that transduce the ECM-derived signal mainly by activating FAK and Src[575,576]. Focal adhesions are crucial for cell adhesion although they are also important in cell migration where stable focal adhesions will be formed in the leading edge of the cell while they will be reduced in the rear[575]. Interestingly, we have found that NRP2-deletion significatively reduced the number of cells attached to a non-coated surface (**fig. 62A, B**), suggesting that NRP2 might increase cell adhesion (**fig. 89**). Based on published results, this could be explained by a down-regulation of focal adhesions.

We have not studied in depth the mechanisms by which NRP2 induces migration and inhibits cell adhesion (**fig. 89**). Nevertheless, a recent study has demonstrated that a small-molecule FAK inhibitor decreased cell migration in endothelial and hepatoblastoma cells[577]. Moreover, there was decreased expression of integrins and a reduction in the number of focal adhesions, which induced F-actin disorganization, cell protrusions rearrangement and the subsequent cell detachment[577]. Furthermore, it has been shown that, either through VEGFR or through integrins, NRP2 up-regulates GLI1 which in turn induces FAK activation by PI3K/AKT and MAPK signalling pathway[409,565,578], all inducing cell migration by interacting with the ECM through focal adhesions to allow cell movement. Therefore, in our models, NRP2 deletion could modulate integrin-derived focal adhesions formation, down-regulating FAK activation and reducing cell adhesions while inhibiting cell migration at the same time. Thus, this will suggest that NRP2 might be promoting cell migration by activating integrin signalling and increasing focal adhesions assembly to be able to move over an ECM matrix.

5.4.5. NRP2 triggers lung DTCs proliferation inducing lung metastases development *in vivo*

Our previous results suggest that NRP2 induces tumour growth by facilitating cell proliferation, survival and stemness. Furthermore, we have found that NRP2 increases cell migration and adhesion suggesting it can have a role in promoting tumour cells dissemination to secondary organs.

To test the role of NRP2 in DTCs biology and metastasis we have first used a cell line that was derived from lung DTCs and has been shown to mimic DTCs behaviour in the lung microenvironment

(Lu-HEp3)[266]. Interestingly, NRP2 is highly expressed in Lu-HEp3 cells (**fig. 23**). When inoculated *in vivo* and treated with the NRP2 blocking antibody to prevent ligand binding to NRP2, we have found less proliferative Lu-HEp3 tumours with higher number of apoptotic cells (**fig. 69**). Hence, our results suggest that NRP2 is necessary to facilitate the proliferation and survival of lung DTCs derived cell lines.

Furthermore, we have shown for the first time that NRP2 is up-regulated in lung DTCs compared to pre-malignant lesions and PT cells (**fig. 70B**). In addition, our results suggest that NRP2 might be essential for lung metastases development since overt lung metastases increase NRP2 expression, even in metastases deriving from NRP2 low expressing PTs (**fig. 70C, 71**). Not only that, but we have also demonstrated that NRP2 has a key role in regulating lung DTCs phenotype, since the percentage of dormant lung DTCs increases in CAM *in vivo* assays when NRP2 is inhibited (**fig. 73**), suggesting NRP2 could be regulating DTCs switch between dormancy and proliferation. The novel function of NRP2 inhibiting p27 expression and thus DTCs quiescence is accompanied by a lower number of lung metastatic lesions and smaller lung micrometastases in mice inoculated with $NRP2^{KO}$ (**fig. 74**). Moreover, single DTCs phenotype was switched towards a more dormant phenotype in $NRP2^{KO}$ T-HEp3 lung DTCs (**fig. 74D**). To corroborate that NRP2 regulates not only PT growth but also lung DTCs proliferation and lung metastases development, we have performed a tail vein *in vivo* mice model and showed that NRP2 deletion reduces proliferative lung metastases *in vivo* either in BrCa or in HNSCC models (**fig. 75, 76**). The number and size of proliferative lung metastatic lesions was clearly smaller in $NRP2^{KO}$ cells, suggesting an entrance in tumour dormancy. Moreover, the number of dormant lung DTCs increases in the lungs of the mice inoculated with $NRP2^{KO}$ cells. Therefore, NRP2 deletion triggers a switch from a proliferative to dormant lung DTCs phenotype, reducing lung metastases development (**fig. 75, 76**).

Altogether, these results underline how crucial NRP2 is for the regulation of the survival and maintenance of the proliferative phenotype of lung DTCs and thus, for lung metastases development (**fig. 90**). Our results are in agreement with recent papers that have demonstrated that NRP2 plays an specific and essential role in lung cancer invasion and metastasis[417,487,573], since the lung microenvironment was shown to up-regulate NRP2 but no NRP1 expression[487].

5.4.6. NRP2 expression is up-regulated in lung DTCs by lung fibroblasts and macrophages-derived TGFβ1

Our previous results suggest that NRP2 has a determinant role in lung metastases, inducing proliferation in lung DTCs and thus, lung metastases development and enlargement. Next, we have studied whether NRP2 could be regulated by factors present in the lung microenvironment. To our surprise, no differences have been observed in NRP2 levels after VEGF-C treatment (**fig. 77A**). VEGF-C is the main ligand of NRP2 and, together with VEGFR-3, induces lymph vessels development[396,405,499,579]. Moreover, NRP2 has been shown to be highly expressed in human cancers with high lymphangiogenesis and lymphatic metastasis[396]. Furthermore, it has been reported that NRP2 up-regulation by VEGF-C could enhance survival and migration of lymphatic endothelial cells[405,435] while its blocking reduced tumour lymphanagiogenesis and more importantly, tumour metastasis[405]. In tumour cells, VEGF-C/NRP2 binding is also associated with the functional regulation of tumour cells such as tumour initiation, cell migration, chemoresistance and metastasis[405,409,499,565,580]. Taking into account these evidences and although many studies demonstrate VEGF-C/NRP2 interaction, a recent study where VEGF-C/NRP2 axis promoted cell adhesion and migration showed no NRP2 increase after

VEGF-C treatment[499]. Hence, our data suggest that NRP2 up-regulation in the lung is independent of VEGF-C, at least in our models.

Several studies have revealed that NRPs can bind other growth factors such as TGFβ1, binding to both the latent and active forms of TGFβ1, promoting tumour growth and progression[412,413,415–417,487]. In agreement with these studies, our data show that NRP2 is activated after TGFβ1 treatment likely in a post-transcriptional manner (**fig. 77B, C**). Moreover, treatment with TGFβ1 increases the expression of the proliferation marker Ki67 as well as the number of bigger cell colonies in 3D cultures (**fig. 78**). TGFβ1 has a dual role in tumour progression, inhibiting tumour growth at early steps but favouring tumour progression and invasion at late stages[503,581]. In agreement with our results, it has been demonstrated that TGFβ1 up-regulates NRP2 promoting migration and invasion in BrCa[551]. Furthermore, TGFβ1 induces metastasis in lung cancer[417,487] and proliferation in dormant bone marrow DTCs[266]. Hence, our results indicate that TGFβ1-NRP2 axis might be a potential target for the progression of lung metastasis in breast and head and neck cancers (**fig. 90**).

Taking into account the effects of TGFβ1 treatment up-regulating NRP2 expression together with inducing cell proliferation and growth, we would have expected that dormancy-inducing signals would have opposite effects down-regulating NRP2 levels. Nothing further from the truth, the BMCM treatment, described as pro-quiescence factor[306,466,467], barely alters NRP2 protein levels (**fig. 79A**). On the other hand, another TGFβ family member studied, TGFβ2, which oppositely to TGFβ1 regulates anti-proliferative DTCs functions[266,291,292], shows minor changes regarding NRP2 expression and cell proliferation (**fig. 79B-E**).

Mechanistically, how NRP2 expression is increased by TGFβ1 remains controversial. Some studies present SMADs-dependent translational regulation of NRP2, where SMAD3 increases NRP2 expression by binding to the 5' untraslated region[582]. As the central mediator of TGFβ signalling, genetic or chemical inhibition of SMAD4 also decreased NRP2 levels impairing tumour cell migration[416]. Conversely, NRP2 up-regulation has also been described to be a SMAD independent process where ERK and AKT signalling pathways could be involved[487]. Therefore, to determine whether NRP2 is regulated by the canonical or non-canonical TGFβ pathway in our models, we have used two different TGFβRI inhibitors (SB431542 and GNB) which would be informative of canonical pathway implication by targeting SMAD2/3 [472]. Type I TGFβ receptor inhibition partially decreases the TGFβ1-driven NRP2 up-regulation in proliferative BrCa and HNSCC cells (**fig. 80**), describing the TGFβ canonical pathway as one of the main regulators of the NRP2 expression in our models.

Interestingly, these results are also validated in HNSCC derived lung DTCs (Lu-HEp3) where the notorious NRP2 up-regulation after TGFβ1 treatment is markedly reduced when inhibiting SMADs proteins activation (**fig. 80**). We have also confirmed that TGFβ1 is one of the lung factors involved in NRP2 up-regulation in lung DTCs since NRP2 induction by lung CM is partially reverted when TGFβ1 is depleted from the lung CM (**fig. 81**). Lung-derived TGFβ1 increases NRP2 protein levels through activation of its canonical signalling pathway, not only in LDS and proliferative cells, but also in HDS and dormant cells (**fig. 82**), suggesting TGFβ1 can reprogram $NRP2^{low}$ cells into $NRP2^{high}$ cells independently of the basal NRP2 levels. Consequently, these results verify that TGFβ1 canonical signalling pathway up-regulates NRP2 expression in proliferative cell lines and propose TGFβ1 as a candidate lung factor regulating NRP2 expression in lung DTCs in the lung microenvironment (**fig. 90**).

However, the source of the TGFβ1 present in the lung still remains a mystery. Macrophages are the most numerous immune-cells present in the lung environment under homoeostatic conditions as well as in pathological conditions[583]. The infiltration of macrophages correlates with poor patients' survival[584,585]. They are easily influenced and rapidly adapt to the changing environment promoting tumour growth and metastasis[583]. TAMs may derive from circulatory monocytes or from resident tissue macrophages. Be that as it may, TAMs contribute to tumour development in lungs where resident TAMs might support cell growth while monocytes-derived macrophages may participate in cell spreading in the lung[586]. Besides being influenced by the stroma, where tumour cells secreted IL-4 and IL-13 trigger their M2 differentiation[172,587], they are also able to modulate their surrounding stroma by secreting several proteases, cytokines and growth factors such as MMPs and IL-β1 [588], that promote cell proliferation and metastases. We have shown that in TAM-tumour cell crosstalk in the lung microenvironment, TGFβ1 could play an essential role. We have corroborated that macrophages synthetized and released TGFβ1 to the media (**fig. 84**). Mimicking results obtained with TGFβ1 and lung CM treatments, NRP2 expression is up-regulated after macrophage CM treatment. Moreover, NRP2 induction is partially reverted after SB431542 treatment, to inhibit type I TGFβ receptor (**fig. 84A**). In agreement with published data and our obtained results, where macrophages are able to secrete TGFβ1, we propose that macrophage-derived TGFβ1 could increase DTCs NRP2 expression prompting lung DTCs proliferation and thus, lung metastases (**fig. 90**). Interestingly, it has been shown that inhibition or ablation of lung TAMs reduced BrCa metastases burden[589–592], even when metastases had already been established[591], confirming the requirement of macrophages for lung metastatic seeding and growth. Moreover, α4-integrin expressing macrophages have been shown to be involved in lung DTCs survival by activating a PI3K/AKT-dependent survival pathway when binding to VCAM-1-positive DTCs[179].

Our results suggest that TAMs could regulate lung DTCs shift to a proliferative phenotype through secretion of TGFβ1 that will promote NRP2 overexpression in lung DTCs (**fig. 90**). However, while TAMs have been suggested to promote tumour progression and metastases through a variety of mechanisms, recent reports suggest they can also have a functional role in promoting tumour dormancy. For instance, TAMs have been shown to promote cancer recurrence by activation of local inflammatory signalling. Using the immunosuppressive corticosteroid dexamethasone CD11c+ pro-inflammatory macrophages were ablated, which led to a reduction of IL-6 and a delay in BrCa recurrence[593]. However, a recent study has demonstrated the protective role of TAMs when binding to BrCa DTCs in the bone marrow, stimulating cell quiescence[594]. Macrophages-DTCs association also induced cell chemoresistance, making them non-targetable. As macrophage phenotype is plastic, they proposed transforming the M2/TAM phenotype into a M1 phenotype, which reversed dormant BrCa cells into proliferative cells and thus responsive to current BrCa therapies such as carboplatin[594]. Not only macrophages present in the metastatic niche could regulate DTCs dormancy[594–596], but also macrophages within the PT have been shown to induce a pro-dormant phenotype in those cells that are prone to disseminate[597]. Tumour cells and macrophages contact in PTs up-regulated Mena protein, which is required for early dissemination as well as for DTCs survival in the lung parenchyma. Moreover, PT macrophages secreted factors induced the expression of the dormancy marker NR2F1 in CTCs, but more notoriously in lung DTCs[597]. Interestingly, recruitment of TAMs promoting tumour progression has been recently associated to NRPs expression. NRP1-SEMA3A signalling pathway is required for TAM attraction[421,598,599], inducing M2 macrophage differentiation and prompting tumour malignant properties[598]. Altogether, these evidence establish macrophages as regulators of the biology

of DTCs, stemness and cell survival in secondary organs where NRPs might have a determinant role in their recruitment and activation.

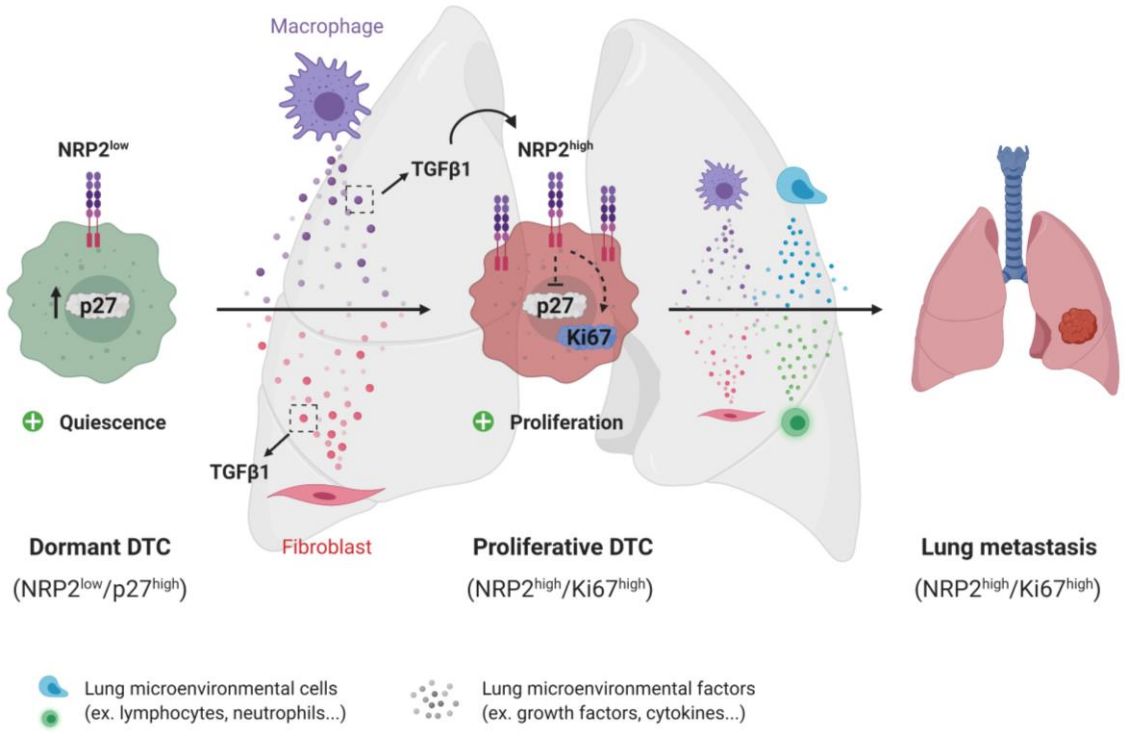

Figure 90. Lung fibroblasts and macrophages-derived TGFβ1 drives NRP2 up-regulation promoting lung DTCs proliferation, in all triggering lung metastases development. Lung stromal cells secreted factors, such as lung fibroblasts and macrophages-secreted TGFβ1, up-regulates NRP2 overexpression in lung DTCs. NRP2 increase will inhibit the cell cycle inhibitor p27 and activate cell proliferation marker, Ki67. Altogether, NRP2 expression will promote lung DTCs quiescence exit and proliferation, hence, favouring lung metastases development.

Tumour-associated fibroblasts are also prominent players in the TME regulating multiple biological and pathological functions. However, their role in the metastatic niche and specifically in regulating tumour dormancy is largely unknown. Few evidence have shown a direct correlation between activated fibroblasts and tumour dormancy, although it might be mainly derived from the secreted factors and ECM remodelling[600]. Stiffness of tumour stroma is mainly regulated by TAFs and it is associated with cell dormancy. The composition of the stroma determines the fate of DTCs, where type I collagen and fibronectin induced the proliferation of dormant BrCa DTCs[283,300], developing proliferative lung metastatic lesions[300]. TAFs produce a wide variety of growth factors related with tumourigenesis, metastases and tumour dormancy. Fibroblasts-derived IL-8 triggered dormant BrCa cells re-awakening and proliferation in the liver and increased their survival as well[601]. Moreover, ILs have also been associated with chemoresistance[602], another prominent feature of quiescent cells. Of all synthetized growth factors, the most abundant factor secreted by activated fibroblasts is TGFβ1 [600]. In agreement with this, we have found that both CCD19 and CF5 lung fibroblasts synthetized and secreted TGFβ1 to the media (**fig. 83**). We have also observed that TGFβ1 is up-regulated in old mice lungs as compared to young mice lungs, which also show higher fibroblasts marker expression indicating old lungs are largely fibrotic (**fig. 85A, B**). Pulmonary fibrosis is an age-related lung disease of unknown cause that constitutes a major cause of morbidity and mortality[505–507]. It is characterized

by an excess of activated fibroblasts which secrete ECM components such as type I collagen and a wide variety of growth factors[505,506]. TGFβ1 is one of the main growth factors involved in lung fibrosis development[506] and it was shown to promote dormant BrCa DTCs re-awakening in TGFβ1-driven type I collagen accumulative lung fibrosis[300]. The proliferation of dormant DTCs was shown to be dependent on β1-integrin expression[300], which regulates the switch from a dormant state to active proliferation and metastasis through the uPA/uPAR complex[311,312]. We have shown that old and fibrotic lungs-derived TGFβ1 up-regulates NRP2 expression (**fig. 85C**), suggesting NRP2 might have a key role in cell quiescence inhibition and proliferation activation in fibrotic lungs in response to fibroblasts-derived TGFβ1 (**fig. 90**). In TGFβ1-mediated fibrosis the canonical Wnt pathway is activated, which in turn stimulates fibroblasts differentiation and activation[603]. Blocking canonical Wnt signalling down-regulated NRP2 expression[562] and resulted in a suppression of tumour growth and lung metastasis[604,605]. With all, our results suggest a new mechanism for TAFs regulation of DTCs escape from dormancy and promotion of lung metastasis through TGFβ1 mediated upregulation of NRP2 (**fig. 90**).

Taking all the results together, we have demonstrated for the first time that NRP2 is up-regulated in lung DTCs, contributing to enhance cell survival and the proliferative phenotype of these cells and thus the development of proliferative lung metastases. Besides the effects on PTs, the enhanced migratory and proliferative capacity of NRP2 expressing cells, accompanied by the stem-cell features activation, might facilitate lung metastases enlargement. Factors present in the tumour microenvironment modulate tumour cell behaviour and stromal lung fibroblasts and macrophages-secreted TGFβ1 induces NRP2 expression, which might contribute to cell quiescence escape highlighting the crosstalk between tumour cells and the microenvironment in tumour dormancy. The mechanisms by which NRP2 prompts quiescence exit and cell proliferation need to be further studied. Nevertheless, the novel function of NRP2 as a negative regulator of p27 expression leads us to think that NRP2 might be hampering cell cycle arrest. This represents a new mechanism for NRP2 expressing DTCs to concertedly escape cell cycle arrest, promoting cell proliferation and metastasis.

There are mainly three strategies to target tumour cell dormancy. The sleeping strategy which plans to maintain the dormant state of DTCs in secondary organs as long as patients do not manifest clinical symptoms. Dormant DTCs awakening strategy that aims to activate dormant cells to increase their sensitivity towards chemotherapy, making them targetable and thus removing them preventing any future problems. And lastly, the killing strategy whose objective is to eliminate dormant tumour cells, which makes it the most appropriate strategy although being quite challenging to assume. All the above results present NRP2 as a metastatic target to prevent the activation of DTCs and the development of overt lung metastases in aggressive and highly proliferative BrCa and HNSCC tumours. To emphasize the metastatic role of NRP2, studies with patient samples show that patients with metastasis with high levels of NRP2 have lower DMFS (**fig. 52**). All these evidences make NRP2 a promising target molecule against metastatic diseases conferring NRP2 a relevant clinical value. All the multiple functions regulated by NRPs in cancer cells make NRPs a formidable point of vulnerability. In recent years, many strategies have been developed for targeting NRP2. NRP2 blocking antibodies[405], microRNAs[560,606], inhibitory soluble peptides[607] and antagonists[356], among others, have been used for tumour progression and metastasis inhibition *in vitro* and *in vivo*. While a monoclonal anti-NRP1 antibody was tested in a phase I clinical trial in patients with locally advanced or metastatic solid tumours (NCT00747734)[608], no NRP2 targeted clinical trials have been published in the literature yet.

However, the promising preclinical studies suggest that some of the described approaches may offer future encouraging potential anti-NRP2 therapeutics in cancer.

5.5. Concluding remarks

According to our work, it is evident that factors present in the TME regulate tumour growth, progression and metastasis development by influencing cell functions and phenotype. We have first seen that SEMA3F, as a soluble factor present in the microenvironment, is able to increase dormancy markers expression in PTs. Moreover, we have also observed a decreased in cell dissemination to secondary organs such as liver and lungs upon SEMA3F treatment. In addition to the lower number of DTCs, the regulation of dormancy markers by SEMA3F causes an increase in the percentage of dormant lung DTCs. As a result, we define SEMA3F as an anti-proliferative factor in BrCa and HNSCC, which make SEMA3F a good prognosis factor.

Afterwards, we have also seen how the expression of the main SEMA3s receptors, PLXNs, can be modulated by several factors present in the TME. On one hand, PLXNA2 inhibits cell migration and invasion as well as it might diminish the stemness capacity of tumour cells, in all hindering ER-negative breast tumour growth. On the other hand, PLXNA3 might be favouring higher dormancy periods of ER-positive breast tumours, inhibiting cell proliferation and tumour growth. PLXNA3 expression is positively regulated by oestrogen signalling pathway and since its expression correlates with higher OS in ER-positive patients, it could be proposed as a good prognosis factor in this BrCa subtype.

Finally, we have deeply focused on deciphering the role of NRP2 as a pro-metastatic protein, where we have demonstrated that it promotes lung metastases by inducing DTCs proliferation. We have first corroborated the pro-tumourigenic role of NRP2 in stimulating cell proliferation, survival, migration, invasion, adhesion and PT growth. Then, focusing on lung metastases development, we have associated high levels of NRP2 with higher number and bigger size of lung metastases as well as with more proliferative metastases *in vivo*, identifying NRP2 pathway as a novel mechanism of DTCs proliferation activation. This activation is mediated by lung stromal cells such as macrophages and fibroblasts, which through the secretion of cytokines and growth factors, such as TGFβ1, up-regulate NRP2 expression in lung DTCs. NRP2 activation, through p27 inhibition, promotes dormant DTCs swing to proliferative DTCs and hence, triggers lung metastases formation and proliferation. Therefore, we have identified a new mechanism for lung DTCs to escape dormancy regulated by lung stroma-DTCs crosstalk. This study demonstrates the importance of the tumour cells-microenvironment crosstalk in promoting tumour growth and metastases development. Furthermore, it reveals the potential clinical value of NRP2 against metastatic diseases upon which no effective treatments are currently designed.

Conclusions

1. LDS BrCa and proliferative HNSCC cell lines overexpress NRP1 and NRP2 while SEMA3F and PLXNA3 are up-regulated in HDS BrCa and dormant HNSCC cell lines. Additionally, PLXNA2 is highly expressed in LDS BrCa and HEp3 DTCs-derived cell lines.

2. SEMA3F expression is up-regulated in luminal breast tumour subtypes and lower grade patients' tumours, which makes SEMA3F a good prognosis factor in BrCa.

3. SEMA3F treatment induces dormancy markers expression (ex. p27, Dec2, TGFβR3) in BrCa and HNSCC proliferative cells and reduces *in vivo* cell dissemination to liver and lungs, increasing the percentage of dormant lung DTCs. Therefore, SEMA3F can be considered a potential dormancy-inducer.

4. PLXNA2 restrains BrCa cells migration and invasion as well as stem cell markers expression and inhibits ER-negative breast tumours growth. Therefore, PLXNA2 could be a potential tumour suppressor in ER-negative BrCa subtype.

5. PLXNA3 expression is differentially regulated by oestrogens and tamoxifen treatment and correlates with higher OS in ER-positive patients, being a potential tumour suppressor as it inhibits luminal A breast tumours growth *in vivo*.

6. High levels of NRP2 correlates with lower survival in BrCa and HNSCC patients with metastatic disease, suggesting it can be a potential biomarker of metastatic risk.

7. NRP2 promotes primary tumour growth *in vivo* by activating cell proliferation, adhesion, migration, invasion and survival whereas it hinders cell cycle arrest and quiescence entrance by inhibiting p27 expression.

8. Stromal TGFβ1, mainly produced by lung fibroblasts and macrophages, positively regulates NRP2 expression in BrCa and HNSCC tumour cells, likely favouring DTCs proliferation and metastatic outgrowth.

9. NRP2 is essential for lung DTCs proliferative phenotype acquisition and hence, for lung metastases growth *in vivo*. Therefore, NRP2 can be considered as an attractive target for advanced tumours.

Bibliography

1. Skandalakis, J. E. Embryology and Anatomy of the Breast. in *Breast Augmentation* 3–24 (2009). doi:10.1007/978-3-642-21837-8_35.

2. Javed, A. & Lteif, A. Development of the human breast. *Semin. Plast. Surg.* **27**, 5–12 (2013).

3. Musumeci, G. *et al.* Mammary gland: From embryogenesis to adult life. *Acta Histochem.* **117**, 379–385 (2015).

4. Pellacani, D., Tan, S., Lefort, S. & Eaves, C. J. Transcriptional regulation of normal human mammary cell heterogeneity and its perturbation in breast cancer. *EMBO J.* **38**, e100330 (2019).

5. Stingl, J. Estrogen and Progesterone in Normal Mammary Gland Development and in Cancer. *Horm. Cancer* **2**, 85–90 (2011).

6. Need, E. F., Atashgaran, V., Ingman, W. v. & Dasari, P. Hormonal Regulation of the Immune Microenvironment in the Mammary Gland. *J. Mammary Gland Biol. Neoplasia* **19**, 229–239 (2014).

7. Siegel, R. L., Miller, K. D. & Jemal, A. Cancer statistics, 2020. *CA. Cancer J. Clin.* **70**, 7–30 (2020).

8. Global Cancer Organization - World Health Organization. https://gco.iarc.fr.

9. European Cancer Information System. https://ecis.jrc.ec.europa.eu/.

10. Howlader, N. *et al.* SEER Cancer Statistics Review, 1975-2016, National Cancer Institute. https://seer.cancer.gov/csr/1975_2016/ (2019).

11. The Cancer Atlas. https://canceratlas.cancer.org/.

12. American Cancer Society. Global Cancer, Facts & Figures. *Am. Cancer Soc.* (2018) doi:http://bit. ly/9NTLj6.

13. Hanahan, D. & Weinberg, R. A. Hallmarks of Cancer: The Next Generation. *Cell* **144**, 646–674 (2011).

14. Polyak, K. Breast cancer: origins and evolution. *J. Clin. Invest.* **117**, 3155–3163 (2007).

15. Turashvili, G. & Brogi, E. Tumor Heterogeneity in Breast Cancer. *Front. Med.* **4**, 227 (2017).

16. Campbell, L. L., Polyak, K. & Polyak, K. Breast Tumor Heterogeneity: Cancer Stem Cells or Clonal Evolution? *Cell Cycle* **6**, 2331–2338 (2007).

17. Martelotto, L. G., Ng, C. K. Y., Piscuoglio, S., Weigelt, B. & Reis-filho, J. S. Breast cancer intra-tumor heterogeneity. *Breast Cancer Res.* **16**, 1–11 (2014).

18. Zhou, J. *et al.* Stem Cells and Cellular Origins of Breast Cancer: Updates in the Rationale, Controversies, and Therapeutic Implications. *Front. Oncol.* **9**, 1–12 (2019).

19. Liu, X. *et al.* Dissecting the Origin of Breast Cancer Subtype Stem Cell and the Potential Mechanism of Malignant Transformation. *PLoS One* **11**, e0165001 (2016).

20. Vermeulen, L., Kemper, K., Stassi, G. & Medema, J. P. Cancer stem cells – old concepts , new insights. *Cell Death Differ.* **15**, 947–958 (2008).

21. Swanton, C. Intratumor heterogeneity: Evolution through space and time. *Cancer Res.* **72**, 4875–4882 (2012).

22. Hiley, C. T. & Swanton, C. Spatial and temporal cancer evolution: causes and consequences of tumour diversity. *Clin. Med. (Northfield. Il).* **14**, s33–s37 (2014).

23. Almendro, V. & Fuster, G. Heterogeneity of breast cancer: etiology and clinical relevance. *Clin. Transl. Oncol.* **13**, 767–773 (2011).

24. Polyak, K. Heterogeneity in breast cancer . *J. Clin. Invest.* **121**, 3786–3788 (2011).

25. Perou, C. M. *et al.* Molecular portraits of human breast tumours. *Nature* **406**, 747–752 (2000).

26. Sørlie, T. *et al.* Gene expression patterns of breast carcinomas distinguish tumor subclasses with clinical implications. *PNAS* **98**, 10869–10874 (2001).

27. Lim, E. *et al.* Aberrant luminal progenitors as the candidate target population for basal tumor development in BRCA1 mutation carriers. *Nat. Med.* **15**, 907–913 (2009).

28. Cserni, G. Histological type and typing of breast carcinomas and the WHO classification changes over time. *Pathologica* **112**, 25–41 (2020).

29. Feng, Y. *et al.* Breast cancer development and progression: Risk factors , cancer stem cells , signaling pathways , genomics , and molecular pathogenesis. *Genes Dis.* **5**, 77–106 (2018).

30. Makki, J. Diversity of Breast Carcinoma: Histological Subtypes and Clinical Relevance. *Clin. Med. Insights Pathol.* **8**, 23–31 (2015).

31. Fabbri, A., Carcangiu, M. L. & Carbone, A. Histological Classification of Breast Cancer. in *Breast Cancer. Nuclear Medicine in Diagnosis and Therapeutic Options.* (eds. Bombardieri, E., Bonadonna, G. & Gianni, L.) 3–14 (2008).

32. Seijen, M. Van *et al.* Ductal carcinoma in situ: to treat or not to treat, that is the question. *Br. J. Cancer* **121**, 285–292 (2019).

33. Van Cleef, A. *et al.* Current view on ductal carcinoma in situ and importance of the margin thresholds: A review. *Facts, Views Vis. ObGyn* **6**, 210–218 (2014).

34. Farabegoli, F. *et al.* Genetic pathways in the evolution of breast ductal carcinoma in situ. *J. Pathol.* **196**, 280–286 (2002).

35. Dossus, L. & Benusiglio, P. R. Lobular breast cancer: incidence and genetic and non-genetic risk factors. *Breast Cancer Res.* **17**, 1–8 (2015).

36. Cardoso, F. *et al.* Global analysis of advanced/metastatic breast cancer: Decade report (2005-2015). *The Breast* **39**, 131–138 (2018).

37. Tao, Z. *et al.* Breast Cancer: Epidemiology and Etiology. *Cell Biochem. Biophys.* **72**, 333–338 (2015).

38. Sawaki, M., Shien, T. & Iwata, H. TNM classification of malignant tumors (Breast Cancer Study Group). *Jpn. J. Clin. Oncol.* **49**, 228–231 (2019).

39. Piñeros, M. *et al.* Essential TNM: a registry tool to reduce gaps in cancer staging information. *Lancet Oncol.* **20**, 103-e111 (2019).

40. Hortobagyi, G. N., Edge, S. B. & Giuliano, A. New and Important Changes in the TNM Staging System for Breast Cancer. *ASCO Educ. B.* **38**, 457–467 (2018).

41. Cserni, G. The new TNM-based staging of breast cancer. *Virchows Arch.* **472**, 697–703 (2018).

42. Hortobagyi, G. N. *et al.* Breast. in *AJCC Cancer Staging Manual* 589–636 (2018).

43. Rakha, E. A. *et al.* Breast cancer prognostic classification in the molecular era: the role of histological grade. *Breast Cancer Res.* **12**, 207 (2010).

44. Rakha, E. A. *et al.* Prognostic Significance of Nottingham Histologic Grade in Invasive Breast Carcinoma. *J. Clin. Oncol.* **26**, 3153–3158 (2008).

45. Schwartz, A. M. Histologic Grade Remains a Prognostic Factor for Breast Cancer Regardless of the Number of Positive Lymph Nodes and Tumor Size. *Arch Pathol Lab Med* **136**, 1048–1052 (2014).

46. Colomer, R. *et al.* Biomarkers in breast cancer: A consensus statement by the Spanish Society of Medical Oncology and the Spanish Society of Pathology. *Clin. Transl. Oncol.* **20**, 815–826 (2017).

47. Mueller, C., Haymond, A., Davis, J. B., Williams, A. & Espina, V. Protein biomarkers for subtyping breast cancer and implications for future research. *Expert Rev. Proteomics* **15**, 131–152 (2018).

48. Fragomeni, S. M., Sciallis, A. & Jeruss, J. S. Molecular subtypes and local-regional control of breast cancer. *Surg. Oncol. Clin. N. Am.* **27**, 95–120 (2018).

49. Wolff, A. *et al.* Human Epidermal Growth Factor Receptor 2 Testing in Breast Cancer: American Society of Clinical Oncology/College of American Pathologists Clinical Practice Guideline Focused Update. *J. Clin. Oncol.* **30**, 2105–2122 (2018).

50. Loibl, S. & Gianni, L. HER2-positive breast cancer. *Lancet* **389**, 2415–2429 (2017).

51. Allott, E. H. *et al.* Intratumoral heterogeneity as a source of discordance in breast cancer biomarker classification. *Breast Cancer Res.* **18**, 1–11 (2016).

52. Prat, A. & Perou, C. M. Deconstructing the molecular portraits of breast cancer. *Mol. Oncol.* **5**, 5–23 (2011).

53. Prat, A. *et al.* Phenotypic and molecular characterization of the claudin-low intrinsic subtype of breast cancer. *Breast Cancer Res.* **12**, R68 (2010).

54. Parker, J. S. *et al.* Supervised Risk Predictor of Breast Cancer Based on Intrinsic Subtypes. *J. Clin. Oncol.* **27**, 1160–1167 (2009).

55. Bustreo, S. *et al.* Optimal Ki67 cut-off for luminal breast cancer prognostic evaluation: a large case series study with a long-term follow-up. *Breast Cancer Res. Treat.* **157**, 363–371 (2016).

56. Prat, A. *et al.* Prognostic significance of progesterone receptor-positive tumor cells within immunohistochemically defined luminal A breast cancer. *J. Clin. Oncol.* **31**, 203–209 (2013).

57. Harbeck, N. *et al.* Breast cancer. *Nat. Rev.* **5**, 1–31 (2019).

58. Coleman, C. Early Detection and Screening for Breast Cancer. *Semin. Oncol. Nurs.* **33**, 141–155 (2017).

59. Moloney, B. M., O'Loughlin, D., Elwahab, S. A. & Kerin, M. J. Breast cancer detection—a synopsis of conventional modalities and the potential role of microwave imaging. *Diagnostics* **10**, 103 (2020).

60. Fernández-Nogueira, P. *et al.* Breast Mammographic Density: Stromal Implications on Breast Cancer Detection and Therapy. *J. Clin. Med.* **9**, 776 (2020).

61. Seely, J. M. & Alhassan, T. Screening for breast cancer in 2018—what should we be doing today? *Curr. Oncol.* **25**, S115–S124 (2018).

62. Greenwood, H., Freimanis, R., Carpentier, B. & Joe, B. Clinical Breast Magnetic Resonance Imaging: Technique, Indications, and Future Applications. *Semin. Ultrasound, CT MR* **39**, 45–59 (2018).

63. Waks, A. G. & Winer, E. P. Breast Cancer Treatment: A Review. *JAMA - J. Am. Med. Assoc.* **321**, 288–300 (2019).

64. Muley, H., Fadó, R., Rodríguez-Rodríguez, R. & Casals, N. Drug uptake-based chemoresistance in breast cancer treatment. *Biochem. Pharmacol.* **177**, 113959 (2020).

65. Rouzier, R. *et al.* Breast cancer molecular subtypes respond differently to preoperative chemotherapy. *Clin. Cancer Res.* **11**, 5678–5685 (2005).

66. Gianni, L. *et al.* 5-Year analysis of neoadjuvant pertuzumab and trastuzumab in patients with locally advanced, inflammatory, or early- stage HER2-positive breast cancer (NeoSphere): a multicentre, open- label, phase 2 randomised trial. *Lancet Oncol.* **17**, 791–80 (2016).

67. Slamon, D. *et al.* Adjuvant Trastuzumab in HER2-Positive Breast Cancer. *N. Engl. J. Med.* **365**, 1273–1283 (2011).

68. Untch, M. & Thomssen, C. Clinical practice decisions in endocrine therapy. *Cancer Invest.* **28**, 4–13 (2010).

69. Early Breast Cancer Trialists' Collaborative Group (EBCTCG) *et al.* Relevance of breast cancer hormone receptors and other factors to the efficacy of adjuvant tamoxifen: patient-level meta-analysis of randomised trials. *Lancet (London, England)* **378**, 771–784 (2011).

70. Sologuren, I., Rodríguez-Gallego, C. & Lara, P. C. Immune effects of high dose radiation treatment: implications of ionizing radiation on the development of bystander and abscopal effects. *Transl. Cancer Res.* **3**, 18–31 (2014).

71. Li, C. H., Karantza, V., Aktan, G. & Lala, M. Current treatment landscape for patients with locally recurrent inoperable or metastatic triple-negative breast cancer: A systematic literature review. *Breast Cancer Res.* **21**, 143 (2019).

72. Schmid, P. *et al.* Atezolizumab and Nab-Paclitaxel in Advanced Triple-Negative Breast Cancer. *N. Engl. J. Med.* **379**, 2108–2121 (2018).

73. Groeger, S. & Meyle, J. Oral Mucosal Epithelial Cells. *Front. Immunol.* **10**, 1–22 (2019).

74. Sharma, A. K. & Kies, M. S. Neck dissection, classification and TNM staging of head and neck cancer. in *American Academy of Otolaryngology* vol. 3 (2008).

75. Muir, C. & Weiland, L. Upper aerodigestive tract cancers. *Cancer Suppl.* **75**, 147–153 (1995).

76. Bray, F. *et al.* Global cancer statistics 2018: GLOBOCAN estimates of incidence and mortality worldwide for 36 cancers in 185 countries. *CA. Cancer J. Clin.* **68**, 394–424 (2018).

77. Gatta, G. *et al.* Prognoses and improvement for head and neck cancers diagnosed in Europe in early 2000s: The EUROCARE-5 population-based study. *Eur. J. Cancer* **51**, 2130–2143 (2015).

78. Dwivedi, R., Royal, T., Nhs, M. & Trust, F. Epidemiology, Etiology and Natural history of Head and Neck Cancer. in *Essentials of head and neck cancer* (2011).

79. Stenson, K. M. Epidemiology and risk factors for head and neck cancer. *UpToDate* (2020) doi:10.1053/j.seminoncol.2004.09.013.

80. Nelson, W. In search of the first head and neck surgeon. *Am. J. Surg.* **154**, 342–346 (1987).

81. Wyss, A. *et al.* Cigarette, cigar, and pipe smoking and the risk of head and neck cancers: Pooled analysis in the international head and neck cancer epidemiology consortium. *Am. J. Epidemiol.* **178**, 679–690 (2013).

82. Pelucchi, C., Gallus, S., Garavello, W., Bosetti, C. & La Vecchia, C. Cancer risk associated with alcohol and tobacco use: Focus on upper aero-digestive tract and liver. *Alcohol Res. Heal.* **29**, 193–198 (2006).

83. Tan, E., Adelstein, D., Droughton, M., Van Kirk, M. & Lavertu, P. Squamous cell head and neck cancer in nonsmokers. *Am. J. Clin. Oncol.* **20**, 146–150 (1997).

84. Seitz, H. & Becker, P. Alcohol metabolism and cancer risk. *Alcohol Res. Heal.* **30**, 38–41 (2007).

85. Madani, A. H. *et al.* Interaction of Alcohol Use and Specific Types of Smoking on the Development of Oral Cancer. *Int. J. High Risk Behav. Addict.* **3**, e12120 (2014).

86. Seitz, H. K. & Stickel, F. Molecular mechanisms of alcoholmediated carcinogenesis. *Nat. Rev.* **7**, 599–612 (2007).

87. Gillison, M. L., Chaturvedi, A. K., Anderson, W. F. & Fakhry, C. Epidemiology of Human Papillomavirus–Positive Head and Neck Squamous Cell Carcinoma. *J. Clin. Oncol.* **33**, 3235–3242 (2015).

88. Kreimer, A., Clifford, G., Boyle, P. & Franceschi, S. Human papillomavirus types in head and neck squamous cell carcinomas worldwide: a systematic review. *Cancer epimediology, biomarkers Prev.* **14**, 467–475 (2005).

89. Ang, K. *et al.* Human papillomavirus and survival of patients with oropharyngeal cancer. *N. Engl. J. Med.* **363**, 24–35 (2010).

90. Wai, K. C., Strohl, M. P., Zante, A. van & Ha, P. K. Molecular Diagnostics in Human Papillomavirus-Related Head and Neck Squamous Cell Carcinoma. *Cells* **9**, 1–14 (2020).

91. Wołączewicz, M., Becht, R., Grywalska, E. & Niedźwiedzka-Rystwej, P. Herpesviruses in head and neck cancers. *Viruses* **12**, 1–11 (2020).

92. Amin, M. B. *et al. AJCC Cancer Staging Manual. 8th Edition.* (Springer US, 2017).

93. Chung, C. H. *et al.* Molecular classification of head and neck squamous cell carcinomas using patterns of gene expression. *Cancer Cell* **5**, 489–500 (2004).

94. Jin, C. *et al.* Cytogenetic abnormalities in 106 oral squamous cell carcinomas. *Cancer Genet. Cytogenet.* **164**, 44–53 (2006).

95. Keck, M. K. *et al.* Integrative analysis of head and neck cancer identifies two biologically distinct HPV and three non-HPV subtypes. *Clin. Cancer Res.* **21**, 870–881 (2015).

96. Zhang, Y. *et al.* Subtypes of HPV-positive head and neck cancers are associated with HPV characteristics, copy number alterations, PIK3CA mutation, and pathway signatures. *Clin. Cancer Res.* **22**, 4735–4745 (2016).

97. Smeets, S. J. *et al.* Genetic classification of oral and oropharyngeal carcinomas identifies subgroups with a different prognosis. *Cell. Oncol.* **31**, 291–300 (2009).

98. Lawrence, M. S. *et al.* Comprehensive genomic characterization of head and neck squamous cell carcinomas. *Nature* **517**, 576–582 (2015).

99. Oganesyan, G. *et al.* Critical role of TRAF3 in the Toll-like receptor-dependent and -independent antiviral response. *Nature* **439**, 208–211 (2006).

100. Petti, S. Pooled estimate of world leukoplakia prevalence: a systematic review. *Oral Oncol.* **39**, 770–780 (2003).

101. Villa, A. & Sonis, S. Oral leukoplakia remains a challenging condition. *Oral Dis.* **24**, 179–183 (2018).

102. Napier, S. & Speight, P. Natural history of potentially malignant oral lesions andconditions: an overview of the literature. *J. Oral Pathol. Med.* **37**, 1–10 (2008).

103. Veeramachaneni, R. *et al.* Analysis of head and neck carcinoma progression reveals novel and relevant stage-specific changes associated with immortalisation and malignancy. *Sci. Rep.* **9**, 1–17 (2019).

104. Leemans, C. R., Snijders, P. J. F. & Brakenhoff, R. H. The molecular landscape of head and neck cancer. *Nat. Rev. Cancer* **18**, 269–282 (2018).

105. Leemans, C. R., Braakhuis, B. J. M. & Brakenhoff, R. H. The molecular biology of head and neck cancer. *Nat. Rev. Cancer* **11**, 9–22 (2011).

106. Slaughter, D. P., Southwick, H. W. & Smejkal, W. "Field cancerization" in oral stratified squamous epithelium. *Cancer* **6**, 963–968 (1953).

107. Castellsagué, X. *et al.* HPV Involvement in Head and Neck Cancers: Comprehensive Assessment of Biomarkers in 3680 Patients. *J. Natl. Cancer Inst.* **108**, 1–12 (2016).

108. Yan, K., Agrawal, N. & Gooi, Z. Head and Neck Masses. *Med. Clin. North Am.* **102**, 1013–1025 (2018).

109. Akhavan-Moghadam, J., Afaaghi, M., Maleki, A. R. & Saburi, A. Fine Needle Aspiration: An Atraumatic Method to Diagnose Head and Neck Masses. *Trauma Mon.* **18**, 117–121 (2013).

110. Vogel, D. W. T. & Thoeny, H. C. Cross-sectional imaging in cancers of the head and neck: How we review and report. *Cancer Imaging* **16**, 1–15 (2016).

111. Srinivasan, A., Mohan, S. & Mukherji, S. Biologic imaging of head and neck cancer: the present and the future. *AJNR* **33**, 586–594 (2012).

112. Pfister, D. G. *et al.* Head and Neck Cancers, Clinical Practice Guidelines in Oncology. *J. Natl. Compr. Cancer Netw.* **12**, 1454–1487 (2014).

113. D'Cruz, A. K. *et al.* Elective versus Therapeutic Neck Dissection in Node-Negative Oral Cancer. *N. Engl. J. Med.* **373**, 521–529 (2015).

114. Chow, L. Q. Head and Neck Cancer. *N. Engl. J. Med.* **382**, 60–72 (2020).

115. Cramer, J. D., Burtness, B., Le, Q. T. & Ferris, R. L. The changing therapeutic landscape of head and neck cancer. *Nat. Rev. Clin. Oncol.* **16**, 669–683 (2019).

116. Bonner, J. A. *et al.* Radiotherapy plus Cetuximab for Squamous-Cell Carcinoma of the Head and Neck. *N. Engl. J. Med.* **354**, 567–578 (2006).

117. Santuray, R. T., Johnson, D. E. & Grandis, J. R. New Therapies in Head and Neck Cancer. *Trends in Cancer* **4**, 385–396 (2018).

118. Seiwert, T. *et al.* Safety and clinical activity of pembrolizumab for treatment of recurrent or metastatic squamous cell carcinoma of the head and neck (KEYNOTE-012): an open-label, multicentre, phase 1b trial. *Lancet Oncol.* **17**, 957–965 (2016).

119. Ferris, R. *et al.* Nivolumab for Recurrent Squamous-Cell Carcinoma of the Head and Neck. *N. Engl. J. Med.* **375**, 1856–1867 (2016).

120. Palma, M. De, Biziato, D. & Petrova, T. V. Microenvironmental regulation of tumour angiogenesis. *Nat. Rev. Cancer* **17**, 457–474 (2017).

121. Bissell, M. J. & Hines, W. C. Why don't we get more cancer? A proposed role of the microenvironment in restraining cancer progression. *Nat. Med.* **17**, 320–329 (2011).

122. Oxford, J. T., Reeck, J. C. & Hardy, M. J. Extracellular Matrix in Development and Disease. *Int. J. Mol. Sci.* **20**, 10–14 (2019).

123. Bonnans, C., Chou, J. & Werb, Z. Remodelling the extracellular matrix in development and disease. *Nat. Rev. Mol. Cell Biol.* **15**, 786–801 (2014).

124. Hartman, C., Isenberg, B., Chua, S. & Wong, J. Extracellular matrix type modulates cell migration on mechanical gradients. *Exp. Cell Res.* **359**, 361–366 (2017).

125. Sharma, P. *et al.* Aligned fibers direct collective cell migration to engineer closing and nonclosing wound gaps. *Mol. Biol. Cell* **28**, 2579–2588 (2017).

126. Malik, R., Lelkes, P. & Cukierman, E. Biomechanical and biochemical remodeling of stromal extracellular matrix in cancer. *Trends Biotechnol.* **33**, 230–236 (2015).

127. Gonzalez-Avila, G. *et al.* Matrix metalloproteinases participation in the metastatic process and their diagnostic and therapeutic applications in cancer. *Crit. Rev. Oncol. Hematol.* **137**, 57–83 (2019).

128. Paolillo, M. & Schinelli, S. Extracellular Matrix Alterations in Metastatic Processes. *Int. J. Mol. Sci.* **20 (19)**, 1–18 (2019).

129. Mehner, C. *et al.* Tumor cell-produced matrix metalloproteinase 9 (MMP-9) drives malignant progression and metastasis of basal-like triple negative breast cancer. *Oncotarget* **5**, 2736–2749 (2014).

130. Moore-Smith, L. D., Isayeva, T., Lee, J. H., Frost, A. & Ponnazhagan, S. Silencing of TGF-β1 in tumor cells impacts MMP-9 in tumor microenvironment. *Sci. Rep.* **7**, 1–10 (2017).

131. Bai, X. *et al.* Role of matrix metalloproteinase-9 in transforming growth factor-β1-induced epithelial–mesenchymal transition in esophageal squamous cell carcinoma. *Onco. Targets. Ther.* **10**, 2837–2847 (2017).

132. Pego, E. R., Fernández, I. & Núñez, M. J. Molecular basis of the effect of MMP-9 on the prostate bone metastasis: A review. *Urol. Oncol.* **36**, 272–282 (2018).

133. Dong, W. *et al.* Matrix metalloproteinase 2 promotes cell growth and invasion in colorectal cancer. *Acta Biochim. Biophys. Sin. (Shanghai).* **43**, 840–848 (2011).

134. Webb, A. H. *et al.* Inhibition of MMP-2 and MMP-9 decreases cellular migration, and angiogenesis in in vitro models of retinoblastoma. *BMC Cancer* **17**, 1–11 (2017).

135. Ametller, E. *et al.* Differential regulation of MMP7 in colon cancer cells resistant and sensitive to oxaliplatin-induced cell death. *Cancer Biol. Ther.* **11**, 4–13 (2011).

136. Maurel, J. *et al.* Serum matrix metalloproteinase 7 levels identifies poor prognosis advanced colorectal cancer patients. *Int. J. Cancer* **121**, 1066–71 (2007).

137. Sahai, E. *et al.* A framework for advancing our understanding of cancer-associated fibroblasts. *Nat. Rev. Cancer* **20**, 174–186 (2020).

138. Liu, T. *et al.* Cancer-associated fibroblasts: an emerging target of anti-cancer immunotherapy. *J. Hematol. Oncol.* **12**, 1–15 (2019).

139. Zeltz, C. *et al.* Cancer-associated fibroblasts in desmoplastic tumors: emerging role of integrins. *Semin. Cancer Biol.* **62**, 166–181 (2019).

140. Allaoui, R. *et al.* Cancer-associated fibroblast-secreted CXCL16 attracts monocytes to promote stroma activation in triple-negative breast cancers. *Nat. Commun.* **7**, 1–14 (2016).

141. Fearon, D. The carcinoma-associated fibroblast expressing fibroblast activation protein and escape from immune surveillance. *Cancer Immunol. Res.* **2**, 187–193 (2014).

142. Ding, X. *et al.* HGF-mediated crosstalk between cancer-associated fibroblasts and MET-unamplified gastric cancer cells activates coordinated tumorigenesis and metastasis. *Cell Death Dis.* **9**, 1–16 (2018).

143. Deying, W. *et al.* CAF-derived HGF promotes cell proliferation and drug resistance by up-regulating the c-Met/PI3K/Akt and GRP78 signalling in ovarian cancer cells. *Biosci. Reports* **37**, 1–12 (2017).

144. Fiori, M. E. *et al.* Cancer-associated fibroblasts as abettors of tumor progression at the crossroads of EMT and therapy resistance. *Mol. Cancer* **18 (1)**, 1–16 (2019).

145. Fernández-Nogueira, P. *et al.* Tumor-Associated Fibroblasts Promote HER2-Targeted Therapy Resistance through FGFR2 Activation. *Clin. Cancer Res.* **26**, 1432–1448 (2020).

146. Pein, M. *et al.* Metastasis-initiating cells induce and exploit a fibroblast niche to fuel malignant colonization of the lungs. *Nat. Commun.* **11**, 1–18 (2020).

147. Calon, A. *et al.* Dependency of Colorectal Cancer on a TGF-b-Driven Program in Stromal Cells for Metastasis Initiation. *Cancer Cell* **22**, 571–584 (2012).

148. Potente, M., Gerhardt, H. & Carmeliet, P. Review Basic and Therapeutic Aspects of Angiogenesis. *Cell* **146**, 873–887 (2011).

149. Abhinand, C. S., Raju, R., Soumya, S. J. & Arya, P. S. VEGF-A / VEGFR2 signaling network in endothelial cells relevant to angiogenesis. *J. Cell Commun. Signal.* **10**, 347–354 (2016).

150. Armulik, A., Genové, G. & Betsholtz, C. Pericytes: Developmental, Physiological, and Pathological Perspectives, Problems, and Promises. *Dev. Cell* **21**, 193–215 (2011).

151. Alitalo, A. & Detmar, M. Interaction of tumor cells and lymphatic vessels in cancer progression. *Oncogene* **21**, 4499–4508 (2012).

152. Wong, S. Y. & Hynes, R. O. Lymphatic or Hematogenous Dissemination: How Does a Metastatic Tumor Cell Decide? *Cell Cycle* **5**, 812–817 (2006).

153. Dadras, S. S. *et al.* Tumor lymphangiogenesis: a novel prognostic indicator for cutaneous melanoma metastasis and survival. *Am. J. Pathol.* **162**, 1951–1960 (2003).

154. Maula, S.-M. *et al.* Intratumoral lymphatics are essential for the metastatic spread and prognosis in squamous cell carcinomas of the head and neck region. *Cancer Res.* **63**, 1920–1926 (2003).

155. Kyzas, P. A., Geleff, S., Batistatou, A., Agnantis, N. J. & Stefanou, D. Evidence for lymphangiogenesis and its prognostic implications in head and neck squamous cell carcinoma. *J. Pathol.* **206**, 170–177 (2005).

156. Hirakawa, S. From tumor lymphangiogenesis to lymphvascular niche. *Cancer Sci.* **100**, 983–989 (2009).

157. Vesely, M. D., Kershaw, M. H., Schreiber, R. D. & Smyth, M. J. Natural Innate and Adaptive Immunity to Cancer. *Annu. Rev. Immunol.* **29**, 235–271 (2011).

158. Shurin, M. R., Lu, L., Kalinski, P., Stewart-Akers, A. M. & Lotze, M. T. Th1/Th2 balance in cancer, transplantation and pregnancy. *Springer Semin. Immunopathol.* **21**, 339–359 (1999).

159. Maimela, N. R., Liu, S. & Zhang, Y. Fates of CD8 + T cells in Tumor Microenvironment. *Comput. Struct. Biotechnol. J.* **17**, 1–13 (2019).

160. Farhood, B. CD8 + cytotoxic T lymphocytes in cancer immunotherapy: A review. *J. Cell. Physiol.* **234**, 8509–8521 (2019).

161. Ye, L.-L., Wei, X.-S., Zhang, M., Niu, Y.-R. & Zhou, Q. The Significance of Tumor Necrosis Factor Receptor Type II in CD8+ Regulatory T Cells and CD8+ Effector T Cells. *Front. Immunol.* **9**, 1–8 (2018).

162. Bhat, P., Leggatt, G., Waterhouse, N. & Frazer, I. H. Interferon-γ derived from cytotoxic lymphocytes directly enhances their motility and cytotoxicity. *Cell Death Dis.* **8**, 1–11 (2017).

163. Binnewies, M. *et al.* Understanding the tumor immune microenvironment (TIME) for effective therapy. *Nat. Med.* **24**, 541–550 (2018).

164. Borst, J., Ahrends, T., Bąbała, N., Melief, C. J. M. & Kastenmüller, W. CD4+ T cell help in cancer immunology and immunotherapy. *Nat. Rev. Immunol.* **18**, 635–647 (2018).

165. Togashi, Y., Shitara, K. & Nishikawa, H. Regulatory T cells in cancer immunosuppression — implications for anticancer therapy. *Nat. Rev. Clin. Oncol.* **16**, 356–371 (2019).

166. Guo, F. F. & Cui, J. W. The Role of Tumor-Infiltrating B Cells in Tumor Immunity. *J. Oncol.* 1–10 (2019) doi:https://doi.org/10.1155/2019/2592419.

167. Mantovani, A., Marchesi, F., Malesci, A. & Laghi, L. Tumor-Associated Macrophages as Treatment Targets in Oncology. *Nat. Rev. Clin. Oncol.* **14**, 399–416 (2017).

168. Yang, M., Mckay, D., Pollard, J. W. & Lewis, C. E. Diverse Functions of Macrophages in Different Tumor Microenvironments. *Cancer Res.* **78**, 5492–5503 (2018).

169. Cassetta, L. & Pollard, J. W. Targeting macrophages : therapeutic approaches in cancer. *Nat. Rev. Drug Discov.* **17**, 887–904 (2018).

170. Zhu, Y. *et al.* Tissue-resident macrophages in pancreatic ductal adenocarcinoma originate from embryonic haematopoiesis and promote tumour progression. *Immunity* **47**, 323–338 (2017).

171. Müller, E. *et al.* Toll-Like Receptor Ligands and Interferon-γ Synergize for Induction of Antitumor M1 Macrophages. *Front. Immunol.* **8**, 1–16 (2017).

172. Gocheva, V. *et al.* IL-4 induces cathepsin protease activity in tumor-associated macrophages to promote cancer growth and invasion. *Genes Dev.* **24**, 241–255 (2010).

173. DeNardo, D. G. *et al.* CD4(+) T cells regulate pulmonary metastasis of mammary carcinomas by enhancing protumor properties of macrophages. *Cancer Cell* **16**, 91–102 (2009).

174. Rahal, O. M. *et al.* Blocking Interleukin (IL)4- and IL13-Mediated Phosphorylation of STAT6 (Tyr641) Decreases M2 Polarization of Macrophages and Protects Against Macrophage-Mediated Radioresistance of Inflammatory Breast Cancer. *Int. J. Radiat. Oncol. Biol. Phys.* **100**, 1034–1043 (2018).

175. Pyonteck, S. M. *et al.* CSF-1R inhibition alters macrophage polarization and blocks glioma progression. *Nat. Med.* **19**, 1264–1272 (2013).

176. Hinshaw, D. C. & Shevde, L. A. The Tumor Microenvironment Innately Modulates Cancer Progression. *Cancer Res.* **79**, 4557–4566 (2019).

177. Lin, E. Y. & Pollard, J. W. Tumor-associated macrophages press the angiogenic switch in breast cancer. *Cancer Res.* **67**, 1–4 (2007).

178. Wyckoff, J. *et al.* A paracrine loop between tumor cells and macrophages is required for tumor cell migration in mammary tumors. *Cancer Res.* **64**, 7022–7029 (2004).

179. Chen, Q., Zhang, X. H.-F. & Massagué, J. Macrophage binding to receptor VCAM-1 transmits survival signals in breast cancer cells that invade the lungs. *Cancer Cell* **20**, 538–549 (2011).

180. Zhang, H. *et al.* Circulating Tumor Microparticles Promote Lung Metastasis by Reprogramming Inflammatory and Mechanical Niches via a Macrophage-Dependent Pathway. *Cancer Immunol. Res.* **6**, 1046–1056 (2018).

181. Chen, X. *et al.* CYP4A in tumor-associated macrophages promotes pre-metastatic niche formation and metastasis. *Oncogene* **36**, 5045–5057 (2017).

182. Wylie, B., Macri, C., Mintern, J. D. & Waithman, J. Dendritic Cells and Cancer: From Biology to Therapeutic Intervention. *Cancers (Basel).* **11 (4)**, 1–21 (2019).

183. Sagiv, J. Y. *et al.* Phenotypic diversity and plasticity in circulating neutrophil subpopulations in cancer. *Cell Rep.* **10**, 562–573 (2015).

184. Shaul, M. E. & Fridlender, Z. G. Tumour-associated neutrophils in patients with cancer. *Nat. Rev. Clin. Oncol.* **16**, 601–620 (2019).

185. Wang, W.-C. *et al.* Survival Mechanisms and Influence Factors of Circulating Tumor Cells. *Biomed Res. Int.* 1–10 (2018) doi:10.1155/2018/6304701.

186. Granot, Z. Neutrophils as a Therapeutic Target in Cancer. *Front. Immunol.* **10**, 1–6 (2019).

187. Shimasaki, N., Jain, A. & Campana, D. NK cells for cancer immunotherapy. *Nat. Rev. Drug Discov.* **19**, 200–218 (2020).

188. Nair, S. & Dhodapkar, M. V. Natural Killer T Cells in Cancer Immunotherapy. *Front. Immunol.* **8**, 1–18 (2017).

189. Arese, M., Bussolino, F., Pergolizzi, M., Bizzozero, L. & Pascal, D. Tumor progression: the neuronal input. *Ann. Transl. Med.* **6**, 89 (2018).

190. Jobling, P. *et al.* Nerve-cancer cell cross-talk: A novel promoter of tumor progression. *Cancer Res.* **75**, 1777–1781 (2015).

191. Entschladen, F., Palm, D., Lang, K., Drell IV, T. L. & Zaenker, K. S. Neoneurogenesis: Tumors may initiate their own innervation by the release of neurotrophic factors in analogy to lymphangiogenesis and neoangiogenesis. *Med. Hypotheses* **67**, 33–35 (2006).

192. Mauffrey, P. *et al.* Progenitors from the central nervous system drive neurogenesis in cancer. *Nature* **569**, 672–678 (2019).

193. Zhao, H. *et al.* The Ron receptor tyrosine kinase activates c-Abl to promote cell proliferation through tyrosine phosphorylation of PCNA in breast cancer. *Oncogene* **33**, 1429–1437 (2014).

194. Zhao, C.-M. *et al.* Denervation suppresses gastric tumorigenesis. *Sci. Transl. Med.* **6**, 1–13 (2014).

195. Magnon, C. *et al.* Autonomic Nerve Development Contributes to Prostate Cancer Progression. *Science (80-.).* **341**, 1236361 (2013).

196. Cole, S. W., Nagaraja, A. S., Lutgendorf, S. K., Green, P. A. & Sood, A. K. Sympathetic nervous system regulation of the tumour microenvironment. *Nat. Rev. Cancer* **15**, 563–572 (2015).

197. Palm, D. & Entschladen, F. Neoneurogenesis and the neuro-neoplastic synapse. *Prog. Exp. Tumor Res.* **39**, 91–98 (2007).

198. Voss, M. J. & Entschladen, F. Tumor interactions with soluble factors and the nervous system. *Cell Commun. Signal.* **8**, 1–6 (2010).

199. Li, Z. & Cho, C. Neurotransmitters, more than meets the eye–neurotransmitters and their perspectives in cancer development and therapy. *Eur. J. Pharmacol.* **667**, 17–22 (2011).

200. Kazi, R. & Bunimovich, Y. L. The nervous system: A new target in the fight against cancer. *Anticancer. Drugs* **29**, 929–934 (2018).

201. Bakst, R. L. & Wong, R. J. Mechanisms of Perineural Invasion. *J. Neurol. Surg.* **77**, 96–106 (2016).

202. Mancino, M., Ametller, E., Gascón, P. & Almendro, V. The neuronal influence on tumor progression. *Biochim. Biophys. Acta* **1816**, 105–118 (2011).

203. Marchesi, F., Piemonti, L., Mantovani, A. & Allavena, P. Molecular mechanisms of perineural invasion, a forgotten pathway of dissemination and metastasis. *Cytokine Growth Factor Rev.* **21**, 77–82 (2010).

204. Bapat, A., Hostetter, G., Von Hoff, D. & Han, H. Perineural invasion and associated pain in pancreatic cancer. *Nat. Rev. Cancer* **11**, 695–707 (2011).

205. Bakst, R. *et al.* Perineural Invasion and Perineural Tumor Spread in Head and Neck Cancer. *Int. J. Radiat. Oncol. Biol. Phys.* **103**, 1109–1124 (2019).

206. Sayar, A. *et al.* Nonanatomic Prognostic Factors in Resected Nonsmall Cell Lung Carcinoma: The Importance of Perineural Invasion as a New Prognostic Marker. *Ann. Thorac. Surg.* **77**, 421–425 (2004).

207. Welch, D. R. & Hurst, D. R. Defining the Hallmarks of Metastasis. *Cancer Res.* **79**, 3011–3027 (2019).

208. Gupta, G. P. & Massagué, J. Cancer Metastasis: Building a Framework. *Cell* **127**, 679–695 (2006).

209. Fidler, I. & Kripke, M. Metastasis Results from Preexisting Variant Cells Within a Malignant Tumor. *Science (80-.).* **197**, 893–895 (1977).

210. Greaves, M. & Maley, C. C. Clonal evolution in cancer. *Nature* **481**, 306–313 (2012).

211. Schmidt-Kittler, O. *et al.* From latent disseminated cells to overt metastasis: Genetic analysis of systemic breast cancer progression. *PNAS* **100**, 7737–7742 (2003).

212. Klein, C. The Systemic Progression of Human Cancer: A Focus on the Individual Disseminated Cancer Cell—The Unit of Selection. *Adv. Cancer Res.* **89**, 35–67 (2003).

213. Stratton, M. Exploring the genomes of cancer cells: progress and promise. *Science (80-.).* **331**, 1553–1558 (2011).

214. Birkbak, N. J. & McGranahan, N. Cancer Genome Evolutionary Trajectories in Metastasis. *Cancer Cell* **37**, 8–19 (2020).

215. Robinson, D. R. *et al.* Integrative clinical genomics of metastatic cancer. *Nature* **548**, 297–303 (2017).

216. Hosseini, H. *et al.* Early dissemination seeds metastasis in breast cancer. *Nature* **540**, 552–558 (2016).

217. Cejalvo, J. M. *et al.* Intrinsic subtypes and gene expression profiles in primary and metastatic breast cancer. *Cancer Res.* **77**, 2213–2221 (2017).

218. Armenia, J. *et al.* The long tail of oncogenic drivers in prostate. *Cancer* **50**, 645–651 (2018).

219. Bertucci, F. *et al.* Genomic characterization of metastatic breast cancers. *Nature* **569**, 560–564 (2019).

220. Stoecklein, N. H. & Klein, C. A. Genetic disparity between primary tumours, disseminated tumour cells, and manifest metastasis. *Int. J. Cancer* **126**, 589–598 (2010).

221. Klein, C. *et al.* Genetic heterogeneity of single disseminated tumour cells in minimal residual cancer. *Lancet* **360**, 683–689 (2002).

222. Stoecklein, N. *et al.* Direct genetic analysis of single disseminated cancer cells for prediction of outcome and therapy selection in esophageal cancer. *Cancer Cell* **13**, 441–453 (2008).

223. Yates, L. R. *et al.* Genomic Evolution of Breast Cancer Metastasis and Relapse. *Cancer Cell* **32**, 169–184 (2017).

224. Hüsemann, Y. *et al.* Systemic Spread Is an Early Step in Breast Cancer. *Cancer Cell* **13**, 58–68 (2008).

225. Celià-Terrassa, T. & Kang, Y. Distinctive properties of metastasis initiating cells. *Genes Dev.* **30**, 892–908 (2016).

226. Strauss, D. & Thomas, J. Transmission of donor melanoma by organ transplantation. *Lancet Oncol.* **11**, 790–796 (2010).

227. Woodle, E. S. *et al.* Prostate cancer prior to solid organ transplantation: the Israel Penn International Transplant Tumor Registry experience. *Transplant. Proc.* **37**, 958–959 (2005).

228. Klein, C. A. The Metastasis Cascade. *Science (80-.).* **321**, 1785–1788 (2008).

229. Vanharanta, S. & Massagué, J. Origins of Metastatic Traits. *Cancer Cell* **24**, 410–421 (2013).

230. Massagué, J. & Obenauf, A. C. Metastatic colonization by circulating tumour cells. *Nature* **529**, 298–306 (2016).

231. Riggi, N., Aguet, M. & Stamenkovic, I. Cancer Metastasis: A Reappraisal of Its Underlying Mechanisms and Their Relevance to Treatment. *Annu. Rev. Pathol. Mech. Dis.* **13**, 117–140 (2018).

232. Chiang, S. P. H., Cabrera, R. M. & Segall, J. E. Tumor cell intravasation. *Am. J. Physiol. Cell Physiol.* **311**, C1–C14 (2016).

233. Lamouille, S., Xu, J. & Derynck, R. Molecular mechanisms of epithelial–mesenchymal transition. *Nat. Rev. Mol. Cell Biol.* **15**, 178–196 (2014).

234. Mani, S. A. *et al.* The epithelial-mesenchymal transition generates cells with properties of stem cells. *Cell* **133**, 704–715 (2008).

235. Jordan, N. V., Johnson, G. L. & Abell, A. N. Tracking the intermediate stages of epithelial-mesenchymal transition in epithelial stem cells and cancer. *Cell Cycle* **10**, 2865–2873 (2011).

236. Te Boekhorst, V., Preziosi, L. & Friedl, P. Plasticity of Cell Migration In Vivo and In Silico. *Annu. Rev. Cell Dev. Biol.* **32**, 491–526 (2016).

237. Westcott, J. M. *et al.* An epigenetically distinct breast cancer cell subpopulation promotes collective invasion. *J. Clin. Invest.* **125**, 1927–1943 (2015).

238. Sökeland, G. & Schumacher, U. The functional role of integrins during intra- and extravasation within the metastatic cascade. *Mol. Cancer* **18**, 1–19 (2019).

239. Vollmann-Zwerenz, A., Leidgens, V., Feliciello, G., Klein, C. A. & Hau, P. Tumor Cell Invasion in Glioblastoma. *Int. J. Mol. Sci.* **21 (6)**, 1–21 (2020).

240. Butler, T. P. & Gullino, P. M. Quantification of cell shedding into efferent blood of mammary adenocarcinoma. *Cancer Res.* **35**, 512–516 (1975).

241. Micalizzi, D. S., Maheswaran, S. & Haber, D. A. A conduit to metastasis: circulating tumor cell biology. *Genes Dev.* **31**, 1827–1840 (2017).

242. Gay, L. & Felding-Habermann, B. Contribution of platelets to tumour metastasis. *Nat. Rev. Cancer* **11**, 123–134 (2011).

243. Coffelt, S., Wellenstein, M. & de Visser, K. Neutrophils in cancer: neutral no more. *Nat. Rev.* **16**, 431–446 (2016).

244. Lorusso, G. & Rüegg, C. New insights into the mechanisms of organ-specific breast cancer metastasis. *Semin. Cancer Biol.* **22**, 226–233 (2012).

245. Strell, C. & Entschladen, F. Extravasation of leukocytes in comparison to tumor cells. *Cell Commun. Signal.* **6**, 1–13 (2008).

246. Reymond, N., D'Água, B. B. & Ridley, A. J. Crossing the endothelial barrier during metastasis. *Nat. Rev. Cancer* **13**, 858–870 (2013).

247. Al-Mehdi, A. *et al.* Intravascular origin of metastasis from the proliferation of endothelium-attached tumor cells: a new model for metastasis. *Nat. Med.* **6**, 100–102 (2000).

248. Baccelli, I. *et al.* Identification of a population of blood circulating tumor cells from breast cancer patients that initiates metastasis in a xenograft assay. *Nat. Biotechnol.* **31**, 539–545 (2013).

249. García, S. A., Weitz, J. & Schölch, S. Circulating Tumor Cells. *Methods Mol. Biol.* **1692**, 213–219 (2018).

250. Cameron, M. *et al.* Temporal progression of metastasis in lung: cell survival, dormancy, and location dependence of metastatic inefficiency. *Cancer Res.* **60**, 2541–2546 (2000).

251. Luzzi, K. *et al.* Multistep nature of metastatic inefficiency: dormancy of solitary cells after successful extravasation and limited survival of early micrometastases. *Am. J. Pathol.* **153**, 865–873 (1998).

252. Paget, S. The distribution of secondary growths in cancer of the breast. *Lancet* **1**, 571–573 (1889).

253. Fares, J., Fares, M. Y., Khachfe, H. H., Salhab, H. A. & Fares, Y. Molecular principles of metastasis: a hallmark of cancer revisited. *Signal Transduct. Target. Ther.* **5**, 1–17 (2020).

254. Zhang, X. H.-F., Giuliano, M., Trivedi, M. V., Schiff, R. & Osborne, C. K. Metastasis Dormancy in Estrogen Receptor-Positive Breast Cancer. *Clin. Cancer Res.* **19**, 1–16 (2013).

255. Ruppender, N. S., Morrissey, C., Lange, P. H. & Vessella, R. L. Dormancy in solid Tumors: Implications for Prostate Cancer. *Cancer Metastasis Rev.* **32**, 501–9 (2013).

256. Aguirre-Ghiso, J. A. & Sosa, M. S. Emerging Topics on Disseminated Cancer Cell Dormancy and the Paradigm of Metastasis. *Annu. Rev. Cancer Biol.* **2**, 377–393 (2018).

257. Peinado, H. *et al.* Pre-metastatic niches : organ-specific homes for metastases. *Nat. Rev. Cancer* **17**, 302–317 (2017).

258. Liu, Y. & Cao, X. Characteristics and Significance of the Pre-metastatic Niche. *Cancer Cell* **30**, 668–681 (2016).

259. Karaca, Z. *et al.* VEGFR1 expression is related to lymph node metastasis and serum VEGF may be a marker of progression in the follow-up of patients with differentiated thyroid carcinoma. *Eur. J. Endcrinology* **164**, 277–284 (2011).

260. Ara, T. & DeClerck, Y. A. Interleukin-6 in Bone Metastasis and Cancer Progression. *Eur. J. Cancer* **46**, 1223–1231 (2010).

261. Lynch, C. Matrix metalloproteinases as master regulators of the vicious cycle of bone metastasis. *Bone* **48**, 44–53 (2011).

262. Lipton, A. & Goessl, C. Clinical development of anti-RANKL therapies for treatment and prevention of bone metastasis. *Bone* **48**, 96–99 (2011).

263. Yousefi, M. *et al.* Organ-specific metastasis of breast cancer: molecular and cellular mechanisms underlying lung metastasis. *Cell. Oncol.* **41**, 123–140 (2018).

264. Gao, H. *et al.* The BMP inhibitor Coco reactivates breast cancer cells at lung metastatic sites. *Cell* **150**, 764–779 (2012).

265. Kobayashi, A. *et al.* Bone morphogenetic protein 7 in dormancy and metastasis of prostate cancer stem-like cells in bone. *J. Exp. Med.* **208**, 2641–2655 (2011).

266. Bragado, P. *et al.* TGFβ2 dictates disseminated tumour cell fate in target organs through TGFβ-RIII and p38α/β signalling. *Nat. Cell Biol.* **15**, 1351–1361 (2013).

267. Turajlic, S. & Swanton, C. Metastasis as an evolutionary process. *Science (80-.).* **352**, 169–175 (2016).

268. Aguirre-Ghiso, J. A. Models, mechanisms and clinical evidence for cancer dormancy. *Nat. Rev. Cancer* **7**, 834–846 (2007).

269. Senft, D. & Ronai, Z. A. Adaptive Stress Responses During Tumor Metastasis and Dormancy. *Trends in Cancer* **2**, 429–442 (2016).

270. Gomis, R. R. & Gawrzak, S. Tumor cell dormancy. *Mol. Oncol.* **11**, 62–78 (2017).

271. Popper, H. H. Progression and metastasis of lung cancer. *Cancer Metastasis Rev.* **35**, 75–91 (2016).

272. Denaro, N., Merlano, M. C. & Russi, E. G. Follow-up in Head and Neck Cancer: Do More Does It Mean Do Better? A Systematic Review and Our Proposal Based on Our Experience. *Clin. Exp. Otorhinolaryngol.* **9**, 287–297 (2016).

273. Trumpp, A., Essers, M. & Wilson, A. Awakening dormant haematopoietic stem cells. *Nat. Rev. Immunol.* **10**, 201–209 (2010).

274. Hamatani, T. *et al.* Global gene expression analysis identifies molecular pathways distinguishing blastocyst dormancy and activation. *PNAS* **101**, 10326–10331 (2004).

275. Morrison, S. J. & Scadden, D. T. The bone marrow niche for haematopoietic stem cells. *Nature* **505**, 327–334 (2014).

276. Naumov, G. N. *et al.* A Model of Human Tumor Dormancy: An Angiogenic Switch From the Nonangiogenic Phenotype. *JNCI* **98**, 316–325 (2006).

277. Wang, H. *et al.* Targeting Immune-Mediated Dormancy: A Promising Treatment of Cancer. *Front. Oncol.* **9**, 1–9 (2019).

278. Müller-Hermelink, N. *et al.* TNFR1 signaling and IFN-gamma signaling determine whether T cells induce tumor dormancy or promote multistage carcinogenesis. *Cancer Cell* **13**, 507–518 (2008).

279. Kim, K., Marquez-palencia, M. & Malladi, S. Metastatic Latency, a Veiled Threat. *Front. Immunol.* **10**, 1–9 (2019).

280. Sosa, M. S., Bragado, P. & Aguirre-Ghiso, J. A. Mechanisms of disseminated cancer cell dormancy: an awakening field. *Nat. Rev. Cancer* **14**, 611–622 (2014).

281. Ghajar, C. M. Metastasis prevention by targeting the dormant niche. *Nature* **15**, 238–247 (2015).

282. Linde, N. & Fluegen, G. The Relationship Between Dormant Cancer Cells and Their Microenvironment. *Adv. Cancer Res.* **132**, 45–71 (2016).

283. Barney, L. E. *et al.* Tumor cell–organized fibronectin maintenance of a dormant breast cancer population. *Sci. Adv.* **6**, 1–13 (2020).

284. Butturini, E., Prati, A. C. De, Boriero, D. & Mariotto, S. Tumor Dormancy and Interplay with Hypoxic Tumor Microenvironment. *Int. J. Mol. Sci.* **20 (17)**, 1–21 (2019).

285. Fluegen, G. *et al.* Phenotypic heterogeneity of disseminated tumour cells is preset by primary tumour hypoxic microenvironments. *Nat. Cell Biol.* **19**, 120–132 (2017).

286. Hoppe-Seyler, K. *et al.* Induction of dormancy in hypoxic human papillomavirus-positive cancer cells. *PNAS* **114**, E990–E998 (2017).

287. Feuerer, M. *et al.* Enrichment of memory T cells and other profound immunological changes in the bone marrow from untreated breast cancer patients. *Int. J. Cancer* **92**, 96–105 (2001).

288. Malladi, S. *et al.* Metastatic Latency and Immune Evasion through Autocrine Inhibition of WNT. *Cell* **165**, 45–60 (2016).

289. Tiram, G. *et al.* Reverting the molecular fingerprint of tumor dormancy as a therapeutic strategy for glioblastoma. *FASEB J.* **32**, 5835–5850 (2018).

290. Shiozawa, Y. *et al.* GAS6/AXL Axis Regulates Prostate Cancer Invasion, Proliferation, and Survival in the Bone Marrow Niche. *Neoplasia* **12**, 116–127 (2010).

291. Yumoto, K. *et al.* Axl is required for TGF-β2-induced dormancy of prostate cancer cells in the bone marrow. *Sci. Rep.* **6**, 1–16 (2016).

292. Yu-Lee, L.-Y. *et al.* Osteoblast-Secreted Factors Mediate Dormancy of Metastatic Prostate Cancer in the Bone via Activation of the TGFbRIII – p38MAPK – pS249 / T252RB Pathway. *Cancer Res.* **78**, 2911–2925 (2018).

293. Sosa, M. S. *et al.* NR2F1 controls tumour cell dormancy via SOX9- and RARb-driven quiescence programmes. *Nat. Commun.* **6**, 1–14 (2015).

294. Cock, J. M. De *et al.* Inflammation triggers Zeb1-dependent escape from tumor latency. *Cancer Res.* **76**, 6778–6784 (2016).

295. Malanchi, I. *et al.* Interactions between cancer stem cells and their niche govern metastatic colonization. *Nature* **481**, 85–89 (2012).

296. Ghajar, C. M. *et al.* The perivascular niche regulates breast tumour dormancy. *Nat. Cell Biol.* **15**, 807–817 (2013).

297. Pape, F. Le, Vargas, G. & Clézardin, P. The role of osteoclasts in breast cancer bone metastasis. *J. Bone Oncol.* **5**, 93–95 (2016).

298. Buijs, J. T., Stayrook, K. R. & Guise, T. A. The role of TGF-β in bone metastasis: novel therapeutic perspectives. *Bonekey Rep.* **1**, 1–10 (2012).

299. Oskarsson, T. *et al.* Breast cancer cells produce tenascin C as a metastatic niche component to colonize the lungs. *Nat. Med.* **17**, 867–874 (2011).

300. Barkan, D. *et al.* Metastatic growth from dormant cells induced by a col-I-enriched fibrotic environment. *Cancer Res.* **70**, 5706–5716 (2010).

301. Lawson, M. A. *et al.* Osteoclasts control reactivation of dormant myeloma cells by remodelling the endosteal niche. *Nat. Commun.* **6**, 1–15 (2015).

302. Decker, A. M. *et al.* Sympathetic Signaling Reactivates Quiescent Disseminated Prostate Cancer Cells in the Bone Marrow. *Mol. Cancer Res.* **15**, 1644–1655 (2017).

303. Kan, C., Vargas, G., Pape, F. Le & Clézardin, P. Cancer Cell Colonisation in the Bone Microenvironment. *Int. J. Mol. Sci.* **17 (10)**, 1–16 (2016).

304. Lu, X. *et al.* VCAM-1 promotes osteolytic expansion of indolent bone micrometastasis of breast cancer by engaging α4β1-positive osteoclast progenitors. *Cancer Cell* **20**, 701–714 (2011).

305. Breuksch, I., Weinert, M. & Brenner, W. The role of extracellular calcium in bone metastasis. *J. Bone Oncol.* **5**, 143–145 (2016).

306. Tivari, S., Lu, H., Dasgupta, T., Lorenzo, M. S. De & Wieder, R. Reawakening of dormant estrogen- dependent human breast cancer cells by bone marrow stroma secretory senescence. *Cell Commun. Signal.* **16 (1)**, 1–18 (2018).

307. Lee, J.-H. *et al.* Lung Stem Cell Differentiation in Mice Directed by Endothelial Cells via a BMP4-NFATc1-Thrombospondin-1 Axis. *Cell* **156**, 440–455 (2013).

308. Carlson, P. *et al.* Targeting the perivascular niche sensitizes disseminated tumour cells to chemotherapy. *Nat. Cell Biol.* **21**, 238–250 (2019).

309. Powe, D. G. *et al.* Beta-Blocker Drug Therapy Reduces Secondary Cancer Formation in Breast Cancer and Improves Cancer Specific Survival. *Oncotarget* **1**, 628–638 (2010).

310. De Giorgi, V. *et al.* β-Blocker use and reduced disease progression in patients with thick melanoma: 8 years of follow-up. *Melanoma Res.* **27**, 268–270 (2017).

311. Aguirre-ghiso, J. A., Liu, D., Mignatti, A., Kovalski, K. & Ossowski, L. Urokinase Receptor and Fibronectin Regulate the ERK MAPK to p38 MAPK Activity Ratios That Determine Carcinoma Cell Proliferation or Dormancy In Vivo. *Mol. Biol. Cell* **12**, 863–879 (2001).

312. Ghiso, J. A. A., Kovalski, K. & Ossowski, L. Tumor Dormancy Induced by Downregulation of Urokinase Receptor in Human Carcinoma Involves Integrin and MAPK Signaling. *J. Cell Biol.* **147**, 89–103 (1999).

313. Aguirre-Ghiso, J. A., Estrada, Y., Liu, D. & Ossowski, L. ERK MAPK Activity as a Determinant of Tumor Growth and Dormancy; Regulation by p38 SAPK. *Cancer Res.* **63**, 1684–1695 (2003).

314. Aguirre-Ghiso, J. A. Inhibition of FAK signaling activated by urokinase receptor induces dormancy in human carcinoma cells in vivo. *Oncogene* **21**, 2513–2524 (2002).

315. Adam, A. P. *et al.* Computational identification of a p38 SAPK-regulated transcription factor network required for tumor cell quiescence. *Cancer Res.* **69**, 5664–5672 (2009).

316. Yamada, S. D. *et al.* Mitogen-activated Protein Kinase Kinase 4 (MKK4) Acts as a Metastasis Suppressor Gene in Human Ovarian Carcinoma. *Cancer Res.* **62**, 6717–23 (2002).

317. Lotan, T. *et al.* Protein Kinase Kinase 4–Mediated Inhibition of SKOV3ip.1 Ovarian Cancer Metastasis Involves Growth Arrest and p21 Up-regulation. *Cancer Res.* **68**, 2166–2175 (2008).

318. Harper, K. L. *et al.* Mechanism of early dissemination and metastasis in Her2+ mammary cancer. *Nature* **540**, 588–592 (2016).

319. Ranganathan, A. C., Zhang, L., Adam, A. P. & Aguirre-Ghiso, J. A. Functional coupling of p38-induced up-regulation of BiP and activation of RNA-dependent protein kinase-like endoplasmic reticulum kinase to drug resistance of dormant carcinoma cells. *Cancer Res.* **66**, 1702–1711 (2006).

320. Ranganathan, A., Zhang, L., Adam, A. & Aguirre-Ghiso, J. Dual Function of Pancreatic Endoplasmic Reticulum Kinase in Tumor Cell Growth Arrest and Survival. *Cancer Res.* **68**, 3260–3268 (2008).

321. Schewe, D. M. & Aguirre-Ghiso, J. A. ATF6α-Rheb-mTOR signaling promotes survival of dormant tumor cells in vivo. *Proc. Natl. Acad. Sci. U. S. A.* **105**, 10519–10524 (2008).

322. Jo, H., Jia, Y., Subramanian, K. K., Hattori, H. & Luo, H. R. Cancer Cell-Derived Clusterin Modulates the Phosphatidylinositol 3 J -Kinase – Akt Pathway through Attenuation of Insulin-Like Growth Factor 1 during Serum Deprivation □ †. *Mol. Cell. Biol.* **28**, 4285–4299 (2008).

323. Humtsoe, J. O. & Kramer, R. H. Differential epidermal growth factor receptor signaling regulates anchorage-independent growth by modulation of the PI3K/AKT pathway. *Oncogene* **29**, 1214–1226 (2010).

324. Lu, Z. *et al.* The tumor suppressor gene ARHI regulates autophagy and tumor dormancy in human ovarian cancer cells. *J. Clin. Invest.* **118**, 3917–3929 (2008).

325. Puig, I. *et al.* TET2 controls chemoresistant slow-cycling cancer cell survival and tumor recurrence. *J. Cell. Physiol.* **128**, 3887–3905 (2018).

326. Scognamiglio, R. *et al.* Myc Depletion Induces a Pluripotent Dormant State Mimicking Diapause. *Cell* **164**, 668–680 (2016).

327. Horak, C. E., Lee, J. H., Marshall, J., Martin, S. & Steeg, P. S. The role of metastasis suppressor genes in metastatic dormancy. *APMIS* **116**, 586–601 (2008).

328. Nash, K. T. *et al.* Requirement of KISS1 secretion for multiple organ metastasis suppression and maintenance of tumor dormancy. *J. Natl. Cancer Inst.* **99**, 309–321 (2007).

329. Bandyopadhyay, S. *et al.* Interaction of KAI1 on tumor cells with DARC on vascular endothelium leads to metastasis suppression. *Nat. Med.* **12**, 933–938 (2006).

330. Sherbet, G. V. KAI1 (CD82) Suppresses Metastasis, Cell Proliferation and Invasion. *Ther. Strateg. Cancer Biol. Pathol.* 91–93 (2013) doi:https://doi.org/10.1016/B978-0-12-416570-0.00013-5.

331. Mátyási, B. *et al.* The Function of NM23-H1/NME1 and Its Homologs in Major Processes Linked to Metastasis. *Pathol. Oncol. Res.* **26**, 49–61 (2020).

332. Takács-Vellai, K. The metastasis suppressor Nm23 as a modulator of Ras/ERK signaling. *J. Mol. Signal.* **9**, 1–8 (2014).

333. Steeg, P. S. Targeting metastasis. *Nat. Rev. Cancer* **16**, 201–218 (2016).

334. Klein, C. A. Parallel progression of tumour and metastases. *Nat. Rev. Cancer* **9**, 302–312 (2009).

335. Pan, H. *et al.* 20-Year Risks of Breast-Cancer Recurrence after Stopping Endocrine Therapy at 5 Years. *N. Engl. J. Med.* **377**, 1836–1846 (2017).

336. Hartkopf, A. D. *et al.* Prognostic relevance of disseminated tumour cells from the bone marrow of early stage breast cancer patients—Results from a large single-centre analysis. *Eur. J. Cancer* **50**, 2550–2559 (2014).

337. Hartkopf, A. *et al.* Disseminated tumor cells from the bone marrow of patients with nonmetastatic primary breast cancer are predictive of locoregional relapse. *Ann. Oncol.* **26**, 1155–1160 (2015).

338. Kim, R. S. *et al.* Dormancy Signatures and Metastasis in Estrogen Receptor Positive and Negative Breast Cancer. *PLoS One* **7 (4)**, 1–8 (2012).

339. Chéry, L. *et al.* Characterization of single disseminated prostate cancer cells reveals tumor cell heterogeneity and identifies dormancy associated pathways. *Oncotarget* **5**, 9939–9951 (2014).

340. Borgen, E. *et al.* NR2F1 stratifies dormant disseminated tumor cells in breast cancer patients. *Breast Cancer Res.* **20**, 1–13 (2018).

341. Ogba, N. *et al.* Luminal breast cancer metastases and tumor arousal from dormancy are promoted by direct actions of estradiol and progesterone on the malignant cells. *Breast Cancer Res.* **16**, 1–14 (2014).

342. Neophytou, C. M., Kyriakou, T. C. & Papageorgis, P. Mechanisms of metastatic tumor dormancy and implications for cancer therapy. *Int. J. Mol. Sci.* **20 (24)**, 1–21 (2019).

343. Jahanban-Esfahlan, R. *et al.* Tumor Cell Dormancy: Threat or Opportunity in the Fight against Cancer. *Cancers (Basel).* **11 (8)**, 1–23 (2019).

344. Summers, M. A., McDonald, M. M. & Croucher, P. I. Cancer Cell Dormancy in Metastasis. *Cold Spring Harb. Perspect. Med.* **10**, a037556 (2019).

345. Byrne, N. M., Summers, M. A. & McDonald, M. M. Tumor Cell Dormancy and Reactivation in Bone: Skeletal Biology and Therapeutic Opportunities. *JBMR Plus* **3**, e10125 (2019).

346. Schewe, D. M. & Aguirre-Ghiso, J. A. Inhibition of eIF2α Dephosphorylation Maximizes Bortezomib Efficiency and Eliminates Quiescent Multiple Myeloma Cells Surviving Proteasome Inhibitor Therapy. *Cancer Res.* **69**, 1545–1552 (2009).

347. Gil, M., Seshadri, M., Komorowski, M. P., Abrams, S. I. & Kozbor, D. Targeting CXCL12/CXCR4 signaling with oncolytic virotherapy disrupts tumor vasculature and inhibits breast cancer metastases. *PNAS* **110**, E1291-1300 (2013).

348. Naume, B. *et al.* Clinical outcome with correlation to disseminated tumor cell (DTC) status after DTC-guided secondary adjuvant treatment with docetaxel in early breast cancer. *J. Clin. Oncol.* **32**, 3848–57 (2014).

349. Guo, H.-F. & Kooi, C. W. Vander. Neuropilin Functions as an Essential Cell Surface Receptor. *J. Biol. Chem.* **290**, 29120–29126 (2015).

350. Parker, M. W., Guo, H., Li, X., Linkugel, A. D. & Kooi, C. W. Vander. Function of Members of the Neuropilin Family as Essential Pleiotropic Cell Surface Receptors. *Biochemistry* **51**, 9437–9446 (2012).

351. Pellet-Many, C., Frankel, P., Jia, H. & Zachary, I. Neuropilins : structure , function and role in disease. *Biochem. J.* **411**, 211–226 (2008).

352. Rossignol, M., Gagnon, M. L. & Klagsbrun, M. Genomic organization of human neuropilin-1 and neuropilin-2 genes: identification and distribution of splice variants and soluble isoforms. *Genomics* **70**, 211–222 (2000).

353. Nakamura, F. & Goshima, Y. Structural and functional relation of neuropilins. in *Neuropilin: From Nervous System to Vascular and Tumor Biology* (ed. Bagnard, D.) 55–69 (Springer, Boston, MA, 2002).

354. Worzfeld, T. & Offermanns, S. Semaphorins and plexins as therapeutic targets. *Nat. Rev. Drug Discov.* **13**, 603–621 (2014).

355. Herzog, B., Pellet-Many, C., Britton, G., Hartzoulakis, B. & Zachary, I. C. VEGF binding to NRP1 is essential for VEGF stimulation of endothelial cell migration, complex formation between NRP1 and VEGFR2, and signaling via FAK Tyr407 phosphorylation. *Mol. Biol. Cell* **22**, 2766–2776 (2011).

356. Geretti, E. *et al.* A mutated soluble neuropilin-2 B domain antagonizes vascular endothelial growth factor bioactivity and inhibits tumor progression. *Mol. Cancer Res.* **8**, 1063–1073 (2010).

357. Werneburg, S. *et al.* Polysialylation and lipopolysaccharide-induced shedding of E-selectin ligand-1 and neuropilin-2 by microglia and THP-1 macrophages. *Glia* **64**, 1314–1330 (2016).

358. Huang, X. *et al.* N-glycosylation-defective splice variants of neuropilin-1 promote metastasis by activating endosomal signals. *Nat. Commun.* **10**, 1–16 (2019).

359. Shintani, Y. *et al.* Glycosaminoglycan modification of neuropilin-1 modulates VEGFR2 signaling. *EMBO J.* **25**, 3045–3055 (2006).

360. Hendricks, C. *et al.* A Novel Physiological Glycosaminoglycan-Deficient Splice Variant of Neuropilin-1 Is Anti-Tumorigenic In Vitro and In Vivo. *PLoS One* **11**, 1–21 (2016).

361. Jongbloets, B. C. & Pasterkamp, R. J. Semaphorin signalling during development. *Development* **141**, 3292–3297 (2014).

362. Yazdani, U. & Terman, J. R. The semaphorins. *Genome Biol.* **7 (3)**, 1–14 (2006).

363. Koppel, A. M., Feiner, L., Kobayashi, H. & Raper, J. A. A 70 amino acid region within the semaphorin domain activates specific cellular response of semaphorin family members. *Neuron* **19**, 531–537 (1997).

364. Janssen, B. J. C. *et al.* Structural basis of semaphorin–plexin signalling. *Nature* **467**, 1118–1124 (2010).

365. Sharma, A., Verhaagen, J. & Harvey, A. R. Receptor complexes for each of the Class 3 Semaphorins. *Front. Cell. Neurosci.* **6**, 1–13 (2012).

366. Adams, R., Lohrum, M., Klostermann, A., Betz, H. & Püschel, A. The chemorepulsive activity of secreted semaphorins is regulated by furin-dependent proteolytic processing. *EMBO J.* **16**, 6077–6086 (1997).

367. Perälä, N., Sariola, H. & Immonen, T. More than nervous: The emerging roles of plexins. *Differentiation* **83**, 77–91 (2012).

368. Franco, M. & Tamagnone, L. Tyrosine phosphorylation in semaphorin signalling: shifting into overdrive. *EMBO Rep.* **9**, 865–871 (2008).

369. Pascoe, H. G., Wang, Y. & Zhang, X. Structural mechanisms of plexin signaling. *Prog. Biophys. Mol. Biol.* **118**, 161–168 (2015).

370. Negishi, M., Oinuma, I. & Katoh, H. R-ras as a key player for signaling pathway of plexins. *Mol. Neurobiol.* **32**, 217–222 (2005).

371. Wang, Y. *et al.* Plexins Are GTPase-Activating Proteins for Rap and Are Activated by Induced Dimerization. *Sci. Signal.* **5**, 1–13 (2012).

372. Bell, C. H., Aricescu, A. R., Jones, E. Y. & Siebold, C. A Dual Binding Mode for RhoGTPases in Plexin Signalling. *PLoS Biol.* **9 (8)**, 1–10 (2011).

373. Nogi, T. *et al.* Structural basis for semaphorin signalling through the plexin receptor. *Nature* **467**, 1123–1127 (2010).

374. Gu, C. *et al.* Semaphorin 3E and Plexin-D1 Control Vascular Pattern Independently of Neuropilins. *Science (80-.).* **307**, 265–268 (2005).

375. Luchino, J. *et al.* Semaphorin 3E Suppresses Tumor Cell Death Triggered by the Plexin D1 Dependence Receptor in Metastatic Breast Cancers. *Cancer Cell* **24**, 673–685 (2013).

376. Goel, H. L., Pursell, B., Standley, C., Fogarty, K. & Mercurio, A. M. Neuropilin-2 regulates α6β1 integrin in the formation of focal adhesions and signaling. *J. Cell Sci.* **125**, 497–506 (2012).

377. Valdembri, D. *et al.* Neuropilin-1/GIPC1 Signaling Regulates α5β1 Integrin Traffic and Function in Endothelial Cells. *PLoS Biol.* **7**, e1000025 (2009).

378. Herzog, Y., Kalcheim, C., Kahane, N., Reshef, R. & Neufeld, G. Differential expression of neuropilin-1 and neuropilin-2 in arteries and veins. *Mech. Dev.* **109**, 115–119 (2001).

379. UniProt. https://www.uniprot.org/uniprot.

380. Gu, C. *et al.* Neuropilin-1 conveys semaphorin and VEGF signaling during neural and cardiovascular development. *Dev. Cell* **5**, 45–57 (2003).

381. Giger, R. J. *et al.* Neuropilin-2 Is Required In Vivo for Selective Axon Guidance Responses to Secreted Semaphorins. *Neuron* **25**, 29–41 (2000).

382. Jin, Z. & Strittmatter, S. Rac1 mediates collapsin-1-induced growth cone collapse. *J. Neurosci.* **17**, 6256–6263 (1997).

383. Zanata, S., Hovatta, I., Rohm, B. & Püschel, A. Antagonistic effects of Rnd1 and RhoD GTPases regulate receptor activity in Semaphorin 3A-induced cytoskeletal collapse. *J. Neurosci.* **22**, 471–477 (2002).

384. Aizawa, H. *et al.* Phosphorylation of cofilin by LIMkinase is necessary for semaphorin 3A-induced growth cone collapse. *Nat. Neurosci.* **4**, 367–373 (2001).

385. Ruiz de Almodovar, C. *et al.* Matrix-binding vascular endothelial growth factor (VEGF) isoforms guide granule cell migration in the cerebellum via VEGF receptor Flk1. *J. Neurosci.* **30**, 15052–15066 (2010).

386. Huber, A. B., Kolodkin, A. L., Ginty, D. D. & Cloutier, J.-F. Signaling at the growth cone: Ligand-Receptor Complexes and the Control of Axon Growth and Guidance. *Annu. Rev. Neurosci.* **26**, 509–563 (2003).

387. Pasterkamp, R. J. & Giger, R. J. Semaphorin Function in Neural Plasticity and Disease. *Curr. Opin. Neurobiol.* **19**, 263–274 (2009).

388. Quintremil, S., Ferrer, F. M., Puente, J., Pando, M. E. & Valenzuela, M. A. Roles of Semaphorins in Neurodegenerative Diseases. in *Neurons - Dendrites and Axons* (eds. Aranda-Abreu, G. E. & Hernández- Aguilar, M. E.) (2018). doi:10.5772/intechopen.82046.

389. Raimondi, C. & Ruhrberg, C. Neuropilin signalling in vessels, neurons and tumours. *Semin. Cell Dev. Biol.* **24**, 172–178 (2013).

390. Chauvet, S., Burk, K. & Mann, F. Navigation rules for vessels and neurons: cooperative signaling between VEGF and neural guidance cues. *Cell Mol. Life Sci.* **70**, 1685–1703 (2013).

391. Takashima, S. *et al.* Targeting of both mouse neuropilin-1 and neuropilin-2 genes severely impairs developmental yolk sac and embryonic angiogenesis. *PNAS* **99**, 3657–3662 (2002).

392. Yuan, L. *et al.* Abnormal lymphatic vessel development in neuropilin 2 mutant mice. *Development* **129**, 4797–4806 (2002).

393. Verlinden, L. *et al.* Nrp2 deficiency leads to trabecular bone loss and is accompanied by enhanced osteoclast and reduced osteoblast numbers. *Bone* **55**, 465–475 (2013).

394. Chen, H. *et al.* Neuropilin-2 Regulates the Development of Select Cranial and Sensory Nerves and Hippocampal Mossy Fiber Projections. *Neuron* **25**, 43–56 (2000).

395. Zachary, I. C., Frankel, P., Evans, I. M. & Pellet-Many, C. The role of neuropilins in cell signalling. *Biochem. Soc. Trans.* **37**, 1171–1178 (2009).

396. Wang, J. *et al.* NRP-2 in tumor lymphangiogenesis and lymphatic metastasis. *Cancer Lett.* **418**, 176–184 (2018).

397. Prud'homme, G. J. & Glinka, Y. Neuropilins are multifunctional coreceptors involved in tumor initiation, growth, metastasis and immunity. *Oncotarget* **3**, 921–939 (2012).

398. Nasarre, P., Gemmill, R. M. & Drabkin, H. A. The emerging role of class-3 semaphorins and their neuropilin receptors in oncology. *Onco. Targets. Ther.* **7**, 1663–1687 (2014).

399. Niland, S. & Eble, J. A. Neuropilins in the Context of Tumor Vasculature. *Int. J. Mol. Sci.* **20 (3)**, 1–44 (2019).

400. Jubb, A. M. *et al.* Neuropilin-1 expression in cancer and development. *J. Pathol.* **226**, 50–60 (2012).

401. Jubb, A. M. *et al.* Neuropilin-2 expression in cancer. *Histopathology* **60**, 340–349 (2012).

402. Peng, K., Bai, Y., Zhu, Q., Hu, B. & Xu, Y. Targeting VEGF–neuropilin interactions: a promising antitumor strategy. *Drug Discov. Today* **24**, 656–664 (2019).

403. Aspalter, I. M. *et al.* Alk1 and Alk5 inhibition by Nrp1 controls vascular sprouting downstream of Notch. *Nat. Commun.* **6**, 1–13 (2015).

404. Pan, Q. *et al.* Blocking Neuropilin-1 Function Has an Additive Effect with Anti-VEGF to Inhibit Tumor Growth. *Cancer Cell* **11**, 53–67 (2007).

405. Caunt, M. *et al.* Blocking Neuropilin-2 Function Inhibits Tumor Cell Metastasis. *Cancer Cell* **13**, 331–342 (2008).

406. Hu, C. & Jiang, X. Role of NRP-1 in VEGF-VEGFR2-Independent Tumorigenesis. *Target. Oncol.* **11**, 501–505 (2016).

407. Raimondi, C. *et al.* Imatinib inhibits VEGF-independent angiogenesis by targeting neuropilin 1-dependent ABL1 activation in endothelial cells. *J. Exp. Med.* **211**, 1167–1183 (2014).

408. Zhang, L. *et al.* VEGF-A/Neuropilin 1 Pathway Confers Cancer Stemness via Activating Wnt/β-Catenin Axis in Breast Cancer Cells. *Cell. Physiol. Biochem.* **44**, 1251–1262 (2017).

409. Elaimy, A. L. *et al.* VEGF–neuropilin-2 signaling promotes stem-like traits in breast cancer cells by TAZ-mediated repression of the Rac GAP β2-chimaerin. *Sci. Signal.* **11**, 1–14 (2018).

410. Goel, H. L. & Mercurio, A. M. Enhancing integrin function by VEGF/neuropilin signaling: Implications for tumor biology. *Cell Adhes. Migr.* **6**, 554–560 (2012).

411. Fukasawa, M., Matsushita, A. & Korc, M. Neuropilin-1 interacts with integrin beta1 and modulates pancreatic cancer cell growth, survival and invasion. *Cancer Biol. Ther.* **6**, 1173–1180 (2007).

412. Grandclement, C. *et al.* Neuropilin-2 Expression Promotes TGF-β1-Mediated Epithelial to Mesenchymal Transition in Colorectal Cancer Cells. *PLoS One* **6**, e20444 (2011).

413. Glinka, Y., Stoilova, S., Mohammed, N. & Prud'homme, G. Neuropilin-1 exerts co-receptor function for TGF-beta-1 on the membrane of cancer cells and enhances responses to both latent and active TGF-beta. *Carcinogenesis* **32**, 613–621 (2011).

414. Kwiatkowski, S. C. *et al.* Neuropilin-1 modulates TGFβ signaling to drive glioblastoma growth and recurrence after anti-angiogenic therapy. *PLoS One* **12**, e0185065 (2017).

415. Ding, Z. *et al.* Neuropilin 1 modulates TGF-β1-induced epithelial-mesenchymal transition in non-small cell lung cancer. *Int. J. Oncol.* **56**, 531–543 (2020).

416. Wittmann, P. *et al.* Neuropilin-2 induced by transforming growth factor-β augments migration of hepatocellular carcinoma cells. *BMC Cancer* **15**, 1–8 (2015).

417. Gemmill, R. M. *et al.* The neuropilin 2 isoform NRP2b uniquely supports TGFb-mediated progression in lung cancer. *Sci. Signal.* **10 (462)**, 1–12 (2017).

418. Yaqoob, U. *et al.* Neuropilin-1 Stimulates Tumor Growth by Increasing Fibronectin Fibril Assembly in the Tumor Microenvironment. *Cancer Res.* **72**, 4047–4059 (2015).

419. Roy, S. *et al.* Macrophage-derived Neuropilin-2 exhibits novel tumor-promoting functions. *Cancer Res.* **78**, 5600–5617 (2018).

420. Roy, S. *et al.* Multifaceted Role of Neuropilins in the Immune System: Potential Targets for Immunotherapy. *Front. Immunol.* **8**, 1–27 (2017).

421. Casazza, A. *et al.* Impeding macrophage entry into hypoxic tumor areas by Sema3A/Nrp1 signaling blockade inhibits angiogenesis and restores antitumor immunity. *Cancer Cell* **24**, 695–709 (2013).

422. Toledano, S., Nir-Zvi, I., Engelman, R., Kessler, O. & Neufeld, G. Class-3 semaphorins and their receptors: Potent multifunctional modulators of tumor progression. *Int. J. Mol. Sci.* **20 (3)**, 1–20 (2019).

423. Neufeld, G. *et al.* The role of the semaphorins in cancer. *Cell Adhes. Migr.* **10**, 652–674 (2016).

424. Herman, J. & Meadows, G. Increased class 3 semaphorin expression modulates the invasive and adhesive properties of prostate cancer cells. *Int. J. Oncol.* **30**, 1231–1238 (2007).

425. Chakraborty, G., Kumar, S., Mishra, R., Patil, T. V. & Kundu, G. C. Semaphorin 3A Suppresses Tumor Growth and Metastasis in Mice Melanoma Model. *PLoS One* **7**, e33633 (2012).

426. Bagci, T., Wu, J., Pfannl, R., Ilag, L. & Jay, D. Autocrine semaphorin 3A signaling promotes glioblastoma dispersal. *Oncogene* **28**, 3537–3550 (2009).

427. Müller, M. W. *et al.* Association of axon guidance factor semaphorin 3A with poor outcome in pancreatic cancer. *Int. J. Cancer* **121**, 2421–2433 (2007).

428. Catalano, A. *et al.* Semaphorin-3A is expressed by tumor cells and alters T-cell signal transduction and function. *Blood* **107**, 3321–3329 (2006).

429. Rolny, C. *et al.* The tumor suppressor semaphorin 3B triggers a prometastatic program mediated by interleukin 8 and the tumor microenvironment. *J. Exp. Med.* **205**, 1155–1171 (2008).

430. Malik, M., Satherley, L., Davies, E., Ye, L. & Jiang, W. Expression of Semaphorin 3C in Breast Cancer and its Impact on Adhesion and Invasion of Breast Cancer Cells. *Anticancer Res.* **36**, 1281–1286 (2016).

431. Man, J. *et al.* Sema3C Promotes the Survival and Tumorigenicity of Glioma Stem Cells through Rac1 Activation. *Cell Rep.* **9**, 1812–1826 (2014).

432. Foley, K. *et al.* Semaphorin 3D autocrine signaling mediates the metastatic role of annexin A2 in pancreatic cancer. *Sci. Signal.* **8**, 1–14 (2015).

433. Zhou, Z. H. *et al.* SEMA3F prevents metastasis of colorectal cancer by PI3K-AKT-dependent down-regulation of the ASCL2-CXCR4 axis. *J. Pathol.* **236**, 467–478 (2015).

434. Doçi, C. L., Mikelis, C. M., Lionakis, M. S., Molinolo, A. A. & Gutkind, J. S. Genetic identification of SEMA3F as an anti-lymphangiogenic metastasis suppressor gene in head and neck squamous carcinoma. *Cancer Res.* **75**, 2937–2948 (2015).

435. Zhang, B. *et al.* Prognostic Significance of VEGF-C, Semaphorin 3F, and Neuropilin-2 Expression in Oral Squamous Cell Carcinomas and Their Relationship With Lymphangiogenesis. *J. Surg. Oncol.* **111**, 382–388 (2015).

436. Zhou, X. *et al.* Effects of SEMA3G on migration and invasion of glioma cells. *Oncol. Rep.* **28**, 269–275 (2012).

437. Vivekanadhan, S. & Mukhopadhyay, D. Divergent roles of Plexin D1 in cancer. *Biochim. Biophys. Acta* **1872**, 103–110 (2019).

438. Hota, P. K. & Buck, M. Plexin structures are coming: opportunities for multilevel investigations of semaphorin guidance receptors, their cell signaling mechanisms, and functions. *Cell. Mol. Life Sci.* **69**, 3765–3805 (2012).

439. Yamada, D., Watanabe, S., Kawahara, K. & Maeda, T. Plexin A1 signaling confers malignant phenotypes in lung cancer cells. *Biochem. Biophys. Res. Commun.* **480**, 75–80 (2016).

440. Kigel, B., Rabinowicz, N., Varshavsky, A., Kessler, O. & Neufeld, G. Plexin-A4 promotes tumor progression and tumor angiogenesis by enhancement of VEGF and bFGF signaling. *Blood* **118**, 4285–96 (2011).

441. Lu, Y. *et al.* Isoprenaline/β2-AR activates Plexin-A1/VEGFR2 signals via VEGF secretion in gastric cancer cells to promote tumor angiogenesis. *BMC Cancer* **17 (1)**, 1–15 (2017).

442. Gabrovska, P. N. *et al.* Semaphorin-plexin signalling genes associated with human breast tumourigenesis. *Gene* **489**, 63–9 (2011).

443. Tian, T. V *et al.* Identification of novel TMPRSS2:ERG mechanisms in prostate cancer metastasis: involvement of MMP9 and PLXNA2. *Oncogene* **33**, 2204–14 (2014).

444. Nguyen, H. *et al.* Progesterone and 1,25-dihydroxyvitamin D_3 inhibit endometrial cancer cell growth by upregulating semaphorin 3B and semaphorin 3F. *Mol. Cancer Res.* **9**, 1479–92 (2011).

445. Joseph, D., Ho, S.-M. & Syed, V. Hormonal regulation and distinct functions of semaphorin-3B and semaphorin-3F in ovarian cancer. *Mol. Cancer Ther.* **9**, 499–509 (2010).

446. Casazza, A. *et al.* Sema3E-Plexin D1 signaling drives human cancer cell invasiveness and metastatic spreading in mice. *J. Clin. Invest.* **120**, 2684–2698 (2010).

447. Worzfeld, T. *et al.* ErbB-2 signals through Plexin-B1 to promote breast cancer metastasis. *J. Clin. Invest.* **122**, 1296–1305 (2012).

448. Haider, M.-T. *et al.* Breast cancer bone metastases are attenuated in a Tgif1-deficient bone microenvironment. *Breast Cancer Res.* **22**, 1–16 (2020).

449. Samuel, S. *et al.* Neuropilin-2 Mediated β-Catenin Signaling and Survival in Human Gastro-Intestinal Cancer Cell Lines. *PLoS One* **6 (10)**, 1–11 (2011).

450. Hillman, R. T. *et al.* Neuropilins are positive regulators of Hedgehog signal transduction. *Genes Dev.* **25**, 2333–2346 (2011).

451. Rao, J. *et al.* Semaphorin-3F suppresses the stemness of colorectal cancer cells by inactivating Rac1. *Cancer Lett.* **358**, 76–84 (2015).

452. Muders, M. H., Zhang, H., Wang, E., Tindall, D. J. & Datta, K. Vascular endothelial growth factor-C protects prostate cancer cells from oxidative stress by the activation of mammalian target of rapamycin complex-2 and AKT-1. *Cancer Res.* **69**, 6042–6048 (2009).

453. Stanton, M. J. *et al.* Autophagy Control by the VEGF-C/NRP-2 Axis in Cancer and Its Implication for Treatment Resistance. *Cancer Res.* **73**, 160–171 (2013).

454. Garcia-Recio, S. *et al.* Substance P autocrine signaling contributes to persistent HER2 activation that drives malignant progression and drug resistance in breast cancer. *Cancer Res.* **73**, 6424–6434 (2013).

455. Garcia-Recio, S., Pastor-Arroyo, E. M., Marín-Aguilera, M., Almendro, V. & Gascón, P. The transmodulation of HER2 and EGFR by substance P in breast cancer cells requires c-Src and metalloproteinase activation. *PLoS One* **10**, e0129661 (2015).

456. Fernández-Nogueira, P. *et al.* Histamine receptor 1 inhibition enhances antitumor therapeutic responses through extracellular signal-regulated kinase (ERK) activation in breast cancer. *Cancer Lett.* **424**, 70–83 (2018).

457. Zubeldia-Plazaola, A. *et al.* Glucocorticoids promote transition of ductal carcinoma in situ to invasive ductal carcinoma by inducing myoepithelial cell apoptosis. *Breast Cancer Res.* **20**, 65 (2018).

458. Fernández-Nogueira, P. *et al.* Differential expression of neurogenes among breast cancer subtypes identifies high risk patients. *Oncotarget* **7**, 5313–5326 (2016).

459. Barkan, D. & Chambers, A. F. β1-integrin: A potential therapeutic target in the battle against cancer recurrence. *Clin. Cancer Res.* **17**, 7219–7223 (2011).

460. Dai, X., Cheng, H., Bai, Z. & Li, J. Breast cancer cell line classification and Its relevance with breast tumor subtyping. *J. Cancer* **8**, 3131–3141 (2017).

461. Neve, R. M. *et al.* A collection of breast cancer cell lines for the study of functionally distinct cancer subtypes. *Cancer Cell* **10**, 515–527 (2006).

462. Kao, J. *et al.* Molecular Profiling of Breast Cancer Cell Lines Defines Relevant Tumor Models and Provides a Resource for Cancer Gene Discovery. *PLoS One* **4**, e6146 (2009).

463. Ossowski, L., Russo, H., Gartner, M. & Wilson, E. Growth of a human carcinoma (HEp3) in nude mice: rapid and efficient metastasis. *J. Cell. Physiol.* **133**, 288–296 (1987).

464. Ossowski, L. & Reich, E. Changes in malignant phenotype of a human carcinoma conditioned by growth environment. *Cell* **33**, 323–333 (1983).

465. Ossowski, L. & Reich, E. Loss of malignancy during serial passage of human carcinoma in culture and discordance between malignancy and transformation parameters. *Cancer Res.* **40**, 2310–5 (1980).

466. Ono, M. *et al.* Exosomes from bone marrow mesenchymal stem cells contain a microRNA that promotes dormancy in metastatic breast cancer cells. *Sci. Signal.* **7**, 1–12 (2014).

467. Marlow, R. *et al.* A novel model of dormancy for bone metastatic breast cancer cells. *Cancer Res.* **73**, 6886–6899 (2013).

468. Bliss, S. A. *et al.* Mesenchymal stem cell-derived exosomes stimulate cycling quiescence and early breast cancer dormancy in bone marrow. *Cancer Res.* **76**, 5832–5844 (2016).

469. Bandari, P. S. *et al.* Hematopoietic growth factor inducible neurokinin-1 type: a transmembrane protein that is similar to neurokinin 1 interacts with substance P. *Regul. Pept.* **111**, 169–178 (2003).

470. Ghazanfari, R. *et al.* Human Primary Bone Marrow Mesenchymal Stromal Cells and Their in vitro Progenies Display Distinct Transcriptional Profile Signatures. *Sci. Rep.* **7**, 10338 (2010).

471. Boxall, S. A. & Jones, E. Markers for Characterization of Bone Marrow Multipotential Stromal Cells. *Stem Cells Int.* **2012**, 975871 (2012).

472. Ikemori, R. *et al.* Epigenetic SMAD3 Repression in Tumor-Associated Fibroblasts Impairs Fibrosis and Response to the Antifibrotic Drug Nintedanib in Lung Squamous Cell Carcinoma. *Cancer Res.* **80**, 276–90 (2020).

473. Thomas, P. & Smart, T. G. HEK293 cell line: A vehicle for the expression of recombinant proteins. *J. Pharmacol. Toxicol. Methods* **51**, 187–200 (2005).

474. Shalem, O. *et al.* Genome-Scale CRISPR-Cas9 Knockout Screening in Human Cells. *Science (80-.).* **343**, 84–87 (2014).

475. Ran, F. A. *et al.* Genome engineering using the CRISPR-Cas9 system. *Nat. Protoc.* **8**, 2281–2308 (2013).

476. Jiang, F. & Doudna, J. A. CRISPR – Cas9 Structures and Mechanisms. *Annu. Rev. Biophys.* **46**, 505–531 (2017).

477. Synthego. https://www.synthego.com (2020).

478. Benchling [biology software]. https://www.benchling.com/crispr (2020).

479. GOBO, Gene Set Analysis. http://co.bmc.lu.se/gobo/gsa.pl.

480. Ringnér, M., Fredlund, E., Häkkinen, J., Borg, Å. & Staaf, J. GOBO: Gene Expression-Based Outcome for Breast Cancer Online. *PLoS One* **6 (3)**, 1–11 (2011).

481. Nagy, Á., Munkácsy, G. & Győrffy, B. Pancancer survival analysis of cancer hallmark genes. *Sci. Rep.* **11 (1)**, 1–10 (2021).

482. Tang, Z. *et al.* GEPIA: a web server for cancer and normal gene expression profiling and interactive analyses. *Nucleis Acids Res.* **45**, 98–102 (2017).

483. Cortazar, A. R. *et al.* CANCERTOOL: a visualization and representation interface to exploit cancer datasets. *Cancer Res.* **78**, 6320–6328 (2018).

484. Denny, S. K. *et al.* Nfib Promotes Metastasis through a Widespread Increase in Chromatin Accessibility. *Cell* **166**, 328–342 (2016).

485. Lu, X. *et al.* Predicting features of breast cancer with gene expression patterns. *Breast Cancer Res. Treat.* **108**, 191–201 (2008).

486. Györffy, B. *et al.* An online survival analysis tool to rapidly assess the effect of 22,277 genes on breast cancer prognosis using microarray data of 1,809 patients. *Breast Cancer Res. Treat.* **123**, 725–31 (2010).

487. Nasarre, P. *et al.* Neuropilin-2 is upregulated in lung cancer cells during TGFβ1-induced epithelial-mesenchymal transition. *Cancer Res.* **73**, 7111–7121 (2014).

488. Belle, M., Parray, A., Belle, M., Chédotal, A. & Nguyen-Ba-Charvet, K. T. PlexinA2 and Sema6A are required for retinal progenitor cell migration. *Dev. Growth Differ.* **58**, 492–502 (2016).

489. Hatanaka, Y. *et al.* Semaphorin 6A-Plexin A2/A4 Interactions with Radial Glia Regulate Migration Termination of Superficial Layer Cortical Neurons. *iScience* **21**, 359–374 (2019).

490. Ribatti, D., Tamma, R. & Annese, T. Epithelial-Mesenchymal Transition in Cancer: A Historical Overview. *Transl. Oncol.* **13 (6)**, 1–9 (2020).

491. Syed, V. *et al.* Profiling estrogen-regulated gene expression changes in normal and malignant human ovarian surface epithelial cells. *Oncogene* **24**, 8128–8143 (2005).

492. Goel, H. L. *et al.* Neuropilin-2 promotes branching morphogenesis in the mouse mammary gland. *Development* **138**, 2969–2976 (2011).

493. Cao, Y. *et al.* Neuropilin-2 Promotes Extravasation and Metastasis by Interacting with Endothelial a5 Integrin. *Cancer Res.* **73**, 4579–90 (2013).

494. Wander, S. A., Zhao, D. & Slingerland, J. M. p27: A Barometer of Signaling Deregulation and Potential Predictor of Response to Targeted Therapies. *Clin. Cancer Res.* **17**, 12–18 (2011).

495. Coqueret, O. New roles for p21 and p27 cell-cycle inhibitors: a function for each cell compartment? *Trends Cell Biol.* **13**, 65–70 (2003).

496. Wang, Y., Yin, H. & Chen, X. Circ-LDLRAD3 Enhances Cell Growth, Migration, and Invasion and Inhibits Apoptosis by Regulating MiR-224-5p/NRP2 Axis in Gastric Cancer. *Dig. Dis. Sci.* 1–10 (2021) doi:https://doi.org/10.1007/s10620-020-06733-1.

497. Ding, G. Y. *et al.* Effect of RNA interference targeting neuropilin-2 gene on proliferation and apoptosis of colon cancer cell line HCT-8. *Zhonghua Fu Chan Ke Za Zhi* **100**, 3879–3883 (2020).

498. Gray, M. J. *et al.* Therapeutic targeting of neuropilin-2 on colorectal carcinoma cells implanted in the murine liver. *J. Natl. Cancer Inst.* **100**, 109–120 (2008).

499. Alghamdi, A. A. A. *et al.* NRP2 as an Emerging Angiogenic Player; Promoting Endothelial Cell Adhesion and Migration by Regulating Recycling of α5 Integrin. *Front. Cell Dev. Biol.* **8**, 1–16 (2020).

500. Fantozzi, A. & Christofori, G. Mouse models of breast cancer metastasis. *Breast Cancer Res.* **8 (4)**, 1–11 (2006).

501. Goel, H. L. & Mercurio, A. M. VEGF targets the tumour cell. *Nat. Rev. Cancer* **13**, 871–882 (2013).

502. Goel, H. L. *et al.* VEGF/neuropilin-2 regulation of Bmi-1 and consequent repression of IGF-IR define a novel mechanism of aggressive prostate cancer. *Cancer Discov.* **2**, 906–21 (2012).

503. Massagué, J. TGFβ signalling in context. *Nature* **13**, 616–630 (2012).

504. Altorki, N. K. *et al.* The lung microenvironment: an important regulator of tumour growth and metastasis. *Nat. Rev. Cancer* **19**, 9–31 (2019).

505. Cox, T. R. & Erler, J. T. Molecular Pathways: Connecting Fibrosis and Solid Tumor Metastasis. *Clin. Cancer Res.* **20**, 3637–43 (2014).

506. Ballester, B., Milara, J. & Cortijo, J. Idiopathic Pulmonary Fibrosis and Lung Cancer: Mechanisms and Molecular Targets. *Int. J. Mol. Sci.* **20 (3)**, 1–28 (2019).

507. Raghu, G., Chen, S.-Y., Hou, Q., Yeh, W.-S. & Collard, H. R. Incidence and prevalence of idiopathic pulmonary fibrosis in US adults 18–64 years old. *Eur. Respir. J.* **48**, 179–186 (2016).

508. Giancotti, F. G. Mechanisms governing metastatic dormancy and reactivation. *Cell* **155**, 750 (2013).

509. Gurrapu, S. & Tamagnone, L. Semaphorins as Regulators of Phenotypic Plasticity and Functional Reprogramming of Cancer Cells. *Trends Mol. Med.* **25**, 303–314 (2019).

510. Taylor Alto, L. & Terman, J. R. Semaphorins and their Signaling Mechanisms. *Methods Mol. Biol.* **1493**, 1–25 (2017).

511. Rehman, M. & Tamagnone, L. Semaphorins in cancer: Biological mechanisms and therapeutic approaches. *Cell Dev. Biol.* **24**, 179–189 (2013).

512. Xiong, G., Wang, C., Evers, B. M., Zhou, B. P. & Xu, R. RORα suppresses breast tumor invasion by inducing SEMA3F expression. *Cancer Res.* **72**, 1728–39 (2012).

513. Nasarre, P. *et al.* Semaphorin SEMA3F Has a Repulsing Activity on Breast Cancer Cells and Inhibits E-Cadherin–Mediated Cell Adhesion. *Neoplasia* **7**, 180–189 (2005).

514. Bielenberg, D. R. *et al.* Semaphorin 3F, a chemorepulsant for endothelial cells, induces a poorly vascularized, encapsulated, nonmetastatic tumor phenotype. *J. Clin. Invest.* **114**, 1260–1271 (2004).

515. Liu, Y., Li, R., Yin, K., Ren, G. & Zhang, Y. The crucial role of SEMA3F in suppressing the progression of oral squamous cell carcinoma. *Cell. Mol. Biol. Lett.* **22**, 1–11 (2017).

516. Futamura, M. *et al.* Possible Role of Semaphorin 3F, a Candidate Tumor Suppressor Gene at 3p21.3, in p53-Regulated Tumor Angiogenesis Suppression. *Cancer Res.* **67**, 1451–60 (2007).

517. Kandoth, C. *et al.* Mutational landscape and significance across 12 major cancer types. *Nature* **502**, 333–339 (2013).

518. Mantovani, F., Collavin, L. & Sal, G. Del. Mutant p53 as a guardian of the cancer cell. *Cell Death Differ.* **26**, 199–212 (2019).

519. Harris, S. L. & Levine, A. J. The p53 pathway: positive and negative feedback loops. *Oncogene* **24**, 2899–2908 (2005).

520. Nakayama, H. *et al.* Regulation of mTOR Signaling by Semaphorin 3F-Neuropilin 2 Interactions In Vitro and In Vivo. *Sci. Rep.* **5**, 1–14 (2015).

521. Bollard, J. *et al.* The axon guidance molecule semaphorin 3F is a negative regulator of tumor progression and proliferation in ileal neuroendocrine tumors. *Oncotarget* **6**, 36731–36745 (2015).

522. Potiron, V. A. *et al.* Semaphorin SEMA3F affects multiple signaling pathways in lung cancer cells. *Cancer Res.* **67**, 8708–15 (2007).

523. Chen, R. *et al.* Phosphorylation of P27 by AKT is required for inhibition of cell cycle progression in cholangiocarcinoma. *Dig. liver Dis.* **50**, 501–506 (2018).

524. Prasad, S. B. *et al.* PI3K/AKT pathway-mediated regulation of p27(Kip1) is associated with cell cycle arrest and apoptosis in cervical cancer. *Cell. Oncol.* **38**, 215–25 (2015).

525. Shanmugasundaram, K. *et al.* PI3K regulation of the SKP-2/p27 axis through mTORC2. *Oncogene* **32**, 2027–2036 (2013).

526. Fu, X. *et al.* SEMA3F-deficient colorectal cancer cells Promote lymphangiogenesis: fatty acid metabolism replace glycolysis for energy supply during lymphatic endothelial cells proliferation in tumor hypoxia microenvironment. *BioRxiv* 1–54 (2019).

527. Giger, R. J. *et al.* Neuropilin-2 Is Required In Vivo for Selective Axon Guidance Responses to Secreted Semaphorins. *Neuron* **25**, 29–41 (2000).

528. Xie, Z. *et al.* Semaphorin 3F Serves as a Tumor Suppressor in Esophageal Squamous Cell Carcinoma and is Associated With Lymph Node Metastasis in Disease Progression. *Technol. Cancer Res. Treat.* **19**, 1–9 (2020).

529. Clarhaut, J. *et al.* ZEB-1, a repressor of the semaphorin 3F tumor suppressor gene in lung cancer cells. *Neoplasia* **11**, 157–66 (2009).

530. Wu, F. *et al.* Endogenous axon guiding chemorepulsant semaphorin-3F inhibits the growth and metastasis of colorectal carcinoma. *Clin. Cancer Res.* **17**, 2702–11 (2011).

531. Sijaona, A., Luukko, K., Kvinnsland, I. H. & Kettunen, P. Expression patterns of Sema3F, PlexinA4, -A3, Neuropilin1 and -2 in the postnatal mouse molar suggest roles in tooth innervation and organogenesis. *Acta Odontol. Scand.* **70**, 140–8 (2012).

532. Takahashi, K., Ishida, M., Hirokawa, K. & Takahashi, H. Expression of the semaphorins Sema 3D and Sema 3F in the developing parathyroid and thymus. *Dev. Dyn.* **237**, 1699–1708 (2008).

533. Zhang, P., Sun, Y. & Ma, L. ZEB1: at the crossroads of epithelial-mesenchymal transition, metastasis and therapy resistance. *Cell cycle* **14**, 481–7 (2015).

534. Wu, H.-T. *et al.* Oncogenic functions of the EMT-related transcription factor ZEB1 in breast cancer. *J. Transl. Med.* **18**, 1–10 (2020).

535. Cagnoni, G. & Tamagnone, L. Semaphorin receptors meet receptor tyrosine kinases on the way of tumor progression. *Oncogene* **33**, 4795–4802 (2014).

536. Delloye-Bourgeois, C. *et al.* Microenvironment-Driven Shift of Cohesion/Detachment Balance within Tumors Induces a Switch toward Metastasis in Neuroblastoma. *Cancer Cell* **32**, 427–443 (2016).

537. Suzuki, H. I. *et al.* Regulation of TGF-b-mediated endothelial-mesenchymal transition by microRNA-27. *J. Biochem.* **161**, 417–420 (2017).

538. Sripathi, S. R. *et al.* Axon Guidance Signaling Modulates Epithelial to Mesenchymal Transition in Stem CellDerived Retinal Pigment Epithelium. *BioRxiv* 1–26 (2018) doi:https://doi.org/10.1101/264705.

539. Oh, J.-E. *et al.* PlexinA2 Mediates Osteoblast Differentiation via Regulation of Runx2. *JBMR* **27**, 552–562 (2012).

540. Sabag, A. D. *et al.* The role of the plexin-A2 receptor in Sema3A and Sema3B signal transduction. *J. Cell Sci.* **127**, 5240–5252 (2014).

541. Zhao, X.-F. *et al.* PlexinA2 Forward Signaling through Rap1 GTPases Regulates Dentate Gyrus Development and Schizophrenia-like Behaviors. *Cell Rep.* **22**, 456–470 (2018).

542. Liu, J. *et al.* SOX4 maintains the stemness of cancer cells via transcriptionally enhancing HDAC1 revealed by comparative proteomics study. *Cell Biosci.* **11**, 1–19 (2021).

543. Peng, X. *et al.* SOX4 contributes to TGF-b-induced epithelialemesenchymal transition and stem cell characteristics of gastric cancer cells. *Genes Dis.* **5**, 49–61 (2018).

544. Huang, H.-Y. *et al.* SOX4 Transcriptionally Regulates Multiple SEMA3/Plexin Family Members and Promotes Tumor Growth in Pancreatic Cancer. *PLoS One* **7 (12)**, 1–12 (2012).

545. Krishnan, A. *et al.* Genome-wide prediction and functional characterization of the genetic basis of autism spectrum disorder. *Nat. Neurosci.* **19**, 1454–1462 (2016).

546. Ben-Zvi, A. *et al.* The Semaphorin receptor PlexinA3 mediates neuronal apoptosis during dorsal root ganglia development. *J. Neurosci.* **28**, 12427–32 (2008).

547. Oleari, R. *et al.* PLXNA1 and PLXNA3 cooperate to pattern the nasal axons that guide gonadotropin-releasing hormone neurons. *Development* **146 (21)**, 1–8 (2019).

548. Kotan, L. D. *et al.* Loss-of-function variants in SEMA3F and PLXNA3 encoding semaphorin-3F and its receptor plexin-A3 respectively cause idiopathic hypogonadotropic hypogonadism. *Genet. Med.* 1–9 (2021) doi:10.1038/s41436-020-01087-5.

549. Huang, J. *et al.* Downregulation of estrogen receptor and modulation of growth of breast cancer cell lines mediated by paracrine stromal cell signals. *Breast Cancer Res. Treat.* **161**, 229–243 (2017).

550. Moriarty, W. F., Kim, E., Gerber, S. A., Hammers, H. & Alani, R. M. Neuropilin-2 promotes melanoma growth and progression in vivo. *Melanoma Res.* **26**, 321–328 (2016).

551. Chen, Y. *et al.* Transforming growth factor-β1 promotes breast cancer metastasis by downregulating miR-196a-3p expression. *Oncotarget* **8**, 49110–49122 (2017).

552. Do, Y. *et al.* MiR-146a Regulates Migration and Invasion by Targeting NRP2 in Circulating-Tumor Cell Mimicking Suspension Cells. *Genes (Basel).* **12**, 1–15 (2021).

553. Fung, T. M. *et al.* Neuropilin-2 promotes tumourigenicity and metastasis in oesophageal squamous cell carcinoma through ERK – MAPK – ETV4 – MMP – E-cadherin deregulation. *J. Pathol.* **239**, 309–319 (2016).

554. Bower, J. J. *et al.* Patterns of cell cycle checkpoint deregulation associated with intrinsic molecular subtypes of human breast cancer cells. *NPJ Breast Cancer* **3**, 1–12 (2017).

555. Ceccarelli, S. *et al.* Neuropilin 1 Mediates Keratinocyte Growth Factor Signaling in Adipose-Derived Stem Cells: Potential Involvement in Adipogenesis. *Stem Cells Int.* **2018**, 1–18 (2018).

556. Jiang, S. X., Sheldrick, M., Desbois, A., Slinn, J. & Hou, S. T. Neuropilin-1 Is a Direct Target of the Transcription Factor E2F1 during Cerebral Ischemia-Induced Neuronal Death In Vivo. *Mol. Cell. Biol.* **27**, 1696–1705 (2007).

557. Bruin, A. de *et al.* Genome-wide analysis reveals NRP1 as a direct HIF1-E2F7 target in the regulation of motorneuron guidance in vivo. *Nucleis Acids Res.* **44**, 3549–3566 (2016).

558. Fujii, T. *et al.* MicroRNA-331-3p Suppresses Cervical Cancer Cell Proliferation and E6/E7 Expression by Targeting NRP2. *Int. J. Mol. Sci.* **17**, 1–13 (2016).

559. Li, L. *et al.* Neuropilin-1 is associated with clinicopathology of gastric cancer and contributes to cell proliferation and migration as multifunctional co-receptors. *J. Exp. Clin. Cancer Res.* **35**, 1–12 (2016).

560. Zhang, M., Song, Y. & Zhai, F. ARFHPV E7 oncogene, lncRNA HOTAIR, miR-331-3p and its target, NRP2, form a negative feedback loop to regulate the apoptosis in the tumorigenesis in HPV positive cervical cancer. *J. Cell. Biochem.* **119**, 4397–4407 (2018).

561. Samuel, S. *et al.* Neuropilin-2 Mediated β-Catenin Signaling and Survival in Human Gastro-Intestinal Cancer Cell Lines. *PLoS One* **6**, (2011).

562. Ji, T. *et al.* Neuropilin-2 expression is inhibited by secreted Wnt antagonists and its down-regulation is associated with reduced tumor growth and metastasis in osteosarcoma. *Mol. Cancer* **14**, 1–14 (2015).

563. Liu, W., Wu, T., Dong, X. & Zeng, Y. A. Neuropilin-1 is upregulated by Wnt/β-catenin signaling and is important for mammary stem cells. *Sci. Rep.* **7**, 1–11 (2017).

564. Steinhusen, U. *et al.* Apoptosis-induced Cleavage of b-Catenin by Caspase-3 Results in Proteolytic Fragments with Reduced Transactivation Potential. *J. Biol. Chem.* **275**, 16345–16353 (2002).

565. Goel, H. L. *et al.* GLI1 regulates a novel neuropilin-2/α6β1 integrin based autocrine pathway that contributes to breast cancer initiation. *EMBO Mol. Med.* **5 (4)**, 488–508 (2013).

566. Gong, C. *et al.* Stimulation of medulloblastoma stem cells differentiation by a peptidomimetic targeting neuropilin-1. *Oncotarget* **9**, 15312–15325 (2018).

567. Siegle, J. M. *et al.* SOX2 is a cancer-specific regulator of tumour initiating potential in cutaneous squamous cell carcinoma. *Nat. Commun.* **4**, 1–12 (2014).

568. Hamerlik, P. *et al.* Autocrine VEGF–VEGFR2–Neuropilin-1 signaling promotes glioma stem-like cell viability and tumor growth. *J. Exp. Med.* **209**, 507–520 (2012).

569. Jiang, L., Li, J. & Song, L. Bmi-1, stem cells and cancer. *Acta Biochim. Biophys. Sin. (Shanghai).* **41**, 527–534 (2009).

570. Batlle, E. & Clevers, H. Cancer stem cells revisited. *Nat. Med.* **23**, 1124–1134 (2017).

571. Roche, J. The Epithelial-to-Mesenchymal Transition in Cancer. *Cancers (Basel).* **10 (2)**, 1–4 (2020).

572. Luo, X. *et al.* Vascular NRP2 triggers PNET angiogenesis by activating the SSH1-coflin axis. *Cell Biosci.* **10**, 1–16 (2020).

573. Lv, T. *et al.* p53-R273H upregulates neuropilin-2 to promote cell mobility and tumor metastasis. *Cell Death Dis.* **8**, 1–12 (2017).

574. Harjunpää, H., Asens, M. L., Guenther, C. & Fagerholm, S. C. Cell Adhesion Molecules and Their Roles and Regulation in the Immune and Tumor Microenvironment. *Front. Immunol.* **10**, 1–24 (2019).

575. Nagano, M., Hoshino, D., Koshikawa, N., Akizawa, T. & Seiki, M. Turnover of Focal Adhesions and Cancer Cell Migration. *Int. J. Cell Biol.* 1–10 (2012) doi:https://doi.org/10.1155/2012/310616.

576. Pascalisa, C. De & Etienne-Manneville, S. Single and collective cell migration: the mechanics of adhesions. *Mol. Biol. Cell* **28**, 1833–1846 (2017).

577. Yu, H. *et al.* Inhibition of cell migration by focal adhesion kinase: Time-dependent difference in integrin-induced signaling between endothelial and hepatoblastoma cells. *Int. J. Mol. Med.* **41**, 2573–2588 (2018).

578. Po, A. *et al.* Noncanonical GLI1 signaling promotes stemness features and in vivo growth in lung adenocarcinoma. *Oncogene* **36**, 4641–4652 (2017).

579. Wang, J. *et al.* Pathway-related molecules of VEGFC/D-VEGFR3/NRP2 axis in tumor lymphangiogenesis and lymphatic metastasis. *Clin. Chim. Acta* **461**, 165–171 (2016).

580. Kong, D. *et al.* VEGF-C mediates tumor growth and metastasis through promoting EMT-epithelial breast cancer cell crosstalk. *Oncogene* **40**, 964–979 (2021).

581. Derynck, R., Akhurst, R. J. & Balmain, A. TGF-β signaling in tumor suppression and cancer progression. *Nat. Genet.* **29**, 117–129 (2001).

582. Xie, X. *et al.* Smad3 Regulates Neuropilin 2 Transcription by Binding to its 5' Untranslated Region. *J. Am. Heart Assoc.* **9 (8)**, 1–20 (2020).

583. Murray, P. J. & Wynn, T. A. Protective and pathogenic functions of macrophage subsets. *Nat. Rev. Immunol.* **11**, 723–737 (2011).

584. Zhao, X. *et al.* Prognostic significance of tumor-associated macrophages in breast cancer: a meta-analysis of the literature. *Oncotarget* **8**, 30576–30586 (2017).

585. Kumar, A. T. *et al.* Prognostic Significance of Tumor-Associated Macrophage Content in Head and Neck Squamous Cell Carcinoma: A Meta-Analysis. *Front. Oncol.* **9**, 1–10 (2019).

586. Loyher, P.-L. *et al.* Macrophages of distinct origins contribute to tumor development in the lung. *J. Exp. Med.* **215**, 2536–2553 (2018).

587. Little, A. C. *et al.* IL-4/IL-13 Stimulated Macrophages Enhance Breast Cancer Invasion Via Rho-GTPase Regulation of Synergistic VEGF/CCL-18 Signaling. *Front. Oncol.* **9**, 1–13 (2019).

588. Sarode, P., Schaefer, M. B., Grimminger, F., Seeger, W. & Savai, R. Macrophage and Tumor Cell Cross-Talk Is Fundamental for Lung Tumor Progression: We Need to Talk. *Front. Oncol.* **10**, 1–11 (2020).

589. Qian, B. *et al.* A Distinct Macrophage Population Mediates Metastatic Breast Cancer Cell Extravasation, Establishment and Growth. *PLoS One* **4**, 1–16 (2009).

590. Kitamura, T. *et al.* CCL2-induced chemokine cascade promotes breast cancer metastasis by enhancing retention of metastasis-associated macrophages. *J. Exp. Med.* **212**, 1043–1059 (2015).

591. Qian, B.-Z. *et al.* FLT1 signaling in metastasis-associated macrophages activates an inflammatory signature that promotes breast cancer metastasis. *J. Exp. Med.* **212**, 1433–1448 (2015).

592. Alhudaithi, S. S. *et al.* Local Targeting of Lung-Tumor-Associated Macrophages with Pulmonary Delivery of a CSF-1R Inhibitor for the Treatment of Breast Cancer Lung Metastases. *Mol. Pharm.* **17**, 4691–4703 (2020).

593. Ruth, J. R. Modeling Breast Cancer Dormancy and Recurrence Following Oncogenic Pathway Inhibition. *Publicly Accessible Penn Dissertations* vol. 1429 (University of Pennsylvania, 2014).

594. Walker, N. D. *et al.* Exosomes from differentially activated macrophages influence dormancy or resurgence of breast cancer cells within bone marrow stroma. *Cell Death Dis.* **10**, 1–16 (2019).

595. Hur, J. *et al.* CD82/KAI1 Maintains the Dormancy of Long-Term Hematopoietic Stem Cells through Interaction with DARC-Expressing Macrophages. *Cell Stem Cell* **18**, 508–521 (2016).

596. Walens, A. *et al.* CCL5 promotes breast cancer recurrence through macrophage recruitment in residual tumors. *Elife* **8**, 1–26 (2019).

597. Borriello, L. *et al.* Primary tumor associated macrophages activate programs of invasion and dormancy in disseminating tumor cells. *BioRxiv* 1–52 (2021) doi:https://doi.org/10.1101/2021.02.04.429798.

598. Chen, X.-J. *et al.* The role of the hypoxia-Nrp-1 axis in the activation of M2-like tumor-associated macrophages in the tumor microenvironment of cervical cancer. *Mol. Carcinog.* **58**, 388–397 (2019).

599. Vlaeminck, Y. De *et al.* Targeting Neuropilin-1 with Nanobodies Reduces Colorectal Carcinoma Development. *Cancers (Basel).* **12**, 1–21 (2020).

600. Dai, L. *et al.* Fibroblasts in cancer dormancy: foe or friend? *Cancer Cell Int.* **21 (1)**, 1–11 (2021).

601. Khazali, A. S., Wells, A. M. & Clark, A. Inflammatory cytokine IL-8/CXCL8 promotes tumour escape from hepatocyte-induced dormancy. *Br. J. Cancer* **118**, 566–576 (2018).

602. Qiao, Y. *et al.* IL6 derived from cancer-associated fibroblasts promotes chemoresistance via CXCR7 in esophageal squamous cell carcinoma. *Oncogene* **37**, 873–883 (2018).

603. Akhmetshina, A. *et al.* Activation of canonical Wnt signalling is required for TGF-β mediated fibrosis. *Nat. Commun.* **3**, 1–12 (2012).

604. Jang, G.-B. *et al.* Blockade of Wnt/β-catenin signaling suppresses breast cancer metastasis by inhibiting CSC-like phenotype. *Sci. Rep.* **5**, 1–15 (2015).

605. DiMeo, T. A. *et al.* A Novel Lung Metastasis Signature Links Wnt Signaling with Cancer Cell Self-Renewal and Epithelial-Mesenchymal Transition in Basal-like Breast Cancer. *Cancer Res.* **69**, 1–12 (2009).

606. Zhao, M. *et al.* miR-331-3p Suppresses Cell Proliferation in TNBC Cells by Downregulating NRP2. *Technol. Cancer Res. Treat.* **19**, 1–9 (2020).

607. Parker, M. W. *et al.* Structural basis for VEGF-C binding to neuropilin-2 and sequestration by a soluble splice form. *Structure* **23**, 677–687 (2015).

608. Weekes, C. D. *et al.* A phase I study of the human monoclonal anti-NRP1 antibody MNRP1685A in patients with advanced solid tumors. *Invest. New Drugs* **32**, 653–660 (2014).